

DYSREGULATION OF BONE METABOLISM
DURING TYPE 2 DIABETES MELLITUS: ROLE OF
TOLL-LIKE RECEPTOR-4 AND AUTOPHAGY

By

ELIZABETH RENDINA-RUEDY

Bachelor of Science in Biochemistry
Oklahoma State University
Stillwater, OK
2007

Master of Science in Nutritional Sciences
Oklahoma State University
Stillwater, OK
2009

Submitted to the Faculty of the
Graduate College of the
Oklahoma State University
in partial fulfillment of
the requirements for
the Degree of
DOCTOR OF PHILOSOPHY
May, 2014

DYSREGULATION OF BONE METABOLISM
DURING TYPE 2 DIABETES MELLITUS: ROLE OF
TOLL-LIKE RECEPTOR-4 AND AUTOPHAGY

Dissertation Approved:

Dr. Brenda J. Smith

Dissertation Adviser

Dr. Stephen L. Clarke

Dr. Edralin A. Lucas

Dr. Barbara J. Stoecker

Dr. Rita K. Miller

ACKNOWLEDGEMENTS

I recognize that it is impossible for me to compose an all-inclusive list to acknowledge all of my peers, mentors, colleagues, and friends that have had an impact on my growth and development during my Ph.D. However, I would like to take this opportunity to recognize my doctoral committee, advisor, and family.

Aside from the classic role of the doctoral committee, I was lucky enough to develop relationships with each of my committee members, Drs. Barbara Stoecker, Edralin Lucas, Rita Miller, Stephen Clarke, and Brenda Smith. Each member has served an integral role in my success. Drs. Stoecker and Lucas have always been incredibly helpful and served as a wealth of information and knowledge during my training. Dr. Miller was such an inspiration for me, from her ideas and opinions, to the courses she instructed. It was in her classes that I discovered many of my current interests and I cannot express enough gratitude or praise. Furthermore, I truly appreciated her teaching style and have tailored my own teaching philosophy around her courses. I like to think of Dr. Clarke as a co-mentor. Dr. Clarke was always in the lab helping every one of the graduate students. At times he was my hardest critic, but it was during these times that I learned I could rise to the occasion. His mentorship and guidance will always be remembered and appreciated. Lastly, I'd like to thank my academic advisor and mentor Dr. Smith. I fall short on words to express my gratitude to Dr. Smith. I know that she has not only molded me into the scientist I am today, but has also helped me grow as a person. She is someone I have always looked up to and held in the highest regards. Every accomplishment I obtain throughout the years will directly reflect back to Dr. Smith, and I only hope I can do her justice.

Finally, I'd like to thank my family. My sister Andrea, who has always been a huge supporter, has helped me out in more ways than I can imagine. Her children, my niece and nephew, have always been a light in my life. When everything was going crazy, being around them helped me find myself, casting all my worries and stresses away. My mother and father, Carmela and Joseph, have supported me from day one. I could not have obtained this degree, or any of my priors, without their help and guidance. I am forever indebted to them for the life that they have afforded me and I only hope to make them proud. Finally my husband, Zach. this degree and lifestyle is one only few can understand and he understood it. Zach has always been my biggest fan, even if some of my dreams may have got in the way of his own. I have appreciated all of his sacrifices and cannot wait for the rest of our lives together.

Although my name will be written on the diploma, it is all of these individuals that deserve as much, if not more, credit than me.

Name: ELIZABETH RENDINA-RUEDY

Date of Degree: MAY, 2014

Title of Study: DYSREGULATION OF BONE METABOLISM DURING TYPE 2
DIABETES MELLITUS: ROLE OF TOLL-LIKE RECEPTOR-4 AND
AUTOPHAGY

Major Field: HUMAN SCIENCES

Abstract:

Patients with type 2 diabetes mellitus (T2DM) have demonstrated a 1.5-3.5 fold increase in fracture risk, but the mechanisms responsible remain in question. Due to the inflammatory response that has been shown to accompany T2DM and impaired insulin signaling, the purpose of this project was to: (1) determine alterations in bone metabolism and their effects on bone microarchitectural and biomechanical properties the development and progression of T2DM in a young, growing animal; (2) determine the role of toll-like receptor (TLR)-4 in this skeletal response; and (3) explore the extent to which the autophagic pathway in bone cells is altered in response to impaired insulin signaling and glucose availability. The initial study was designed to characterize long-term metabolic and skeletal response between two commonly used C57BL/6 substrains (i.e., C57BL/6 and C57BL/6N) on a high fat (HF) diet. The findings of this study show that the C57BL/6J and the C57BL/6N mouse differ in their metabolic response to a HF diet over a 24 wk study period, but their skeletal response was similar. The subsequent study demonstrated that C3H/HeJ mice with a non-functional TLR-4, were somewhat protected from the metabolic changes induced by a HF diet and were also protected from the deleterious impact a HF diet exerted on bone. The final study demonstrated that autophagy was up-regulated in bone and as impaired glucose tolerance progressed, autophagic flux was enhanced as evidenced by the increased pBeclin1 protein expression. Furthermore, the development and progression of impaired glucose tolerance was associated with osteoblast maturation and an apparent increase in osteocytes. The ability of autophagy to drive osteoblast maturation was further confirmed by the ability of rapamycin-mediated autophagy to shift the phenotype of MC3T3-E1 towards that of a more mature osteoblast. Therefore, the results from these studies (1) establish an appropriate mouse model for the pathogenesis of T2DM; (2) suggest that the metabolic changes associated with a HF diet attenuate bone accrual by altering bone turnover, and that TLR-4 is involved in this skeletal phenotype; and (3) Beclin1-mediated autophagy appears to be up-regulated during impaired glucose tolerance, driving the osteoblast towards a more mature, non-mineralizing phenotype.

TABLE OF CONTENTS

Chapter	Page
I. INTRODUCTION.....	1
Background Information.....	1
Specific Aims.....	9
Limitations.....	10
II. REVIEW OF LITERATURE.....	12
Obesity and Type 2 Diabetes (T2DM) Significance and Background.....	12
Clinical Investigation of Fracture Risk Associated with T2DM.....	15
Rodent Models of T2DM and its Impact on Bone.....	18
Glucose Homeostasis and Insulin Signaling.....	20
Inflammation Induced via Toll-like receptor (TLR)-4 and its Impact on Insulin Signaling.....	23
TLR-4 Signaling Involved in T2DM: Lessons from Animal Models.....	27
Bone Metabolism and Turnover.....	28
Inflammation and TLR-4's Impact on Bone Metabolism.....	32
Implications of RAGE Signaling and Accumulation of AGE's on Bone Strength.....	35
Regulation of Macroautophagy.....	37
Evidence of Altered Autophagy during T2DM.....	44
Autophagy in Osteoblasts, Osteocytes, and Osteoclasts.....	45
Glucose Transporters (GLUTs) of Osteoblasts and Osteoclasts.....	49
Summary of Potential Mechanisms in the Dysregulation of Bone Metabolism in T2DM.....	51
III. A Comparative Study of the Metabolic and Skeletal Response of C57BL/6J and C57BL/6N Mice in a Diet-Induced Model of Type 2 Diabetes.....	53
Introduction.....	57
Materials and Methods.....	58
Results.....	63
Discussion.....	66
References.....	73
Tables.....	77
Figure Legends and Figures.....	83
Supplemental Table.....	89

Chapter	Page
IV. The Attenuation of Bone Accrual in Young, Growing Mice in a Diet-Induced Obesity Model of Type 2 Diabetes Mellitus Involves TLR-4	90
Abstract	92
Introduction.....	94
Materials and Methods.....	97
Results.....	103
Discussion.....	110
References.....	117
Figure Captions.....	123
Tables.....	125
Figures.....	128
V. Glucose Intolerance Attenuates Bone Accrual in the Young Growing Skeleton by Promoting the Maturation of Osteoblasts Through Beclin1-Mediated Autophagy	132
Abstract	134
Introduction.....	136
Materials and Methods.....	139
Results.....	143
Discussion.....	147
Figure Legends.....	151
References.....	153
Tables.....	156
Figures.....	158
VI. SUMMARY, CONCLUSIONS, AND RECOMMENDATIONS	163
Summary.....	163
Conclusions.....	165
Recommendations.....	167
LITERATURE CITED.....	172
APPENDICES	187
Appendix A.....	188
Appendix B.....	191
Appendix C.....	199
INSTITUTIONAL ANIMAL CARE AND USE COMMITTEE (IACUC)	216

LIST OF ABBREVIATIONS.....218

LIST OF TABLES

Table	Page
CHAPTER III	
1. Body Composition, Tissues Weights, Food Intake, Total White Blood Cell Counts and Adipokines	77
2. Pathological Scoring of Hepatic Tissue after 24 wk on a Control of High Fat Diet.....	78
3. Bone Densitometry of the Whole Body and Bone Microarchitectural Parameters of the Spine and Tibia	79
4. Relative Fold Change of Gene Expression in the Liver and Bone Marrow in Mice Fed a High Fat Diet Compared to the Control Diet	80
Supplemental Table 1.....	89
CHAPTER IV	
1. Final Bodyweight and Body Composition of C57BL/6 and C3H/HeJ Mice Following a Control or High Fat Diet.....	125
2. Plasma Insulin and Indicators of Glucose Homeostasis	126
3. Transcriptional Fold Changes of Genes Involved in Osteoblastogenesis and TLR-4 Signaling	127
CHAPTER V	
1. Alterations in Trabecular Microarchitecture of the Femoral Neck after 2, 8, and 16 wks	156
Target Genes used for qPCR Analyses	157

LIST OF FIGURES

Figure		Page
CHAPTER II		
1.....		21
2.....		25
3.....		38
4.....		41
CHAPTER III		
1. Weekly Body Weights		83
2. Blood Glucose and Plasma Insulin Over Time.....		84
3. Glucose Tolerance Test Results After 24 Weeks on a High Fat Diet		85
4. Strain Comparison of Carboxylation Status of Plasma OCN After 24 Wk on a Control or High Fat Diet		86
5. Representative Micrographs of Liver Histology.....		87
6. Alterations in Trabecular Bone Microarchitecture in the Lumbar Vertebra.....		88
CHAPTER IV		
1.		128
2.		129
3.		130
4.		131
CHAPTER V		
1.		158
2.		159
3.		160
4.		161
5.		162

CHAPTER I

INTRODUCTION

Background Information

Obesity is a major public health problem that affects 35.7% of adults and 17% of youth in the United States (Center for Disease Control and Prevention, 2011; Ogden et al., 2012). These statistics represent an increase in obesity rates of approximately 3-fold over the past 5 decades (Parikh et al., 2007). National medical costs associated with obesity are estimated at \$147 billion per year, which accounts for 10% of all healthcare expenditures (Finkelstein et al., 2009). These estimates include both direct and indirect costs associated with treating obesity and its co-morbidities, including stroke, hypertension, peripheral vascular diseases, and type 2 diabetes mellitus (T2DM). In fact, 80-90% of people diagnosed with T2DM are also clinically defined as obese (Berenson, 2012).

Currently, 24 million Americans have T2DM and the prevalence is expected to rise sharply over the next 40 years due to an increase in the aging population, increases in minority groups at high risk for T2DM, and individuals with T2DM living longer (Centers for Disease Prevention and Control, 2011). The Centers for Disease Control

and Prevention (CDC) has projected that the number of Americans with T2DM will double or triple by 2050, which translates to 1 in 3 adults being diagnosed with T2DM (Centers for Disease Prevention and Control, 2011). While T2DM was once considered to be “adult-onset” diabetes, health care providers have been diagnosing more children with T2DM (Centers for Disease Control and Prevention, 2013). Children and adolescents diagnosed with T2DM are usually between 10-19 years of age, obese, and have a family history of diabetes (Centers for Disease Control and Prevention, 2013). The annual medical costs related to treating the diabetes and its complications have been estimated at \$116 billion in the U.S. and these expenditures are 2.3 times higher than the health care costs of patients without diabetes (Centers for Disease Prevention and Control, 2011). The costs and the projected increase in T2DM over the next several decades highlight the negative impact T2DM will have on the health of both adults and children if better prevention strategies and treatment options are not developed.

T2DM is a condition that results in elevated blood glucose or hyperglycemia due to the inability of cells to take up glucose from the circulation. This impairment in glucose uptake is particularly affected in cells dependent upon insulin (e.g., white adipose tissue and skeletal muscle). Although pancreatic insulin secretion often increases as a compensatory mechanism to clear glucose from the blood during the early stages of glucose intolerance, impaired insulin signaling is responsible for the observed hyperglycemia. If blood glucose is not controlled with a regimen of diet, exercise and oral hypoglycemic agents, over time damage to the pancreatic β -cells can result in the cessation of insulin production and secretion (Porte, Jr., 1991). It is at this point that patients may become dependent upon insulin therapy for control and regulation of blood glucose.

Aside from the effects on pancreatic β -cells, failure to control blood glucose can lead to other long-term debilitating complications. Classic complications associated with T2DM include macro- and micro-vascular diseases, which contribute to an increased risk of stroke, myocardial infarction, blindness, renal failure and upper and lower extremity amputation (Hajer et al., 2008). As a result, T2DM is considered the 7th leading cause of death in the U.S. (i.e., ~230,000 deaths/ year) when all contributing factors are taken into account (Centers for Disease Prevention and Control, 2011). Interest in identifying other long-term complications associated with T2DM has led to the investigation of hyperglycemia's effects on other tissue and organ systems, including connective tissue. As early as 1946, researchers began to explore the relationship between T2DM and bone health (Kenney, 1946). While initial studies supported a positive association between T2DM and bone density, continued research with fracture as the primary outcome has depicted a very different relationship between T2DM and fracture risk (Schwartz et al., 2001; Nicodemus et al., 2001; de Liefde et al., 2005; Janghorbani et al., 2006; Melton, III et al., 2008).

Bone mineral density (BMD) determined by dual-energy x-ray absorptiometry (DXA), is commonly used as a determinant of fracture risk (World Health Organization, 2004). Early studies examining fracture risk in adult type 2 diabetics often concluded that these patients were not at increased risk of fracture due to reports of a normal or even elevated BMD (Rishaug et al., 1995; van Daele et al., 1995; Stolk et al., 1996). Further support of this concept was data from the Rochester cohort in 1980 that showed diabetes (i.e., T1DM and T2DM) was not associated with increased fracture incidence (Heath, III et al., 1980). However, continued concern of fracture incidence in this population caused some investigators involved with large scale studies to examine the relationship between fracture

incidence and T2DM as a secondary outcome using previous data sets. In 2001, data from the Study of Osteoporotic Fractures (SOF) demonstrated that women with T2DM had an ~2-fold increase in fracture incidence of the hip and proximal humerus (Schwartz et al., 2001). The Iowa Women's Health Study reported a similar increase in fracture risk in women with T2DM, and importantly the duration (i.e., >12 yr) of T2DM was considered an important contributing factor that increased relative risk (RR) by ~3 fold (Nicodemus et al., 2001). The Nurses' Health Study also reported a RR of hip fracture ~2 fold, and concluded that duration (i.e., >5 yr) of the condition was associated with an exacerbated increase in fracture risk (Janghorbani et al., 2006). These studies were followed by similar reports from the Rotterdam Study describing an increase in fracture incidences among patients with T2DM of ~2 fold (Nicodemus et al., 2001; de Liefde et al., 2005; Janghorbani et al., 2006). Interestingly, in 2008 a follow-up report from the Rochester cohort, which originally reported no increase in fracture incidence in patients with diabetes (i.e., T1DM and T2DM), concluded that both men and women with T2DM had an ~2-fold increase in fracture of the hip, and as duration of T2DM increased 10 years and beyond, this risk was exacerbated (Melton, III et al., 2008; Heath, III et al., 1980). The discrepancy in these results compared to the original findings was attributed to stricter inclusion/exclusion criteria, more stringent classification of T2DM, delineating T1DM and T2DM, and consideration of T2DM duration (Melton, III et al., 2008; Melton, III et al., 2008). Collectively, these studies have provided support that independent of BMD, both men and women with T2DM experience an increased risk of fracture 5-10 yrs post diagnosis. While considerably less research has been done relative to the influence of impaired glucose tolerance on the young, growing skeleton, recent evidence has also established a connection between childhood obesity and increased risk of

fracture (Goulding et al., 2000; Goulding et al., 2001). Due to the importance of optimizing peak bone mass during this early stage of life and its effects on lifetime osteoporosis risk, if bone accrual is inhibited in these children they are not only at increased risk for fracture in the short-term, but also their long-term risk of osteoporotic-related fractures is increased (Goulding et al., 2005). In light of the prevalence of T2DM across all age groups and their potential short- and long-term complications associated with fracture, more research is needed to understand the mechanisms through which altered glucose homeostasis affects bone quality, so that appropriate prevention and therapeutic strategies can be developed.

While the disconnect between BMD and fracture risk in T2DM has perplexed clinicians and researchers alike, common confounders associated with T2DM and bone (e.g., increased adiposity, decreased physical activity, and/or chronic inflammation) have made this clinical observation difficult to unravel. Recent research, however, has focused on the role of the inflammatory response in T2DM and offers a potential explanation of an impact on bone metabolism. A number of different potential sources of inflammation exist among diabetic patients. For instance, most type 2 diabetics are obese and adipose tissue can serve as a source of many adipocytokines that alter the immune response and act as either insulin sensitizers (i.e., leptin and adiponectin) or insulin antagonists (i.e., resistin and tumor necrosis factor or TNF- α) (Mathieu et al., 2010). In addition to adipocytokines, another source of inflammatory signaling in T2DM has been attributed to the pathogen pattern recognition receptors (PRR), toll like receptor (TLR)-4 and the receptor for advanced glycation end-products (RAGEs) (Schiller et al., 2006). Obesity has been linked to gut leakage of lipopolysaccharide (LPS) and increased circulating saturated free fatty acids, both of which are considered TLR-4 ligands (Cani et al., 2008; Lee et al., 2001). Elevated blood

glucose has also been shown to increase the expression of TLR-4 on human monocytes (Dasu et al., 2008). These findings suggest that increased TLR-4 and its ligands enhance the activation of the downstream inflammatory signaling pathway in T2DM.

More direct evidence establishing a role for TLR-4 in T2DM has come from animal models. Mouse models deficient in TLR-4 (e.g., *TLR4*^{-/-} deletion or C3H/HeJ strain with a naturally occurring mutation in TLR-4), have been reported to be protected against the development of diet-induced obesity and insulin resistance (Poggi et al., 2007; Tsukumo et al., 2007; Shi et al., 2006). Another PRR, RAGE, has also been of interest as it relates to the inflammation and complications of T2DM. Hyperglycemia accelerates nonenzymatic glycation and oxidation of proteins and the formation of advanced glycation end products (AGEs). The increase in this ligand as well as the RAGE receptor during T2DM not only promotes inflammation, but has also been shown to promote cross-talk with TLR-4 resulting in similar downstream responses (Ramasamy et al., 2011; Hofmann et al., 1999). The role of these pathways is of particular interest in understanding how T2DM impacts bone metabolism due to the intimate relationship of TLR-4 and RAGE on bone cellular differentiation and function.

The interplay between bone metabolism and the immune response, especially inflammation, has led to the proposed notion that enhanced stimulation of TLR-4 and RAGE during T2DM contributes to the increase in fracture incidence. Bone forming osteoblasts express receptor activator for NF-κB ligand (RANKL), which promotes bone resorption by up-regulating osteoclast differentiation (Kearns et al., 2008). In turn, osteoclastogenesis induced by RANKL signaling also increases the release of the high mobility group box (HMGB) 1, another ligand of both TLR-4 and RAGE (Zhou et al., 2008). Pro-inflammatory

cytokines that are downstream targets of TLR-4 and RAGE signaling (e.g. TNF- α , interleukin 1 β or IL-1 β , and IL-6) have been shown to stimulate the production of RANKL and increase osteoclastogenesis (Roggia et al., 2001). Moreover, TNF- α has been shown to reduce bone formation by inhibiting the maturation of pre-osteoblast cells (Gilbert et al., 2000), decreasing osteoblast activity (Bu et al., 2008) and stimulating osteoblast apoptosis (Jilka, 1998). Due to the regulatory effects of these cytokines on bone turnover, the inflammatory state that occurs with T2DM has the potential to negatively impact bone metabolism, which could ultimately contribute to an increase in fracture.

Aside from AGE/RAGE signaling, increased AGEs observed in T2DM may also be incorporated into the protein matrix of the skeleton, resulting in compromised bone quality. Cross-linking of collagen in bone tissue is catalyzed by the enzyme lysyl oxidase (Lox), leading to the formation of aldehydes from lysine residues in collagen and elastin precursors, assembling the protein matrix for bone mineralization (Robins et al., 1972). The incorporation of AGEs into the mineralized matrix involved in collagen cross-linking has the ability to incorporate AGEs and can directly affect bone fragility (i.e., strength, stiffness, and toughness) (Vashishth, 2007). The increased potential for AGEs to be incorporated into collagen cross-links of bone with increased duration of T2DM could explain the increase in fracture risk, despite the maintenance or increase in BMD.

Another potential cellular process that could contribute to the dysregulation of bone metabolism during the initiation and progression of T2DM is autophagy. Autophagy, a process that is controlled by proteins downstream of the insulin receptor and involved in glucose (energy) sensing, can effectively influence cell survival or cell death by means of organelle recycling (Bursch et al., 2008). Increased circulating insulin observed relatively

early in the development of T2DM could lead to the over-activation of the insulin signaling pathway and promotion of osteoblast maturation and mineralization. Conversely, when serum insulin decreases as in the case of attenuated pancreatic β -cell production, the osteoblast's growth and proliferation could decline as a result of autophagy, resulting in a decrease in bone formation that could lead to reduced bone mass and increased incidence of fracture. Understanding how impaired insulin signaling and altered glucose homeostasis influence autophagy in osteoblasts and osteoclasts may provide novel insights into the alterations in skeletal metabolism that are occurring over time in patients with T2DM. Moreover, the lack of information describing the mechanism by which osteoblasts and osteoclasts transport glucose, and the role of insulin and glucose availability in the function of these cells needs to be investigated in both cell types.

The *purpose* of this project is to: 1) determine the alterations in bone metabolism and their effects on bone microarchitectural and biomechanical properties during the development and progression of T2DM in a young, growing animal; 2) determine the role of TLR-4 in this skeletal response; and (3) explore the extent to which the autophagic pathway in bone cells is altered in response to impaired insulin signaling and glucose availability. We hypothesize that 1) the young growing C57BL/6 mice will exhibit compromised bone mass, structure and quality with increasing time on the high fat diet compared to their C3H/HeJ counterparts; and 2) autophagy associated with the metabolic changes occurring in T2DM will contribute to the dysregulation of skeletal metabolism, resulting in deterioration of bone quality. A series of *in vitro* and *in vivo* experiments have been designed that to test these hypotheses. The *in vivo* experiments will utilize rapidly growing, male C57BL/6 and C3H/HeJ mice fed a high fat (60% kcal from fat) over a 2, 8, and 16 wk time course to track

metabolic alterations occurring in conjunction with the alterations in bone mass, microarchitecture and strength. The second set of experiments will utilize a well-characterized system of pre-osteoblasts (MC3T3-E1 cells, RIKEN) and primary cells that can be differentiated into osteoblasts to further examine the role of TLR-4, and how autophagy is impacting bone cell function in T2DM. To test these hypotheses, the following specific aims have been developed.

Specific Aim 1. To determine the alterations in bone metabolism (i.e., bone formation and bone resorption) that occur at times corresponding to pre-, short, and long term glucose intolerance (i.e., 2, 8 and 16 wks) and the implications of these changes on bone structural and biomechanical properties in C3H/HeJ and C57BL/6 mice consuming a high fat or control diet.

Specific Aim 2. Investigate the role TLR-4 has on the differentiation of osteoclasts and osteoblasts *ex vivo*, and to determine how these alterations contribute to the *in vivo* phenotype.

Specific Aim 3. Investigate glucose transport of osteoblasts using *in vivo* and *in vitro* models.

Specific Aim 4. Determine the extent to which autophagy induced by rapamycin affects osteoblast differentiation and activity using an established cell line.

Specific Aim 5. Determine how indicators of autophagy in bone tissue are altered in diet-induced obese mice over time (2, 8, and 16 weeks) and to compare these changes with the alterations in glucose tolerance, bone density, microarchitecture and strength.

Limitations:

Despite efforts to design scientifically sound experiments to test the hypotheses, limitations do exist.

- 1) The study of the skeletal effects of high fat diet induced obesity and glucose intolerance on bone is a complex issue due to the influences of weight-bearing and insulin in the early stages followed by the effects of inflammation and by-products of hyperglycemia with increasing duration. To address these issues, a time course study was developed to evaluate the alterations in bone metabolism and structure occurring over time.
- 2) While fasting the animals prior to sacrifice allows for optimal assessment of plasma glucose, insulin, leptin, and adiponectin, it may have impaired the ability to determine alterations in intracellular insulin signaling *in vivo*.
- 3) Cell culture systems serve only as a model for the physiological responses that occur *in vivo*. The *in vitro* experiments described used either single cell populations or subsets of cells enriched for stromal and hematopoietic cells. A more realistic

- depiction of the cellular responses would include tissue culture systems that allow cell-to-cell interaction, but such experiments would limit the ability to investigate a specific cell population's response.
- 4) The induction of autophagy with rapamycin serves only as a model and may not mimic all aspects of the cellular response to altered glucose homeostasis and insulin signaling. To address this issue, the mechanism by which autophagy is induced during impaired glucose tolerance *in vivo* and that of the phenotype in the rapamycin-treated osteoblasts was characterized.
 - 5) The mutation in TLR-4 was one of the first genetic variations to be described in the C3H/HeJ mice, however, after beginning Study 1, a genetic variation in the leptin receptor gene (*Lepr*) was also described (REF). While the most classic role of leptin is its action regulating appetite and metabolism, leptin can also regulate the inflammatory response and the skeletal response to mechanical stimulation. The difference in C3H/HeJ's response to leptin in this animal strain is dually noted as it could contribute to the impaired metabolic and skeletal response observed in these mice upon high fat diet feeding. To address this issue, (1) plasma leptin was assessed, and (2) genes involved in TLR-4 signaling were determined to attempt to characterize the modulation of this response.

Each of these limitations was addressed as conclusions were drawn related to the given results. Therefore, there is no foreseeable reason that these issue would prohibit the accomplishment of the specific aims described.

CHAPTER II

LITERATURE REVIEW

Obesity and Type 2 Diabetes Significance and Background

Obesity is a condition of excess adiposity defined as a body mass index (BMI) greater than or equal to 30 kg/m^2 in adults (National Institutes of Health, 1998). In the U.S. a significant increase in the prevalence of obesity has occurred over the past five decades, and current estimates indicate that approximately 35% of adults and 17% of children and adolescents are obese (Ogden et al., 2013). No state has an adult obesity rate lower than 20%, and 12 states located in the southern region of the U.S. reported obesity rates greater than 30% (May et al., 2013; Center for Disease Control and Prevention, 2008). Although obesity has classically been reported in adults, childhood obesity has more than doubled in children, and tripled in adolescents in the past 30 yr (Ogden et al., 2012). While more recent data suggests obesity rates may have reached a plateau, the prevalence rates remain high and continue to negatively affect our nation's health (Ogden et al., 2012; Flegal et al., 2010). One of the most striking health

consequences related to the prevalence of obesity has been the staggering increase in cases of type 2 diabetes (T2DM).

T2DM is the most common form of diabetes in adults and accounts for an estimated 16 million cases (95%) of diabetes in adults in the U.S. (Centers for Disease Prevention and Control, 2011). Among type 2 diabetics, 80-90% are obese and the associated hyperglycemia is primarily due to impaired insulin signaling (Centers for Disease Prevention and Control, 2011). The Center for Disease Control and Prevention (CDC) has projected that the prevalence of T2DM will double or even triple by 2050 to affect 1 in 3 adults if current trends continue (Centers for Disease Prevention and Control, 2011). While T2DM was once considered to be “adult-onset” diabetes, health care providers have been diagnosing children with T2DM with greater frequency (Centers for Disease Control and Prevention, 2013). Children and adolescents diagnosed with T2DM are usually between 10-19 years old, obese, and have a family history of diabetes (Centers for Disease Control and Prevention, 2013). Generating accurate estimates of the prevalence of childhood T2DM has been difficult due to undiagnosed symptoms, a lack of routine monitoring of blood glucose, and the normal changes in glucose tolerance that occur during puberty (Centers for Disease Prevention and Control, 2011; Reinehr, 2013). However, in response to the growing health concerns with T2DM in children, the CDC funded the SEARCH for Diabetes in Youth Study in 2000 to provide a surveillance system for childhood diabetes. The systemic nature of the hyperglycemia associated with T2DM predisposes adults and children to a number of health complications that can negatively impact one’s quality of life.

Direct and indirect medical costs to treat diabetes in the U.S. have been estimated at \$174 billion annually, which includes medical coverage for glucose monitoring supplies, hypoglycemic agents (e.g., thiazolidinediones or TZDs and metformin) and treatment of complications (Centers for Disease Prevention and Control, 2011). Hypoglycemic agents are generally prescribed to adults during the earlier stages of T2DM; but long-term loss of β -cell function can result in a patient becoming dependent on insulin therapy. While these therapeutic agents have improved the overall prognosis for the type 2 diabetic, T2DM is still listed as the seventh leading cause of death in the U.S. (Centers for Disease Prevention and Control, 2011). Cause of death associated with T2DM is attributed to its complications, including micro- and macro vascular diseases and loss of renal function (Berenson, 2012).

Several of the complications (e.g., peripheral vascular disease, retinopathy, nephropathy, impaired wound healing, and neuropathy) are known to result from alterations in connective tissues (Robins et al., 1972; Schmidt et al., 1999; Berenson, 2012). Interest in how the metabolic perturbations in T2DM affect connective tissues led investigators to examine the relationship between T2DM and bone health. Early studies indicated that patients with T2DM were not at increased risk for fracture based on the assessment of bone density (Rishaug et al., 1995; van Daele et al., 1995; Stolk et al., 1996). However, subsequent studies with fracture as the primary outcome variable have challenged these initial findings (Valerio et al., 2012; Schwartz et al., 2001; van Daele et al., 1995; Nicodemus et al., 2001; de Liefde et al., 2005; Janghorbani et al., 2006; Farr et al., 2013; Cole et al., 2012; Goulding et al., 2000).

Clinical Investigation of Fracture Risk Associated with T2DM

One of the earliest studies documenting an impact of diabetes mellitus on the skeletal system was published in 1946, by William Kenney in the Department of Orthopedics at Yale University. Kenney asserted that diabetes mellitus (i.e., T1DM and T2DM) was found in cases of femoral neck fracture more frequently than in cases of intertrochanteric fracture (Kenney, 1946). While this observation focused on fracture as an outcome in patients with diabetes, other reports began to appear in the literature indicating that based on their bone mineral density (BMD), type 2 diabetics were not at increased risk for fracture (Rishaug et al., 1995; van Daele et al., 1995; Stolk et al., 1996). Many of these early reports were limited by the fact that they did not differentiate based on the type of diabetes, tended to have a small sample size, and used BMD as a surrogate indicator of fracture risk (World Health Organization, 2004). The result was a number of published reports with conflicting findings. One of the first large-scale studies published in 1980, on a cohort of residents in Rochester, MN, reported that neither male or female diabetic patients (i.e., both T1DM and T2DM) experienced a greater incidence of fractures (Heath, III et al., 1980). As additional reports began to focus on T1DM or T2DM separately, it became apparent that T1DM was associated with low BMD (i.e., osteopenia), whereas BMD in the type 2 diabetics was typically normal (de Liefde et al., 2005; Melton, III et al., 2008; Nicodemus et al., 2001; van Daele et al., 1995; van Daele et al., 1995). Based on the findings from these early studies, investigators concluded that type 2 diabetics were not at increased risk of fracture.

Continued clinical concerns with fracture incidence among type 2 diabetics caused some investigators involved with large scale osteoporosis studies to begin to

examine the relationship between fracture incidence and T2DM in their cohorts. In 2001, data from the Study of Osteoporotic Fractures (SOF) research group, revealed a relative risk (RR) for fracture in women (≥ 65 years of age) who were not on insulin ($n = 551$) of 1.82 and 1.94 in the hip and proximal humerus, respectively (Schwartz et al., 2001). These authors also reported a RR of 2.66 for fracture of the foot in diabetic patients on insulin ($n = 106$) (Schwartz et al., 2001). Similar to this study, data from the Iowa Women's Health Study showed an increase in fracture risk (1.7-fold) of the hip among postmenopausal women with T2DM compared to woman without diabetes (Nicodemus et al., 2001). The author's also demonstrated that patients in the highest tertile for duration of T2DM (i.e., ≥ 12 yr) had a 2.3-fold increase in fracture risk, and insulin treatment further increased this risk to 2.66 (Nicodemus et al., 2001). These studies were followed by similar reports from the Rotterdam Study and the Nurses' Health Study describing an increase in RR for hip fracture among patients with T2DM of 1.8 and 2.2, respectively (de Liefde et al., 2005; Janghorbani et al., 2006). Interestingly, in 2008 a follow-up report from the Rochester cohort, which originally reported no increase in fracture incidence in patients with T1DM and T2DM, concluded that both men and women with T2DM had a 1.8-fold increase in fractures of the axial skeleton, and that diabetes duration greater than 10 years exacerbated this risk (Melton, III et al., 2008; Heath, III et al., 1980). The discrepancy in these findings compared to their original report was attributed to stricter inclusion/exclusion criteria, more stringent classification of T2DM, distinguishing between T1DM and T2DM, and consideration of diabetes duration as a covariant.

The results of these studies demonstrate that BMD underestimates fracture incidence in patients with T2DM and have brought into question the relevance of BMD as a screening tool for fracture risk in some populations. Schwartz *et al.* collected data from 3 large prospective studies (e.g., SOF, Osteoporotic Fractures in Men Study, and Health, Aging, and Body Composition study) and demonstrated that femoral neck BMD and the World Health Organization Fracture Risk Algorithm (FRAX) underestimate fracture risk in older adults with T2DM (Schwartz *et al.*, 2011). However, the development of reference point indentation (RPI) testing has provided a means by which scientists can test the biomechanical properties of bone and evaluate bone “quality” *in vivo*. Biomechanical testing allows for the measurement of a parameter directly associated with bone strength and fracture. Although reference point indentation is not yet approved for routine clinical use, recently, an elegant study by Farr *et al.*, (Farr *et al.*, 2013) showed that bone material strength (BMS) is compromised in patients with T2DM. This study provides further evidence that the skeleton is an important target tissue that is adversely affected by T2DM, and that the current, clinical assessments (i.e., DXA and FRAX) are likely inadequate at predicting fracture in patients with T2DM.

Information related to complications fracture risk among young children who are type 2 diabetics is more scarce than the data available on the adult population. Similar to observations among overweight and obese adults, studies reporting DXA results suggest that obese children have a higher BMD compared to non-obese children (Klein *et al.*, 1998; Leonard *et al.*, 2004). However, when bone mass is expressed relative to bone size and body weight, this is not the case (Goulding *et al.*, 2000). Childhood obesity has also been shown to be associated with a modest increase in risk for fractures (Valerio *et al.*,

2012; Kim et al., 2013b; Kessler et al., 2013; Adams et al., 2013). For example, obesity increased fracture incidence of the upper and lower limbs in girls, and increased fracture incidence of the lower limbs in boys (Valerio et al., 2012). Moreover, increased BMI (i.e., overweight, moderately obese, and extremely obese categories) has been associated with increased odds ratio of foot, ankle, leg, and knee fractures among children (Kessler et al., 2013). Compromised bone mass accrual during these critical years of skeletal growth not only predispose overweight children to fractures during childhood and adolescence, but also increase osteoporosis risk throughout the course of their lifetime (National Institutes of Health, 2000; Goulding et al., 2005).

To begin to unravel the phenomenon of increased skeletal fragility in T2DM, it is imperative that the alterations in bone metabolism be investigated during the initiation and progression of glucose intolerance. Contributing factors (e.g., inflammation, glucose availability/transport, and insulin signaling) have been hypothesized to play pivotal roles in the pathogenesis of T2DM and have the potential to alter bone metabolism. Due to the prevalence of T2DM, taken together with the devastating consequences associated with fracture in this population, continued research is needed to identify the mechanisms involved, so that appropriate prevention and therapeutic strategies can be developed.

Rodent Models of T2DM and its Impact on Bone

Complications associated with T2DM often require decades to develop. Therefore, animal models provide important tools for studying the molecular aspects and pathological effects of obesity-induced changes in glucose homeostasis and progression

to severe glucose intolerance. In 1949, Ingle (INGLE, 1949) was the first to report on an obesity model in which rats were fed diet *ad libitum* and their physical activity was restricted. Since then, there have been many studies aimed at characterizing the metabolic responses of rodent models exposed to high fat diets. The C57BL/6 mouse fed a high fat is a particularly good model because it mimics many of the metabolic alterations observed with obesity and T2DM in humans, including hyperinsulinemia, hyperglycemia, and hypertension (Collins et al., 2004).

In addition to the metabolic and cardiovascular changes, mouse models have shown that a compromise in bone structure, biomechanics, and metabolism occurs with obesity and T2DM. Parhami *et al.* (Parhami et al., 2001) reported that an atherogenic high fat diet (i.e., 1.25% cholesterol, 15.8% fat, and 0.5% cholate) fed for 4 and 7 mo to C57BL/6 mice resulted in decreased bone mineral content and density. Patsch and colleagues (Patsch et al., 2011) showed that a high fat diet (i.e., 60% lipid) fed to C57BL/6 mice for short and long term (i.e., 3 or 24 wk) periods decreased BMD and attributed this response to increased bone resorption or an increase in serum cross-linked telopeptides of type I collagen (CTX). Moreover, a high fat diet (i.e., 60% kcal from fat) administered for 16 wk to young (3 wk) and aged (15 wk) C57BL/6 mice resulted in compromised biomechanical properties (e.g., lower bone strength, stiffness, and toughness) (Ionova-Martin et al., 2011). More recently, Lu *et al.* (Lu et al., 2013) presented data showing that a high fat diet also impacts bone acquisition in young male mice. The authors reported that a high fat diet (i.e., 45% total calories from fat) fed for 8 wk to 17 day old male C57BL mice resulted in lower bone mineral content that was attributed to decreased osteoblast differentiation (i.e., as evidenced by a reduction in β -

catenin and *Runx2* mRNA) and reduced colony-forming osteoblasts (CFU-Ob) (Lu et al., 2013). These studies provide important evidence that mouse models of high fat diet-induced obesity are invaluable tools for studying mechanistic alterations occurring in bone metabolism during glucose intolerance.

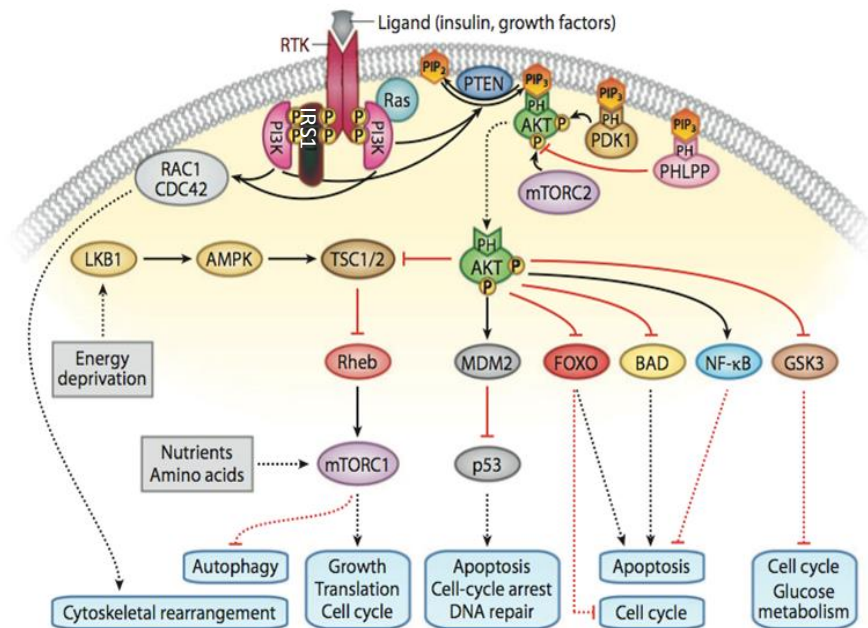
Glucose Homeostasis and Insulin Signaling

As described previously, T2DM is a condition in which hyperglycemia occurs due to diminished ability for insulin to stimulate cellular glucose uptake. Under normal conditions, blood glucose is controlled by an efficient homeostatic mechanism that is dependent on various hormonal responses including cortisol, sex hormones, and insulin (Hedeskov, 1980). Of these hormones, insulin is considered to be the primary regulator of blood glucose by enhancing peripheral glucose uptake and down-regulating hepatic glucose liberation (WINEGRAD et al., 1958; Exton et al., 1973). Insulin is secreted from pancreatic β -cells into the circulation when blood glucose reaches a threshold concentration of 4 mM (Ashcroft, 1976). Insulin secretion has been described as a “square wave pulse” pattern, which ensures insulin is secreted in a biphasic manner (Curry et al., 1968; Grodsky et al., 1968). The first or rapid phase, typically lasts from 1-8 min, with a spike occurring after approximately 4 min (Grodsky et al., 1969). This is followed by second, prolonged phase, that has been compared to a large compartment of stored insulin being released at a much slower rate and lasts from ~8-30 min postprandial (Grodsky et al., 1969). Circulating insulin interacts with cells that express its membrane-bound receptor (IR) to regulate many cellular processes, including glucose transport and

metabolism, protein translation, cell cycle, as well as autophagy and apoptosis (**Figure 1**) (Chalhoub et al., 2009). Although profound changes occur in β -cell function, number, and insulin secretion, it is widely accepted that the initiation of T2DM results from peripheral insulin resistance.

Under normal circumstances, insulin binds to its receptor tyrosine kinase (RTK) and a conformational change occurs that allows for activation or autophosphorylation of the receptor. These activated tyrosine residues are then recognized by the docking

Figure 1.



Chalhoub and Baker, 2009

Figure 1: Activated receptor tyrosine kinases (RTKs) recruit and activate PI3K, leading to increased phosphatidylinositol-3,4,5-trisphosphate (PIP₃) levels. PIP₃ recruits many proteins to the membrane by binding to their pleckstrin homology (PH) domains, including the serine/threonine kinases AKT, 3-phosphoinositide-dependent kinase (PDK1), and the phosphatase PH domain and leucine rich repeat protein phosphatase (PHLPP). Membrane-bound AKT is rendered fully active through its phosphorylation by PDK1 and the rapamycin-insensitive mammalian target of rapamycin (mTOR) complex (mTORC2), and it is inactivated when dephosphorylated by PHLPP. Activated AKT may phosphorylate a range of substrates, thereby activating or inhibiting these targets and resulting in cellular growth, survival, and proliferation through various mechanisms. Abbreviations: AMPK, protein, insulin receptor substrate (IRS) via their phosphotyrosine binding domain (PTB)

(Avruch, 1998) (**Figure 1**). With IRS1 located at the plasma membrane, docked on the cytoplasmic portion of IR, it may be phosphorylated at multiple tyrosine residues. Next, phosphatidylinositol 3 kinase (PI3K) is recruited to IRS1 via the Src homology 2 (SH2) domain, and phosphorylates phosphatidylinositol 4, 5-bisphosphate (PIP₂) at the 3' position, yielding phosphatidylinositol 3, 4, 5-triphosphate (PIP₃). Akt (or protein kinase B) is then phosphorylated at Thr308 and Ser473 by 3-phosphoinositide dependent protein kinase (PDK) and mechanistic target of rapamycin complex 2 (mTORC2), respectively. Activated Akt then translocates from the plasma membrane to the cytosol where it acts to regulate many cellular processes via multiple protein targets (Chalhoub et al., 2009). It is this signaling cascade that has been proposed to be attenuated in some capacity in T2DM, affecting multiple cellular responses such as the translocation of insulin-sensitive glucose transporters (i.e., GLUT4) from cytoplasmic vesicles to the plasma membrane, resulting in the inability of glucose uptake by skeletal muscle and adipose tissue. It has been speculated that the impaired insulin signaling that occurs with T2DM is due to defects in the IR docking protein, IRS (Copps et al., 2012). For example, the systemic knockout of IRS1 and IRS2 results in insulin resistance and impaired glucose tolerance (Araki et al., 1994; Abe et al., 1998; Burks et al., 2000; Previs et al., 2000). However, the newer paradigm that IR has the potential to act as a nuclear transcription factor may provide further insights into the molecular mechanisms responsible for T2DM (Sarfstien et al., 2013). Factors that have been proposed to contribute to the development of insulin resistance include changes in fatty acid uptake and lipogenesis, alterations in adipocytokines (e.g., leptin, resistin, and adiponectin), and systemic chronic, low grade inflammation.

Inflammation Induced via TLR-4 and its Impact on Insulin Signaling

Clues as to a relationship between inflammation and diabetes have existed since 1876 when the non-steroidal anti-inflammatory drug (NSAID), sodium salicylate, was shown to diminish sugar excretion (Ebstein, 1876). This connection between diabetes and inflammation was further demonstrated in 1957 when Reid and colleagues (REID et al., 1957) reported an insulin-dependent diabetic patient treated with a high dose of aspirin for rheumatic fever, no longer needed daily insulin injections. More recently, mechanistic studies have described how activation of some inflammatory pathways, especially toll-like receptor-4 or TLR-4, can impact insulin signaling (Shi et al., 2006). Toll receptors were first described in *Drosophila* and shown to exhibit a means for the host to detect invasions by microorganisms (Lemaitre et al., 1996). Currently, 13 mammalian homologues of the receptor have been identified (i.e., TLR1-TLR13) all of which have specific immunological responses belonging to the family of pattern recognition receptors (PRR) (Tilich et al., 2011).

Medzhitov and *et al.* (Medzhitov et al., 1997) was the first to show that a Toll receptor, now termed TLR-4, was able induce the expression of genes involved in inflammatory responses. TLR-4 is a transmembrane protein containing repeated leucine-rich motifs in its extracellular portion and a cytoplasmic domain that is homologous to the signaling domain of the IL-1 receptor. Known ligands for TLR-4 include LPS found in the wall of gram negative bacteria, heat shock protein (HSP) 60 and 70, hyaluronic acid, oxidized low density lipoprotein (LDL), fibrinogen, amyloid protein, fetuin A

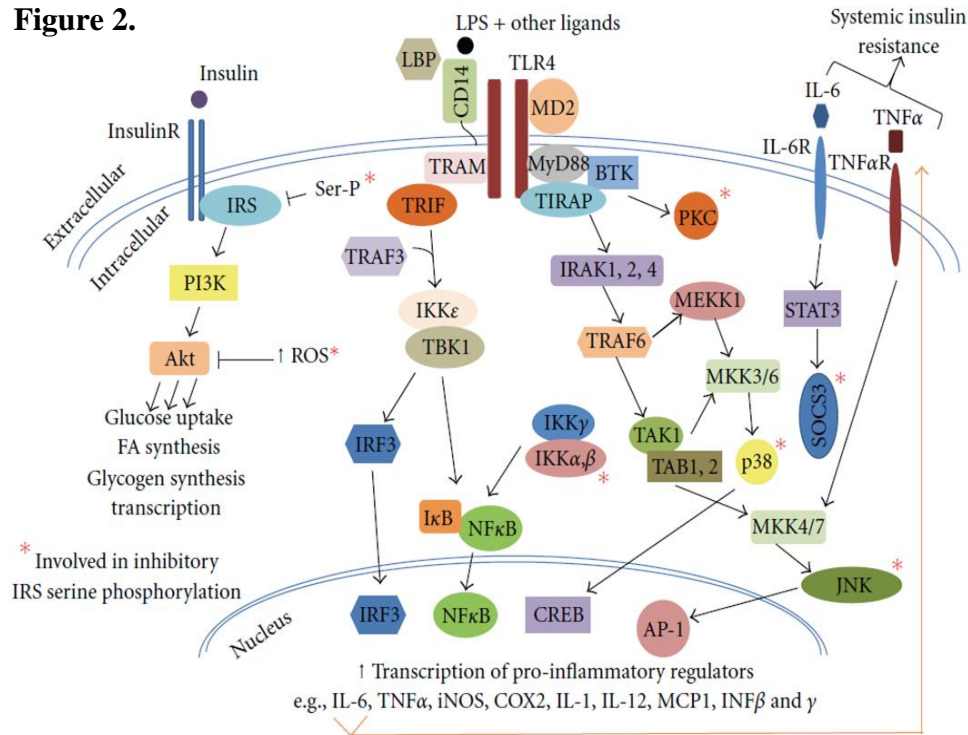
(FetA)-bound saturated free fatty acids (sFFA), and some glycoproteins located on viral envelopes (Pal et al., 2012; Tilich et al., 2011). Interestingly, in T2DM and obesity, TLR-4 and two of its ligands, LPS and sFFA, are up-regulated, leading to increased levels of both tissue specific and circulating pro-inflammatory cytokines (e.g., TNF- α , IL-1 β , and IL-6) (Dasu et al., 2012; Pal et al., 2012; Lee et al., 2001; Schaeffler et al., 2009; Reyna et al., 2008; Medvedev et al., 2007).

Stimulation of TLR-4 by both LPS and sFFA leads to the activation of MyD88 dependent and/or MyD88 independent (i.e., TIR domain-containing adaptor inducing IFN- β or TRIF dependent) pathway. For example, LPS circulates bound to LPS binding protein (LBP) and interacts with the anchored protein, CD14 (cluster of differentiation 14), which facilitates the transfer LPS to the TLR-4/MD2 complex (**Figure 2**) (Kim et al., 2010). While genetic models confirm that TLR-4 is essential for LPS-induced immune response, it is not clear if LPS directly binds to TLR-4. Understanding how these signaling pathways function normally versus during the initiation and progression of T2DM could provide mechanistic explanations related to impaired insulin sensitivity and may lead to novel therapeutic interventions.

As shown in Figure 2, once LPS is bound to the TLR-4/MD2 complex, MyD88 dependent or MyD88 independent signaling cascades can be elicited. Upon ligand binding, TLR-4, MyD88, along with the toll/interleukin-1 receptor (TIR) adaptor protein, TIRAP or MAL (MyD88-adaptor-like) recruit IL-1 receptor-associated kinase (IRAK)

through the interaction of death domains (Takeda et al., 2007). Activated IRAK1

Figure 2.



Kim and Sears, 2010

Figure 2. Schematic of TLR-4 signaling cascades. The My88 dependent pathway is responsible for the up-regulation of many pro-inflammatory cytokines including IL-6, IL-1 β , and TNF- α , whereas the MyD88 independent pathway, sometimes referred to as the TIR domain-containing adaptor inducing IFN- β (TRIF) pathway, activates the transcription factor interferon regulatory factor (IRF) 3. Upon stimulation, MyD88, along with the adaptor protein TIRAP or MAL (TIR domain-containing adaptor protein or MyD88-adaptor-like) recruit IL-1 receptor-associated kinase (IRAK) through the interaction of death domains between both proteins. TGF- β -activated kinase 1 (TAK1), and TAK1 binding proteins, TAB1 and TAB2, form a large cytoplasmic complex that phosphorylates the IKK (IKK α , IKK β , and NEMO/IKK γ) and MAP kinases such as JNK. In contrast to the MyD88 pathway, the TRIF dependent pathway is responsible for regulating type 1 interferons, which modulate the innate immune response. Upon activation, TRIF acts on two different proteins, receptor-interacting protein 1 (RIP1) and TRAF3. Unique to this pathway is the recruitment of TRAF3 by TRIF and the association of TRAF3 with TRAF family member-associated NF- κ B activator (TANK), TANK binding kinase 1 (TBK1), and Ikki. It is through this pro-inflammatory/TLR-4 signaling cascade that the insulin signaling pathway may be impaired due to NF- κ B and JNK activation.

phosphorylates TNF receptor-associated factor 6 (TRAF6) forming a large, cytoplasmic complex with TGF- β -activated kinase 1 (TAK1), and TAK1 binding proteins, which in

turn, activates a heterodimeric complex composed of I κ Bs kinases (i.e., I κ ka, I κ kb, and NEMO/IKK γ). This IKK complex primes I κ B for proteasomal degradation, allowing for the dissociation and translocation of NF- κ B to the nucleus where it can function as a transcription factor, up-regulating many pro-inflammatory genes (e.g., TNF α , IL-1 β , and IL-6) that are critical for the innate immune response elicited by TLR-4. In contrast to the MyD88 pathway, the MyD88 independent pathway or TIR domain-containing adaptor inducing IFN- β (TRIF) dependent pathway is responsible for regulating type 1 interferons. Unique to this pathway is the recruitment of TRAF3 by TRIF and the association with TRAF family member-associated NF- κ B activator. This complex is important for the dimerization and translocation of IRF3 to the nucleus, where it can regulate transcriptional targets (e.g., *Cxcl10* and *Ifit1*) central to the function and role of TLR-4 modulating of the immune system. While these TLR-4 signaling cascades are critical for the immune system to respond to foreign microorganisms, chronic or unwarranted activation of this pathway may lead to adverse side effects, including alterations in insulin response.

Both of the pathways downstream of TLR-4, MyD88-dependent and MyD88-independent, can result in phosphorylation of IRS1 at Ser307 as opposed to tyrosine residues (Kim et al., 2010). This alternative phosphorylation leads to the attenuation of IRS function and the corresponding signaling cascade, ultimately impairing the activation of downstream targets (e.g., Akt, GLUT-4, and mTORC1) (Kim et al., 2010). Moreover, two specific inflammatory signal cascades stimulated via TLR-4, NF- κ B and c-Jun NH(2)-terminal protein kinases (JNK), have also been shown to be activated with increased adiposity and have been implicated in insulin resistance (Tilich et al., 2011).

For example, when NF- κ B is activated as a result of TLR-4 stimulation, a subunit of the IKK complex (i.e., IKK β) has been shown to phosphorylate IRS1 at serine 307.

Moreover, TLR-4 signaling can also increase the activation of the serine-threonine kinase, JNK, and similar to NF- κ B, results in the alternative phosphorylation of IRS1 (Ser307). In addition to these two mechanisms through which TLR-4 activation alters IRS1 phosphorylation, suppressor of cytokines (Socs) 1 and 3 can ubiquitinate IRS1, resulting in its degradation, and thereby attenuating the insulin signaling pathway. Thus, in addition to the classic innate immune response, stimulation of TLR-4 can also result in the attenuation of the insulin signaling cascade, thereby contributing to the onset of glucose intolerance.

TLR-4 Signaling Involved in T2DM: Lessons from Animals Models

Animal models have provided direct evidence linking various metabolic alterations associated with T2DM to TLR-4. In 1968, Sultzter showed that the inbred mouse strain, C3H/HeJ, was immune to a lethal challenge of LPS *in vivo* (Sultzter, 1968). Upon further investigation and genotyping it was determined that C3H/HeJ mice have a naturally occurring point mutation (P712H) in the cytoplasmic TIR domain of TLR-4, which attenuates the downstream signaling cascade (Medvedev et al., 2007; Piao et al., 2008). While the C3H/HeJ and TLR-4 knockout (*Tlr4*^{-/-}) models have classically been valuable tools for immunological and microbial research, recent studies have demonstrated an altered metabolic response to a high fat diet in this strain (Poggi et al., 2007; Shi et al., 2006; Tsukumo et al., 2007). Poggi *et al.* (Poggi et al., 2007) provided

the first evidence that the C3H/HeJ mice were protected from a high fat diet induced insulin resistance. This study compared the C3H/HeJ mice to their control, C3H/HeOuJ mice, which have a functional TLR-4, on a high fat diet (i.e., 42 or 35% kcal fat) (Poggi et al., 2007). The study showed that the C3H/HeJ mice on a high fat diet had lower serum insulin and higher glucose utilization rate after 22 weeks compared to C3H/HeOuJ. Interestingly, in this same study mRNA from epididymal and adipose tissue revealed that the C3H/HeJ mice had lower TNF- α and IL-1 β expression compared to controls (Poggi et al., 2007). Histological evaluation also showed that the C3H/HeJ mice were protected from non-alcoholic fatty liver disease (NAFLD). A subsequent study showed that the C3H/HeJ mice on a high fat diet (i.e., 55% kcal from fat) were protected from decreased activation of the IR and IRS in white adipose tissue and skeletal muscle, two proteins that are critical for proper insulin signaling (Tsukumo et al., 2007). Moreover, Davis *et al.* (Davis et al., 2008) showed that C57BL/10ScN mice with a deletion of TLR-4 are completely protected from diet-induced obesity by a saturated fatty acid diet vs. a high unsaturated fat diet. These studies present convincing evidence that mice, with a non-functional or deleted TLR-4, are protected from many of the metabolic changes classically induced by a high fat diet.

Bone Metabolism and Turnover

Bone tissue is continually remodeled throughout life and this process maintains the integrity and function of the skeleton. Bone metabolism is a tightly coupled process primarily involving bone resorbing cells or osteoclasts, and bone forming cells or

osteoblasts. The osteoblast-derived, mechanosensing osteocyte has been described as playing a role in this process, however, far less is known about these cells (Lanyon, 1993). Osteoclasts are members of the monocytic-macrophage family, derived from hematopoietic stem cells (HSC). Differentiation of osteoclasts is initiated by the activation of receptor activator for NF- κ B (RANK), a membrane-bound homotrimeric protein from the TNF receptor family. RANK's ligand, RANKL, can be detected circulating in a secreted form from activated T-cells as well as expressed on the membrane on osteoblasts. Similar to the MyD88 dependent- TLR-4 pathway, activation of RANK recruits TRAF6 to form a complex, which induces the translocation of NF- κ B to the nucleus. Activated, nuclear NF- κ B up-regulates a component of the dimeric transcription factor activator protein-1 (AP-1), known as c-Fos, which then interacts with nuclear factor of activated T-cells (NFAT)-c1. This activation leads to the induction of various osteoclast-related genes including, *Hmgb1*, tartrate resistant acid phosphatase (TRAP or *Acp5*), Fos-related antigen 1 (*Fra1* or *Fosl1*), and cathepsin K (*CTSK* or *Ctsk*). The induction of osteoclastogenesis results in mature, multinucleated, TRAP positive cells that have a ruffled border, due to actin reorganization. The mature osteoclast can then form a sealing zone with the bone, often through integrins. For example, the $\alpha\beta3$ integrin recognizes the arginine-glycine-aspartate (RGD) amino acid motif of osteopontin (OPN encoded by the *Spp1* gene) and bone sialoprotein (BSP encoded by the *Ibsp* gene), whereas the $\beta1$ family integrins recognize collagen and fibronectin. When the osteoclast attaches to the surface of the bone, it creates an acidic microenvironment by an electrogenic proton pump and a chloride channel, reducing the pH to ~ 4.5 . This acidic milieu mobilizes the mineralized component, where calcium and phosphorus are

endocytosed and released into the extracellular fluid (ECF). Cathepsin K then degrades type 1 collagen and TRAP acts to hydrolyze OPN and BSP, which in turn releases the osteoclast from the bone. The process of resorption is estimated to take approximately 3 weeks in humans and approximately 7 days in mice.

In contrast to osteoclasts, osteoblasts are derived from mesenchymal stem cells (MSC) by initially signaling through the Indian hedgehog (Ihh) pathway, which commits the cells to an osteoblast lineage. Runt-related transcription factor 2 (Runx2 or *Cbfa1*) and osterix (or *Sp7*), along with Wnt/ β -catenin signaling, act to differentiate these progenitor cells to osteoblast precursors and bone-secreting osteoblasts. Bone morphogenic proteins (BMPs) belong to the transforming growth factor (TGF) β superfamily and were first identified as the active component in bone extracts that could induce ectopic calcification. BMP-2,-4,-5,-6, and -7 all have strong osteogenic capacity. Early markers of osteoblast differentiation include alkaline phosphatase (ALP), BSP, and collagen type 1 alpha 1 (Col1a1), whereas parathyroid hormone/PTH-related peptide (PTH/PTHrP) and osteocalcin (OCN encoded by the *Bglap* gene) are considered markers of mature osteoblasts (Chatakun et al., 2014). Another protein important for osteoblastogenesis is OPN, which peaks during differentiation and then again at later stages of osteoblast maturation. While OPN has been shown to be important for many cellular responses (e.g., apoptosis, autophagy, and the immune response), in bone it is critical for the regulation of matrix mineralization. Mature osteoblasts lay down the matrix portion of bone that will become mineralized with the aid of ALP, acting to hydrolyze inhibitors of mineral deposition (i.e., pyrophosphates) and BSP, which initiates mineralization. The mineralized portion of bone or the osteoid is composed of

hydroxyapatite, $\text{Ca}_{10}(\text{PO}_4)_6(\text{OH})_2$, and this mineralization process has been shown to be halted by OCN as the osteoblast becomes entombed by calcified bone matrix. Mature osteoblasts also regulate osteoclastogenesis through their expression of RANKL, and their secretion of osteoprotegerin (OPG), a receptor decoy for RANKL. Although the mechanisms are not fully understood, the osteoblast has been shown to have three potential fates; (1) become a bone lining cell, (2) undergo apoptosis, or (3) become an embedded osteocyte (Nakashima et al., 2003).

Osteocytes are regularly dispersed throughout the mineralized matrix and make up about 90-95% of bone cells in the adult skeleton. The cell body is encased in a lacuna while the dendritic processes extend in to the bone through tiny canals called canaliculi. This unique niche of mineralized matrix along with the complex morphology of the osteocyte, make it a difficult cell to study, and many of their functions have remained elusive. Recent advances in the field, however, have shown that one of the functions of the osteocyte is to act as a sensory cell mediating the effects of mechanical loading (Lanyon, 1993; Lanyon, 1992). For example, a novel protein secreted by osteocytes, sclerostin (*Sost1*), responds to load-bearing by decreasing *Sost1* production, resulting in an increase in BMD (Li et al., 2005). Likewise, in the absence of load-bearing activity (e.g., bed rest and microgravity), sclerostin exerts its effect by binding to low density lipoprotein receptor-related protein (LRP) 5/6 and attenuating the Wnt/ β -catenin pathway (Li et al., 2005). In fact, results from a multicenter phase II clinical trial demonstrated that the sclerostin monoclonal antibody, Romosozumab (Amgen, Thousand Oaks, CA) increases BMD and bone formation, and reduces bone resorption in postmenopausal women (McClung et al., 2014). In addition to their function as sensory cells, osteocyte

cell death, triggered by trauma or apoptosis, has been shown to act as a stimulus for osteoclast migration and resorption (Emerton et al., 2010). These orchestrated signals between osteoclasts, osteoblasts, and osteocytes that contribute to the maintenance of a healthy skeleton. Therefore, the uncoupling of these processes due to inflammation or altered glucose homeostasis may contribute to the pathophysiology of increased fracture risk.

Inflammation and TLR-4's Impact on Bone Metabolism

Recent evidence has provided insights into the connection between skeletal metabolism and the immune response, termed “osteimmunology”. For instance, it is established that post-menopausal women experience an uncoupling of bone turnover, resulting in accelerated bone resorption and increased risk of osteoporotic-related fracture (Manolagas et al., 2010). In conjunction with bone loss, post-menopausal women have been shown to have high circulating pro-inflammatory cytokines (e.g., TNF- α , IL-1 β , IL-6), demonstrating that estrogen has anti-inflammatory characteristics (Pacifci et al., 1989; Abrahamsen et al., 2000; Scheidt-Nave et al., 2001; Pfeilschifter, 2003). Further evidence of the regulation of bone turnover by the immune response is evidenced by the fact that bone loss and fracture are complications associated with rheumatoid arthritis (RA), chronic obstructive pulmonary disease (COPD), periodontal disease, human immunodeficiency virus (HIV), and systemic lupus erythematosus (SLE) (Agusti et al., 2008; Grassi et al., 1998; Anastos et al., 2007; Almedhed et al., 2007; Geurs, 2007). These clinical observations provided some of the early evidence that bone turnover was

regulated by the immune response, and the subsequent inflammation. Confounding factors such as the use of corticosteroids, which are known to be detrimental to bone, made it difficult to determine if bone loss was a result of the disease pathology or side-effects of treatment. However, the development of rodent models and *in vitro* studies with osteoclasts and osteoblasts have provided insights into the regulation of bone metabolism by inflammatory mediators including those inflammatory mediators induced by TLR-4 activation.

The osteoclast is essentially a specialized macrophage, derived from cells of the monocytic lineage and as such, is inherently regulated by the immune response. Stimulation of the MyD88 dependent pathway through TLR-4 interaction recruits TRAF6, which in turn potentiates osteoclastogenesis by NFATc1 translocation to the nucleus (Mabilleau et al., 2011; Lamothe et al., 2007). Activation of the NF- κ B pathway has also been shown to be essential for RANK-mediated osteoclast differentiation (Ogasawara et al., 2004). Furthermore, TAK1 deficient monocytes do not differentiate into osteoclasts in the presence of RANKL, demonstrating that TAK1 activation via TLR-4 signaling is indispensable for RANKL-stimulated osteoclastogenesis (Lamothe et al., 2013). Not only do the various intracellular pathways activated by TLR-4 signaling alter osteoclast function, subsequent cytokines produced downstream of TLR-4 also impact osteoclastogenesis. For example, it has been demonstrated that TNF- α up-regulates RANKL, increasing osteoclast differentiation and number, as well as enhancing osteoclast activity (Zou et al., 2002; Wei et al., 2005). Moreover, Wei *et al* (Wei et al., 2005) established that IL-1 β is a potent stimulator of bone resorption, and exerts this effect by enhancing stromal cell expression of RANKL. Furthermore, the development

of a novel rodent model of chronic, systemic inflammation supported these mechanistic, *in vitro* studies by demonstrating that a low dose LPS pellet was able to induce bone loss in conjunction with the up-regulation of IL-1 β and TNF- α in the bone (Smith et al., 2006). These data demonstrate that the activation of TLR-4 and the downstream signaling pathways contribute to altered bone turnover by increasing osteoclast differentiation and activity.

In addition to osteoclasts, osteoblasts have also been shown to constitutively express TLR-4 and be responsive to TLR-4 ligands, as well as cytokines produced from this activation. Previous *in vitro* and *in vivo* studies have shown that LPS suppresses the transcription of *Cbfa2* and *Sp7* as well as activating transcription factor 4 (*Atf4*), thereby down-regulating osteoblast differentiation (Bandow et al., 2010). It has been proposed that the mechanism involves TLR-4 signaling, as *Myd88*^{-/-} primary osteoblasts do not appear to respond to LPS stimulation (Bandow et al., 2010). LPS has also been shown to stimulate osteoblast apoptosis by increasing caspase 3 (*Casp3*) mRNA and protein abundance in MC3T3-E1 cells (Guo et al., 2013). Moreover, TNF- α has also been shown to decrease osteoblast differentiation via means downstream of insulin-like growth factor (IGF-1) and BMPs (Gilbert et al., 2000). Collectively, these studies indicate that TLR-4 stimulation leads to decreased osteoblast differentiation and mineralization, as well as increased apoptosis, resulting in impaired bone formation.

Various animal models have also supported the role TLR-4 plays on regulating bone metabolism *in vivo*, impacting bone structure, microarchitecture, and biomechanics. For example, in 1996 Beamer *et. al* (Beamer et al., 1996) reported that the C3H/HeJ mice have higher bone density of the femur, vertebra, and the proximal phalanges compared to

all other strains examined (i.e., AKR.J, BALB/cByJ, C57BL/6J, C57L/J, DBA/2J, NZB/B1NJ, SM/J, SJL/BmJ, SWR/BmJ, and 129/J) (Beamer et al., 1996). This elevated BMD was explained by the fact that the C3H/HeJ mice have fewer osteoclast precursor cells compared to C57BL/6J and A/J mice (Gerstenfeld et al., 2010). The C3H/HeJ mice demonstrated an attenuated response to LPS-induced bone resorption compared to control, C3H/HeN mice (Nakamura et al., 2008). Furthermore, it has been shown that C3H/HeJ mice have a higher bone formation rate, increased osteoblast activity, and lower apoptosis of osteoblasts compared to C57BL/6J mice (Linkhart et al., 1999; Sheng et al., 2002; Sheng et al., 2004; Sheng et al., 2006). Not only do these animals exhibit a high BMD, 3-pt bending revealed that the C3H/HeJ mice have improved biomechanical properties (e.g., ultimate force, yield force, and stiffness) when compared with C57BL/6 (Schriefer et al., 2005). Additionally, Johnson and colleagues (Johnson et al., 2004) demonstrated that mice harboring mutations in TLR-4 (i.e., C57Bl/10SnJ and C3H/HeJ) or in its co-receptor, CD14 (i.e., B6.129S-Cd14^{tm1Fmm}), exhibit a high BMC, BMA, and BMD. Collectively, these results provide evidence that TLR-4 mediated signaling has an integral role in bone metabolism.

Implications of RAGE Signaling and Accumulation of AGE's on Bone Strength

Cross-talk has been shown to occur between the downstream signaling cascades initiated by TLR-4 and another well-characterized PRR, the receptor of advanced glycation end-products (RAGE). Similar to TLR-4, RAGE interacts with many damage-associated molecular pattern (DAMP) molecules including advanced glycation end-products (AGEs), S-100s, HMGB1, β -amyloid, and adhesion molecules (Mac-1 and

ICAM1), all of which have been demonstrated to be up-regulated during T2DM (Gonzalez et al., 2013). In addition to the similarity in ligands, the downstream inflammatory response resembles that of TLR-4 response in bone, as well. For example, the RAGE ligand, HMGB1, has been shown to be essential for RANKL-induced terminal differentiation of osteoclasts (Zhou et al., 2008). Conversely osteoblast proliferation, differentiation, and mineralization are inhibited when cultured with AGEs (Ogawa et al., 2007; Cortizo et al., 2003). Consistent with these *in vitro* studies, *Rage*^{-/-} mice demonstrate elevated bone mass along with decreased osteoclast number compared to wild type controls (Zhou et al., 2006). The convergence of the TLR-4 and RAGE signaling cascades and their known effects on bone metabolism under normal conditions raises the question as to pathway's contribution to the bone phenotype in T2DM.

The primary ligands for RAGE are AGEs, and have been shown to be elevated during T2DM through a series of dehydrogenation and oxidation reactions. While all proteins are prone to AGE formation, deleterious AGE accumulation occurs in tissues with lower turnover, such as bone. Collagen is the most abundant protein in bone and is susceptible to glycation at arginine and lysine residues, forming the AGE pentosidine. Diabetic rats have been shown to exhibit increased bone pentosidine, in conjunction with a decrease in bone strength (Saito et al., 2006). Ionova-Martin *et. al* (Ionova-Martin et al., 2011) showed increased accumulation of pentosidine in the tibia of older animals after 16 weeks on a high fat diet (60% kcal from fat). The increased glycation of proteins such as collagen can reduce the elastic properties of bone, translating to clinical applicability and would allow for a maintained or even increased BMD, with an increase in fracture incidence. Although compelling evidence exists to support the role of TLR-4

and RAGE as critical factors contributing to the dysregulation of bone metabolism during T2DM, other mechanisms and cellular responses downstream of the IR may play a central role.

Regulation of Macroautophagy

Alterations occurring in cellular processes regulated by insulin sensitivity and glucose transport in osteoblasts and osteoclasts during T2DM may contribute to the dysregulation of bone metabolism. One such cellular process, macroautophagy, referred to hereafter as autophagy, is controlled by proteins downstream of the IR and is involved in energy (i.e., glucose) sensing, effectively regulating cell survival or cell death by means of organelle recycling (Bursch et al., 2008). This multi-step cellular process involves initiation, membrane nucleation, phagophore formation, sequestration and autophagosome formation, followed by autophagosome-lysosome fusion. Autophagy is centrally regulated by mTORC1 or AMPK.

As the name suggests, mTOR was first described as a target protein for the immunosuppressant drug, rapamycin, and was originally developed as an anti-fungal agent. In recent years mTOR and one of its associated complexes, mTORC1, has been demonstrated to act as a central regulator of autophagy as well. In addition to mTOR, the mTORC1 complex consists of adaptor proteins known as Raptor (regulatory-associated protein of mTOR) and mLST8 (mammalian lethal with SEC13 protein 8 or sometimes referred to as G protein β subunit-like protein; G β L) (Yang et al., 2010; Ravikumar et al., 2010) (**Figure 3**). Upon insulin binding to IR, Akt becomes activated (Ser473, Thr308),

which leads to the inhibition of TSC1/2 (tuberous sclerosis complex) and Rheb (ras homology enriched in brain), ultimately leading to the phosphorylation of mTORC (Ser2448). Phosphorylated mTORC1 regulates mRNA translation by activating ribosomal s6 kinase (RSK) and blocking the translational repressors, eIF4EBP1 and eEF2 kinase, and therefore promoting cell growth. Conversely, mTORC1 can exist as an inactive complex via multiple mechanisms including being bound to inhibitors known as Pras40 (proline-rich AKT1 substrate 1) and/ or Deptor (DEP domain-containing mTOR-interacting protein), or by the displacement of Raptor. It is this inactive form of mTORC1, which dissociates from the lysosome, thereby initiating autophagy by activating unc-like kinase (ULK1) (dephosphorylation at Ser757).

AMPK is another protein altered in various tissues during T2DM which can regulate autophagy, both by direct and indirect mechanisms. AMPK exists as an obligate

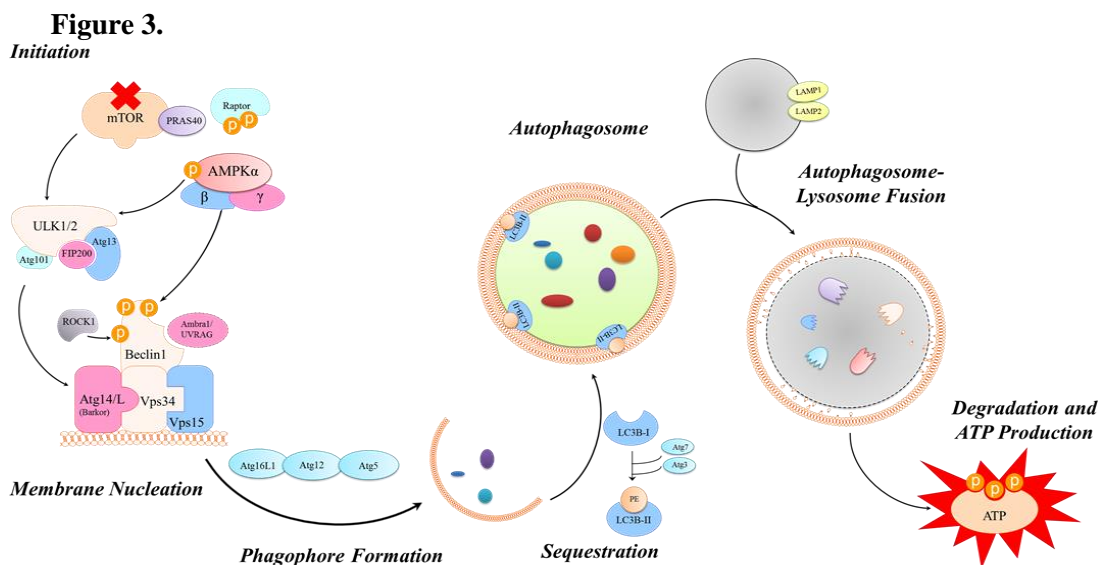


Figure 3. Schematic diagram of autophagy initiation, membrane nucleation and phagophore formation, sequestration of proteins and/ or organelles, autophagosome formation and autophagosome-lysosomal fusion resulting degradation and ATP production.

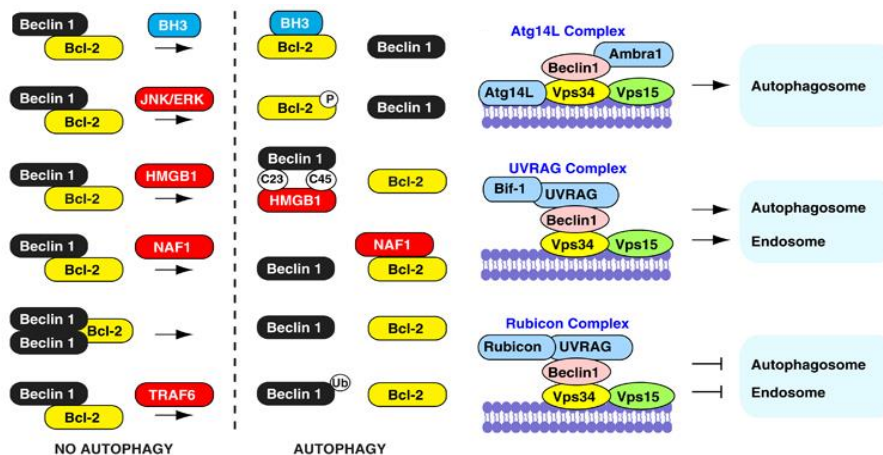
heterotrimer consisting of a catalytic α subunit and two regulatory subunits (β and γ) (**Figure 3**). When intracellular energy or concentrations of ATP are low, AMP binds to the γ subunit promoting the phosphorylation and activation of AMPK α (Thr172). This phosphorylation catalyzes the reaction of 2 ADP molecules into 1 ATP and 1 AMP, thereby sustaining cellular function. Activated AMPK due to low cellular energy or a high [AMP]/[ATP] ratio, can also phosphorylate TSC1/2 (Ser1387) and/ or Raptor, directly controlling mTORC1 and autophagy. Regulation of autophagy from AMPK also occurs independent of mTORC1, by phosphorylating ULK1 (Ser317, 555, and 777) and Beclin1. Activation of the ULK1 complex is the critical step for the initiation of canonical autophagy.

One of the first autophagy related proteins, Atg1, described in yeast (*S. cerevisiae*) coordinates the initiation of autophagy and downstream protein conjugation systems (Chan, 2012). The mammalian homologue of Atg1, ULK1/2, is a serine/threonine kinase found in a complex with FIP200 (focal adhesion kinase family-interacting protein of 200 kDa), Atg13, and Atg101 (Wirth et al., 2013). In addition to phosphorylation, ULK1/2 can be acetylated by TIP60 (HIV-1 Tat interactive protein, 60 kD) (Lys162 and 606), thereby activating autophagy. Although the mechanism is not entirely clear, this core machinery orchestrates the downstream events prior to autophagy initiation. Membrane nucleation and assembly of the initial phagophore membrane requires the class III phosphatidylinositol 3-kinase (PtdInsK) complex, composed of the PtdInsK, Beclin1, Barkor (beclin 1-associated autophagy-related key regulator or Atg14L), and Vps34 (vacuole protein sorting).

Beclin1 was discovered in the late 1990's to interact with the anti-apoptotic B-cell lymphoma-2 (Bcl-2) protein, hence the name (Bcl-2-interacting myosin-like coiled-coil protein). More recently, however, Beclin1 has been identified as a key regulator of autophagy. Beclin1 is a multifunctional protein with many post-translational fates, including phosphorylation, calpain-mediated cleavage, ubiquitination, and existence in multi-protein complexes. Pro-autophagic Beclin1 complexes include Barkor-Vps34-Vps15-Beclin1-AMBRA (activating molecule in beclin-1 regulator autophagy) and Vps34-Vps15-Beclin1-Bif-1-UVRAG (UV radiation resistance-associated gene), whereas Rubicon (RUN domain protein as Beclin1 interacting and cysteine-rich containing) bound Vps34-Vps15-Beclin1-UVRAG complex negatively functions in autophagosome maturation (**Figure 4**) (Kang et al., 2011). Two phosphorylation sites that regulate autophagy have been identified on Beclin1, Thr119 and Ser91/94. DAPK (death-associated protein kinase) has been demonstrated to phosphorylate Beclin1 at Thr119 position, thereby dissociating it from Bcl-x_L, initiating membrane nucleation and autophagosome formation. Additionally, Gurkar *et al.* (Gurkar et al., 2013) demonstrated that activated ROCK1 or ROK β (Rho kinase 1) promotes autophagy by phosphorylating Beclin1 at Thr119. The authors went on to describe that inactive ROCK1 leads to autophagy impairment, resulting in cell death in glucose-starved HeLa cells (Gurkar et al., 2013). In addition to cytokinesis and cytoskeletal arrangement, ROCK1 has been studied due to its implications on IRS phosphorylation and glucose metabolism (Chun et al., 2012; Lee et al., 2014; Lee et al., 2009a). Lee *et al.* (Lee et al., 2014) recently showed that the enzymatic activity of ROCK1 is elevated in obese mice (e.g., diet-induced, *db/db*, and *ob/ob*), which could activate autophagy by means of Beclin1

phosphorylation. Moreover, AMPK has been shown to activate the pro-autophagy Vsp34 complex by phosphorylating Beclin1 at the Ser91/94 position in mouse embryonic fibroblasts (MEFs), and this phosphorylation was critical for AMPK induced autophagy (i.e., glucose starvation) vs. mTORC1 (i.e., rapamycin treatment) (Kim et al., 2013a). These two, newly identified phosphorylation sites on Beclin1, appear to be dependent on autophagy induction and provide another means by which to study this process. Although little is known about the transcriptional regulation of Beclin1, there is evidence that *Becn1* mRNA is controlled by several transcription factors (e.g., EF1, c-jun, NF- κ B, FoxO3, and HIF1 α), microRNAs (e.g., miRNA30a), and epigenetic silencing due to hypermethylation. Furthermore, the critical role of Beclin1 in membrane nucleation and

Figure 4.



Kang et al., 2011

Figure 4. Post-translational fates of Beclin1.

phagophore formation has demonstrated robust cross-talk between autophagy and apoptosis.

Following autophagy initiation and membrane nucleation, two ubiquitin-like conjugation systems are used to isolate and sequester cargo to the autophagosome. Atg12

is conjugated to Atg5 by Atg7 to form an isopeptide bond between Atg12-glycine and Atg5-lysine (i.e., Atg12-Atg5) and then interacts with Atg16. The Atg8 or mammalian homolog microtubule associated protein light chain 3 (LC3) exists as an A and B form (other mammalian homologues for Atg8 include GABARAP-1 and GATE16) and is essential for autophagosome formation as well as autophagosome-lysosome fusion (Tanida et al., 2004). ProLC3 is processed by the protease Atg4, which results in the cleavage of proLC3 to its cytosolic form LC3-I. Similar to Atg12 conjugation, Atg7 is conjugated to LC3I, followed by Atg3, ultimately resulting in the conjugation LC3I to phosphatidyl ethanolamine (PE) or LC3-II. This step initiates the sequestration process and leads to the fusion of the autophagosome to the lysosome, where LC3-II and autophagosome contents are degraded to nucleotides, amino acids, and free fatty acids. This material can then be recycled for macromolecular synthesis and ATP generation. Although LC3-II is a larger protein than LC3-I, interestingly, LC3-II has greater mobility in SDS-PAGE than LC3-I, which allows for a methods to indirectly observe autophagosome formation. It should be noted that since LC3-II is located on the membrane of the autophagosome and this protein is degraded upon lysosomal fusion. Therefore, it is necessary to inhibit lysosomal degradation (i.e., bafilomycin A1 or chloroquine) if LC3-II is going to be used as an indicator of autophagy. Although great strides have been made in the field of autophagy many questions and gaps in knowledge remain, bringing this complex cellular process to the forefront of research related to cancer, aging, neurodegenerative diseases, as well as obesity and T2DM.

Transmission electron microscopy (TEM) continues to be the “gold standard” for monitoring autophagy since the term was first coined by Christian D Duve in 1963;

however, other techniques and assays have been and are continuing to be developed. One of the earliest assays was established in yeast following the observation that these autophagosomal vacuoles contain high amounts of ALP (Noda et al., 1995). Assessing ALP is based on the premise that upon starvation conditions (i.e., glucose and amino acids), ALP was processed from its inactive precursor to the mature form (Noda et al., 1995). Measurement of ALP activity, however, would prove to be a non-specific indicator in cells such as hepatocytes and osteoblasts, which express high levels of ALP. Therefore, aside from TEM, the most commonly used techniques to monitor autophagy includes western blot analysis of the molecular weight shift in LC3-I (14 kDa) to LC3-II (16 kDa) and translocation of green fluorescence protein (GFP)-LC3 from the cytoplasm (LC3-I) to the distinct puncta (LC3-II). Although these tools have been critical for the advancement of the field of autophagy they do have limitations. For example, LC3-II is generally accepted as an appropriate indicator of autophagosome formation, but it is readily degraded in the lysosome, making *in vivo* assessment challenging (Mizushima et al., 2007). While it is not commonly used, Iwai-Kanai et al., (Iwai-Kanai et al., 2008) utilized the anti-malaria drug, chloroquine, to prevent LC3-II degradation in cardiac tissue, allowing for data interpretation of autophagic flux. Transgenic models can also be used to observe autophagy *in vivo*, but due to the cost, these models are not always an option. Other techniques have been reported (e.g., acridine orange fluorescence, indirect immunofluorescence, and western blot of various proteins), but they are not specific and require a combination of methods to validate conclusions. As the science continues to advance in the field of autophagy, so too does the development and refinement of methods suitable for monitoring this dynamic process.

Evidence of Altered Autophagy during T2DM

Due to the control of autophagy by proteins involved in insulin signaling and intracellular energy sensors (e.g., mTORC1 and AMPK), investigation as to how this process is altered in T2DM has yielded novel and seemingly conflicting results. For example, in the pancreas autophagy has been shown to be essential for maintenance of β -cell mass, structure, and function (Masini et al., 2009; Chen et al., 2011). Contrary to initial expectations, β -cells experience a decrease in autophagy during diabetes, which has been speculated to be a contributing factor in the progression from obesity to T2DM. Autophagy is activated in myocardial tissues from diet-induced obesity model of T2DM; however, a disruption in the autophagic flux (i.e., autophagosome-lysosome fusion) was shown to contribute to cardiac injury (Iwai-Kanai et al., 2008). Lastly, white adipose tissue has been shown to undergo increased autophagy in animal models and in patients with T2DM. Adipocytes from human subjects with T2DM demonstrate decreased mTORC1 activity and increased autophagosomes as evidenced by TEM and LC3-II (Ost et al., 2010). Nunez *et al* (Nunez et al., 2013) confirmed the observation of enhanced autophagy in subcutaneous adipose tissue from an animal model of diet-induced obesity and in obese-diabetic patients. Interestingly, a subset of human obese-diabetic patients who underwent bariatric surgery exhibited a decrease in autophagy with decreasing BMI (Nunez et al., 2013). While no reports have been published regarding bone cells undergoing altered autophagy in type 2 diabetics, osteoblasts are derived from the same MSC population as adipocytes and may therefore act in a similar manner. It should be noted that in all of these tissues and cells it remains unclear whether autophagy is playing

a protective or a harmful role during diabetes. However, making a general, all-encompassing statement may not be appropriate since autophagy can be beneficial and function as a pro-survival mechanism to deal with acute stress, or has the potential to be lethal when autophagic activity persists.

Autophagy in Osteoblasts, Osteocytes, and Osteoclasts

While limited work has been published on the role of autophagy in osteoblasts, osteocytes, and osteoclasts, some advances have been made within the past 5 years. Results from *in vitro* osteoblast cultures have implicated alterations of autophagy as a cellular response to nitric oxide, estradiol treatment, and palmitate-induced cell death. For example, glutathione-depleted human osteoblastic osteosarcoma cells (U2-OS) treated with the vasodilating drug, sodium nitroprusside (SNP), induced large increases in LC3-II protein expression and autophagosome formation (i.e., TEM) (Son et al., 2010). These data suggest that during excessive, uncontrolled oxidative stress, osteoblasts will undergo increased autophagy. Although the authors discuss a modest increase in LC3-II protein abundance following SNP treatment, the data was expressed as LC3-II/ LC3-I, which has been described to be an inaccurate approach (Mizushima et al., 2007; Klionsky et al., 2008). Recently, Yang *et al.* (Yang et al., 2013) induced autophagy in osteoblast-like MC3T3-E1 cells by serum deprivation and noted increased autophagosome formation, along with increased abundance of Beclin1, LC3-II, and ULK1 after 48 hrs. Interestingly, estradiol treatment decreased the apoptotic events (e.g., caspase 3 cleavage and Hoechst staining of fragmented DNA) in these cells, while enhancing autophagy (i.e., decreased p-mTORC1 and increased LC3-II). These findings suggest that estrogen plays

a cellular protective role in osteoblasts by increasing autophagy, and therefore, offers a novel means by which postmenopausal osteoporosis is induced when estrogen levels decline (Yang et al., 2013). While no studies to date have investigated autophagy in bone during obesity or T2DM, a recent publication has shown that sFFA, palmitate, can induce cell death of human osteoblasts via apoptosis and autophagy as demonstrated by LC3 puncta and TEM (Gunaratnam et al., 2013). Recent interest has also focused on autophagy's role in osteocytes during glucocorticoid treatment (Xia et al., 2010). This publication showed that the osteocyte-like cell line of MLO-Y4 cells transfected with GFP-LC3 increased GFP-LC3 puncta following 10^{-6} M of dexamethasone treatment for 24 hr, consistent with increased autophagosome formation. Similar to Son and colleagues' (Son et al., 2010) report on SNP's effect on osteoblasts, LC3-II protein expression was also reported as a ratio of LC3-I form, although actin appears to be an appropriate control in this publication (Xia et al., 2010). While the work of Xia et. al., undeniably advanced the field of how glucocorticoids affect osteocytes, there are major limitations that make data interpretation and understanding the implications difficult.

While the prior literature reviewed was designed to investigate autophagy, other studies have described how osteoblasts respond to rapamycin treatment. Rapamycin, also known as sirolimus, is an immunosuppressant drug isolated from the bacterium *S. hygrosopicus* that is commonly utilized in autophagy research due to its ability to inactivate mTORC1. Specifically, rapamycin binds to the FKBP12–rapamycin-binding (FRB) domain of mTOR, directly blocking substrate recruitment (i.e., Raptor) of mTORC1, thereby up-regulating autophagy. A review of the literature reveals conflicting data as to how rapamycin affects osteoblasts. For example 10 nM of

rapamycin for 12, 24, 28, and 72 hr has been shown to impair osteoblast differentiation by decreasing Runx2 and cyclin D1 protein expression in osteoblastic MC-4 (MC3T3-E1 subclone 4) cells (Singha et al., 2008). Conversely, 1 nM rapamycin has been shown to induce osteogenic differentiation of human embryonic stem cells (hESC) by up-regulating *Bmp2* and *Runx2* mRNA, as well as increasing nodule formation (Lee et al., 2009b). The osteogenic potential was attributed to rapamycin's ability to regulate TGF β /BMP signaling by blocking the interaction of FKBP12 and the TGF β type 1 receptor to induce BMP4 expression and Smad activity. It is important to note that although rapamycin was used in both of these experiments, autophagy was never assessed.

Some of the most informative data related to autophagy and bone come from conditional knockout models. The work of Onal *et al.* (Onal et al., 2013) described the generation of a dentin matrix protein (DMP)-1-Cre transgenic mouse crossed with a floxed *Atg7* allele, resulting in suppressed *Atg7* expression in osteocytes (~75% reduction). As anticipated, autophagy was suppressed in these animals based on a decrease in LC3-II protein abundance (Onal et al., 2013). Interestingly, these animals exhibited decreased BMD of the femur, spine and whole body, presumably due to a decrease in trabecular bone (vertebral and femoral BV/TV) (Onal et al., 2013). Suppression of autophagy in osteocytes was sufficient to mimic the osteopenia associated with advanced age even in young adult mice. Further insight was provided by another transgenic mouse model which was generated to express an osteoblast specific (Osx or Osterix-Cre) deletion of FIP200 (Liu et al., 2013). The authors described an increase in LC3-II abundance during the differentiation of primary osteoblasts, which suggested that

autophagy was involved in the terminal differentiation of osteoblasts (Liu et al., 2013). This conditional knockout model confirmed that these animals had dramatically lower trabecular and cortical bone at 1, 2, and 6 mo of age (Liu et al., 2013). These bone structural changes were attributed to decreased bone formation as determined by static and dynamic bone histomorphometry (Liu et al., 2013). Together, these two groundbreaking studies demonstrate that basal autophagy promotes osteocyte function, supports nodule formation by osteoblasts and contributes to the terminal differentiation of osteoblasts.

While the direct role autophagy plays in osteoclast differentiation and/or osteoclast function in the context of T2DM remains unclear, it has been suggested that autophagy is a pivotal regulator for osteoclastogenesis induced by hypoxia, Paget's disease of bone, and TNF- α mediated joint destruction (Zhao et al., 2011; Tresse et al., 2010; Lin et al., 2013). However, it has recently been discovered that autophagic proteins (i.e., Atg5, Atg7, Atg4B, and LC3) are involved in the polarized secretion of lysosomal contents by the osteoclast (DeSelm et al., 2011). These proteins are essential for proper bone resorption by the osteoclast in what has been described as "non-canonical" autophagy. The description of autophagic proteins being involved in cellular processes aside from canonical autophagy (e.g., actin-ring organization and resorption of osteoclasts as well as phagocytosis and degradation of photoreceptor outer segments of retinal pigment epithelium), makes the osteoclast particularly difficult to study especially given the current validated methods in the field (Kim et al., 2013c).

Glucose Transporters (GLUTs) on Osteoblasts and Osteoclasts

It is reasonable to conceive that autophagy can be induced during T2DM due to the impaired ability to transport glucose for cellular utilization. For autophagy to be activated due to inadequate cellular glucose, the subcellular localization of the cell's major glucose transporter (GLUT) would need to be dependent upon insulin, similar to GLUT4. Therefore, characterization of the major GLUTs expressed on osteoblasts and osteoclasts is fundamental to understanding how these cells may be impacted during T2DM. In 1989, Ituarte *et al.* (Ituarte et al., 1989) showed that rat osteosarcoma cells (e.g., UMR 106-01) possessed a stereospecific, saturable, active glucose transport system, similar to that of insulin sensitive cells (i.e., myocytes and adipocytes). Further investigation using this osteosarcoma cell line revealed that both GLUT1 and GLUT3 were expressed by osteoblast-like cells and were responsible for glucose up-take (Thomas et al., 1996). Moreover, Hahn *et al.*, (Hahn et al., 1988) showed that insulin rapidly stimulated 2-deoxyglucose uptake in osteoblast-enriched rat bone explant preparations. Although GLUT3 was originally considered the “neuronal glucose transporter” several studies have shown that GLUT3 is expressed on osteoblasts (e.g., UMR 106-01, UMR 201-10B, PyMS, and primary osteoblasts) and its expression increases with maturation of the osteoblasts (Zoidis et al., 2011; Ma et al., 2011; Thomas et al., 1996; Fang et al., 2006; Ituarte et al., 1989). Additionally, subcellular fractionation has shown that L6 myotubes exhibit an intracellular pool of GLUT3 that is redistributed to the plasma membrane upon insulin stimulation (Bilan et al., 1992). More recently, insulin has been shown to increase the expression of GLUT3 on the plasma membrane in human monocytes and B-lymphocytes (Maratou et al., 2007). While homozygous

mutations in GLUT3 (*Glut3*^{-/-}) are embryonic lethal, male heterozygous *Glut3*^{+/-} mice develop adult-onset adiposity with insulin resistance (Ganguly et al., 2008). These studies provide evidence that GLUT3 is an insulin-sensitive transporter, and tissues that express this GLUT (i.e., bone, testes, and brain) should be considered as contributing sources to the hyperglycemia observed during T2DM.

More recently, preliminary data presented by Li and colleagues (Zhu Li et al., 2013) demonstrated that primary mouse osteoblasts isolated from the calvaria express GLUT1, GLUT3, and GLUT4. It is important to note that given the relatively low K_m of GLUT3 ($K_m=1.4$ mM) compared to GLUT1 ($K_m= 6.9$ mM) and GLUT4 ($K_m = 4.6$ mM), GLUT3 may still act as the primary glucose transporter in osteoblasts due to its high affinity for glucose. Due to the evidence that osteoblasts express GLUTs (i.e., GLUT3 and GLUT4) whose subcellular localization is regulated by insulin, the potential exists that osteoblasts experience increased autophagy due to inadequate intracellular energy during T2DM.

In contrast to osteoblasts, glucose transport in osteoclasts or their precursor cell population (i.e., monocyte/macrophage lineage) has not been extensively studied. One of the only publications related to GLUTs and these bone resorbing cells showed that osteoclasts differentiated from peripheral blood mononuclear cells (PBMC) increase GLUT1 protein expression in response to hypoxia (Knowles et al., 2008). Previous research has shown that cell lines of human monocytic lineage express GLUT1, GLUT3, and GLUT5 (Fu et al., 2004). Due to the lack of evidence describing the molecular mechanism by which osteoclasts transport glucose, additional research is needed.

Alterations that occur in insulin sensitivity during T2DM have been observed in peripheral tissues such as skeletal muscle and adipose tissue to diminish glucose transport, contributing to elevated blood glucose. If GLUT4 is expressed on osteoblasts as reported (Zhu Li et al., 2013) and/or if GLUT3 acts in a similar manner to GLUT4, it is conceivable that bone may also contribute to the systemic hyperglycemia that occurs in T2DM. Furthermore, if glucose uptake is attenuated in osteoblasts, osteoclasts, as well as osteocytes, these cells may be metabolically stressed, resulting in the up-regulating autophagy. Given the protective nature of autophagy, it is plausible that during T2DM a cell such as the osteoblast could experience an increase maturation and activity due to autophagy initially, but chronic activation of autophagy would eventually result in cell death by means of apoptosis (Bursch et al., 2008). This unique scenario, of accelerated osteoblast maturation followed by cell death, could provide a novel explanation for the apparent paradox in T2DM of having an increased risk of fracture with increasing duration in type 2 diabetics, while simultaneously maintaining BMD.

Summary of Potential Mechanisms in the Dysregulation of Bone Metabolism in T2DM

Based on this review of the literature, it is apparent that investigation into the role of TLR-4 and autophagy in bone metabolism could provide new insights into the alterations in bone microarchitecture and biomechanical properties that ultimately result in increased fracture risk with T2DM. Given the literature supporting the potential for increased TLR-4 signaling in the development and progression of glucose intolerance,

and the potential negative effects of these pro-inflammatory mediators on bone cell differentiation, activity and apoptosis, it is imperative to investigate the role of TLR-4 on the skeletal response over time in T2DM. Due to the fact that autophagy is regulated by both the insulin signaling pathway (mTORC1) and intracellular energy (AMPK), the potential exists for this cellular process to be altered in osteoblasts and osteoclasts during hyperglycemia. Although information on how autophagy impacts osteoblast and osteoclast differentiation and function is limited, the literature supports the notion that autophagy may initially provide protection from cellular stresses occurring with T2DM (Liu et al., 2013; Eisenberg-Lerner et al., 2009). If the autophagy is increased during the early stages of T2DM and hyperglycemia, this dynamic process may provide a protective role, maintaining bone metabolism, however, prolonged hyperglycemia could alter bone metabolism, resulting in increased fracture risk. Therefore, a series of studies have been designed to investigate the role of TLR-4 and autophagy in an animal model of T2DM. The findings from these studies will advance the field of bone and mineral research related to TLR-4 signaling and the role of autophagy, and may lead to the identification of potential therapeutic targets to decrease fracture incidence in the population.

CHAPTER III

A COMPARATIVE STUDY OF THE METABOLIC AND SKELETAL RESPONSE OF C57BL/6J AND C57BL/6N MICE IN A DIET-INDUCED MODEL OF TYPE 2 DIABETES.

The following manuscript has been submitted for publication in *Metabolism*

Title: A Comparative Study of the Metabolic and Skeletal Response of C57BL/6J and C57BL/6N Mice in a Diet-Induced Model of Type 2 Diabetes.

Authors: Elizabeth Rendina-Ruedy¹, Kelsey D. Hembree¹, Angela Sasaki¹, McKale R. Davis¹, Stan A. Lightfoot², Stephen L. Clarke¹, Edralin A. Lucas¹, Brenda J. Smith¹

¹Department of Nutritional Sciences, Oklahoma State University, Stillwater, OK.

²Center for Cancer Prevention and Drug Development, University of Oklahoma Health Sciences Center, Oklahoma City, OK.

Corresponding Author: Brenda J. Smith, Department of Nutritional Sciences, HSci 420 Oklahoma State University, Stillwater OK 74078; (405) 744-3866; bjsmith@okstate.edu

Abstract:

Objective: Type 2 diabetes mellitus (T2DM) represents a complex clinical scenario of altered energy metabolism and increased fracture incidence. The C57BL/6 mouse model of diet-induced obesity has been used to study the mechanisms by which glucose intolerance alters bone mass and quality, but genetic variations in substrains of C57BL/6 may confound the interpretation of results. Therefore, this study was designed to investigate the long-term metabolic and skeletal response of two commonly used C57BL/6 substrains to a high fat (HF) diet.

Methods: C57BL/6J and C57BL/6N and the negative control strain, C3H/HeJ mice, were fed a control or HF diet for 24 wks. Blood glucose, plasma insulin, and a glucose tolerance test were determined to characterize the metabolic response of each strain. The skeletal response was determined by assessing trabecular and cortical bone microarchitecture.

Results: C57BL/6N mice on a HF diet demonstrated an increase in plasma insulin and blood glucose as early as 4 wk, whereas the hyperinsulinemic and hyperglycemic response of the C57BL/6J mice to the HF diet was delayed until 16 and 24 wks, respectively. Only the C57BL/6N mice lost significant trabecular bone in the vertebra in response to the high fat diet. The C3H/HeJ mice were protected from bone loss.

Conclusions: These data show that the C57BL/6J and C57BL/6N on a high fat diet differ in their metabolic and skeletal response, which could have implications for data interpretation and should be considered when designing animal studies.

Keywords: glucose, insulin, osteocalcin, substrain, bone

Abbreviations: Type 2 diabetes mellitus, T2DM; high fat, HF; bone mineral density, BMD; bone mineral area, BMA; bone mineral content, BMC; toll-like receptor 4, TLR-4;

lipopolysaccharide, LPS; saturated free fatty acids, sFFAs; nicotinamide nucleotide transhydrogenase, NNT; white blood cells, WBC; dual energy x-ray absorptiometry, DXA; intraperitoneal glucose tolerance test, IGTT; area under the curve, AUC; osteocalcin, OCN; gamma carboxylated OCN, Gla-OCN; undercarboxylated OCN, Glu-OCN; micro-computerized tomography, microCT; volume of interest, VOI; bone volume/ total volume, BV/TV; trabecular number, Tb.N.; trabecular thickness, Tb.Th.; trabecular separation, Tb.Sp.; connectivity density, ConnDens; structural model index, SMI; non-alcoholic fatty liver disease, NAFLD; fatty acid synthase, *Fasn*; sterol regulatory element-binding protein, *Srebp1c*; glucose transporter 2 or solute carrier family, *Slc2a2*; peroxisome proliferative-activator α , *Ppara*; glutathione peroxidase, *Gpx1*; peptidylprolyl isomerase B, *Ppib*; leptin receptor, *Lepr*; ribonucleic acid, RNA; complementary deoxyribonucleic acid, cDNA; quantitative real-time polymerase chain reaction, qPCR; statistical analysis software, SAS; standard error, SE; kilocalorie, kcal; adenosine triphosphate, ATP.

1. Introduction

Increasing prevalence of type 2 diabetes mellitus (T2DM) has stimulated research focused on the pathogenesis and treatment of T2DM and its complications. Initial studies examining fracture as a possible complication of T2DM indicated that type 2 diabetics were not at risk of fracture based on bone mineral density (BMD), the clinical standard for screening [1-3]. However, data analyzed from clinical trials with fracture as an outcome variable instead of BMD revealed that both men and women with T2DM experience an increase in fracture (i.e., 1.5-3 fold) beginning 5-10 years post diagnosis [4-8]. Collectively, the clinical evidence indicates that independent of BMD, type 2 diabetics are at increased risk of fracture that is exacerbated over time.

Rodent models have enabled investigators to study the molecular mechanisms contributing to the alterations in bone quality associated with T2DM. One of the most commonly utilized models has been the C57BL/6J mouse fed a high fat (HF) diet, which exhibit an increase in adiposity, hyperinsulinemia, hyperglycemia, and dyslipidemia similar to humans [9-11]. Additionally, C57BL/6J mice exhibit decreased BMD in response to long-term intake of a HF diet, which results from altered adipokines and/or hormones [12-15]. Alterations in bone mass in these animals are also accompanied by impaired bone quality as evidenced by compromised biomechanical properties [13;15-19]. In contrast, C3H/HeJ mice, which have a nonfunctional toll-like receptor (TLR) 4 due to a point mutation in the toll-interleukin 1 receptor domain, exhibit a blunted metabolic and skeletal response to HF diets [20-22]. TLR-4 is expressed on bone forming osteoblasts and bone resorbing osteoclasts, and TLR-4 ligands (e.g., lipopolysaccharide or LPS, and saturated free fatty acids or sFFAs) as well as downstream inflammatory mediators may uncouple bone turnover [23;24]. Because of interest in sFFAs and

gut-derived LPS in the pathophysiology of T2DM and its complications, the C3H/HeJ strain has become an important research tool. Other rodent models of T2DM have included the Zucker fatty diabetes mellitus rat and the fat-fed, streptozotocin-treated rat, but mouse models are often preferred due to the lower cost of housing and the range of available genetically modified models [25;26].

A review of published reports revealed that studies utilizing different C57BL/6 substrains (e.g., C57BL/6J and C57BL/6N) are often discussed without mention of genetic variations that could have important implications on the results and their interpretation. For example, the C57BL/6J mouse (Jackson Laboratory) has a missense mutation in the gene encoding nicotinamide nucleotide transhydrogenase (*Nnt*) that alters RNA splicing and leads to the deletion of exons 7-11 [27-29]. The C57BL/6J mouse's genetic alteration may contribute to the discrepancies in the literature in regards to metabolic alterations and corresponding complications using a diet-induced obesity model of T2DM [9;11;12;15]. To date, the metabolic and skeletal responses of the C57BL/6J substrain to a HF diet has not been directly compared to other substrains. If, as we hypothesized, the metabolic response to a HF diet in these two substrains differs due to genetic variations, this may alter hormones and adipokines that can subsequently affect the skeletal response. Such differences would be important relative to the interpretation of results and could assist researchers in selecting the most appropriate model.

2. Methods

2.1. Animal Care and Diets

Eight-week old male mice, C57BL/6N from Charles River (Wilmington, MA) and C57BL/6J and C3H/HeJ mice from Jackson Labs (Bar Harbor, ME), were obtained ($n = 30$ mice/strain) for these studies. The C3H/HeJ mice served as a negative control based on reports of their resistance to diet-induced obesity and TLR-4 mutation [20;21]. Animals were acclimated for 7 days and then randomly assigned to a control AIN-93M (10 % kcals from fat) or a HF (45% kcals from fat; Harlan Teklad, TD.06415) diet for 24 wk. Body weight and food intake were recorded throughout the study and venous tail blood was collected following a 6 hr fast for evaluation of glucose and insulin at 4 wk intervals. After 24 wks, mice were anesthetized (ketamine/xylazine cocktail 70 and 30 mg/kg body weight, respectively) as previously reported and whole body DXA (LunarPIXI, GE Medical Systems, Madison, WI) scans were performed. Mice were exsanguinated via the carotid artery. An aliquot of blood was collected for total white blood cell (WBC) counts and the remainder processed for plasma in EDTA coated tubes and stored at -80°C . All procedures were approved by the Institutional Animal Care and Use Committee of Oklahoma State University.

2.2. Intraperitoneal Glucose Tolerance Test

One week prior to the end of the study (23rd wk), mice were fasted for 6 hrs and an intraperitoneal (IP) glucose tolerance test (IGTT) was performed. Mice were administered an IP glucose solution (2 g glucose/ kg bodyweight) followed by blood glucose monitoring at 15, 30, 60, 90, and 120 min. Area under the curve (AUC) was determined by calculating the sum of rectangular area between each time point.

2.3. Analysis of Insulin, Adipokines, and Osteocalcin

Plasma insulin was assessed at 4 wk intervals, whereas plasma leptin, adiponectin and osteocalcin (OCN), both total -OCN (GlaOCN) and undercarboxylated OCN (Glu-OCN), were determined only at the final time point. All assays were performed using commercially-available ELISA kits including (Crystal Chem, Downers Grove, IL), leptin and adiponectin (EMD Millipore, Billerica, MA) and Gla-OCN and Glu-OCN, Clontech Takara Bio, Mountain View, CA), following the manufacturer's protocol. The ratio of Glu-OCN/ Gla-OCN is commonly reported as a means to indicate whether carboxylation status of OCN is being altered.

2.4. Body Composition and Bone Densitometry

Whole body DXA scans were performed to determine body composition, bone mineral area (BMA), content (BMC), and BMD. All scans were analyzed using PIXImus Series Software version 1.4x (GE Lunar Pixi, Madison, WI).

2.5. Micro-Computerized Tomography (MicroCT)

MicroCT (microCT40, SCANCO Medical, Switzerland) was used to evaluate bone microarchitecture at the proximal tibial metaphysis, tibial mid-diaphysis as well, and 4th lumbar vertebra. Analysis of trabecular bone was performed at the proximal tibial metaphysis on high resolution scans (2048 x 2048 pixels) and the volume of interest (VOI) included 750 μ m of secondary spongiosa. The VOI was analyzed using a threshold of 300, a sigma of 0.7, and support of 1.0. Trabecular bone of the vertebra was assessed on images 80 μ m from the dorsal and caudal growth plates at medium resolution (1024 x 1024 pixels) and included only secondary

spongiosa. Images generated from the scans of the vertebrae were analyzed at a threshold of 340, and a sigma and support of 1.2 and 2.0, respectively. Trabecular parameters evaluated included trabecular bone volume expressed as a percentage of total volume (BV/TV), trabecular number (Tb.N.), trabecular thickness (Tb.Th.), trabecular separation (Tb.Sp.) connectivity density (ConnDens) and structural model index (SMI).

Cortical bone was evaluated by analyzing a 120 μm section at the mid-diaphysis of the tibia. Assessment of cortical bone parameters included cortical porosity, thickness, area, and medullary area of the tibial mid-diaphysis. The acquired images were analyzed at a threshold of 300, a sigma of 0.7, and support of 1.0.

2.6. Analysis of Biomechanical Properties of the Tibia

Tibias were cleaned of soft-adhering tissue and stored in phosphate buffered saline (PBS) at 4°C until analyses were performed. Reference point indentation (RPI) was applied laterally at the tibia-fibula junction using a BioDent (Active Life Scientific, Inc, Santa Barbara, CA), and the first cycle indentation distance and touchdown distance was recorded. Each tibia was subjected to a testing protocol of 2 N force, 2 Hz, and 10 cycles.

2.7. Histology of the Liver

Fixed (10% neutral buffered formalin) liver samples were processed and sectioned (5 μm) for staining with hematoxylin and eosin to assess histological changes associated with nonalcoholic fatty liver disease (NAFLD) that occurs in obesity and/or diabetes. Steatosis and fibrosis were scored on a scale from 0-4, with 0 indicating the absence of hepatic lipid droplets

or fibrosis, whereas 4 indicated of pronounced steatosis or fibrosis. Lobular and portal inflammation was scored using a range of 0-3, with 0 indicating the absence of macrophage infiltration and 3 corresponding to severe inflammation. Balloon degeneration was scored using a 0-2 system, with 0 defined as the lack of degeneration and 2 indicating modest presence of parenchymal cell death. All scoring was performed by the study pathologist who was blinded to treatments.

2.8. RNA Isolation and Gene Expression Analysis

Total RNA was isolated from the liver and bone marrow tissues using TriZol Reagent (Invitrogen, Grand Island, NY) as previously described [30;31]. cDNA was synthesized following a standardized laboratory protocol [30;31] and qPCR was performed using SYBR green chemistry (7900HT Fast Real-Time, Applied Biosystems, Foster City, CA). Hepatic genes of interest included fatty acid synthase (*Fasn*), sterol regulatory element-binding protein (*Srebp1c*), glucose transporter 2 or solute carrier family (*Slc2a2*), peroxisome proliferative-activator α (*Ppara*), and glutathione peroxidase (*Gpx1*), and in the bone marrow *Fasn*, *Ppara* and *Gpx1* (**Table S1**). All qPCR results were evaluated by the comparative cycle number at threshold (C_T) method (User Manual #2, Applied Biosystems) using peptidylprolyl isomerase B or cyclophilin B (*Ppib*) as the invariant control.

2.9. Statistical Analysis

Statistical analyses were performed using Statistical Analysis Software version 9.3 (SAS Institute, NC). The primary objective was to determine the difference in response to a HF diet of a given strain and therefore, student's paired t-test was used unless stated otherwise.

Furthermore, when the C57BL/J and C57BL/6N substrains exhibited a response to the HF diet, the magnitude of the response (i.e., percent change) was calculated and comparisons were made between strains using one-way ANOVA. When the F value was < 0.05 , *post hoc* analyses were performed with the Fischer's least square means separation test. Chi-squared tests were used for histological scoring of liver specimens. All data are presented as mean \pm standard error (SE) and a $P < 0.05$ was considered statistically significant.

3. Results

3.1. Body and Fat Pad Weight, Body Composition, and Food Intake

At baseline, body weight between strains differed with the C57BL/6J, C57BL/6N, and C3H/HeJ; however, no differences existed between the two dietary treatment groups (i.e., Con or HF) within a given strain (*data not shown*). After 5 wk on the HF diet, the C57BL/6J exhibited a significant increase in bodyweight compared to the C57BL/6J Con, whereas the C57BL/6N on the HF diet had a higher ($P < 0.05$) body weight after only 3 wk (**Figure 1**). The C3H/HeJ mice on the HF diet also exhibited a more rapid increase in body weight after only 1 wk compared to their respective Con (**Figure 1**). Analysis of body composition revealed the increase in body weight was due to a significant increase in both lean and fat mass for the two C57BL/6 substrains and the C3H/HeJ mice (**Table 1**). The amount of food consumed was lower for the mice on the HF diet in each strain (**Table 1**), however, the C57BL/6N mice on the HF diet consumed +2.1 kcal/day compared to C57BL/6N-Con. The C57BL/6J and C3H/HeJ on the HF diet consumed +1.2 kcal/day compared to their respective controls (*data not shown*).

3.2. Tissue Weights and White Blood Cells

After 24 wk on a HF diet the C57BL/6N mice exhibited splenomegaly, thymic hypertrophy, and decreased WBC, but the C57BL/6J mice failed to demonstrate these immunological changes (**Table 1**). C3H/HeJ mice had a similar response to HF diet in terms of tissue weights and total WBC's compared to the C57BL/6N mice (**Table 1**).

3.3. Blood Glucose, Plasma Insulin, and Glucose Tolerance Test,

C57BL/6N mice on the HF diet were the only strain that had elevated fasting blood glucose (**Figure 2A**) and plasma insulin (**Figure 2B**) after 4, 8, 12, 16, 20, and 24 wk of treatment compared to their Con counterparts. The C57BL/6J substrain on the HF diet was hyperglycemic at 16 and 20 wk (**Figure 2A**) and hyperinsulinemic at 24 wk (**Figure 2B**). Similar to the C57BL/6J substrain, the C3H/HeJ mice on the HF diet exhibited delayed-onset of hyperglycemia (**Figure 2A**), while their plasma insulin was increased at 12, 20 and 24 wk (**Figure 2B**).

At the end of the study, IGTT showed that the C57BL/6J and C57BL/6N, as well as the C3H/HeJ mice on the HF diet exhibited glucose intolerance (**Figure 3A & B**). The C3H/HeJ mice also exhibited glucose intolerance after 24 wk on a HF diet (**Figure 3**). It should be noted that despite elevated AUC, the C3H/HeJ mice on the HF diet maintained the ability to restore blood glucose by the final IGTT time point. The percent difference in AUC of the HF animals compared to their respective Con demonstrates that that the magnitude of response was similar across the C57BL/6J and C57BL/6N (*data not shown*).

3.4. Plasma Adipokines and Osteocalcin

Both the C57BL/6J and C57BL/6N substrains had elevated plasma leptin after 24 wk on a HF diet (**Table 1**). Similarly, the C3H/HeJ mice on the HF diet also had higher plasma leptin (**Table 1**). Interestingly, at 24 wk the C57BL/6J mice, but not the C57BL/6N substrain, exhibited a decrease in plasma adiponectin in response to a HF diet (**Table 1**).

The carboxylation status of OCN (i.e., Glu/Gla-OCN ratio), which has been shown to influence systemic energy metabolism, was reduced only in the C57BL/6N mice after 24 wk on a HF diet (**Figure 4**).

3.5. Histological Evaluation of Hepatic Tissue

Representative micrographs of liver sections from each group show that the C57BL/6J and C57BL/6N strains as well as the C3H/HeJ strain experienced some degree of hepatic steatosis in response to the HF diet (**Figure 5**). Ninety-two percent of the C57BL/6N mice on the HF diet had lobular inflammation, while 77% had portal inflammation (**Table 2**). The frequency of the inflammatory response was markedly lower in the C57BL/6J mice (54% lobular and 23% portal inflammation) (**Table 2**). While none of the C57BL/6J mice on the HF diet exhibited liver fibrosis, 23% of the treated C57BL/6N mice had fibrotic changes (**Table 2**). Balloon degeneration was also more severe in the C57BL/6N mice on the HF diet compared to the C57BL/6J (**Table 2**). Despite a lack of lobular and portal inflammation and fibrosis in the C3H/HeJ mice, balloon degeneration was severe in this strain (**Table 2**).

3.6. Whole Body Bone Densitometry

Both the C57BL/6J and C57BL/6N mice demonstrated a decrease in whole body BMC and BMA, but no change in whole body BMD in response to the HF diet after 24 wk (**Table 3**). When BMD was expressed relative to body weight, differences due to diet were observed suggesting that the bone did not increase relative to the increase in body weight (**Table 3**).

3.7. Microarchitectural Changes in Trabecular and Cortical Bone

MicroCT analyses of the lumbar vertebra revealed significant loss of trabecular bone or BV/TV with the HF diet in C57BL/6N, while the C57BL/6J did not reach the level of statistical significance ($P < 0.0579$) (**Figure 6A**). In contrast, the C3H/HeJ mice were protected from vertebral bone loss (**Figure 6**) or non-morphometric parameters with HF diet (**Table 3**). Both the C57BL/6J and C57BL/6N mice on the HF diet had a higher SMI indicative of a weaker, more rod-like trabecular bone in the vertebra (**Table 3**).

In contrast to the vertebra, no changes were observed in trabecular or cortical parameters analyzed at the proximal tibial metaphysis or the tibial mid-diaphysis in the C57BL/6J or the C57BL/6N mice. The C3H/HeJ mice failed to demonstrate alterations in trabecular bone of the proximal tibia but did exhibit an increase in the medullary area at the mid-diaphysis (**Table 5**).

3.8. Changes in Biomechanical properties of the Tibia

Based on reference point indentation testing at the tibia-fibula junction, no changes were observed in first cycle indentation distance or touchdown distance in any strain following 24 wk on a HF diet when compared to their respective Con (**Table 3**).

3.9. Characterization of Genes Involved in Energy Metabolism and Inflammation from the Liver and Bone Marrow

Determination of genes involved in hepatic metabolism and inflammation revealed that the C57BL/6N mice on the HF diet had altered metabolic processes, including the up-regulation of glucose uptake (*Slc2a2*) and triglyceride storage (*Fasn* and *Srebp1c*), adipogenesis (*Ppara*), as well as antioxidant capacity (*Gpx1*) (**Table 4**). Interestingly, none of these alterations in gene expression were observed in the C57BL/6J mice after 24 wk on the HF diet.

To determine the degree to which oxidative stress and adipogenesis contributed to bone loss with the HF diet model, *Gpx1* and *Pparg* mRNA abundance was determined in the bone marrow. Similar to the hepatic tissue, the abundance of *Gpx1* mRNA was increased in the C57BL/6N mice on the HF diet, suggesting an increase in antioxidant capacity (**Table 4**). In contrast, the C57BL/6J mice on the HF diet demonstrated a decrease in the relative abundance of *Gpx1* (**Table 4**). Additionally, no alterations were observed in the transcriptional regulator of adipogenesis, *Pparg*, in any strain after 24 wk (**Table 4**).

4. Discussion

The findings of this study show that the C57BL/6J and the C57BL/6N mouse differ in their metabolic response to a HF diet over a 24 wk study period. Discrepancies in the metabolic response between the two strains are most likely attributed to the missense mutation (M35T) in exon 1 and a multi-exon deletion of *Nnt* in the C57BL/6J mice [32;33]. This mutation in *Nnt* has been reported to uncouple β cell mitochondrial metabolism leading to less ATP production in pancreatic islets, enhanced K_{ATP} channel activity, and consequently, impaired glucose-stimulated insulin secretion [28;32;34]. Only fasting insulin was assessed in the current study, however,

early onset of hyperinsulinemia with HF diet was only observed in the C57BL/6N mice with an intact, functional *Nnt*.

The C57BL/6J and C57BL/6N mice had a markedly different hepatic response to the HF diet after 24 wk. Increased mRNA abundance of *Fasn* and a modest increase in *Srebp1c*, in the presence of severe liver steatosis in the C57BL/6N mice on the HF diet suggests an increase in hepatic triglyceride synthesis and storage. Conversely, the C57BL/6J substrain, which has lower glucokinase activity and thus impaired glucose sensing, may explain the lack of transcription regulation of *Fasn* and *Srebp1c* [32]. Furthermore, C57BL/6N mice on the HF diet demonstrated an increase in *Slc2a2* gene expression, which encodes for the non-insulin-sensitive glucose transporter 2, and has been reported to be up-regulated in response to a HF diet [35]. Histological evaluation suggests that the C57BL/6N mice on the HF diet also experienced the most pronounced hepatic inflammation, compared to the C57BL/6J mice.

The findings of this study also demonstrate that the C3H/HeJ mice may not be completely resistant to diet-induced obesity and the subsequent metabolic changes. Differences in the C3H/HeJ strain's response to a high fat diet compared to previous reports may be attributed to the difference in the control strain used [21;22]. Specifically, previous studies have compared the C3H/H3J response to HF diet to C3H/HeOuJ or C3H/HeN, both of which have a functional TLR-4 [21;22]. No comparisons were made with C3H/HeJ mice on a control diet. Therefore, it is not possible to determine if the differences in metabolic response to a HF diet are a result of TLR-4 or genetic variability in the control substrain background. Furthermore, the C3H/HeJ strain has recently been shown to have a genetic variation in the leptin receptor gene (*Lep^r*) [36]. This mutation may account for the impaired metabolic response observed in the

C3H/HeJ strain on a HF diet due to the central role leptin has on regulating energy intake and expenditure as well as having implications on bone [16;17;37].

In conjunction with the metabolic comparisons, the other primary objective of this study was to compare the skeletal response of the two commonly used C57BL/6 substrains' to a HF diet. The C57BL/6J mice on the HF diet exhibited a 13.6% reduction in trabecular bone of the vertebra, although not statistically significant. The C57BL/6N was the only strain that exhibited significant trabecular bone loss which occurred only in the vertebra. In the absence of alterations in tibia trabecular and cortical bone microarchitecture, it is conceivable that the increase in adiposity loaded the skeletal at sites exposed to greater weight-bearing and offset some of the negative effects of glucose intolerance on bone [38;39]. The C57BL/6N mice had more prolonged exposure to hyperglycemia and hyperinsulinemia in response to the HF diet compared to the C57BL/6J substrain, and C57BL/6N were the only substrain to lose significant trabecular bone. While there have been conflicting reports on how a HF diet impacts bone in C57BL/6 mice [11-15], the results of this study indicate the skeletal response may be linked to the duration of disrupted insulin signaling and glucose intolerance. This idea is further supported by the response of the C3H/HeJ mice in which case an attenuated glucose, leptin and insulin response to the HF diet failed to induce bone loss. Several reports have shown that a high fat diet uncouples bone turnover by increasing bone resorption and decreasing bone formation in various rodent models [14;15;19]. Future studies are needed to investigate the mechanism involved in the site-specific loss of bone observed in this animal model.

Based on recent literature describing the hormone OCN as a regulator of systemic energy metabolism [40-42], the role of OCN on both metabolic and skeletal changes induced by HF were investigated. After 24 wk, the C57BL/6N mice on the HF diet had a lower ratio of plasma

Glu-OCN/ Gla-OCN. Because circulating under-carboxylated (Glu-OCN) can act directly on pancreatic β cells to stimulate insulin secretion [18;43-45], it would be expected that a reduction in Glu-OCN would lead to a decrease in insulin secretion. Instead, fasting plasma insulin was elevated in the C57BL/6N mice on the HF diet compared to their respective controls. Plasma insulin in the C57BL/6N mice was reduced at 24 wks relative to earlier time points (i.e., 16 and 20 wk), but the role of OCN on bone and energy metabolism during glucose intolerance warrants further investigation.

To date, this is the first study to directly compare the C57BL/6J and C57BL/6N substrains' response to a HF diet from a metabolic and skeletal perspective. The data presented here show that C57BL/6N mice exhibit an earlier metabolic response to the HF diet compared to the C57BL/6J mice. Moreover, the skeletal response followed that of the metabolic changes in that significant trabecular bone loss occurred in the C57BL/6N substrain with only a trend observed in the C57BL/6J mice. Whole body BMC and BMA was also lower following a HF diet than control in both of the C57BL/6 substrains and C3H/HeJ. (In large part, the C3H/HeJ strain was protected from the metabolic and skeletal changes induced by a HF diet. While a number of questions remain including how bone metabolism is being altered in response to a high fat diet on a molecular level. This study highlights the need to consider not only the most appropriate strain but the most appropriate substrain of mouse when designing experiments. Other important factors to consider when studying the relationship between glucose intolerance and bone include the site-specific skeletal response and the study duration. These decisions could significantly impact data interpretation and the translational implications as they relate to understanding how bone metabolism is altered in the context of T2DM.

Acknowledgments

We would like to express our gratitude to Kristen Hester and Sandra Peterson (Department of Nutritional Sciences, Oklahoma State University, Stillwater, OK 74078) for their technical assistance.

Funding

Oklahoma Center for the Advancement of Science and Technology (HR10-068); Oklahoma Agriculture Experiment Station (OKL02867); United States Department of Agriculture (2012-67011-19906).

Disclosure Statement

None of the authors have any conflicts to disclose.

Author Contributions

Elizabeth Rendina-Ruedy materially participated in the research and article preparation by substantially contributing to the conception design and conduct of the study, acquisition of data, and analysis and interpretation of data, drafting the article and revising it critically for important intellectual content, and providing final approval of the version being submitted.

Kelsey Hembree materially participated in the research by substantially contributing to acquisition of data, revising the article critically for important intellectual content, and providing final approval of the version being submitted.

Angela Sasaki materially participated in the research by substantially contributing to acquisition of data, revising the article critically for important intellectual content, and providing final approval of the version being submitted.

McKale Davis materially participated in the research and article preparation by substantially contributing analysis and interpretation of data, revising the article critically for important intellectual content, and providing final approval of the version being submitted.

Stan Lightfoot materially participated in the research and article preparation by substantially contributing to acquisition of data and analysis and interpretation of data, revising the article critically for important intellectual content, and providing final approval of the version being submitted.

Stephen Clarke materially participated in the research and article preparation by substantially contributing to the conception design and interpretation of data, revising the article critically for important intellectual content, and providing final approval of the version being submitted.

Edralin Lucas materially participated in the research and article preparation by substantially contributing to the conception design and interpretation of data, revising the article critically for important intellectual content, and providing final approval of the version being submitted.

Brenda Smith materially participated in the research and article preparation by substantially contributing to the conception design and conduct of the study, acquisition of data, and analysis and interpretation of data, drafting the article and revising it critically for important intellectual content, and providing final approval of the version being submitted.

References

- [1] Rishaug U, Birkeland KI, Falch JA, et al. Bone mass in non-insulin-dependent diabetes mellitus. *Scand J Clin Lab Invest* 1995 May;55(3):257-62.
- [2] van Daele PL, Stolk RP, Burger H, et al. Bone density in non-insulin-dependent diabetes mellitus. The Rotterdam Study. *Ann Intern Med* 1995 Mar 15;122(6):409-14.
- [3] Stolk RP, van Daele PL, Pols HA, et al. Hyperinsulinemia and bone mineral density in an elderly population: The Rotterdam Study. *Bone* 1996 Jun;18(6):545-9.
- [4] Nicodemus KK, Folsom AR. Type 1 and type 2 diabetes and incident hip fractures in postmenopausal women. *Diabetes Care* 2001 Jul;24(7):1192-7.
- [5] Melton LJ, III, Leibson CL, Achenbach SJ, et al. Fracture risk in type 2 diabetes: update of a population-based study. *J Bone Miner Res* 2008 Aug;23(8):1334-42.
- [6] Schwartz AV, Sellmeyer DE, Ensrud KE, et al. Older women with diabetes have an increased risk of fracture: a prospective study. *J Clin Endocrinol Metab* 2001 Jan;86(1):32-8.
- [7] Janghorbani M, Feskanich D, Willett WC, et al. Prospective study of diabetes and risk of hip fracture: the Nurses' Health Study. *Diabetes Care* 2006 Jul;29(7):1573-8.
- [8] Schwartz AV, Vittinghoff E, Bauer DC, et al. Association of BMD and FRAX score with risk of fracture in older adults with type 2 diabetes. *JAMA* 2011 Jun 1;305(21):2184-92.
- [9] Surwit RS, Kuhn CM, Cochrane C, et al. Diet-induced type II diabetes in C57BL/6J mice. *Diabetes* 1988 Sep;37(9):1163-7.
- [10] Collins S, Martin TL, Surwit RS, et al. Genetic vulnerability to diet-induced obesity in the C57BL/6J mouse: physiological and molecular characteristics. *Physiol Behav* 2004 Apr;81(2):243-8.
- [11] Gallou-Kabani C, Vige A, Gross MS, et al. C57BL/6J and A/J mice fed a high-fat diet delineate components of metabolic syndrome. *Obesity (Silver Spring)* 2007 Aug;15(8):1996-2005.
- [12] Patsch JM, Kiefer FW, Varga P, et al. Increased bone resorption and impaired bone microarchitecture in short-term and extended high-fat diet-induced obesity. *Metabolism* 2011 Feb;60(2):243-9.
- [13] Ionova-Martin SS, Wade JM, Tang S, et al. Changes in cortical bone response to high-fat diet from adolescence to adulthood in mice. *Osteoporos Int* 2011 Aug;22(8):2283-93.

- [14] Parhami F, Tintut Y, Beamer WG, et al. Atherogenic high-fat diet reduces bone mineralization in mice. *J Bone Miner Res* 2001 Jan;16(1):182-8.
- [15] Halade GV, Rahman MM, Williams PJ, et al. High fat diet-induced animal model of age-associated obesity and osteoporosis. *J Nutr Biochem* 2010 Dec;21(12):1162-9.
- [16] Steppan CM, Crawford DT, Chidsey-Frink KL, et al. Leptin is a potent stimulator of bone growth in ob/ob mice. *Regul Pept* 2000 Aug 25;92(1-3):73-8.
- [17] Ducy P, Amling M, Takeda S, et al. Leptin inhibits bone formation through a hypothalamic relay: a central control of bone mass. *Cell* 2000 Jan 21;100(2):197-207.
- [18] Lee NK, Sowa H, Hinoi E, et al. Endocrine regulation of energy metabolism by the skeleton. *Cell* 2007 Aug 10;130(3):456-69.
- [19] Lu XM, Zhao H, Wang EH. A high-fat diet induces obesity and impairs bone acquisition in young male mice. *Mol Med Rep* 2013 Apr;7(4):1203-8.
- [20] Tsukumo DM, Carvalho-Filho MA, Carvalheira JB, et al. Loss-of-function mutation in Toll-like receptor 4 prevents diet-induced obesity and insulin resistance. *Diabetes* 2007 Aug;56(8):1986-98.
- [21] Poggi M, Bastelica D, Gual P, et al. C3H/HeJ mice carrying a toll-like receptor 4 mutation are protected against the development of insulin resistance in white adipose tissue in response to a high-fat diet. *Diabetologia* 2007 Jun;50(6):1267-76.
- [22] Nakamura H, Fukusaki Y, Yoshimura A, et al. Lack of Toll-like receptor 4 decreases lipopolysaccharide-induced bone resorption in C3H/HeJ mice in vivo. *Oral Microbiol Immunol* 2008 Jun;23(3):190-5.
- [23] Rauner M, Sipos W, Pietschmann P. Osteoimmunology. *Int Arch Allergy Immunol* 2007;143(1):31-48.
- [24] Bandow K, Maeda A, Kakimoto K, et al. Molecular mechanisms of the inhibitory effect of lipopolysaccharide (LPS) on osteoblast differentiation. *Biochem Biophys Res Commun* 2010 Nov 26;402(4):755-61.
- [25] Reed MJ, Meszaros K, Entes LJ, et al. A new rat model of type 2 diabetes: the fat-fed, streptozotocin-treated rat. *Metabolism* 2000 Nov;49(11):1390-4.
- [26] Yokoi N, Hoshino M, Hidaka S, et al. A Novel Rat Model of Type 2 Diabetes: The Zucker Fatty Diabetes Mellitus ZFDM Rat. *J Diabetes Res* 2013;2013:103731.
- [27] Mekada K, Abe K, Murakami A, et al. Genetic differences among C57BL/6 substrains. *Exp Anim* 2009 Apr;58(2):141-9.

- [28] Freeman HC, Hugill A, Dear NT, et al. Deletion of nicotinamide nucleotide transhydrogenase: a new quantitative trait locus accounting for glucose intolerance in C57BL/6J mice. *Diabetes* 2006 Jul;55(7):2153-6.
- [29] Huang TT, Naeemuddin M, Elchuri S, et al. Genetic modifiers of the phenotype of mice deficient in mitochondrial superoxide dismutase. *Hum Mol Genet* 2006 Apr 1;15(7):1187-94.
- [30] Rendina E, Lim YF, Marlow D, et al. Dietary supplementation with dried plum prevents ovariectomy-induced bone loss while modulating the immune response in C57BL/6J mice. *J Nutr Biochem* 2012 Jan;23(1):60-8.
- [31] Rendina E, Hembree KD, Davis MR, et al. Dried plum's unique capacity to reverse bone loss and alter bone metabolism in postmenopausal osteoporosis model. *PLoS One* 2013;8(3):e60569.
- [32] Toye AA, Lippiat JD, Proks P, et al. A genetic and physiological study of impaired glucose homeostasis control in C57BL/6J mice. *Diabetologia* 2005 Apr;48(4):675-86.
- [33] Nicholson A, Reifsnnyder PC, Malcolm RD, et al. Diet-induced obesity in two C57BL/6 substrains with intact or mutant nicotinamide nucleotide transhydrogenase (Nnt) gene. *Obesity (Silver Spring)* 2010 Oct;18(10):1902-5.
- [34] Freeman H, Shimomura K, Horner E, et al. Nicotinamide nucleotide transhydrogenase: a key role in insulin secretion. *Cell Metab* 2006 Jan;3(1):35-45.
- [35] Riu E, Ferre T, Hidalgo A, et al. Overexpression of c-myc in the liver prevents obesity and insulin resistance. *FASEB J* 2003 Sep;17(12):1715-7.
- [36] Kapur S, Amoui M, Kesavan C, et al. Leptin receptor (Lepr) is a negative modulator of bone mechanosensitivity and genetic variations in Lepr may contribute to the differential osteogenic response to mechanical stimulation in the C57BL/6J and C3H/HeJ pair of mouse strains. *J Biol Chem* 2010 Nov 26;285(48):37607-18.
- [37] Hamann A, Matthaei S. Regulation of energy balance by leptin. *Exp Clin Endocrinol Diabetes* 1996;104(4):293-300.
- [38] Looker AC, Flegal KM, Melton LJ, III. Impact of increased overweight on the projected prevalence of osteoporosis in older women. *Osteoporos Int* 2007 Mar;18(3):307-13.
- [39] Kuruvilla SJ, Fox SD, Cullen DM, et al. Site specific bone adaptation response to mechanical loading. *J Musculoskelet Neuronal Interact* 2008 Jan;8(1):71-8.
- [40] Clemens TL, Karsenty G. The osteoblast: an insulin target cell controlling glucose homeostasis. *J Bone Miner Res* 2011 Apr;26(4):677-80.

- [41] Ferron M, Hinoi E, Karsenty G, et al. Osteocalcin differentially regulates beta cell and adipocyte gene expression and affects the development of metabolic diseases in wild-type mice. *Proc Natl Acad Sci U S A* 2008 Apr 1;105(13):5266-70.
- [42] Hinoi E, Gao N, Jung DY, et al. An Osteoblast-dependent mechanism contributes to the leptin regulation of insulin secretion. *Ann N Y Acad Sci* 2009 Sep;1173 Suppl 1:E20-E30.
- [43] Ferron M, Wei J, Yoshizawa T, et al. Insulin signaling in osteoblasts integrates bone remodeling and energy metabolism. *Cell* 2010 Jul 23;142(2):296-308.
- [44] Ferron M, McKee MD, Levine RL, et al. Intermittent injections of osteocalcin improve glucose metabolism and prevent type 2 diabetes in mice. *Bone* 2012 Feb;50(2):568-75.
- [45] Rached MT, Kode A, Silva BC, et al. FoxO1 expression in osteoblasts regulates glucose homeostasis through regulation of osteocalcin in mice. *J Clin Invest* 2010 Jan;120(1):357-68.

Table 1. Body Composition, Tissue Weights, Food Intake, Total White Blood Cell Counts and Adipokines

	C57BL/6J		C57BL/6N		C3H/HeJ	
	Con	HF	Con	HF	Con	HF
Final Bodyweight (g)	32.4 ± 0.7	41.2 ± 0.9*	33.7 ± 0.7	47.5 ± 0.7*	30.5 ± 0.6	39.3 ± 1.1*
Body Composition						
<i>Lean (g)</i>	21.8 ± 0.4	24.9 ± 0.3*	22.1 ± 0.3	27.7 ± 0.5*	19.8 ± 0.3	23.9 ± 0.5*
<i>Fat (g)</i>	7.1 ± 0.4	12.0 ± 1.2*	9.6 ± 0.6	18.3 ± 0.6*	6.7 ± 0.3	11.1 ± 0.6*
<i>Percent Fat (%)</i>	24.2 ± 1.0	31.8 ± 1.4*	29.4 ± 1.2	39.7 ± 0.9*	25.2 ± 0.8	31.5 ± 0.8*
Fat Pad (g)	0.68 ± 0.08	1.67 ± 0.13*	1.14 ± 0.11	1.69 ± 0.07*	0.52 ± 0.07	0.90 ± 0.06*
Food Intake (g/day)	3.17 ± 0.04	2.74 ± 0.06*	3.22 ± 0.04	2.98 ± 0.04*	3.19 ± 0.04	2.78 ± 0.06*
Thymus (g)	0.042 ± 0.002	0.048 ± 0.003	0.055 ± 0.004	0.076 ± 0.006*	0.019 ± 0.002	0.024 ± 0.002
Spleen (g)	0.091 ± 0.005	0.098 ± 0.004	0.106 ± 0.006	0.132 ± 0.009*	0.101 ± 0.004	0.123 ± 0.006*
Total White Blood Cells (1 x 10⁵)	17.04 ± 1.80	18.55 ± 1.61	21.69 ± 1.55	16.14 ± 1.72*	7.60 ± 0.71	11.48 ± 1.05*
Adipokines						
<i>Leptin (ng/mL)</i>	3.64 ± 1.14	16.13 ± 3.67*	8.92 ± 1.87	44.96 ± 5.06*	0.84 ± 0.15	11.08 ± 2.72*
<i>Adiponectin (µg/mL)</i>	9.94 ± 0.76	7.45 ± 0.72*	6.36 ± 0.34	6.97 ± 0.25	5.05 ± 0.40	5.13 ± 0.17

Final body weight, body composition, food intake, tissue weight, and total white blood cell counts (WBC) and adipokines after 24 wk on a fed a control (Con=AIN-93M) or a high fat diet (HF=45% kcal from fat) in C57BL/6J, C57BL/6N, C3H/HeJ mice. Values are means ± SE, n = 15 mice in each group. Symbol, *, represents a significant difference (P < 0.05) between dietary treatments within a given strain

Table 2. Pathological Scoring of Hepatic Tissue after 24 wk on a Control or High Fat Diet

	C57BL/6J							C57BL/6N							C3H/HeJ							
	0	1	2	3	4	Mean	P-value	0	1	2	3	4	Mean	P-value	0	1	2	3	4	Mean	P-value	
Steatosis																						
<i>Con</i>	10	1	0	0	0	0.09	0.0028	6	2	3	0	0	0.73	0.0020	10	0	0	0	0	0.00	0.0001	
<i>HF</i>	2	4	6	1	0	1.46		0	2	1	2	8	3.23		1	4	5	4	0	1.86		
Fibrosis																						
<i>Con</i>	0	0	0	0	0	0.00	-	11	0	0	0	0	0.00	0.0885	10	0	0	0	0	0.00	-	
<i>HF</i>	0	0	0	0	0	0.00		10	3	0	0	0	0.23		14	0	0	0	0	0.00		
	0	1	2	3								0	1	2	3							
Lobular Inflammation																						
<i>Con</i>	11	0	0	0	0	0.00	0.0038	11	0	0	0	0	0.00	<0.0001	10	0	0	0	0	0.00	0.0641	
<i>HF</i>	6	7	0	0	0	0.54		1	12	0	0	0	0.92		10	4	0	0	0	0.29		
Portal Inflammation																						
<i>Con</i>	11	0	0	0	0	0.00	0.0885	11	0	0	0	0	0.00	0.0001	10	0	0	0	0	0.00	-	
<i>HF</i>	10	3	0	0	0	0.23		3	10	0	0	0	0.77		14	0	0	0	0	0.00		
	0	1	2								0	1	2									
Balloon Degeneration																						
<i>Con</i>	0	0	0	0	0	0.00	0.0062	11	0	0	0	0	0.00	<0.0001	10	0	0	0	0	0.00	<0.0001	
<i>HF</i>	5	7	1	0	0	0.69		0	0	13	0	0	2.00		1	3	10	0	0	1.64		

Frequency of steatosis (0-4), lobular and portal inflammation (0-3), fibrosis (0-4), and balloon degeneration (0-2), along with mean scores and P-values for control vs. high fat diet within a given strain based on chi-squared statistical analyses.

Table 3. Bone Densitometry of the Whole Body and Bone Microarchitectural Parameters of the Spine and Tibia

	C57BL/6J		C57BL/6N		C3H/HeJ	
	Con	HF	Con	HF	Con	HF
Whole Body Bone Densitometry						
<i>BMC (mg)</i>	731.2 ± 30.3	622.8 ± 23.6*	614.5 ± 24.1	492.9 ± 11.8*	878.5 ± 25.1	810.1 ± 14.3*
<i>BMA (cm²)</i>	12.31 ± 0.40	10.87 ± 0.42*	11.03 ± 0.33	8.91 ± 0.12*	12.90 ± 0.15	11.76 ± 0.22*
<i>BMD (mg/cm²)</i>	59.0 ± 0.8	57.2 ± 0.6	55.9 ± 0.8	55.4 ± 0.6	69.5 ± 0.7	68.6 ± 0.7
<i>BMD/ body weight [(mg/cm²)/g]</i>	1.84 ± 0.05	1.39 ± 0.05*	1.67 ± 0.04	1.17 ± 0.02*	2.29 ± 0.05	1.76 ± 0.05*
Lumbar Vertebra Trabecular						
<i>Connectivity Density (1/mm³)</i>	232.45 ± 13.37	249.77 ± 10.96	221.21 ± 14.25	214.62 ± 16.73	145.78 ± 18.26	116.81 ± 10.83
<i>SMI</i>	0.30 ± 0.09	0.67 ± 0.02*	0.59 ± 0.10	1.00 ± 0.09*	1.10 ± 0.11	1.07 ± 0.09
<i>Apparent Density (mg HA/ ccm)</i>	395.86 ± 20.97	364.38 ± 7.04	358.84 ± 7.84	318.54 ± 8.85*	279.49 ± 10.48	287.93 ± 11.99
<i>Material Density (mg HA/ ccm)</i>	1093.1 ± 6.7	1084.0 ± 8.9	1078.5 ± 8.3	1076.9 ± 8.2	1123.5 ± 10.2	1135.5 ± 11.1
Tibial Midshaft						
<i>Cortical Porosity (%)</i>	4.30 ± 0.26	4.35 ± 0.13	4.50 ± 0.14	4.71 ± 0.10	3.07 ± 0.08	3.69 ± 0.45
<i>Cortical Thickness (mm)</i>	0.17 ± 0.04	0.19 ± 0.04	0.14 ± 0.03	0.16 ± 0.03	0.18 ± 0.05	0.20 ± 0.04
<i>Cortical Area (mm²)</i>	0.011 ± 0.001	0.010 ± 0.001	0.010 ± 0.001	0.011 ± 0.001	0.014 ± 0.001	0.013 ± 0.001
<i>Medullary Area (mm²)</i>	0.035 ± 0.001	0.032 ± 0.001	0.034 ± 0.004	0.037 ± 0.002	0.030 ± 0.001	0.034 ± 0.001*

Whole body bone densitometry and trabecular and cortical bone microarchitecture after 24 wk on a control (AIN-93M) or a HF (45% kcal from fat). Values are means ± SE, *n* = 10-15 mice per group for bone densitometry and *n* = 6 mice per group for MicroCT data. Symbol, *, represents a significant difference (*P* < 0.05) between dietary treatments within a given strain. Values are means ± SE.

Table 4. Relative Fold Change of Gene Expression in the Liver and Bone Marrow in Mice Fed a High Fat Diet Compared to the Control Diet

	C57BL/6J		C57BL/6N		C3H/HeJ	
	HF	<i>P-value</i>	HF	<i>P-value</i>	HF	<i>P-value</i>
Liver						
<i>Fasn</i>	1.55 ± 0.31	0.1748	2.20 ± 0.36*	0.0248	1.23 ± 0.35	0.5934
<i>Gpx1</i>	0.89 ± 0.12	0.6197	1.54 ± 0.15*	0.0127	1.31 ± 0.14	0.1653
<i>Ppara</i>	1.10 ± 0.16	0.5427	1.41 ± 0.11*	0.0478	0.98 ± 0.10	0.8582
<i>Slc2a2</i>	0.99 ± 0.10	0.9792	1.56 ± 0.14*	0.0096	1.08 ± 0.21	0.7756
<i>Srebp1c</i>	1.20 ± 0.26	0.4985	2.07 ± 0.51	0.0997	0.93 ± 0.21	0.8329
<i>Tnf</i>	1.76 ± 0.40	0.2237	1.12 ± 0.28	0.7238	2.09 ± 0.51	0.0703
Bone Marrow						
<i>Fasn</i>	0.94 ± 0.05	0.6811	0.94 ± 0.07	0.5619	1.20 ± 0.15	0.2388
<i>Gpx1</i>	0.56 ± 0.08*	0.0053	1.45 ± 0.13*	0.0228	1.05 ± 0.18	0.7983
<i>Pparg</i>	1.35 ± 0.39	0.4349	0.78 ± 0.10	0.1829	1.21 ± 0.18	0.3279

Mean fold regulation of genes involved in systemic metabolism and inflammation are presented for the animals on the high fat diet (45% kcal from fat) relative to their control (AIN-93M). All target genes were normalized to invariant control (*Ppib*). Symbol, *, represents a significant difference ($P = 0.05$) between dietary treatments within a given strain.

Figure Legends.

Figure 1. Weekly Body Weights. Body weights of C57BL/6J, C57BL/6N, and C3H/HeJ mice fed a control (Con; AIN-93M) or a high fat diet (HF; 45% kcal from fat) were recorded weekly. Data is presented as the mean \pm SE, $n = 15$ mice in each group. Symbols, * for C57BL/6J, † for C57BL/6N, or § for C3H/HeJ indicate significant differences ($P < 0.05$) of dietary treatment within a given mouse strain.

Figure 2. Fasting Blood Glucose and Plasma Insulin Over Time. Blood glucose (A) and plasma insulin (B) was determined at 4 wk intervals in mice from each of the three strains fed a control (Con; AIN-93M) or a high fat diet (HF; 45% kcal from fat). Symbols, * for C57BL/6J, † for C57BL/6N, or § for C3H/HeJ indicate significant differences ($P < 0.05$) of dietary treatment for a given mouse strain.

Figure 3. Glucose Tolerance Test Results Following 24 wk on Control or High Fat Diet.

One week prior to the end of the study, an intraperitoneal glucose tolerance test was administered (2 g glucose/ kg body weight) in the C57BL/6J, C57BL/6N, and C3H/HeJ mice fed a control (Con; AIN-93M) or a high fat diet (HF; 45% kcal from fat). (A) Tail blood was collected following 15, 30, 60, 90, and 120 min following glucose injection and symbols, * for C57BL/6J, † for C57BL/6N, or § C3H/HeJ indicate significant differences ($P < 0.05$) of dietary treatment for a given mouse strain. (B) Area under the curve (AUC) was calculated for the IGTT and symbol, *, represents a significant difference ($P < 0.05$) between dietary treatments for a given strain.

Figure 4. Alterations in Plasma Osteocalcin due to a High Fat Diet. Plasma osteocalcin (OCN) expressed as percent of undercarboxylated (Glu)-OCN per total (Gla)-OCN in C57BL/6J, C57BL/6N, and C3H/HeJ mice on a control (Con; AIN-93M) or a high fat diet (HF; 45% kcal from fat) after 24 wk. Symbol, *, represents a significant difference ($P < 0.05$) between dietary treatments for a given strain.

Figure 5. Representative Micrographs of Liver Histology Sections of liver were harvested, processed and stained with hematoxylin and eosin from C57BL/6J, C57BL/6N, and C3H/HeJ mice following 24 wk on a control (Con; AIN-93M) or a high fat diet (HF; 45% kcal from fat). Representative images were photographed and are presented at a 10 x magnification.

Figure 6. Alterations in Trabecular Bone Microarchitecture in the Lumbar Vertebra. MicroCT analyses of trabecular bone in the lumbar vertebra (L4) in C57BL/6J, C57BL/6N, and C3H/HeJ mice on a control (Con; AIN-93M) or a high fat diet (HF; 45% kcal from fat) for 24 wk. Parameters include (A) bone volume/ total volume (BV/TV), (B) trabecular number (Tb.N.), (C) Trabecular thickness (Tb.Th.), and (D) trabecular separation (Tb.Sp.). Symbol, *, represents a significant difference ($P < 0.05$) between dietary treatments for a given strain.

Figure 1. Weekly Body Weight

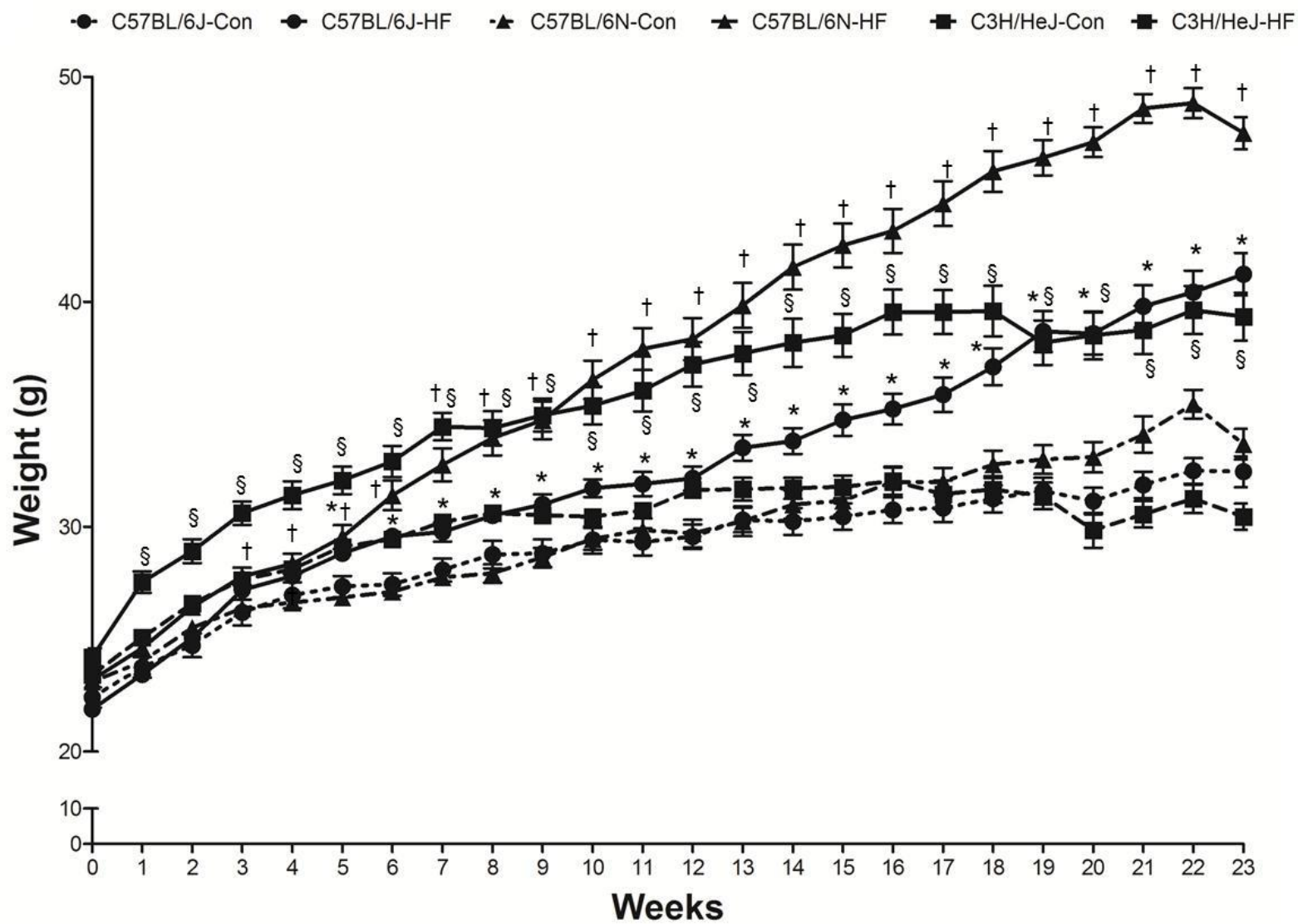


Figure 2. Blood Glucose and Plasma Insulin Over Time

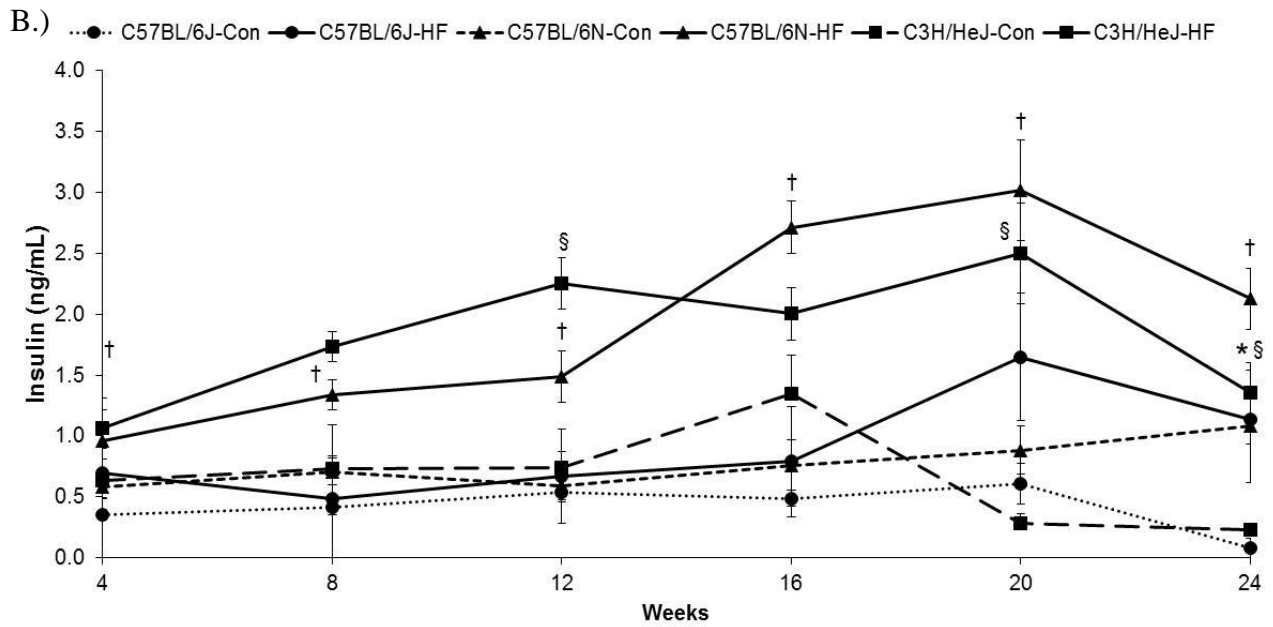
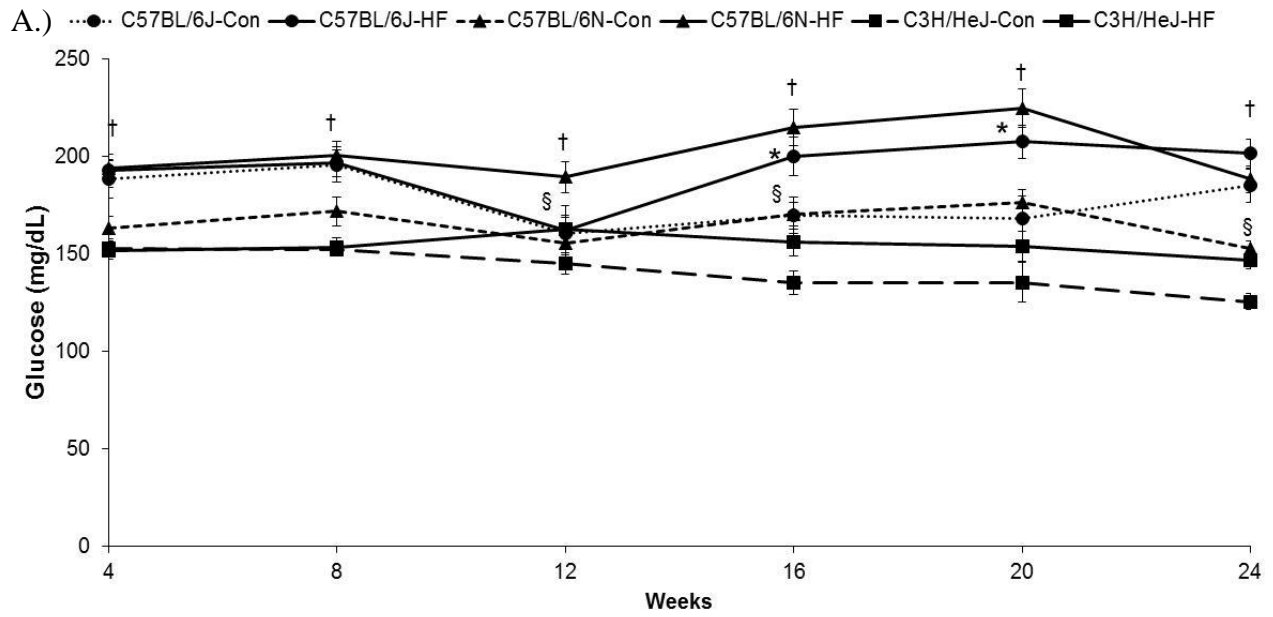


Figure 3. Glucose Tolerance Test Results After 24 Weeks on a High Fat Diet

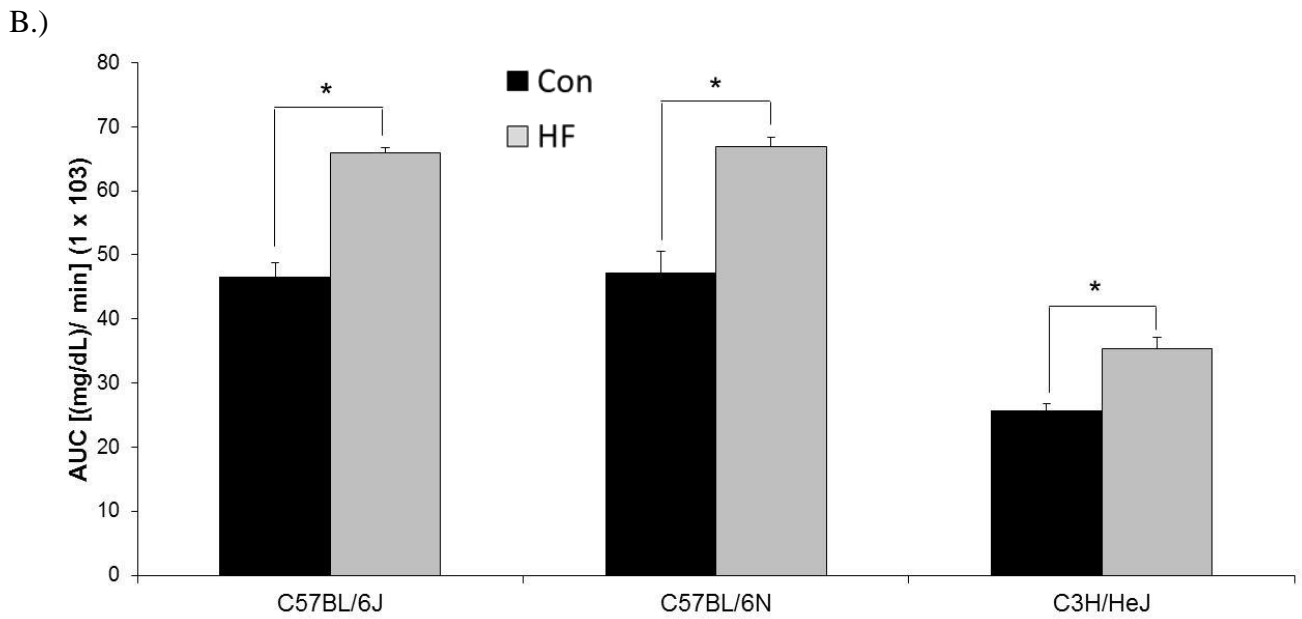
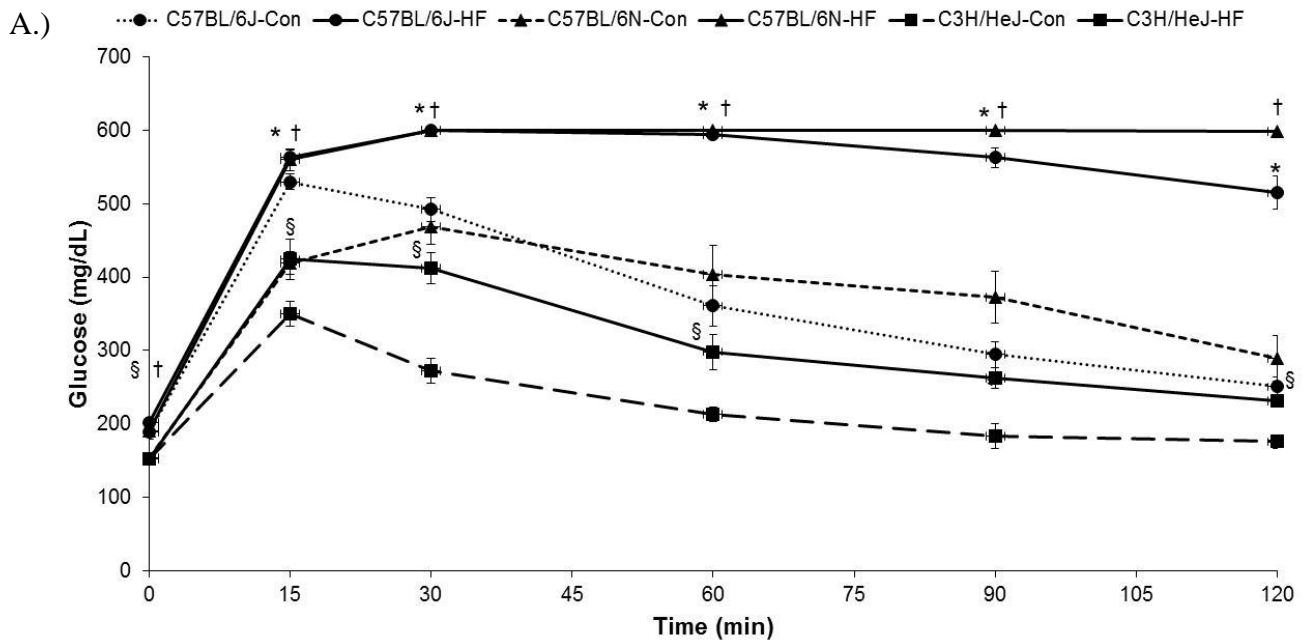


Figure 4. Strain Comparison of Carboxylation Status of Plasma OCN After 24 Wk on a Control or High Fat Diet

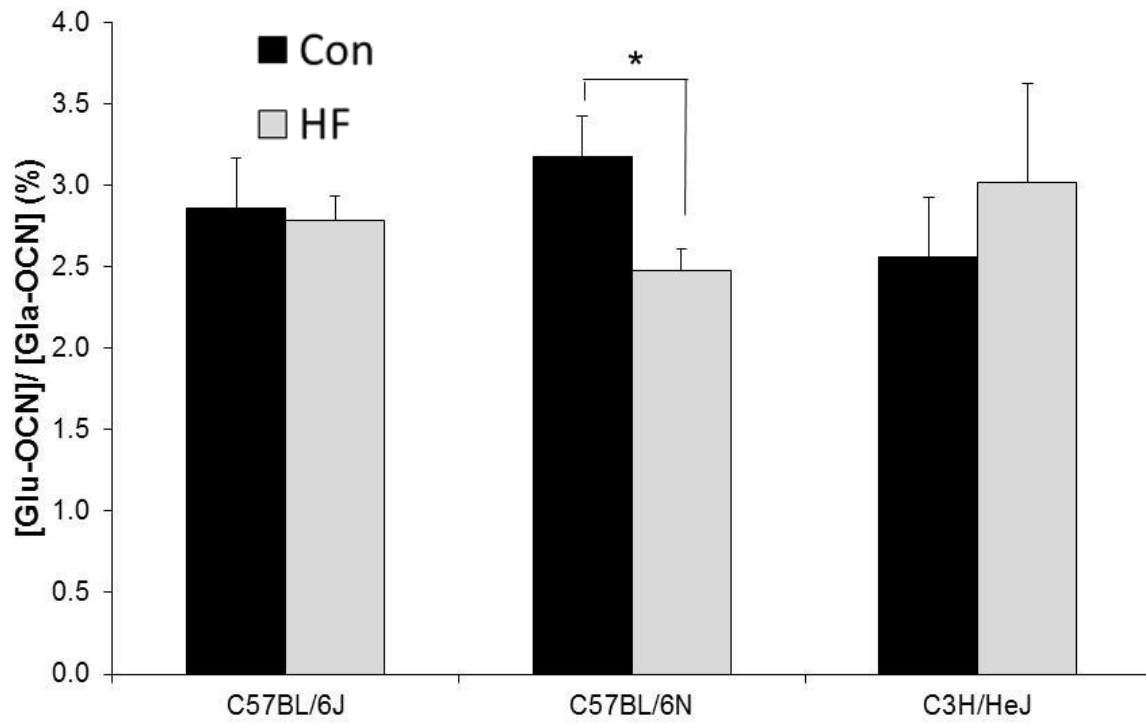


Figure 5. Representative Micrographs of Liver Histology

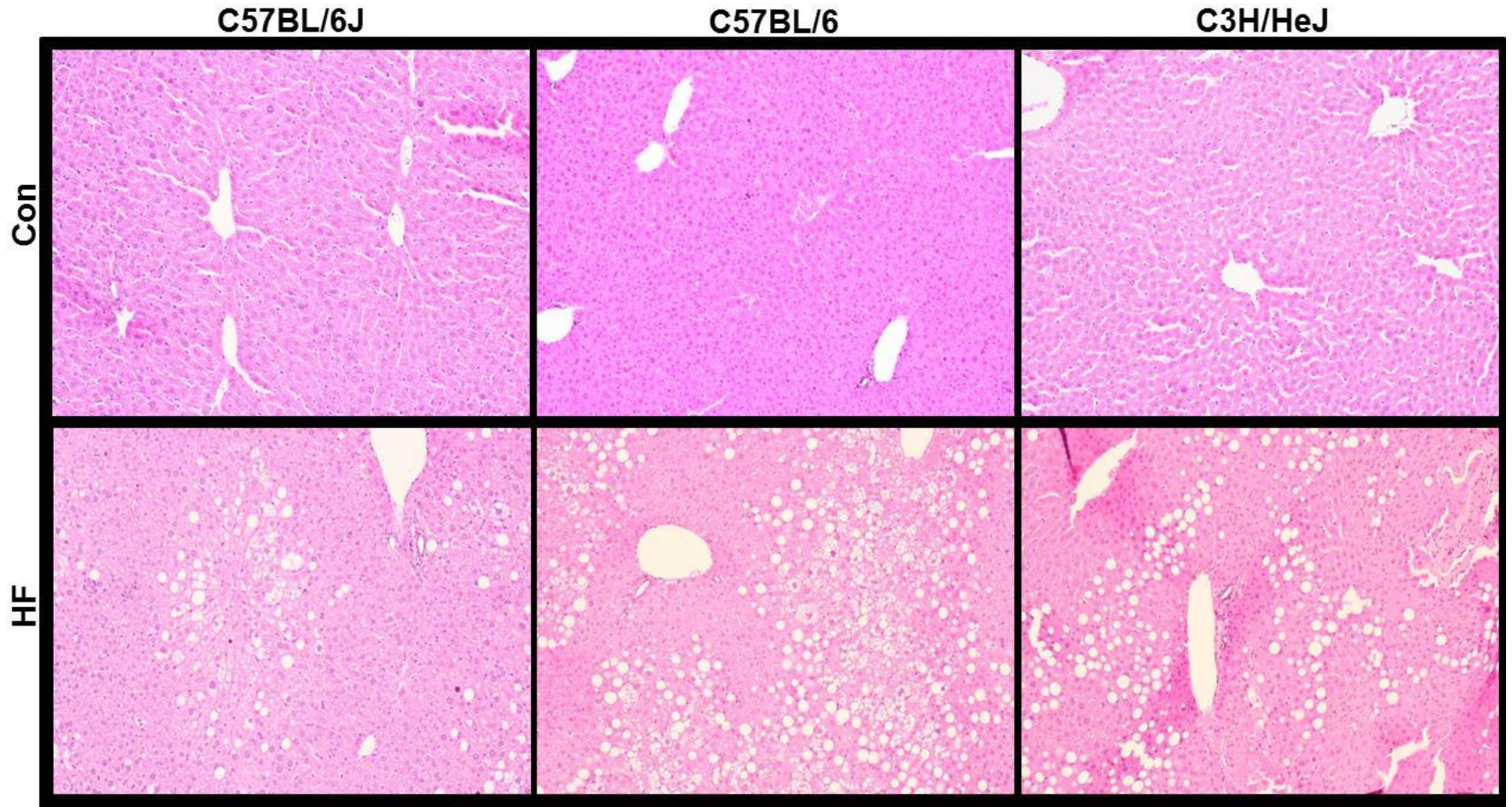
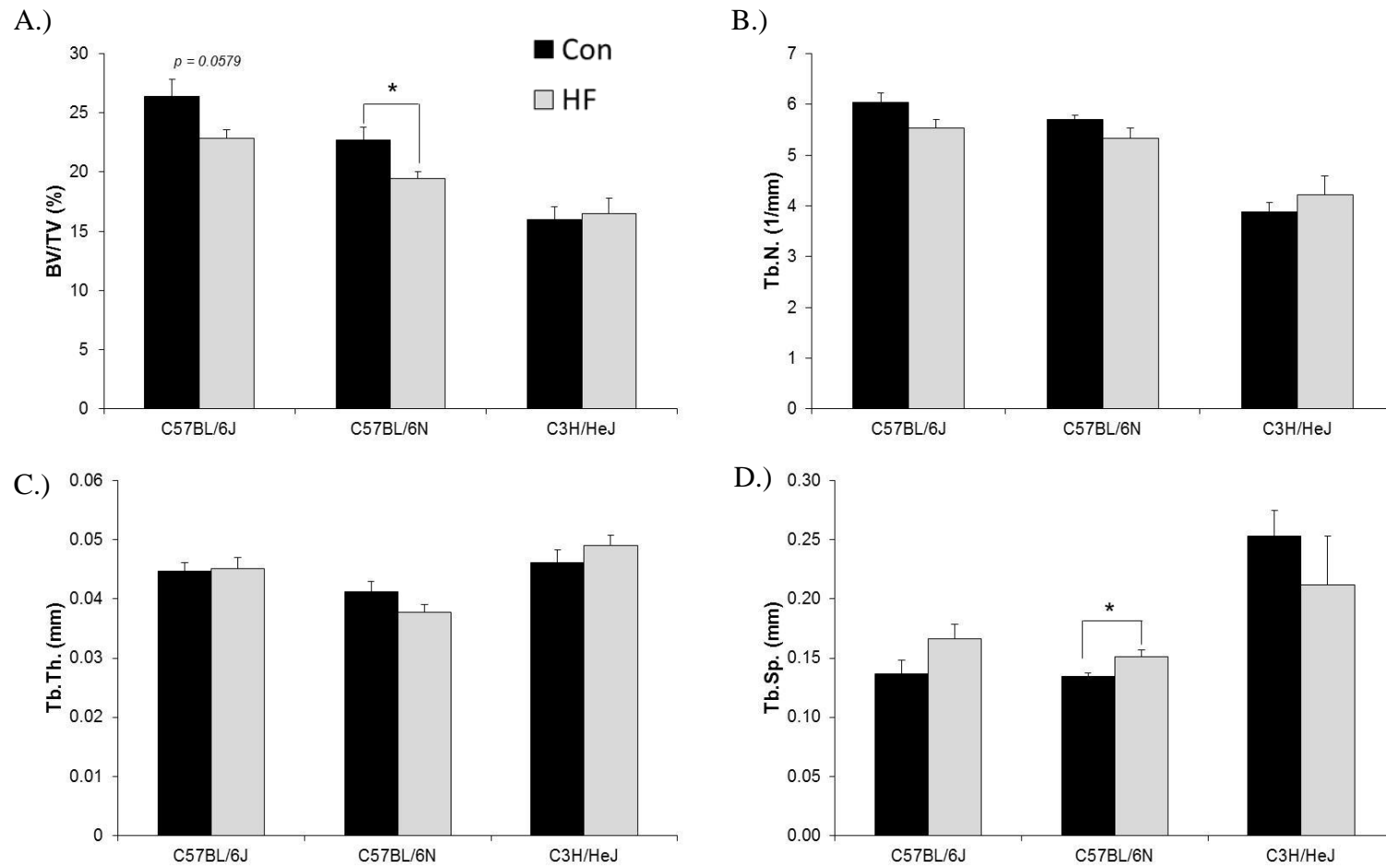


Figure 6. Alterations in Trabecular Bone Microarchitecture in the Lumbar Vertebra



Supplemental Table 1. qPCR Primer List

NCBI Gene Accession Reference	Symbol	Name	Sequence
NM_007988.3	<i>Fasn</i>	Fatty acid synthase	QF 5'- GCT GCG GAA ACT TCA GGA AAT -3'
			QR 5'- AGA GAC GTG TCA CTC CTG GAC TT -3'
NM_008160.6	<i>Gpx1</i>	Glutathione peroxidase	QF 5'- CGG TTT CCC GTG CAA TC -3'
			QR 5'- GAG GGA ATT CAG AAT CTC TTC AT -3'
XM_006520619.1	<i>Ppara</i>	Peroxisome proliferator activated receptor alpha	QF 5'- CGT ACG GCA ATG GCT TTA TC -3'
			QR 5'- AAC GGC TTC CTC AGG TTC TT -3'
XM_006505737.1	<i>Pparg</i>	Peroxisome proliferator activated receptor gamma	QF 5'- CAA GAA TAC CAA AGT GCG ATC AA -3'
			QR 5'- GAG CTG GGT CTT TTC AGA ATA ATA AG -3'
NM_011149.2	<i>Ppib</i>	Peptidylprolyl isomerase B	QF 5'- TGG AGA GCA CCA AGA CAG ACA -3'
			QR 5'- TGC CGG AGT CGA CAA TGA T -3'
NM_031197.2	<i>Slc2a2</i>	Solute carrier family 2 (facilitated glucose transporter), member 2	QF 5'- CAA CTG GGT CTG CAA TTT TGT C -3'
			QR 5'- GAA CAC GTA AGG CCC AAG GA -3'
XM_006532716.1	<i>Srebp1c</i>	Sterol regulatory element-binding protein	QF 5'- GGA GCC ATG GAT TGC ACA TT -3'
			QR 5'- GGC CCG GGA AGT CAC TGT -3'
NM_001278601.1	<i>Tnf</i>	Tumor necrosis factor	QF 5'- CTG AGG TCA ATC TGC CCA AGT AC -3'
			QR 5'- CTT CAC AGA GCA ATG ACT CCA AAG -3'

CHAPTER IV

THE ATTENUATION OF BONE ACCRUAL IN YOUNG, GROWING MICE IN A
DIET-INDUCED OBESITY MODEL OF TYPE 2 DIABETES MELLITUS INVOLVES

TLR-4

Title: The Attenuation of Bone Accrual in Young, Growing Mice in a Diet-Induced Obesity Model of Type 2 Diabetes Mellitus Involves TLR-4

Authors: Elizabeth Rendina-Ruedy¹, Jennifer L. Graef¹, McKale R. Davis¹, Kelsey D. Hembree¹, Jeff M. Gimble², Stephen L. Clarke¹, Edralin A. Lucas¹, Brenda J. Smith¹

¹Department of Nutritional Sciences, Oklahoma State University, Stillwater, OK, United States of America.

²Stem Cell Biology Laboratory, Pennington Biomedical Research Center, Louisiana State University, Baton Rouge, LA, United States of America

Corresponding Author: Brenda J. Smith, Department of Nutritional Sciences, HSci 420 Oklahoma State University, Stillwater OK 74078; (405) 744-3866; bjsmith@okstate.edu

Grant Supporters: Oklahoma Center for the Advancement of Science and Technology (HR10-068) and United States Department of Agriculture (2012-67011-19906).

Keywords: hyperglycemia, insulin, inflammation, fracture, osteoblasts

Abstract

It has previously been demonstrated that activation of toll-like receptor (TLR)-4 is involved in the initiation and progression of T2DM. TLR-4 has also been shown to coordinate bone metabolism by decreasing osteoblast differentiation, activity, and survival while increasing osteoclastogenesis. Therefore, the current study aimed to investigate the role TLR-4 contributes to the dysregulation of bone metabolism during the initiation and progression of T2DM. Four-week old male C3H/HeJ mice, which possess a non-functional TLR-4, and C57BL/6 control were randomly assigned to a control (Con=10% kcal fat) or high fat (HF=60% kcal fat) diet for 2, 8, or 16 wk. Metabolic changes including fasting blood glucose, plasma insulin, and glucose tolerance were monitored over time in conjunction with alterations occurring in bone structure and metabolism. Elevated fasting blood glucose was observed in both the C57BL/6 and C3H/HeJ strains on the HF diet at 2 and 8 wk, but only in the C57BL/6 strain at 16 wk. Both strains on the HF diet demonstrated impaired glucose tolerance at 2, 8, and 16 wk. The C57BL/6 mice on the HF diet exhibited lower whole body BMD by 8 and 16 wk, but C3H/HeJ strain had no evidence of bone loss until 16 wk. Analyses of bone microarchitecture revealed that the C57BL/6 mice on the HF diet experienced attenuated trabecular bone accrual in the distal femur metaphysis at 8 and 16 wk. Interestingly, the C3H/HeJ mice were protected from the deleterious impact of the HF diet on trabecular bone, suggesting TLR-4-mediated mechanisms responsible for attenuated bone formation in T2DM. These structural changes were accompanied with a decrease in osteoblastogenesis after 8 and 16 wk on the HF diet only in the C57BL/6 mice. Both the C57BL/6 and C3H/HeJ mice on a HF diet demonstrated an increase in osteoclastogenesis after 8 wk on HF diet, however, bone turnover was apparently decreased in the C57BL/6 during prolonged hyperglycemia. Further investigation is needed to understand the effects of TLR-4

signaling on osteoblasts and osteoclasts and changes that occur in bone microarchitectural and biomechanical properties in the context of T2DM.

Introduction

Current estimates indicate that approximately 35% of adults are obese and 17% of children and adolescents are overweight [1]. One of the most striking health consequences related to the prevalence of obesity has been the increase in the incidence of type 2 diabetes (T2DM), especially among children [2]. Classic complications associated with T2DM in adults have included micro- and macro vascular diseases, and more recently increased risk of fracture with increasing duration of diabetes has recently been added to the list [3-5]. Accumulating evidence suggests that overweight and obese children also experience an increased risk of fracture, but it is not clear whether these fractures result from compromised bone mass and quality or issues related to balance and risk of falls [6-10]. Similar to observations among overweight and obese adults, studies reporting DXA results suggest that obese children have a higher BMD compared to non-obese children [11;12]. However, when bone mass is expressed relative to bone size and body weight this is not the case [10]. Because bone accrual takes place in the first 2-3 decades of life, obese children are both at greater risk of fracture in their youth as well as being predisposed to greater risk of osteoporotic fractures later in life [10;13]. The increasing prevalence of T2DM among children and potential increase in lifetime fracture risk highlights the need for more research to understand the mechanisms through which altered glucose homeostasis affects bone.

Complications associated with T2DM usually require several years to develop. Therefore, animal models provide important tools for studying the molecular aspects and pathological effects of obesity-induced changes in glucose homeostasis and progression to severe glucose intolerance. Diet-induced obesity models of T2DM have been reported to have decreased bone mineral density (BMD), compromised trabecular and cortical bone, and reduced

bone strength, but the mechanisms involved have remained unclear [14-17]. For example, increased bone resorption due to the up-regulation of osteoclastogenesis has been proposed to be the central mechanism contributing to the deleterious effects on bone [15;16]. Conversely, Lu *et al.* [17] demonstrated that bone accrual is attenuated in young mice consuming a high fat diet in response to decreased osteoblast differentiation and subsequent impaired bone formation. Discrepancies in the findings related to bone metabolism may be attributed to differences in the duration of hyperglycemia and glucose intolerance, age at which the onset of impaired glucose tolerance is initiated, and alterations in insulin sensitivity. For instance, the insulin receptor (IR) is found abundantly expressed on the osteoblast [18;19]. Insulin has been shown to exert an anabolic effect on bone, increasing markers of osteoblast function (i.e., collagen synthesis and alkaline phosphatase or ALP) as well as to increase osteoclastogenesis by up-regulating the expression of receptor of NF- κ B ligand (RANKL) on the osteoblast [20;21]. Thus, with T2DM osteoblasts and osteoclasts are potentially exposed to scenarios of hyper- and hypo- glycemia and insulinemia. The described complexity of the metabolic profile during the initiation and progression of T2DM has contributed to the illusive nature of the mechanisms involved in dysregulating of bone metabolism.

Clues as to a relationship between inflammation and diabetes have existed since 1876 when the non-steroidal anti-inflammatory drug (NSAID), sodium salicylate, was shown to diminish sugar excretion [22]. More recently, mechanistic studies have described how activation of inflammatory pathways, such as toll-like receptor-4 or TLR-4 signaling, diminishes insulin sensitivity [23]. Interestingly, two ligands of TLR-4 (i.e., lipopolysaccharide or LPS and saturated free fatty acids or sFFA) have been shown to be up-regulated during the initiation and progression of T2DM [24-29] as well as many of the downstream inflammatory cytokines (e.g.,

tumor necrosis factor or TNF- α , interleukin or IL-1 β , and IL-6) [24-29]. Further evidence of the link between the immune response and insulin resistance has come from animal models such as the C3H/HeJ mouse, which possess a non-functional TLR-4. This mouse strain has been reported to be protected from developing insulin resistance in response to a high fat diet, as demonstrated by lower plasma insulin, higher glucose utilization, and preserved insulin sensitivity compared to control strains [30;31].

Bone cells, including bone resorbing osteoclasts and bone forming osteoblasts, constitutively express TLR-4 and are responsive to TLR-4 ligands, as well as cytokines produced from TLR-4 activation [32-34]. A novel rodent model of chronic, systemic inflammation induced by a slow release LPS pellet demonstrated that these animals experience a compromise in bone structure and microarchitecture [32;35-37]. LPS activation of the TLR-4 pathway has also been shown to increase osteoclastogenesis and osteoclast resorption activity. In addition to enhancing osteoclast differentiation and activity, TLR-4 stimulation has a profound impact on osteoblasts. LPS has not only been shown to suppress osteoblast differentiation and mineralization, but also stimulate osteoblast apoptosis [33;38]. The C3H/HeJ mice which fail to respond to LPS, exhibit a high BMD relative to other mouse strains [39] and have a higher bone formation rate and reduced osteoblast apoptosis [40-42]. Moreover, the C3H/HeJ strain appears to be protected from a bone phenotype in response to a high fat/ atherogenic diet [14]. Collectively, these data suggest that TLR-4 signaling has potent effects on bone metabolism.

To date, no study has investigated how the initial phases of impaired glucose tolerance and increasing duration of glucose intolerance associated with T2DM impact skeletal metabolism during a critical stage of bone accrual and how TLR-4 contributes to this bone phenotype. Therefore, the purpose of the current study was to investigate (1) how bone structure

and metabolism are altered over time in response to a diet-induced obesity model of T2DM in young, growing mice and (2) whether TLR-4 is contributing to the increase in fracture incidence during T2DM.

Materials and Methods

Animal Use and Care Procedures

Four-week old male C57BL/6N (Charles Rivers, Wilmington, MA), referred to hereafter as C57BL/6, and C3H/HeJ (Jackson Labs, Wilmington, MA) mice were utilized for the current study. The rationale for choosing the C57BL/6 mice was due to their responsiveness to high fat diet treatment [43], while the C3H/HeJ mice were utilized given their non-functional TLR-4 [29;44]. Following a one-week acclimation period, mice were divided into six groups ($n = 16$ mice/group) within each strain and assigned to a control (Con; AIN-93M, 10 % kcals from fat) or the high fat (HF; 60% kcals from fat) diet for 2, 8, or 16 wks. Bodyweight and food intake were monitored weekly throughout the duration of the study. Three to five days prior to the termination of each study (i.e., 2, 8, and 16 wk), mice were fasted for 6 hr and blood glucose was determined. At the end of each time point mice were anesthetized (ketamine/xylazine cocktail 70 and 30 mg/kg body weight, respectively) and whole body DXA scans (LunarPIXI, GE Medical Systems, Madison, WI) were performed with mice placed in the prone position. Mice were exsanguinated via the carotid artery, and blood was processed for plasma using EDTA and stored at -80°C for further analysis. Left femurs were cleaned of soft-adhering tissue and stored in phosphate buffered saline (PBS) at 4°C until microCT analyses and biomechanical testing was performed. PBS was also used to flush the bone marrow from the iliac crest for *ex vivo* cell

culture experiments and from the femur for bone marrow RNA extraction. Calvaria samples were collected at the time of sacrifice and frozen immediately in liquid nitrogen until RNA extraction procedure was carried out. All procedures performed in this study were approved by the Institutional Animal Care and Use Committee of Oklahoma State University.

Evaluation of Body Composition and Whole Body BMD by DXA

Body composition and whole body bone mineral area (BMA), bone mineral content (BMC) and BMD were determined using PIXImus Series Software version 2.10 (Lunar Corporation, Madison, WI).

Fasting Blood Glucose, Intraperitoneal Glucose Tolerance Test (IGTT), and Plasma Insulin

To determine if glucose tolerance was affected by treatment, mice received an intraperitoneal injection of glucose solution (2 g glucose/ kg bodyweight) and blood glucose was monitored at 15, 30, 60, 90, and 120 minutes. Area under the curve (AUC) was calculated by determining the sum of each rectangular area between two time points.

Fasting plasma insulin was determined at 2, 8 and 16 wks using a commercially available ELISA kit (Crystal Chem, Downers Grove, IL) and the manufacturer's protocol was followed.

Determination of Trabecular and Cortical Bone by MicroCT

Micro-computerized tomography (microCT40, SCANCO Medical, Switzerland) was performed to determine changes in the trabecular and cortical bone microarchitecture. The distal femur metaphysis and mid-diaphysis were used to evaluate trabecular and cortical bone within the appendicular skeleton, and were scanned at a resolution of 2048 x 2048 pixels. The trabecular bone volume of interest (VOI) was identified as a 900 μm region of secondary spongiosa within the distal femur metaphysis. The trabecular parameters evaluated included trabecular bone volume expressed as a percentage of total volume (BV/TV), trabecular number (Tb.N.), trabecular thickness (Tb.Th.), trabecular separation (Tb.Sp.) connectivity density (ConnDens) and structural model index (SMI). Evaluation of cortical bone was performed by analyzing a 270 μm section at the mid-point of the femur. Cortical bone parameters assessed included cortical porosity, thickness, area, and medullary area. All of the acquired images of cortical and trabecular bone were analyzed at a threshold of 340, and a sigma and support of 1.2 and 2.0, respectively.

Analysis of trabecular bone of the axial skeleton was accomplished by evaluating the lumbar vertebra. Images were acquired at a resolution of 1024 x 1024 pixels, beginning 80 μm from the dorsal and caudal growth plates. Similar to the femoral analysis, trabecular bone was determined based on analysis of secondary spongiosa only within the VOI. The images obtained of the vertebra were analyzed at a threshold of 310, and a sigma of 1.2 and support of 2.0.

Analysis of Biomechanical Properties of the Femur

Reference point indentation (RPI) was used (BioDent, Active Life Scientific, Inc, Santa Barbara, CA) to determine alterations in the biomechanical properties of the femur due to altered

glucose homeostasis [45;46]. Testing was performed at two sites, the anterior surface of the femur mid-diaphysis, a primarily cortical bone site, and the lateral region of the distal femur metaphysis, a site that consists of both cortical and trabecular bone. At both sites a testing protocol of 2 N force, 2 Hz, and 10 cycles was used. The first cycle indentation distance (ID) was reported as a distance parameter reflective of the touchdown distance to the retraction distance on the initial cycle, indicative of bone biomechanical properties.

Ex vivo Osteoblastogenesis and Osteoclastogenesis Experiments

Bone marrow cells were harvested from the iliac crest using sterile phosphate buffered saline (PBS) for evaluation of the effect of treatment on osteoblast and osteoclast precursor cells. Bone marrow samples were pooled from 4-5 animals in each experimental group and pelleted by centrifugation at 4°C for 5 min at 1000 x g. The cells were then resuspended in 20 mL of complete alpha MEM (10 % FBS, 1% penicillin/ streptomycin, 20 mM L-glutamine), plated in flasks, and maintained at 37.0°C in 5% CO₂. Following 2 days in culture, the adherent stromal-cell population was harvested for osteoblast experiments while the non-adherent cells were used for osteoclastogenesis experiments.

For osteoblast experiments, stromal cells were plated at a density of 1×10^6 cells/mL. Cells were allowed to become 80-100% confluent and then changed to an osteogenic medium (i.e., complete α MEM supplemented with 50 μ g/mL ascorbic acid and 10 mM β -glycerol phosphate). Following 7 days in culture, cells were stained for alkaline phosphatase (ALP) using a commercially available kit (Sigma-Aldrich, St. Louis, MO) and photographed. ALP activity was also measured by a colorimetric assay using nitro-blue tetrazolium chloride and 5-bromo-4-

chloro-3'-indolyphosphate p-toluidine salt (NBT/ BCIP). Quantification of ALP ($n=9$ wells/group) was performed by releasing the stain and determining the absorbance as previously reported [47]. For nodule formation experiments, stromal cells were allowed to differentiate in the presence of osteogenic medium for 21 days. Mineralized nodules were stained for calcium salts using Von Kossa stain, counterstained with nuclear fast red, and photographed ($n=9$ wells/group).

Osteoclast experiments were performed with the non-adherent hematopoietic cell populations and plated at a density of 4×10^6 cells/mL. Cells were allowed to adhere for 24 hr, and then treated with 30 ng/mL M-CSF and 50 ng/mL RANKL to stimulate osteoclast differentiation. On the fifth day of M-CSF and RANKL exposure, cells were stained for tartrate resistant acid phosphatase (TRAP) and counterstained with hematoxylin. Osteoclasts were identified as large, multinucleated, TRAP positive cells (TRAP⁺) and counted per well ($n=6$ wells/group).

Characterization of Genes Involved in Osteoblastogenesis, Osteoclastogenesis and TLR-4 Signaling by qPCR

The calvaria was used as a tissue source rich in osteoblasts while the bone marrow was flushed with sterile PBS and pelleted via centrifugation and used as a niche for osteoclasts and osteoclast progenitor cells. RNA was extracted from the calvaria using TriZol Reagent (Invitrogen, Grand Island, NY) as previously reported [48;49]. Briefly, 2 μ g of total RNA was DNase treated and reverse transcribed (Superscript II, Invitrogen) [48;49]. qPCR was then performed using SYBR green chemistry (7900HT Fast Real-Time, Applied Biosystems, Foster

City, CA). All qPCR results were evaluated by the comparative cycle number at threshold (C_Q) method (User Manual #2, Applied Biosystems) using peptidylprolyl isomerase B (*Ppib*) as the invariant control. Target genes involved in osteoblastogenesis included *Cbfa1* (F: 5'CGACAGTCCCAACTTCCTGT; R: 5'CGGTAACCACAGTCCCATCT), *Sp7* (F: 5'GAAGTTCACCTGCCTGCTCTGT; R: 5'CGTGGGTGCGCTGATGT), *Colla1* (F: 5'CGTCTGGTTTGGAGAGAGCAT; R: 5'GGTCAGCTGGATAGCGACATC), *Atf4* (F: 5'GCAGTGTTGCTGTAACGGACA; R: 5'TCGCTGTTTCAGGAAGCTCATC), *Bmp2* (F: 5'GGACATCCGCTCCACAAA; R: 5'GGCGCTTCCGCTGTTT), while *Socs3* (F: 5'CACCTGGACTCCTATGAGAAAGTG; R: 5'GAGCATCATACTGATCCAGGAACT) and *Tlr4* (F: 5'ACTGTTCTTCTCCTGCCTGACA; R: 5'TGATCCATGCATTGGTAGGTAATA) were investigated due to their involvement in TLR-4 signaling. The master regulator of osteoclastogenesis, *Nfatc1*, (F: 5'GCGAAGCCCAAGTCTCTTTCC; R: 5'GTATGGACCAGAATGTGA) was also assessed.

Statistical Analyses

Statistical analyses were performed using Statistical Analysis Software version 9.3 (SAS Institute, NC). Student's paired t-test was used to determine the difference in response to the high fat diet of a given strain at each time point. To determine changes occurring over time in bone mass, trabecular and cortical bone (BMD, BV/TV, and cortical area), a factorial analysis was performed with time and diet as factors. When F values were < 0.05 , *post hoc* analyses were performed with Fischer's least square means separation test. Data are presented as mean \pm standard error (SE) and a $P < 0.05$ was considered statistically significant.

Results

Bodyweight and Body Composition

To determine changes occurring in body weight due to a high fat (HF) diet, weekly body weight and body composition data were determined. Both the C57BL/6 and C3H/HeJ mice on the HF diet exhibited an increase in body weight ($P < 0.05$) compared to their Con counterparts at 2, 8, and 16 wks (**Table 1**). In particular, after 2 wk on the HF diet, the C57BL/6 mice weighed 8% more than the mice on the control diet, while the C3H/HeJ had an 18% increase in body weight with the HF diet compared to Con. By week 8, the C57BL/6 and C3H/HeJ mice on the HF diet weighed ~35% more than their Con counterparts. However, at 16 wks the C57BL/6 mice on the HF diet weighed ~70% more than their Con counterparts, whereas the C3H/HeJ animals on the HF diet weighed 44% more than their respective Con (**Table 1**).

Body composition analysis using DXA revealed that at the 2 wk time point, weight gain was primarily attributed to a significant increase in fat mass in both mouse strains (**Table 1**). Fat mass was also increased in the C57BL/6 mice on the HF diet at 8 wk, whereas the C3H/HeJ mice on the HF diet exhibited an increase in lean mass in addition to fat mass (**Table 1**). After 16 wk on the HF diet, both strains demonstrated an increase in lean and fat mass compared to their respective controls (**Table 1**).

The mean food intake was 2.9 and 2.5 g/mouse/day for the C57BL/6 mice on the Con and HF, and 3.2 and 3.0 g/mouse/day for the C3H/HeJ mice consuming the Con and HF diets (*data not shown*).

Alterations in Blood Glucose, Plasma Insulin, and IGTT

Both the C57BL/6 and C3H/HeJ mice on the HF diet exhibited signs of impaired glucose tolerance as early as 2 wk based on elevated fasting blood glucose and an increase in AUC during an IGTT (**Table 2**). Interestingly, at the 2 wk time point the C57BL/6 on the HF diet had a lower fasting plasma insulin ($P<0.05$), whereas no differences were observed in plasma insulin in the C3H/HeJ mice (**Table 2**). At 8 wk both the C57BL/6 and C3H/HeJ strains on the HF diet exhibited hyperglycemia, elevated AUC and although final blood glucose (120 min) of the IGTT remained elevated, there was an apparent “normalization” (**Table 2**). A marked increase in fasting blood glucose and plasma insulin was observed at 16 wk in the C57BL/6 on the HF diet compared to their Con (**Table 2**). After 16 wk on a HF diet, the C57BL/6 mice also demonstrated severe glucose intolerance as evidence by the increased AUC and the inability for their blood glucose to normalize at 120 min of the IGTT, which was ~3-fold higher than the Con group (**Table 2**). This data shows that diet-induced obesity in the C57BL/6 mice results in impaired glucose tolerance and hyperglycemia after 2 and 8 wk on a HF diet, indicative of a pre-diabetes state. Conversely, at the 16 wk time point, blood glucose remained elevated throughout the duration of the IGTT, despite hyperinsulinemia, which suggests the impaired blood glucose clearance was attributed to altered insulin sensitivity. These data show that the metabolic changes occurring in response to a HF diet for 16 wk are similar to the pathophysiology observed during the early stages of T2DM. In contrast to the C57BL/6 mice, after 16 wk on the HF diet, fasting blood glucose was not elevated in the C3H/HeJ mice, but they had elevated plasma insulin (**Table 2**). Although AUC from the IGTT remained high in the C3H/HeJ mice on a HF diet at the 16 wk time point, it was evident that their blood glucose at the final time (i.e., 120 min) was able to normalize to some degree (**Table 2**). These data suggest that the C3H/HeJ mice

are able to counter long term hyperglycemia induced by a HF diet by increasing plasma insulin, and, given their ability to maintain insulin sensitivity, resulting in the clearance of blood glucose.

Bone Growth and Bone Mineral Density

Long term hyperglycemia observed in the C57BL/6 mice on the HF diet at 16 wk was accompanied with an apparent decrease (3.6%) in longitudinal bone growth of the tibia (**Figure 1a**). However, no changes were observed in bone growth in the C3H/HeJ mice on the HF diet (**Figure 1a**). Furthermore, whole body BMD was lower in the C57BL/6 mice with prolonged hyperglycemia at 8 and 16 wk (**Figure 1b**). Similar to the delayed-onset of the metabolic changes consistent with T2DM, the C3H/HeJ mice were also protected to some extent from bone loss as they only demonstrated a decrease in whole body BMD compared to their Con at the later, 16 wk time point (**Figure 1b**).

Given the alterations in bone density occurring in response to diet in the two strains at each time point, changes in bone growth and BMD were evaluated using a factorial analysis with time and diet as factors. As shown in **Figure 2a**, the C57BL/6 mice demonstrate a diminished rate of bone accrual in conjunction with altered glucose homeostasis in the mice consuming the HF diet compared to the Con diet. Similar to the delayed metabolic and skeletal response observed in the C3H/HeJ mice, bone accrual did not appear to be impacted until the 16 wk time point (**Figure 2a**). These results demonstrate prolonged hyperglycemia attenuates bone mineralization as evidenced by whole body BMD.

Microarchitectural Changes in Trabecular and Cortical Bone

Trabecular and cortical bone were assessed to further characterize how glucose intolerance affects the different bone compartments. After 8 and 16 wk of hyperglycemia the C57BL/6 mice on the HF had reduced trabecular bone (i.e., BV/TV) in the distal femur metaphysis (**Figure 1c**) compared to their respective Con, but not in the vertebra (**Figure 1d**). This lower BV/TV in the femur metaphysis was primarily attributed to a decrease in trabecular thickness with a correspondingly higher Tb.Sp. (*data not shown*). In contrast to the C57BL/6 strain, BV/TV of the C3H/HeJ mice on the HF diet did not differ from mice on the control diet at the 2, 8 or 16 wk time point (**Figure 1c**).

Impaired glucose tolerance at 8 wk in the C57BL/6 mice on a HF diet demonstrate a decrease in cortical thickness (**Figure 1e**) and cortical area (**Figure 1f**), when compared to their respective Con. In contrast, the C3H/HeJ mice on a HF diet exhibited higher cortical thickness at the 16 wk (**Figure 1e**)

When trabecular BV/TV in the distal femur metaphysis was plotted over time, it is apparent that bone accrual was attenuated in the C57BL/6 mice on the HF diet, as the Con animals increased BV/TV between wk 2 and 8 (**Figure 2b**). Furthermore, these mice exhibited a decrease in BV/TV between the 8 wk and the 16 wk time points (**Figure 2b**). In the C3H/HeJ strain, BV/TV of the distal femur metaphysis was not altered in the mice on the HF compared to Con diet at any time point (**Figure 2b**). These data suggest that the C3H/HeJ mice, with a nonfunctional TLR-4, are protected from the negative effects of the high fat diet on trabecular bone at this site. Within the lumbar vertebra, both the C57BL/6 and C3H/HeJ mice continued to accrue trabecular bone irrespective of diet (**Figure 2c**).

Analyses of cortical bone area of the femur mid-diaphysis over time revealed the impact of hyperglycemia to be less severe in this bone compartment. However, the attenuation of cortical bone accrual primarily occurred within the early phase of impaired glucose homeostasis (i.e., 8 wks) in the C57BL/6 mice on a HF diet (**Figure 2d**). A time effect across all time points, was the only observed alteration in cortical area in the C3H/HeJ mice (**Figure 2d**).

Alterations in Bone Quality by Bone Microindentation Testing

Determination of the effects of glucose homeostasis on bone biomechanical properties was accomplished by assessing the initial cycle indentation distance (ID) at two sites. Consistent with changes occurring in trabecular bone of the distal femur metaphysis, only the C57BL/6 receiving the HF diet demonstrated an increase in ID, suggesting compromised bone strength at 8 and 16 wks (**Figure 1g**). Despite the less pronounced alterations occurring in cortical bone parameters, the C3H/HeJ mice on the HF diet exhibited an improvement in mid-diaphysial strength (i.e., decreased ID) at the 2 wk time point (**Figure 1h**). By 16 wk, both the C57BL/6 and C3H/HeJ mice on the HF diet had a weaker bone as evidenced by an increase in ID of the femur mid-diaphysis (**Figure 1h**).

Ex vivo Osteoblastogenesis and Osteoclastogenesis Experiments

Further mechanistic insight into the influence of hyperglycemia on bone was gained by evaluating osteoblastogenesis and osteoclastogenesis *ex vivo*. No changes occurred in osteoblastogenesis at the earliest time point of impaired glucose tolerance investigated (i.e., 2 wk

on a HF diet) determined visually by staining for ALP (**Figure 3a**) and by quantification techniques (**Figure 3b**). Von Kossa staining revealed that osteoblast mineralization was also not altered in the C57BL/6 mice at this time point (**Figure 3c**). However, beginning at the 8 wk (**Figure 3e**) time point and throughout the 16 wk time point (**Figure 3h**), the C57BL/6 mice on the HF diet had impaired osteoblast differentiation potential as evidenced by lower ALP compared to their respective Con. Representative images of ALP stain following 8 wk (**Figure 3d**) and 16 wk (**Figure 3g**) are shown to depict staining pattern. Consistent with changes occurring in ALP staining, increasing duration of glucose intolerance in the C57BL/6 mice resulted in decreased osteoblast nodule formation at the 8 wk (**Figure 3f**) and 16 wk (**Figure 3i**) time point. Furthermore, no differences were observed in osteoblast differentiation and nodule formation determined by ALP staining (**Figure 3a, 3d and 3g**) and quantification (**Figure 3b, 3e, and 3h**) as well as Von Kossa (**Figure 3c, 3f, 3i**) staining in the C3H/HeJ mice on the Con and HF diet at 2, 8, and 16 wk

While altered bone accrual is primarily a phenotype associated with the osteoblast, *ex vivo* osteoclastogenesis experiments were performed with hematopoietic bone marrow populations to investigate how the potential for forming bone resorpting osteoclasts was affected due to altered metabolism induced by a high fat diet. No changes were observed visually (**Figure 4a**) or quantitatively (**Figure 4b**) in the number of TRAP⁺ cells at the 2 wk time point in either the C57BL/6 or C3H/HeJ mice on the HF diet compared to their respective Con group. However, impaired glucose tolerance at the 8 wk time point resulted in an increase in TRAP⁺ cells based on visual observation (**Figure 4c**) and confirmed by actual quantification (**Figure 4d**) in both the C57BL/6 and C3H/HeJ mice. Interestingly, prolonged hyperglycemia and elevated plasma insulin observed at the 16 wk time point in the C57BL/6 was also accompanied a decrease in the

presence of large, multinucleated TRAP⁺ cells depicted by representative images (**Figure 4e**) and confirmed by quantification (**Figure 4f**). This decrease in osteoclastogenesis combined with suppressed osteoblastogenesis, suggests that the longer duration of glucose intolerance may be associated with an overall decrease in bone turnover.

Transcriptional Regulation of Genes Involved in Osteoblastogenesis, Osteoclastogenesis and TLR-4 Signaling

Given the differences in bone accrual following prolonged hyperglycemia (i.e., 8 and 16 wk on a HF diet), along with the *ex vivo* data suggesting an altered osteoblast phenotype, mRNA abundance of genes involved in osteoblast differentiation and activity were assessed. At the 2 wk time point, osteoblast differentiation and activity was down-regulated in the C57BL/6 as evidenced by the decrease in mRNA abundance of *Cbfa1* and *Coll1a1* (**Table 3**). The decrease in *Coll1a1* mRNA abundance was apparent with increasing duration of hyperglycemia (i.e., 2, 8 and 16 wks on HF diet) in the C57BL/6 mice (**Table 3**). This apparent down-regulation of osteoblastogenesis was also noted at the 8 wk time point in the C57BL/6 mice, given a decrease in the transcription factor involved in osteoblast differentiation (i.e., *Sp7*) and, *Alpl*, a gene encoding the ALP protein responsible for mineralization (**Table 3**).

Although no change was observed in bone structure or the number of TRAP⁺ during impaired glucose tolerance at the 2 wk time point in the C57BL/6 mice, mRNA abundance of *Nfatc1* was down-regulated (0.56 fold) when compared to Con (*data not shown*). Furthermore, no changes were observed in *Nfatc1* mRNA at any other time points, in either strain (*data not shown*).

Due to the data suggesting that TLR-4 contributes to the dysregulation of bone metabolism during hyperglycemia, mRNA abundance of genes involved in TLR-4 signaling in the osteoblast were determined. Genes involved in TLR-4 activation including *Atf4*, *Bmp2*, and *Socs3* were up-regulated in the C57BL/6 mice experiencing mild or short-term glucose intolerance (**Table 3**). Interestingly, the C57BL/6 mice on a HF diet demonstrated lower mRNA expression of *Tlr4* (**Table 3**). Conversely, the C3H/HeJ mice did not exhibit any of these changes in genes involved in osteoblast-regulation or TLR-4 signaling during the development or progression of impaired glucose tolerance (**Table 3**).

Discussion

The current study demonstrates that the prolonged hyperglycemia and impaired glucose tolerance attenuate bone mass accrual in young, growing mice and at some time points may promote bone loss. Additionally, these data provide evidence that this skeletal phenotype involves TLR-4. Characterization of changes occurring in blood glucose, glucose tolerance, and plasma insulin overtime revealed that the C57BL/6 and C3H/HeJ mice respond differently to a high fat diet. While the C3H/HeJ mice have been reported to be protected from diet-induced obesity and the corresponding glucose intolerance, these previous studies [30;31] made comparisons back to different control strains, C3H/HeOuJ and C3H/HeN. Both of these strains have an intact and functional TLR-4, therefore, comparisons between these control strains to the C3H/HeJ mice on a high fat diet were confounded by genetic differences. Thus, it remained unclear whether the C3H/HeJ mice on a high fat diet would differ in their metabolic response when compared back to the same strain on a control diet. The findings from the current study

show that the C3H/HeJ mice on a high fat diet gained weight and experienced hyperglycemia, hyperinsulinemia, and impaired glucose tolerance when compared to their respective control. However, when the metabolic response to a HF diet was compared to that of the C57BL/6 mice, it was apparent that the C3H/HeJ mice were protected from the development of glucose intolerance and diminished insulin sensitivity. This ability for the C3H/HeJ mice to clear blood glucose in response to the hyperinsulinemic state after 16 wk on a high fat diet is consistent with the maintenance of insulin signaling in the skeletal muscle and adipose tissue [31]. It was also evident that while both the C57BL/6 and C3H/HeJ mice demonstrated hyperinsulinemia after 16 wk on a HF diet, this increase in insulin was only able to normalize blood glucose in C3H/HeJ mice. These data demonstrate insulin sensitivity was maintained in the C3H/HeJ mice despite being on a HF diet for 16 wk. The difference in metabolic response between the C57BL/6 and C3H/HeJ are consistent with changes that have been previously observed in our lab over a 24 wk time course (*manuscript under review*). An interesting and unexpected finding from the current study was that the C57BL/6 mice on a high fat diet for 2 wk were hypoinsulinemic; however, there is precedence in the literature for the hypoglycemic response. For example, insulin secretion has been described as a “square wave pulse” pattern, which ensures insulin is secreted in a biphasic manner (i.e., a first or rapid phase, followed by second, prolonged phase) [50-52]. Both the first and second phase of insulin secretion are lower in type 2 diabetic patients compared to controls [53;54]. Furthermore, C57BL/6 mice fed a high fat diet have been shown to demonstrate hyperglycemia and hypoinsulinemia after 15 wk, attributed to impaired insulin secretion [55]. This study goes on to describe that an attenuation of insulin secretion due to the dissociation of voltage gated Ca^{2+} channels impairs exocytosis in pancreatic β -cells.

The skeletal changes that occurred in conjunction with the development and progression of impaired glucose tolerance and glucose intolerance provides new insight into the mechanism of which T2DM impacts bone metabolism. Moreover, the unique aspect comparing the skeletal response of the C57BL/6 mice to that of the C3H/HeJ mice allowed for the investigation of TLR-4's contribution to the skeletal phenotype. The deleterious impact of a high fat diet was consistent with previously published data [14-17]. However, of these studies, only one investigated how metabolic changes occurring after 8 wk on a HF diet affected an immature, growing skeleton [17]. The results from this study demonstrated that a high fat diet resulted in the attenuation of bone accrual, leading to lower bone mineral content. Consistent with the data presented in the current study, during later stages of impaired glucose tolerance (i.e., 8 wk) osteoblast differentiation and activity are decreased. As impaired glucose tolerance progresses and glucose intolerance develops (i.e., 8 and 16 wk on HF diet) in the C57BL/6 mice, bone accrual is impaired, resulting in lower whole body BMD and trabecular BV/TV. While insulin has been shown to exert an anabolic effect on bone, high glucose concentrations have been reported to decrease osteoblast mineralization *in vitro* [56]. Furthermore, the *ex vivo* osteoblastogenesis and osteoclastogenesis cell cultures suggest that a decrease in bone turnover is occurring during glucose intolerance at the 16 wk time point in the C57BL.6 mice. It is interestingly that this later 16 wk time point represented the most similar metabolic profile to that of a human during the onset of T2DM, and that suppressed bone turnover has been demonstrated to contribute to the increased risk of fragility fractures in type 2 diabetic patients [4]. The difference in transcriptional regulation of osteoclastogenesis and the primary cell culture experiments indicate that while osteoclastogenesis may not have been elevated at a given time point, their progenitor cell populations were being altered. Contrary to the C57BL/6 mice, the

C3H/HeJ mice were able to accrue trabecular bone in the distal femur metaphysis demonstrating that the delayed-progression of impaired glucose tolerance to glucose intolerance plays an osteoprotective role. While it is recognized that the C3H/HeJ mice exhibit altered bone mineralization partly attributed to a mutation in their leptin receptor (*Lepr*), given TLR-4's ability to modulate bone metabolism, further investigation was carried out to tease apart its contribution.

The characterization of genes involved in TLR-4 signaling suggested that this receptor was in fact contributing to the dysregulation of bone metabolism, and provided a further explanation between the difference in skeletal phenotype observed between the C57BL/6 and C3H/HeJ mice. Although *Cbfa1*, *Sp7* and *Alpl* are critical for osteoblast differentiation and matrix mineralization, these genes have also been shown to be down-regulated in response to the TLR-4 ligand, LPS [33;57]. Furthermore, osteoblasts treated with LPS up-regulate *Socs3* expression [58;59] and it has recently been shown that osteoblast differentiation is suppressed through LIF/STAT3/SOCS3 signaling pathways [60]. The approximately 5-fold increase in *Socs3* mRNA abundance occurring after 8 wk on a high fat diet, only in the C57BL/6 mice, suggests that activation of the TLR-4 pathway may contribute to the attenuated osteoblast phenotype. Interestingly SOCS3 has been shown to alter intracellular insulin signaling, resulting in attenuated insulin sensitivity [61]. Given that it has recently been shown that osteoblasts can function as global regulators of metabolism [20;62-64], the up-regulation of *Socs3* mRNA may be contributing to development of glucose intolerance in the C57BL/6 mice. In addition to *Socs3*, ligands for TLR-4 have been shown to regulate *Atf4* and *Bmp2* in the osteoblast. For example, it has been demonstrated that ATF4 is down-regulated in osteoblasts challenged with LPS [57]. However, ATF4 can also co-localize with FoxO1 in osteoblasts to increase blood

glucose and decrease glucose tolerance [65]. Therefore, given the opposite effects TLR-4 signaling and glucose homeostasis exert on ATF4 in the osteoblast, the interpretation of changes occurring in this gene is complicated in a high fat diet induced model of T2DM. In the current study, the increase in *Atf4* mRNA expression in the C57BL/6 mice on the high fat diet after 8 wk could be an indication of alterations in glucose regulation of the osteoblast as opposed to direct implications of TLR-4. Similar to *Atf4*, conflicting data exist about how TLR-4 activation impacts *Bmp2* expression in the osteoblast [38;66]. The increase observed in *Bmp2* mRNA during impaired glucose tolerance at the 8 wk time point in the C57BL/6 mice may also be explained by the coordination of BMP2 by the master regulator of the cellular energy stress response, AMP kinase (AMPK) [67]. Therefore, given the complexity of genes involved in osteoblast function versus how they are regulated by glucose homeostasis or TLR-4 signaling, further studies should be developed to tease apart these pathways.

The findings of these studies depict differences in the metabolic and skeletal response between C57BL/6 and C3H/HeJ mice throughout the progression of impaired glucose tolerance and the development of glucose intolerance. The diminished bone accrual due to prolonged hyperglycemia in the C57BL/6 mice was attributed to a decrease in bone turnover, and regulated, in part, by TLR-4. This study provides novel insight into how metabolic changes induced by a high fat diet (i.e., hyperglycemia, impaired glucose tolerance, and hyperinsulinemia) can impact the young, growing skeleton over time. While future studies are warranted to determine the precise mechanisms involved, the results presented herein suggest TLR-4 contributes to impaired bone metabolism during the development and progression of T2DM.

Acknowledgments

This study was sponsored by Oklahoma Center for the Advancement of Science and Technology (HR10-068) and United States Department of Agriculture (2012-67011-19906). We would also like to express our gratitude to Sandra Peterson (Department of Nutritional Sciences, Oklahoma State University, Stillwater, OK 74078) for her technical assistance.

Conflict of interest

None of the authors have any conflicts to disclose.

References

1. Ogden CL, Carroll MD, Kit BK, Flegal KM (2013) Prevalence of obesity among adults: United States, 2011-2012. NCHS.Data Brief.1-8
2. Centers for Disease Control and Prevention. Children and Diabetes. 2013.
Ref Type: Report
3. Schwartz AV, Vittinghoff E, Bauer DC, Hillier TA, Strotmeyer ES, Ensrud KE, Donaldson MG, Cauley JA, Harris TB, Koster A, Womack CR, Palermo L, Black DM (2011) Association of BMD and FRAX score with risk of fracture in older adults with type 2 diabetes. JAMA 305:2184-2192
4. Farr JN, Drake MT, Amin S, Melton LJ, III, McCready LK, Khosla S (2013) In Vivo assessment of bone quality in postmenopausal women with type 2 diabetes. J.Bone Miner.Res.
5. Gorman E, Chudyk AM, Madden KM, Ashe MC (2011) Bone health and type 2 diabetes mellitus: a systematic review. Physiother.Can. 63:8-20
6. Foley S, Quinn S, Jones G (2009) Tracking of bone mass from childhood to adolescence and factors that predict deviation from tracking. Bone 44:752-757
7. Goulding A, Jones IE, Williams SM, Grant AM, Taylor RW, Manning PJ, Langley J (2005) First fracture is associated with increased risk of new fractures during growth. J.Pediatr. 146:286-288
8. Goulding A, Jones IE, Taylor RW, Williams SM, Manning PJ (2001) Bone mineral density and body composition in boys with distal forearm fractures: a dual-energy x-ray absorptiometry study. J.Pediatr. 139:509-515
9. Goulding A, Jones IE, Taylor RW, Manning PJ, Williams SM (2000) More broken bones: a 4-year double cohort study of young girls with and without distal forearm fractures. J.Bone Miner.Res. 15:2011-2018
10. Goulding A, Taylor RW, Jones IE, McAuley KA, Manning PJ, Williams SM (2000) Overweight and obese children have low bone mass and area for their weight. Int.J.Obes.Relat Metab Disord. 24:627-632
11. Klein KO, Larmore KA, de LE, Brown JM, Considine RV, Hassink SG (1998) Effect of obesity on estradiol level, and its relationship to leptin, bone maturation, and bone mineral density in children. J.Clin.Endocrinol.Metab 83:3469-3475
12. Leonard MB, Shults J, Wilson BA, Tershakovec AM, Zemel BS (2004) Obesity during childhood and adolescence augments bone mass and bone dimensions. Am.J.Clin.Nutr. 80:514-523

13. Matkovic V, Jelic T, Wardlaw GM, Ilich JZ, Goel PK, Wright JK, Andon MB, Smith KT, Heaney RP (1994) Timing of peak bone mass in Caucasian females and its implication for the prevention of osteoporosis. Inference from a cross-sectional model. *J.Clin.Invest* 93:799-808
14. Parhami F, Tintut Y, Beamer WG, Gharavi N, Goodman W, Demer LL (2001) Atherogenic high-fat diet reduces bone mineralization in mice. *J.Bone Miner.Res.* 16:182-188
15. Ionova-Martin SS, Wade JM, Tang S, Shahnazari M, Ager JW, III, Lane NE, Yao W, Alliston T, Vaisse C, Ritchie RO (2011) Changes in cortical bone response to high-fat diet from adolescence to adulthood in mice. *Osteoporos.Int.* 22:2283-2293
16. Patsch JM, Kiefer FW, Varga P, Pail P, Rauner M, Stupphann D, Resch H, Moser D, Zysset PK, Stulnig TM, Pietschmann P (2011) Increased bone resorption and impaired bone microarchitecture in short-term and extended high-fat diet-induced obesity. *Metabolism* 60:243-249
17. Lu XM, Zhao H, Wang EH (2013) A high-fat diet induces obesity and impairs bone acquisition in young male mice. *Mol.Med.Rep.* 7:1203-1208
18. Thomas DM, Hards DK, Rogers SD, Ng KW, Best JD (1996) Insulin receptor expression in bone. *J.Bone Miner.Res.* 11:1312-1320
19. Clemens TL, Karsenty G (2011) The osteoblast: an insulin target cell controlling glucose homeostasis. *J.Bone Miner.Res.* 26:677-680
20. Ferron M, Wei J, Yoshizawa T, Del FA, DePinho RA, Teti A, Ducy P, Karsenty G (2010) Insulin signaling in osteoblasts integrates bone remodeling and energy metabolism. *Cell* 142:296-308
21. Confavreux CB, Levine RL, Karsenty G (2009) A paradigm of integrative physiology, the crosstalk between bone and energy metabolisms. *Mol.Cell Endocrinol.* 310:21-29
22. Ebstein W (1876) Zur therapie des Diabetes mellitus, insbesondere uber die Anwendung des salicylsauren Matron bei demselben. *Berliner Klinische Wochenschrift* 13:337-340
23. Shi H, Kokoeva MV, Inouye K, Tzameli I, Yin H, Flier JS (2006) TLR4 links innate immunity and fatty acid-induced insulin resistance. *J.Clin.Invest* 116:3015-3025
24. Dasu MR, Ramirez S, Isseroff RR (2012) Toll-like receptors and diabetes: a therapeutic perspective. *Clin.Sci.(Lond)* 122:203-214
25. Pal D, Dasgupta S, Kundu R, Maitra S, Das G, Mukhopadhyay S, Ray S, Majumdar SS, Bhattacharya S (2012) Fetuin-A acts as an endogenous ligand of TLR4 to promote lipid-induced insulin resistance. *Nat.Med.* 18:

26. Lee JY, Sohn KH, Rhee SH, Hwang D (2001) Saturated fatty acids, but not unsaturated fatty acids, induce the expression of cyclooxygenase-2 mediated through Toll-like receptor 4. *J Biol.Chem.* 276:16683-16689
27. Schaeffler A, Gross P, Buettner R, Bollheimer C, Buechler C, Neumeier M, Kopp A, Schoelmerich J, Falk W (2009) Fatty acid-induced induction of Toll-like receptor-4/nuclear factor-kappaB pathway in adipocytes links nutritional signalling with innate immunity. *Immunology* 126:233-245
28. Reyna SM, Ghosh S, Tantiwong P, Meka CS, Eagan P, Jenkinson CP, Cersosimo E, DeFronzo RA, Coletta DK, Sriwijitkamol A, Musi N (2008) Elevated toll-like receptor 4 expression and signaling in muscle from insulin-resistant subjects. *Diabetes* 57:2595-2602
29. Medvedev AE, Piao W, Shoenfelt J, Rhee SH, Chen H, Basu S, Wahl LM, Fenton MJ, Vogel SN (2007) Role of TLR4 tyrosine phosphorylation in signal transduction and endotoxin tolerance. *J.Biol.Chem.* 282:16042-16053
30. Poggi M, Bastelica D, Gual P, Iglesias MA, Gremeaux T, Knauf C, Peiretti F, Verdier M, Juhan-Vague I, Tanti JF, Burcelin R, Alessi MC (2007) C3H/HeJ mice carrying a toll-like receptor 4 mutation are protected against the development of insulin resistance in white adipose tissue in response to a high-fat diet. *Diabetologia* 50:1267-1276
31. Tsukumo DM, Carvalho-Filho MA, Carvalheira JB, Prada PO, Hirabara SM, Schenka AA, Araujo EP, Vassallo J, Curi R, Velloso LA, Saad MJ (2007) Loss-of-function mutation in Toll-like receptor 4 prevents diet-induced obesity and insulin resistance. *Diabetes* 56:1986-1998
32. Droke EA, Hager KA, Lerner MR, Lightfoot SA, Stoecker BJ, Brackett DJ, Smith BJ (2007) Soy isoflavones avert chronic inflammation-induced bone loss and vascular disease. *J Inflamm.(Lond)* 4:17
33. Guo C, Yuan L, Wang JG, Wang F, Yang XK, Zhang FH, Song JL, Ma XY, Cheng Q, Song GH (2014) Lipopolysaccharide (LPS) Induces the Apoptosis and Inhibits Osteoblast Differentiation Through JNK Pathway in MC3T3-E1 Cells. *Inflammation* 37:621-631
34. Roggia C, Gao Y, Cenci S, Weitzmann MN, Toraldo G, Isaia G, Pacifici R (2001) Up-regulation of TNF-producing T cells in the bone marrow: a key mechanism by which estrogen deficiency induces bone loss in vivo. *Proc.Natl.Acad.Sci U.S.A* 98:13960-13965
35. Smith BJ, Lerner MR, Bu SY, Lucas EA, Hanas JS, Lightfoot SA, Postier RG, Bronze MS, Brackett DJ (2006) Systemic bone loss and induction of coronary vessel disease in a rat model of chronic inflammation. *Bone* 38:378-386
36. Shen CL, Yeh JK, Samathanam C, Cao JJ, Stoecker BJ, Dagda RY, Chyu MC, Wang JS (2010) Protective actions of green tea polyphenols and alfacalcidol on bone microstructure in female rats with chronic inflammation. *J.Nutr.Biochem.*

37. Tomomatsu N, Aoki K, Alles N, Soysa NS, Hussain A, Nakachi H, Kita S, Shimokawa H, Ohya K, Amagasa T (2009) LPS-induced inhibition of osteogenesis is TNF-alpha dependent in a murine tooth extraction model. *J.Bone Miner.Res.* 24:1770-1781
38. Bandow K, Maeda A, Kakimoto K, Kusuyama J, Shamoto M, Ohnishi T, Matsuguchi T (2010) Molecular mechanisms of the inhibitory effect of lipopolysaccharide (LPS) on osteoblast differentiation. *Biochem.Biophys.Res.Comm.* 402:755-761
39. Sheng MH, Baylink DJ, Beamer WG, Donahue LR, Lau KH, Wergedal JE (2002) Regulation of bone volume is different in the metaphyses of the femur and vertebra of C3H/HeJ and C57BL/6J mice. *Bone* 30:486-491
40. Sheng MH, Lau KH, Mohan S, Baylink DJ, Wergedal JE (2006) High osteoblastic activity in C3H/HeJ mice compared to C57BL/6J mice is associated with low apoptosis in C3H/HeJ osteoblasts. *Calcif.Tissue Int.* 78:293-301
41. Sheng MH, Baylink DJ, Beamer WG, Donahue LR, Rosen CJ, Lau KH, Wergedal JE (1999) Histomorphometric studies show that bone formation and bone mineral apposition rates are greater in C3H/HeJ (high-density) than C57BL/6J (low-density) mice during growth. *Bone* 25:421-429
42. Sheng MH, Lau KH, Beamer WG, Baylink DJ, Wergedal JE (2004) In vivo and in vitro evidence that the high osteoblastic activity in C3H/HeJ mice compared to C57BL/6J mice is intrinsic to bone cells. *Bone* 35:711-719
43. Surwit RS, Kuhn CM, Cochrane C, McCubbin JA, Feinglos MN (1988) Diet-induced type II diabetes in C57BL/6J mice. *Diabetes* 37:1163-1167
44. Piao W, Song C, Chen H, Wahl LM, Fitzgerald KA, O'Neill LA, Medvedev AE (2008) Tyrosine phosphorylation of MyD88 adapter-like (Mal) is critical for signal transduction and blocked in endotoxin tolerance. *J.Biol.Chem.* 283:3109-3119
45. Diez-Perez A, Guerri R, Nogues X, Caceres E, Pena MJ, Mellibovsky L, Randall C, Bridges D, Weaver JC, Proctor A, Brimer D, Koester KJ, Ritchie RO, Hansma PK (2010) Microindentation for in vivo measurement of bone tissue mechanical properties in humans. *J.Bone Miner.Res.* 25:1877-1885
46. Aref M, Gallant MA, Organ JM, Wallace JM, Newman CL, Burr DB, Brown DM, Allen MR (2013) In vivo reference point indentation reveals positive effects of raloxifene on mechanical properties following 6 months of treatment in skeletally mature beagle dogs. *Bone* 56:449-453
47. Lee KN, Jang WG, Kim EJ, Oh SH, Son HJ, Kim SH, Franceschi R, Zhang XK, Lee SE, Koh JT (2012) Orphan nuclear receptor chicken ovalbumin upstream promoter-transcription factor II (COUP-TFII) protein negatively regulates bone morphogenetic protein 2-induced osteoblast differentiation through suppressing runt-related gene 2 (Runx2) activity. *J.Biol.Chem.* 287:18888-18899

48. Rendina E, Lim YF, Marlow D, Wang Y, Clarke SL, Kuvibidila S, Lucas EA, Smith BJ (2012) Dietary supplementation with dried plum prevents ovariectomy-induced bone loss while modulating the immune response in C57BL/6J mice. *J.Nutr.Biochem.* 23:60-68
49. Rendina E, Hembree KD, Davis MR, Marlow D, Clarke SL, Halloran BP, Lucas EA, Smith BJ (2013) Dried plum's unique capacity to reverse bone loss and alter bone metabolism in postmenopausal osteoporosis model. *PLoS.One.* 8:e60569
50. Curry DL, Bennett LL, Grodsky GM (1968) Dynamics of insulin secretion by the perfused rat pancreas. *Endocrinology* 83:572-584
51. Grodsky GM, Curry DL, Bennett LL, Rodrigo JJ (1968) [Factors influencing different rates of insulin release in vitro]. *Acta Diabetol.Lat.* 5 Suppl 1:140-161
52. Grodsky GM, Curry D, Landahl H, Bennett L (1969) [Further studies on the dynamic aspects of insulin release in vitro with evidence for a two-compartmental storage system]. *Acta Diabetol.Lat.* 6 Suppl 1:554-578
53. Ward WK, Bolgiano DC, McKnight B, Halter JB, Porte D, Jr. (1984) Diminished B cell secretory capacity in patients with noninsulin-dependent diabetes mellitus. *J.Clin.Invest* 74:1318-1328
54. van Haefen TW, Van Maarschalkerweerd WW, Gerich JE, Van der Veen EA (1991) Decreased insulin secretory capacity and normal pancreatic B-cell glucose sensitivity in non-obese patients with NIDDM. *Eur.J.Clin.Invest* 21:168-174
55. Collins SC, Hoppa MB, Walker JN, Amisten S, Abdulkader F, Bengtsson M, Fearnside J, Ramracheya R, Toye AA, Zhang Q, Clark A, Gauguier D, Rorsman P (2010) Progression of diet-induced diabetes in C57BL6J mice involves functional dissociation of Ca²(+) channels from secretory vesicles. *Diabetes* 59:1192-1201
56. Garcia-Hernandez A, Arzate H, Gil-Chavarria I, Rojo R, Moreno-Fierros L (2012) High glucose concentrations alter the biomineralization process in human osteoblastic cells. *Bone* 50:276-288
57. Bandow K, Maeda A, Kakimoto K, Kusuyama J, Shamoto M, Ohnishi T, Matsuguchi T (2010) Molecular mechanisms of the inhibitory effect of lipopolysaccharide (LPS) on osteoblast differentiation. *Biochem.Biophys.Res.Commun.* 402:755-761
58. Gao A, Kantarci A, Herrera BS, Gao H, Van Dyke TE (2013) A critical role for suppressors of cytokine signaling 3 in regulating LPS-induced transcriptional activation of matrix metalloproteinase-13 in osteoblasts. *PeerJ.* 1:e51
59. Yan C, Cao J, Wu M, Zhang W, Jiang T, Yoshimura A, Gao H (2010) Suppressor of cytokine signaling 3 inhibits LPS-induced IL-6 expression in osteoblasts by suppressing CCAAT/enhancer-binding protein {beta} activity. *J.Biol.Chem.* 285:37227-37239

60. Matsushita K, Itoh S, Ikeda S, Yamamoto Y, Yamauchi Y, Hayashi M (2014) LIF/STAT3/SOCS3 Signaling Pathway in Murine Bone Marrow Stromal Cells Suppresses Osteoblast Differentiation. *J.Cell Biochem.*
61. Kim JJ, Sears DD (2010) TLR4 and Insulin Resistance. *Gastroenterol.Res.Pract.* 2010:
62. Lee NK, Sowa H, Hinoi E, Ferron M, Ahn JD, Confavreux C, Dacquin R, Mee PJ, McKee MD, Jung DY, Zhang Z, Kim JK, Mauvais-Jarvis F, Ducy P, Karsenty G (2007) Endocrine regulation of energy metabolism by the skeleton. *Cell* 130:456-469
63. Rached MT, Kode A, Silva BC, Jung DY, Gray S, Ong H, Paik JH, DePinho RA, Kim JK, Karsenty G, Kousteni S (2010) FoxO1 expression in osteoblasts regulates glucose homeostasis through regulation of osteocalcin in mice. *J.Clin.Invest* 120:357-368
64. Ferron M, McKee MD, Levine RL, Ducy P, Karsenty G (2012) Intermittent injections of osteocalcin improve glucose metabolism and prevent type 2 diabetes in mice. *Bone* 50:568-575
65. Kode A, Mosialou I, Silva BC, Joshi S, Ferron M, Rached MT, Kousteni S (2012) FoxO1 protein cooperates with ATF4 protein in osteoblasts to control glucose homeostasis. *J.Biol.Chem.* 287:8757-8768
66. Cho JH, Lee SK, Lee JW, Kim EC (2010) The role of heme oxygenase-1 in mechanical stress- and lipopolysaccharide-induced osteogenic differentiation in human periodontal ligament cells. *Angle Orthod.* 80:552-559
67. Kanazawa I, Yamaguchi T, Yano S, Yamauchi M, Sugimoto T (2009) Activation of AMP kinase and inhibition of Rho kinase induce the mineralization of osteoblastic MC3T3-E1 cells through endothelial NOS and BMP-2 expression. *Am.J.Physiol Endocrinol.Metab* 296:E139-E146

Figure Captions

Fig. 1 Changes in tibia length (A), whole body bone mineral density (BMD) (B), trabecular bone volume/ total volume (BV/ TV) of the distal femur metaphysis (C) and vertebra (D), cortical thickness (E) and area (F), first cycle indentation distal (ID) of the distal metaphysis (G) and mid-diaphysis of the femur (H) in C57BL/6 and C3H/HeJ mice on a control (Con; AIN93M) or high fat (HF; 60% kcal from fat) for 2, 8, or 16 wk. Data presented as the mean \pm SE. Symbol * represents a significant difference ($P < 0.05$) between dietary treatments for a given strain, at a given time point.

Fig. 2 Alterations occurring overtime in whole body bone mineral density (BMD) (A), trabecular bone volume/ total volume (BV/ TV) of the distal femur metaphysis (B) and vertebra (C), and cortical area (D) for C57BL/6 and C3H/HeJ mice on a control (Con; AIN93M) or high fat (HF; 60% kcal from fat). Data are presented as the mean \pm SE. Comparisons were made using 2-way ANOVA to determine the effect of diet, time, and diet by time interactions. Points that share the same superscript letter are not significantly different from each other ($P < 0.05$).

Fig. 3 Primary osteoblastogenesis experiments performed using stromal cell population from bone marrow of C57BL/6 and C3H/HeJ mice on a control (Con; AIN93M) or high fat (HF; 60% kcal from fat) for 2, 8, or 16 wk. Following 7 days in osteogenic medium, alkaline phosphatase (ALP) activity was measured by a colorimetric assay using nitro-blue tetrazolium chloride and 5-bromo-4-chloro-3'-indolyphosphate p-toluidine salt (NBT/ BCIP), representative images of ALP staining are shown (A, D,G) as well as quantification data (B, E, H). After 21 days in osteogenic medium, nodule formation was visualized by Von Kossa (C, F, I). Data presented as the mean \pm

SE. Symbol * represents a significant difference ($P < 0.05$) between dietary treatments for a given strain, at a given time point.

Fig. 4 At 2, 8, and 16 wk on a control (Con; AIN93M) or high fat (HF; 60% kcal from fat) bone marrow was harvested from C57BL/6 and C3H/HeJ mice. Non-adherent cells were plated and differentiated in the presence of 30 ng/ mL M-CSF and 50 ng/ mL RANKL. On day 5, cells were stained for tartrate resistant acid phosphatase (TRAP) and counterstained with hematoxylin. TRAP positive (TRAP+) cells were, representative images were captured (A, C, E) and TRAP= cells were quantified by counting each well (B, D, F). Data presented as the mean \pm SE.

Symbol * represents a significant difference ($P < 0.05$) between dietary treatments for a given strain, at a given time point.

Table 1. Final Bodyweight and Body Composition of C57BL/6 and C3H/HeJ mice Following a Control of High Fat Diet

	C57BL/6		C3H/HeJ	
	Control	HF	Control	HF
2 Week				
<i>Bodyweight (g)</i>	21.8 ± 0.2	23.6 ± 0.3*	23.1 ± 0.3	27.2 ± 0.5*
<i>Body Composition</i>				
<i>Lean (g)</i>	17.1 ± 0.2	17.6 ± 0.3	17.5 ± 0.4	18.2 ± 0.3
<i>Fat (g)</i>	4.56 ± 0.1	5.47 ± 0.2*	4.56 ± 0.2	6.28 ± 0.3*
<i>Percent Fat (%)</i>	21.1 ± 0.4	23.7 ± 0.6*	20.6 ± 0.7	25.6 ± 0.6*
8 Week				
<i>Bodyweight (g)</i>	25.7 ± 0.4	34.7 ± 1.0*	27.0 ± 0.5	36.6 ± 0.8*
<i>Body Composition</i>				
<i>Lean (g)</i>	20.4 ± 0.6	20.5 ± 0.5	19.6 ± 0.5	23.6 ± 0.6*
<i>Fat (g)</i>	6.14 ± 0.2	13.14 ± 1.0*	5.30 ± 0.2	12.22 ± 0.4*
<i>Percent Fat (%)</i>	23.1 ± 0.8	38.6 ± 1.6*	21.1 ± 0.5	34.1 ± 0.4*
16 Week				
<i>Bodyweight (g)</i>	26.6 ± 0.5	45.1 ± 1.7*	27.6 ± 0.6	39.6 ± 1.1*
<i>Body Composition</i>				
<i>Lean (g)</i>	19.4 ± 0.4	24.4 ± 0.62*	19.7 ± 0.4	25.0 ± 0.5*
<i>Fat (g)</i>	6.53 ± 0.2	21.25 ± 1.1*	6.36 ± 0.3	13.92 ± 0.4*
<i>Percent Fat (%)</i>	25.1 ± 0.5	46.2 ± 3.1*	24.3 ± 0.6	34.9 ± 0.9*

Control (Con; AIN93M) and high fat (HF; 60% kcal from fat). Values are expressed as mean ± SE. Symbol * indicates significant differences ($P < 0.05$) between dietary treatments within either the C57BL/6 or C3H/HeJ mouse strains at a given time point.

Table 2. Plasma Insulin and Indicators of Glucose Homeostasis

	C57BL/6		C3H/HeJ	
	Con	HF	Con	HF
2 Week				
<i>Fasting Glucose (mg dL)</i>	156.1 ± 7.2	185.9 ± 5.5*	163.8 ± 4.4	195.3 ± 6.2*
<i>Fasting Insulin (pg/mL)</i>	206.4 ± 13.2	148.0 ± 9.5*	202.0 ± 34.1	199.3 ± 9.6
IGTT				
<i>Final Glucose at 120 min (mg/dL)</i>	169.2 ± 6.7	237.7 ± 15.3*	177.5 ± 11.5	254.1 ± 20.5*
<i>AUC [(mg/dL)*min] (1 x 10³)</i>	29.3 ± 1.2	52.8 ± 2.8*	30.6 ± 4.1	41.1 ± 2.7*
8 Week				
<i>Fasting Glucose (mg dL)</i>	151.1 ± 5.4	182.3 ± 7.3*	132.5 ± 4.8	161.3 ± 5.9*
<i>Fasting Insulin (pg/mL)</i>	248.9 ± 31.6	257.3 ± 27.9	245.7 ± 35.3	382.9 ± 56.9
IGTT				
<i>Final Glucose at 120 min (mg/dL)</i>	188.1 ± 8.4	280.3 ± 19.6*	131.6 ± 9.8	202.5 ± 6.3*
<i>AUC [(mg/dL)*min] (1 x 10³)</i>	29.4 ± 1.2	53.8 ± 3.3*	20.4 ± 0.7	36.4 ± 1.7*
16 Week				
<i>Fasting Glucose (mg dL)</i>	147.9 ± 2.1	178.2 ± 6.1*	129.3 ± 3.4	134.9 ± 6.0
<i>Fasting Insulin (pg/mL)</i>	370.8 ± 144.1	736.5 ± 161.2*	189.0 ± 20.9	485.8 ± 104.0*
IGTT				
<i>Final Glucose at 120 min (mg/dL)</i>	204.8 ± 13.2	617.3 ± 37.6*	148.7 ± 7.3	220.0 ± 10.1*
<i>AUC [(mg/dL)*min] (1 x 10³)</i>	36.1 ± 1.9	74.0 ± 2.6*	25.8 ± 1.4	40.1 ± 2.4*

Fasting (6 hours) blood glucose, plasma insulin, and intraperitoneal glucose tolerance test (IGTT) at 2, 8, and 16 weeks on a control (Con=10 % kcal from fat) or HF (60% kcal from fat) diet. IGTT was performed by injecting (IP) glucose solution and blood glucose was tracked at 0, 15, 30, 60, and 120 min. Calculated area under the curve (AUC) and the final (120 min) blood glucose are reported. Values are expressed as mean ± SE. Symbol * indicates significant differences ($P < 0.05$) between dietary treatments within mouse strain at a given time point.

Table 3. Transcriptional Fold Changes of Genes Involved in Osteoblastogenesis and TLR-4 Signaling

	C57BL/6			C3H/HeJ		
	2 Wk	8 Wk	16 Wk	2 Wk	8 Wk	16 Wk
<i>Cbfa1</i>	0.31	0.80	0.64	1.29	1.40	0.73
<i>Sp7</i>	0.83	0.55	0.56	0.92	1.28	0.64
<i>Col1a1</i>	0.78	0.48	0.42	0.78	0.97	1.05
<i>Alpl</i>	0.84	0.68	0.27	0.63	1.16	1.24
<i>Atf4</i>	1.08	1.89	0.97	1.33	0.87	1.03
<i>Bmp2</i>	1.53	2.30	1.11	1.82	1.76	0.95
<i>Socs3</i>	1.80	5.15	1.04	1.69	1.12	1.08
<i>Tlr4</i>	0.97	1.27	0.30	0.86	0.95	1.38

Total RNA was extracted from the calvaria of the C57BL/6 and C3H/HeJ mice after 2, 8, and 16 weeks on a control (Con; AIN93M) or high fat (HF; 60% kcal from fat). cDNA was then used to determine gene expression. All target genes were normalized to invariant control (*Ppib*) and fold change was calculated using the 2^{-ddCQ} method at a given time point within a given strain. Bold, italicized font corresponds to a statistically significant ($P < 0.05$) difference in gene expression in the HF diet relative to Con.

Figure 1.

■ C57BL/6-Con ▨ C57BL/6-HF □ C3H/HeJ-Con ▩ C3H/HeJ-HF

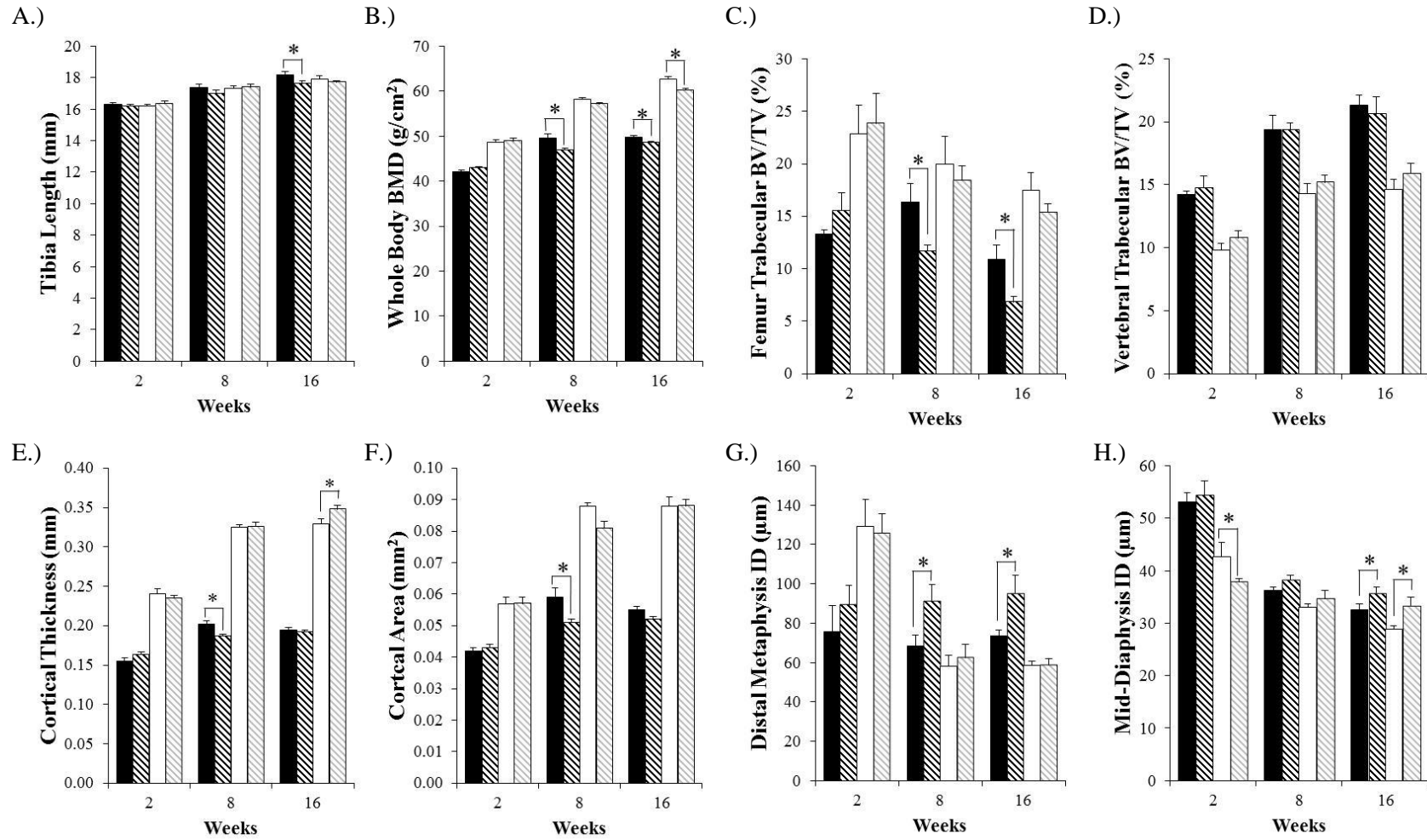


Figure 2.

● C57BL/6-Con ■ C57BL/6-HF ● C3H/HeJ-Con ● C3H/HeJ-HF

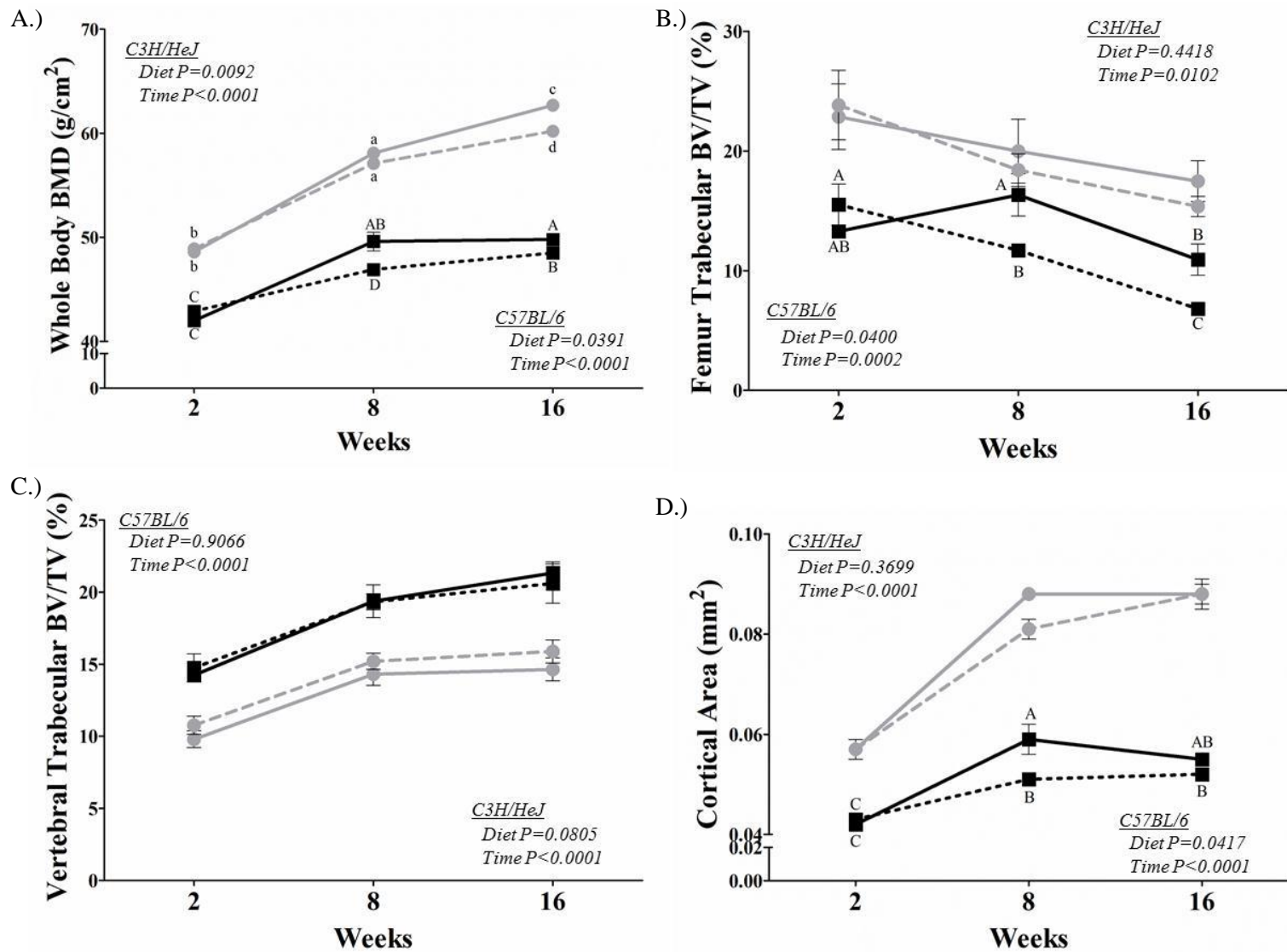


Figure 3.

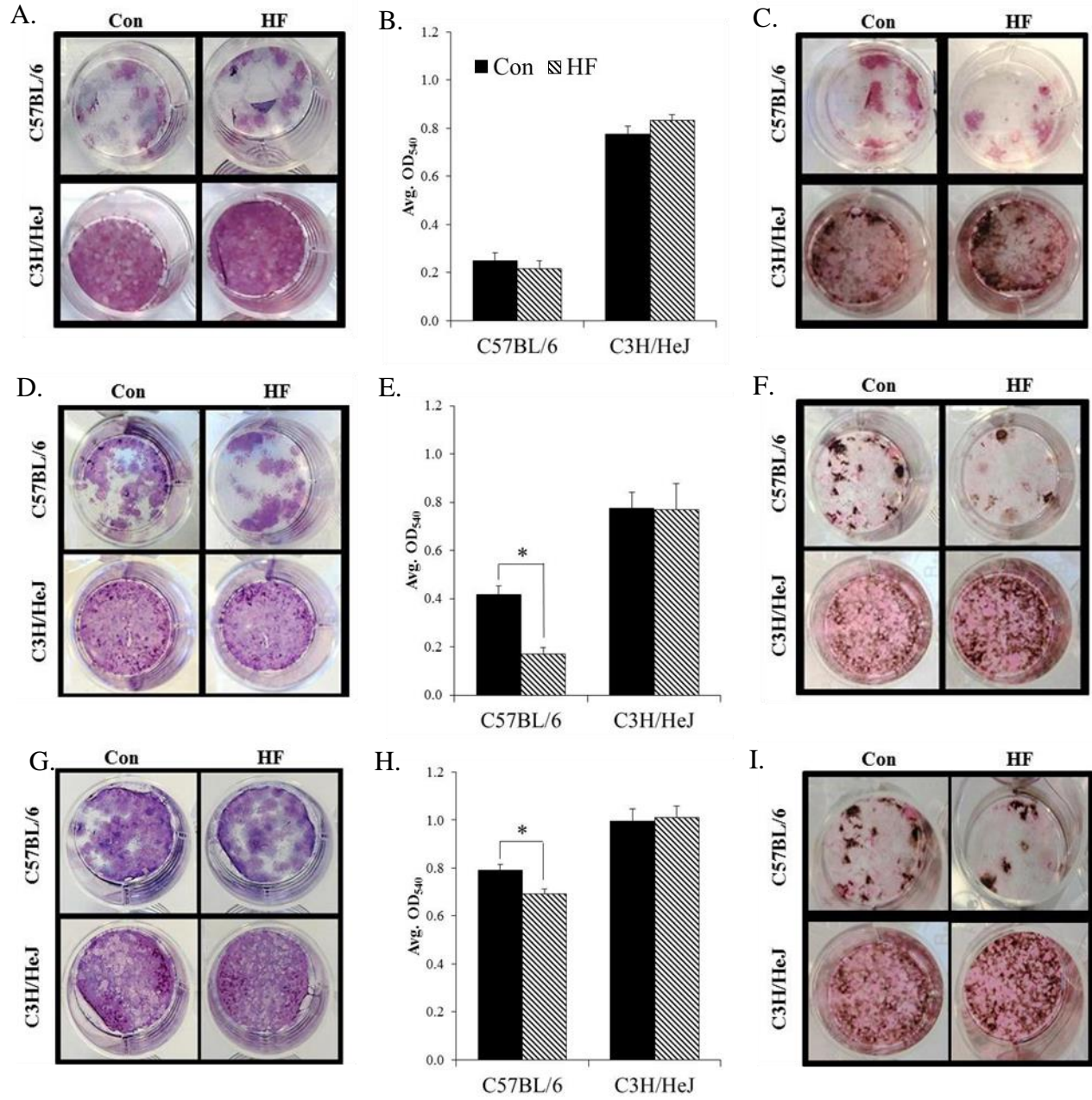
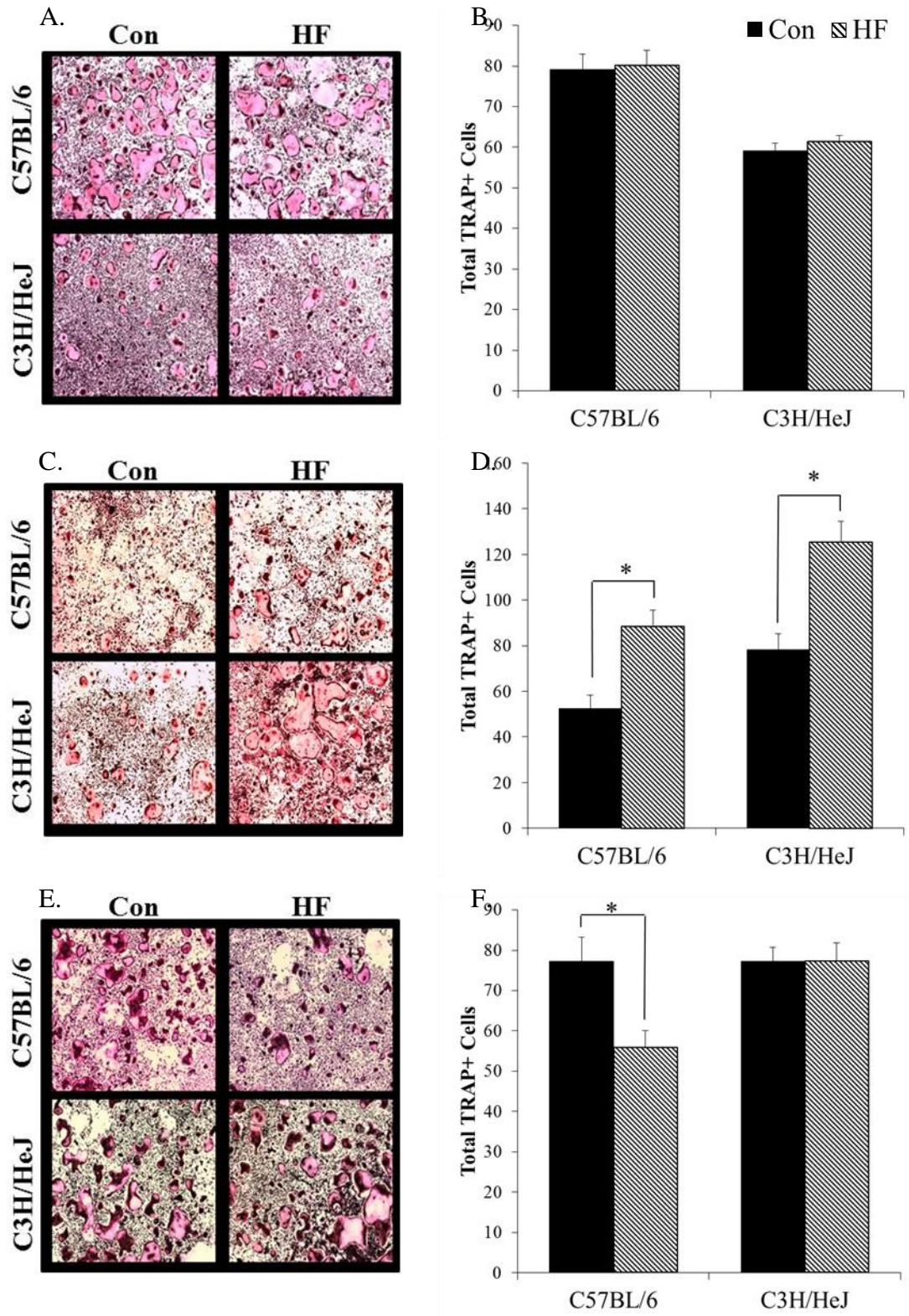


Figure 4.



CHAPTER V

GLUCOSE INTOLERANCE ATTENUATES BONE ACCRUAL IN YOUNG
GROWING SKELETON BY PROMOTING THE MATURATION OF OSTEOBLASTS
THROUGH BECLIN1-MEDIATED AUTOPHAGY

Title: Glucose Intolerance Attenuates Bone Accrual in Young Growing Skeleton by Promoting the Maturation of Osteoblasts through Beclin1-Mediated Autophagy

Authors: E Rendina-Ruedy¹, J.L. Graef¹, SA Lightfoot², JW Ritchey³, SL Clarke¹, EA Lucas¹, BJ Smith¹

¹Department of Nutritional Sciences, Oklahoma State University, Stillwater, OK.

²Center for Cancer Prevention and Drug Development, University of Oklahoma Health Sciences Center, Oklahoma City, OK.

³Department of Veterinary Pathology, Oklahoma State University, Stillwater, OK.

Corresponding Author: Brenda J. Smith, Department of Nutritional Sciences, HSci 420 Oklahoma State University, Stillwater OK 74078; (405) 744-3866; bjsmith@okstate.edu

Grant Supporters: United States Department of Agriculture (2012-67011-19906) and Oklahoma Center for the Advancement of Science and Technology (HR10-068).

Keywords: Hyperglycemia, insulin, macroautophagy, fracture, osteocyte

Abstract

Patients with type 2 diabetes mellitus (T2DM) have demonstrated a 1.5-3.5 fold increase in fracture risk, but the mechanisms responsible for these skeletal changes remain elusive. Macroautophagy, referred to hereafter as autophagy, is regulated by signaling downstream of the insulin receptor. Metabolic changes associated with the initiation and progression of glucose intolerance have been shown to alter autophagy in various tissues, but limited information is available in relation to bone cells. The aim of this study was to (1) investigate whether autophagy is altered in the bone during the initiation and progression of T2DM and (2) determine how autophagy impacts osteoblast differentiation, activity, and maturation. To accomplish this aim, 4-week old, male C57BL/6 mice were fed a control (Con) or high fat (HF) diet for 2, 8, and 16 wks. Consistent with reduced insulin sensitivity, mice on the HF diet demonstrated elevated fasting blood glucose and impaired glucose tolerance. Micro-computerized tomography (microCT) analyses revealed reduced trabecular bone at 8 and 16 wks in the femoral neck, which resulted in lower trabecular bone volume compared to Con mice. Histological evaluation of the tibia and characterization of osteoblast-related genes in the flushed femur suggested that hyperglycemia decreased bone mineralization and may promote terminal osteocyte differentiation. This shift of the osteoblasts towards a non-mineralizing, osteocyte phenotype appears to be coordinated by Beclin1 mediated autophagy during impaired glucose tolerance. However, long-term glucose intolerance resulted in an increase in apoptosis of the osteoblast based on an increase in *Casp3* mRNA. Consistent with changes occurring in the osteoblast *in vivo*, the induction of autophagy by rapamycin was able to direct MC3T3-E1 cells towards a more mature osteoblast phenotype. The current study provides evidence that glucose intolerance contributes to the skeletal dysregulation of bone metabolism by up-regulating autophagy in

osteoblasts, directing this cell towards a non-mineralizing osteocyte, ultimately attenuating bone accrual. Further investigation is warranted to determine if Beclin1-mediated autophagy is essential for the terminal differentiation of the osteoblasts and whether autophagy is having a protective or deleterious effect on bone in T2DM.

Introduction

Type 2 diabetes mellitus (T2DM) is a major public health problem in the U.S. affecting ~25 million adults [1]. The CDC has projected that the prevalence of T2DM will double or even triple, affecting 1 in 3 adults, by 2050 if current trends continue [1]. In addition to classic complications associated with T2DM (e.g., peripheral vascular disease, retinopathy, nephropathy, impaired wound healing, and neuropathy) it has recently been determined that type 2 diabetics are also at greater risk of fracture, primarily at the hip region [2-6]. Furthermore, it was demonstrated that the clinical determinant of fracture risk, bone mineral density (BMD), and the World Health Organization Fracture Risk Algorithm (FRAX) underestimates fracture risk in adults with T2DM [7]. Recent studies have described the attenuation of bone accrual in mice during the development and progression of glucose intolerance, and attribute this observation, in part, to an altered osteoblast phenotype [8]. Therefore, to begin to understand why T2DM increases skeletal fragility, it is imperative that alterations in bone metabolism be investigated both during the progression of hyperglycemia and glucose intolerance.

The hyperglycemia associated with T2DM is attributed, in part, to diminished insulin sensitivity and alterations in the downstream signaling cascade. Although several different types of autophagy exist (i.e., microautophagy, chaperone mediated autophagy and macroautophagy), macroautophagy is the most studied and is, therefore, commonly referred to simply as “autophagy”. Autophagy is a cellular process that is controlled by proteins downstream of the insulin receptor (IR) and is involved in energy (i.e., glucose) sensing and effectively regulates cell survival or cell death by means of organelle recycling [9]. This multi-step cellular process involves initiation, membrane nucleation, phagophore formation, sequestration and autophagosome formation, followed by autophagosome-lysosome fusion. Like many other cells,

bone forming osteoblasts express the IR; therefore, during glucose intolerance osteoblasts may experience alterations in insulin signaling, resulting in the up-regulation of autophagy. Although changes in autophagy have been demonstrated in β -cells, hepatocytes, cardiac myocytes, and adipocytes in type 2 diabetics, no published reports have examined whether autophagy is altered in bone cells during glucose intolerance [10-14].

While significant advances in the field of autophagy as it relates to bone has made in the past 5 yr, conflicting evidence exists on how alterations in the autophagic process will impact osteoblast differentiation, maturation, and activity. For example, Yang *et al.* [15] described a serum-deprivation model of autophagy in osteoblast-like MC3T3-E1 cells in which growth factors and insulin are absent from the culture and noted increased initiation of autophagy and autophagosome formation as evidenced by increased Beclin1, LC3-II, and ULK1 protein abundance. Interestingly, when osteoblasts were treated with estradiol apoptotic events were decreased while autophagy was enhanced [15]. In this case autophagy induction by estradiol is associated with a cytoprotective process, however, publications on glucocorticoid treatment and the free fatty acid, palmitate, describe autophagy as a means by which osteoblasts and osteocytes undergo cell death [16;17]. Two ground-breaking studies related to autophagy and bone have utilized conditional knockout models. For example, Onal *et al.* [18] knocked out the autophagic protein, Atg7, in terminally differentiated osteocytes. Interestingly, these animals exhibited a decrease in femoral, spinal, and total BMD, which was attributed to a decrease in both trabecular and cortical bone. Further insight into how autophagy impacts bone metabolism was provided in an osteoblast conditional knockout of FIP200, in which the animals demonstrated dramatically lower trabecular and cortical bone at 1, 2, and 6 mo of age [19]. These structural changes in the bone were attributed to decreased bone formation as determined by dynamic bone

histomorphometry [19]. Together, these two studies demonstrate that basal autophagy promotes osteocyte function, supports nodule formation by osteoblasts and contributes to the terminal differentiation of osteoblasts. Moreover, one of the earliest assays established to assess autophagy involved determining alkaline phosphatase (ALP) activity in yeast [20]. However, the measurement of ALP would prove to be a non-specific indicator in cells such as the osteoblast, which express high levels of ALP to aid in the mineralization of bone. Given that the attenuation of bone formation associated with the progression of glucose intolerance is primarily attributed to altered osteoblastogenesis, alterations in autophagy in the osteoblasts may contribute to the skeletal phenotype.

Based on the regulation of autophagy by the insulin signaling pathway, insulin resistance during T2DM may increase autophagy in osteoblasts initially providing protection from cellular stress and, possibly, induce cellular maturation. Although information on how autophagy impacts osteoblast differentiation and function is limited, previous studies have supported the notion that autophagy may initially provide protection from cellular stresses occurring during T2DM [19;21]. If the autophagy is increased during the early stages of T2DM and hyperglycemia, this dynamic process may provide a protective role and maintaining normal bone turnover. However, prolonged hyperglycemia could uncouple bone metabolism, resulting in a compromised bone structure and ultimately increased fracture risk. Therefore, this study was designed to (1) investigate whether autophagy is altered in the bone during the initial development and progression of glucose intolerance; and (2) determine how autophagy impacts osteoblast differentiation, activity, and maturation.

Materials and Methods

Animal Use and Care

Four week old male C57BL/6N (Charles Rivers, Wilmington, MA), referred to hereafter as C57BL/6, were utilized for the current study. The rationale for choosing this strain was based on their metabolic and skeletal response to high fat diet, which was more similar to clinical pathophysiology of T2DM versus the C57BL/6J strain (*unpublished data*). These animals were allowed to acclimate for 1 wk and then divided into six groups ($n = 8-10$ mice/group) to receive the control (Con; AIN-93M, 10 % kcals from fat) or a high fat (HF; 60% kcals from fat) diet for 2, 8, or 16 wk. Bodyweight and food intake were recorded throughout the study. At the end of each time point, mice were anesthetized (ketamine/ xylazine cocktail 70 and 30 mg/kg body weight, respectively) and exsanguinated via the carotid artery. At the time of sacrifice tibia and femurs were disarticulated and cleaned of surrounding soft tissue. Femurs to be used for microCT were stored in phosphate buffered saline (PBS) at -4°C , while femurs used for RNA and protein extraction were flushed of their bone marrow and stored in a cryotank (-140°C). Tibias were stored in 10% neutral buffered formalin (NBF) until histological processing. All procedures were approved by the Institutional Animal Care and Use Committee of Oklahoma State University.

Intraperitoneal Glucose Tolerance Test and Plasma Insulin

Three to five days prior to the termination of each study period, mice were fasted for 6 hrs and blood glucose was determined at baseline. Mice then received an intraperitoneal injection of glucose solution (2 g glucose/ kg bodyweight) and their blood glucose was

monitored at 15, 30, 60, 90, and 120 min. Plasma insulin was determined at 2, 8 and 16 wks using a commercially available ELISA kit (Crystal Chem, Downers Grove, IL).

Determination of Alterations in Microarchitecture by MicroCT

Given the profound impact glucose intolerance has on fracture occurring in the hip, micro-computerized tomography (microCT40, SCANCO Medical, Switzerland) was performed to determine changes occurring in the microarchitecture of the femoral neck. Trabecular bone of the femoral neck was determined by scanning each specimen at a resolution of 2048 x 2048 pixels, followed by identifying an approximately 280 μm volume of interest (VOI) beginning 30 μm distal from the femoral neck growth plate. The analyses focused exclusively on secondary spongiosa. Trabecular bone parameters evaluated included bone volume expressed as a percentage of total volume (BV/TV), trabecular number (Tb.N.), trabecular thickness (Tb.Th.), trabecular separation (Tb.Sp.) connectivity density (Conn.Dens.) and structural model index (SMI). All of the acquired images for trabecular and cortical bone were analyzed at a threshold of 340, and a sigma and support of 1.2 and 2.0, respectively.

Morphological Changes in the Tibia

Fixed tibia samples were processed by exposure to sequential dehydration steps with ethanol, cleared with toluene, and paraffin embedded. Tibial sections were cut on a longitudinal axis (5 μm each) using a microtome (Leica RM2165, Wetzlar, Germany) and sections were stained with hematoxylin and eosin. Tibia specimens were then read by the study pathologist

and changes in morphology were noted for osteoblasts (e.g., lining trabeculae and on the endocortical surface) and osteocytes (e.g., in developed lacuna).

Cell Culture Experiments

Mouse pre-osteoblast MC3T3-E1 cells (Riken BioResource Center, Ibaraki, Japan) were maintained in complete α MEM containing 10% fetal bovine serum (FBS), 100 U/L penicillin G and 100 mg/L streptomycin, and 2 mM L-glutamine at 37°C in a humidified atmosphere of 5% CO₂. For osteoblast differentiation experiments, osteogenic medium containing complete α MEM supplemented with 10 mM β -glycerophosphate and 25 μ g/ mL ascorbic acid. Rapamycin and bafilomycin A1 was purchased from Cayman Chemical Company (Ann Arbor, MI), and both were dissolved in DMSO purged with N₂ according to the manufacture's specifications.

Undifferentiated pre-osteoblastic MC3T3-E1 cells were plated (2.0 x 10⁶ cells/ mL) and allowed to adhere for 24 hrs in complete α MEM (i.e., 0 day differentiation). Cells were than subjected to treatment with 0 μ M (Con and DMSO) or 10 μ M rapamycin for 24 hr. Due to the lysosomal degradation of LC3B-II protein 0 or 200 nM of bafilomycin A1 (BafA1) was added to cultures 2 hr prior to RNA and protein harvest (e.g., 22 hr). To determine changes induce by autophagy in a more mature osteoblast, osteogenic medium was added to MC3T3-E1 cultures, and cells were allowed to differentiate for 7 days. Following this differentiation period, cells were treated with 0 or 10 μ M rapamycin for 24 hr, while bafilomycin was added 2 hr before the RNA and protein was extracted.

RNA Extraction and qPCR Analyses

Total RNA was extracted from pulverized, flushed femurs (Spex 6770 Freezer Mill, Metuchen, NJ) and MC3T3-E1 cells using TriZol Reagent (Life Technology, Rockville, MD), following the manufacturers protocol. RNA was quantified using a Nanodrop Spectrophotometer (Rockland, DE) while gel electrophoresis was carried out to verify the quantity and quality of all RNA samples. cDNA was synthesized using 2 µg of total RNA pre-treated with DNase I and subjected to reverse-transcription (Superscript II, Invitrogen, Carlsbad, CA). Each qPCR reaction was performed in duplicate or triplicate using SYBR green chemistry (SABiosciences, Valencia, CA) on the Applied Biosystems 7900HT Fast Real-Time PCR System (Foster City, CA). All qPCR results were evaluated by the comparative cycle number at threshold (C_Q) method (User Manual #2, Applied Biosystems), using peptidylprolyl isomerase B (*Ppib*) as the invariant control. Primer sets for target genes can be found in supplemental materials.

Protein Extraction and Western Blot Analyses

Crude protein was prepared from femur tissues with the bone marrow flushed and MC3T3-E1 cells. Both the homogenized flushed femur and cell pellet were lysed using RIPA buffer containing a protease/ phosphatase inhibitor cocktail (Cell Signaling Technologies, Dancers, MA). Lysates were incubated on ice for 40 min, with vortexing and sonication every 10 min. Samples were then centrifuged at 16,000 x g for 15 min at 4°C, supernatant containing total protein was then aliquoted and stored at -80°C. Prior to western blot analyses, protein concentration was determined by bicinchoninic acid (BCA) assay. Primary antibodies for Beclin1 (Novus Biologicals, Littleton, CO), pBeclin1 (EMD Millipore, Billerica, MA), β-Actin

(Santa Cruz Biotechnology, Dallas, TX), and LC3B and ROCK1 (Cell Signaling Technology, Danvers, MA).

Statistical Analyses

Statistical analyses were accomplished using SAS Version 9.3 (SAS Institute, NC). Comparisons were made between dietary treatment groups across all time points using one-way ANOVA, followed by *post hoc* analysis with Fischer's least square means separation test when F values were significant ($P < 0.05$), unless otherwise stated. Results from the IGTT were analyzed by performing student's paired t-test to make comparisons at a given time point following glucose administration (e.g., 15, 30, 60, 90, 120 min) for a given treatment period (e.g., 2, 8, or 16 wk). Randomized control block design (RCBD) was used for western blot analyses to account for blot-to-blot variability. Similar to ANOVA, when F values were significant ($P < 0.05$) *post hoc* analysis was performed with Fischer's least square means separation test. All data are presented as mean \pm standard error (SE) and α was set at 0.05.

Results

Metabolic and Skeletal Changes Occurring in Response to a High Fat Diet Overtime

Mice on the HF diet exhibited elevated fasting blood glucose at the 2, 8, and 16 wk time point prior to administration of IGTT (**Figure 1A-C**). At the 2 (**Figure 1A**) and 8 (**Figure 1B**) mice on the HF diet were able to restore blood glucose to some extent which suggests s impaired glucose tolerance, often referred to as pre-diabetes. However, given the results of the IGTT at 16

wk, it was evident that mice on the HF diet were unable to restore blood glucose, exhibiting a phenotype consistent with glucose intolerance (**Figure 1C**). As we have previously shown, mice on the HF diet were hypoinsulinemic at the 2 wk time point (Con=206.4 pg/mL; HF=148.0 pg/mL). Fasting plasma insulin was similar between dietary groups at 8 wk (Con=248.9 pg/mL; HF=257.3 pg/mL) and after 16 wk these mice demonstrated elevated plasma insulin (Con=370.8 pg/mL; HF=736.7 pg/mL). Therefore, mice at the 2 and 8 wk time on the HF diet demonstrated metabolic changes corresponding to pre-diabetes, while the metabolic response at the later 16 wk time point (i.e., hyperglycemia, hyperinsulinemia, and glucose intolerance) was consistent with T2DM,

Trabecular BV/TV in the femoral neck was the highest in the Con groups after 8 and 16 wk, while the lowest BV/TV was observed in the 2 wk Con, as well as in the animals that received the HF diet for 2, 8, and 16 wk (**Table 1**). Based on this data, it is evident that trabecular bone accrual stopped as early as 2 wk on the high fat diet and remained impaired through the duration of the study, suggesting that the initiation of glucose intolerance halts bone formation. A similar trend was observed in Tb.Th., Conn.Dens., and SMI (**Table 1**). Cortical bone (i.e., cortical thickness) was previously shown to be reduced by 7.4% at the femur mid-diaphysis.

Interestingly, histological evaluation of the proximal tibia metaphysis in the 2 wk Con group demonstrated cuboidal, active osteoblasts (**Figure 2A**). In contrast, mice on the HF diet for 2 wk had a marked decrease in osteoblasts and a notable increase in number of osteocytes, suggestive of decreased bone formation (**Figure 2A**). Consistent with changes occurring in femoral BV/TV over time, the 8 wk Con animals appeared to have increased calcification than previously reported at the 2 wk time point. Mice on the HF diet had fewer active osteoblasts,

more inactive, spindle-shaped osteoblasts, and an apparent marked increase in osteocyte number (**Figure 2A**). In agreement with the microCT data, at the 16 wk time point mice on the HF diet had noticeably thinner trabeculae, in addition to the rare observation of active osteoblasts (**Figure 2A**).

During the altered metabolic state consistent with pre- and early stage diabetes, there was an increase in the relative abundance of *Ccnd1* (**Figure 2B**), *Bmp4* (**Figure 2D**), and *Colla1* mRNA (**Figure 2F**). While the change in *Atf4* did not reach the level of statistical significance ($P=0.0643$), the relative mRNA abundance of *Atf4* was the highest in the 2 wk HF group, and the lowest in the 2 wk Con group (**Figure 2E**). These changes in transcriptional regulation of osteoblastogenesis were not present between Con animals and those experiencing progressive stages of glucose intolerance at the 16 wk time point. Moreover, no dietary change was observed in *Spp1* (**Figure 2I**) and *Bglap* (**Figure 2J**) mRNA, which may be a reflection of the mixed cell population in the flushed femur. No changes were observed in *Bmp2* (**Figure 2C**).

Determination of Altered Autophagy in Bone during Pre-, Short, and Long Glucose Intolerance

To test the hypothesis that autophagy is up-regulated during impaired glucose tolerance and contributing to the induction of osteoblast maturation, proteins involved in autophagy regulation were visualized in the flushed femur (**Figure 3A**). Total Beclin1 protein expression was highest at the 8 and 16 wk time point in mice fed the HF diet (**Figure 3B**), however further analysis was needed due to the variation in post-translational modifications and functions of Beclin1. pBeclin1 (Thr119) protein abundance was shown to be the highest at 8 wk in the control group and both the Con and HF diet groups at the 16 wk time point (**Figure 3C**). No changes were observed in LC3B-II abundance, however this was predicted as LC3B-II was

presumably degraded in the lysosome (**Figure 3D**). No consistent changes were observed in protein abundance of ROCK1 (**Figure 3E**). While no changes were observed in *Maplc3a* (**Figure 3F**) the induction of autophagy by *Maplc3b* (**Figure 3G**) and *Becn1* (**Figure 3H**) appeared to be initiated during the early stages of impaired glucose tolerance (i.e., after 2 wk on HF diet), preceding the changes in pBeclin1 protein abundance. Furthermore, autophagy induction during early hyperglycemia appears to lower apoptosis given the *Casp3* mRNA abundance, while apoptotic events appears to be elevated in the bone due to prolonged glucose intolerance (**Figure 3I**).

In vitro Model of Autophagy Induction and Transcriptional Regulation of Osteoblastogenesis

To determine how the up-regulation of autophagy with glucose intolerance affects osteoblastogenesis, MC3T3-E1 cells were cultured with 10 μ M Rapamycin with the addition of 200 nM BafA1 for the last 2 hrs of the study. Although it appears that immature (**Figure 4A**) and mature osteoblasts (**Figure 4B**) have high levels of basal autophagy based on the abundance of LC3B-II in control cells (i.e., Con and DMSO), the addition of 10 μ M rapamycin for 24 hr was able to increase autophagy as evidenced by LC3-II protein abundance (**Figure 4C**) and *Maplc3a* (**Figure 4D**) and *Maplc3b* (**Figure 4E**) mRNA. However, no changes were observed in *Becn1* mRNA or protein abundance of pBeclin1 or Beclin1 in undifferentiated (0d) or differentiated (7d) MC3T3-E1 cells (*data not shown*).

Once this model autophagy induction in the osteoblast was established, genes involved in osteoblast differentiation, activity, and maturation were determined. Immature, osteoblast MC3T3-E1 cells undergoing autophagy induced via rapamycin treatment demonstrated a

decrease in mRNA abundance of genes critical for osteoblast differentiation and early osteoblast activity including *Atf4* (**Figure 5D**), *Cbfa1* (**Figure 5E**), *Alpl* (**Figure 5F**), and *Colla* (**Figure 5G**). Conversely, an up-regulation was noted in the cell cycle regulator *Ccnd1* (**Figure 5A**) and the gene that encodes osteopontin, *Spp1*, an indicator of late osteoblast activity (**Figure 5H**). While a similar pattern was observed when autophagy was up-regulated in a more mature osteoblasts (i.e., 7 day differentiation), *Ccnd1* mRNA (**Figure 5A**) was lower in the rapamycin treated group compared to controls (Con and DMSO) and no changes were observed in *Cbfa* (**Figure 5E**), *Alpl* (**Figure 5F**) and *Colla1* (**Figure 5G**). In these more mature osteoblasts, a significant increase in osteocalcin gene expression (*Bglap*) was also noted (**Figure 4**). The differences in the regulation of these genes are presumably indicative of the difference in transcriptional machinery essential during the different stages of osteoblastogenesis. However, in both the undifferentiated and differentiated MC3T3-E1 cells, enhanced autophagy appears to drive the osteoblast towards a more mature, non-mineralizing phenotype.

Discussion

These data demonstrate that during the onset and progression of impaired glucose tolerance and early stages of T2DM, bone accrual is attenuated. This phenotype is observed concurrently with alterations in osteoblast maturation and up-regulated autophagy. These findings suggest that autophagy appears to be driving the terminal differentiation of osteoblasts towards a non-mineralizing cell, via Beclin1-mediated mechanism. While bone accrual appeared to be normal during up until 2 wk, trabecular bone accrual was halted as impaired glucose tolerance progressed. These microarchitecture changes from the femoral neck are consistent

with our previous observations in this model in that bone accrual was attenuated in the distal femur metaphysis. Although it has been shown by our lab and others that hyperglycemia attenuates bone accrual due to decreased osteoblast differentiation, elaboration of the possible mechanisms or fates of the osteoblasts has not been investigated [8]. Histological evaluation of the proximal tibia revealed that while osteoblast number and activity was apparently decreased during glucose intolerance, it appeared that osteocyte numbers were increased in these young animals. Given that the primary role of the osteocyte is to function as a mechanosensing cell, although it is differentiated from an osteoblast, the osteocyte does not form bone [22;23]. Therefore, these data suggest that the apparent increase in osteocyte number during the initiation of glucose intolerance was driven by an increase in osteoblast maturation, and is detrimental to bone accrual.

The possible rationale for a scenario of increased autophagy contributing to osteoblast maturation is two-fold. First, due to the control of autophagy by proteins involved in insulin signaling and intracellular energy sensors (e.g., mTORC1 and AMPK) this process could be altered during different stages of glucose intolerance [10;13;24]. Second, autophagy has been suggested to be essential in the terminal differentiation of osteoblasts to osteocytes [19]. While, one of the most widely accepted indicators of autophagosome formation is LC3-II protein abundance, a major limitation in using this method is that LC3-II is readily degraded in the lysosome, making *in vivo* assessment a challenge [25]. Due to these limitations, Beclin1 protein expression was determined given its recently identified function as a key regulator of membrane nucleation and autophagosome formation [26]. Beclin1 protein abundance was shown to be elevated in the flushed femur following the more prolonged periods of glucose intolerance. Beclin1 has been demonstrated to regulate autophagy by its existence in pro-autophagic

complexes including Barkor-Vps34-Vps15-Beclin1-AMBRA and Vps34-Vps15-Beclin1-Bif-1-UVRAG, whereas Rubicon bound Vps34-Vps15-Beclin1-UVRAG complex negatively functions in autophagosome maturation [27]. Given the multi-functionality of Beclin1, protein abundance of pBeclin1 (Thr119) was identified to be a specific indicator of autophagy activation and demonstrated to be increased following 8 wk on a HF diet in the flushed femur. Active ROCK1 has been previously described to phosphorylate Beclin1 at Thr119, up-regulating Beclin1-mediated autophagy by dissociated the Beclin1-Bcl-x_L complex [28]. Moreover, ROCK1 kinase activity has been shown to be increased during glucose intolerance, making it a suitable protein of interest in the current model. Although, no changes were observed in ROCK1 protein abundance, ROCK1 activity was not assessed and may still provide an explanation for the up-regulated Beclin1-mediated autophagy in this model. The fact that no changes were observed in LC3B-II protein abundance, along with the changes occurring in Beclin1 and *Maplc3a*, *Maplc3b*, suggests an increase in autophagic flux or the degradation and turnover of sequestered cargo. Therefore, in the flushed femur, a sample enriched for osteoblasts and osteocytes, autophagy appears to be increased in response to early and short term glucose intolerance, however, a prolonged hyperglycemic state results in apoptosis these cells.

The up-regulation of autophagy in osteoblast-like MC3T3-E1 cells resulted in their maturation and terminal differentiation. This *in vitro* model was able to confirm some of the changes occurring in the femur which was importance because the flushed femur preparations likely represent a heterogeneous cell population. Although we attempted to enrich for osteoblast and osteocyte cell populations by flushing the bone marrow, these cells are expected to be at different stages of differentiation, ranging from osteoblast progenitor cells, to terminally differentiated osteocytes. This difference in cell populations from the flushed femur versus the

isolated MC3T3 cells may be the reason some conflicting results are reported. The mechanism for autophagy induction in impaired glucose tolerance in the bone appears to involve a different mechanism than rapamycin-induced autophagy in the MC3T3-E1 cells. Beclin1 mediated autophagy has previously been reported to be a mechanism that is critical during glucose deprivation in mouse embryonic fibroblasts (MEFs), and not essential for autophagy initiated by rapamycin [29]. Furthermore, the addition of BafA1 to the MC3T3-E1 cell cultures allowed for the reliable visualization and quantification LC3B-II, however no lysosomal inhibitor was used *in vivo*.

This study is the first to provide data that suggests that glucose intolerance contributes to the skeletal dysregulation of bone metabolism by up-regulating autophagy in osteoblasts, directing this cell towards a non-mineralizing osteocyte, ultimately attenuating bone accrual. Further investigation is warranted to determine if Beclin1-mediated autophagy is essential for the terminal differentiation of the osteoblasts and whether the promotion of autophagy during T2DM results in lower bone volume. Moreover, given the biphasic nature of autophagy (i.e., cytoprotective vs. cell death), it may be possible that this process exerts different mechanisms on these bone cells resulting in different alterations in bone structure and/or biomechanics. Therefore, these data provide evidence of an the up-regulation of autophagy during T2DM, which dysregulates osteoblast maturation, and possibly fate, altering the bone phenotype.

Figure 1. Alterations in glucose tolerance was determined by injecting (IP) glucose solution and tracking blood glucose in mice that were maintained on a control (Con; AIN93M) or high fat (HF; 60% kcal from fat) for 2 (A), 8 (B), and 16 (C) wk. Data is presented as the mean \pm SE. Symbol * represents a significant difference ($P < 0.05$) between dietary treatments at a given time point.

Figure 2. Histological evaluation of hematoxylin and eosin (H&E) stained tibias were read for changes in osteoblast abundance and morphology, along with osteocyte development in mice maintained on a control (Con; AIN93M) or high fat (HF; 60% kcal from fat) for 2, 8, and 16 wk, representative images are shown (A). qPCR was performed on flushed femur samples to determine alterations occurring in genes involved in osteoblast differentiation and activity, to characterize osteoblast maturation. Genes of interest included *Ccnd1* (B), *Bmp2* (C), *Bmp4* (D), *Atf4* (E), *Cbfa1* (F), *Alpl* (G), *Colla1* (H), *Spp1* (I), and *Bglap* (J). All qPCR results were evaluated by the comparative cycle number at threshold (C_Q) method, and genes of interest were normalized to the invariant control, peptidylprolyl isomerase B (*Ppib*) and expressed as relative mRNA abundance. Data is presented as the mean \pm SE ($n=6$). Bars that share the same superscript letter are not significantly different from each other ($P<0.05$).

Figure 3. Western blot analyses and qPCR was performed to determine changes in proteins and genes involved in autophagy from flushed femur samples after mice were fed a control (Con; AIN93M) or high fat (HF; 60% kcal from fat) for 2, 8, and 16 wk,. Representative images ($n=5$) of western blots probed for Beclin1, pBeclin1 (Thr119), LC3B, ROCK1 and β -Actin (A). Quantification of Beclin1 (B), pBeclin1 (C), LC3B-II (D), and ROCK1 (E) was carried out by determining density light units (DLU) for a given protein, and expressed normalized back to β -Actin ($n=5$). qPCR results for *Maplc3a* (F), *Maplc3b* (G), *Becn1* (H), and *Casp3* (I) are

normalized to peptidylprolyl isomerase B (*Ppib*) and expressed as relative mRNA abundance ($n=6$). Data is presented as the mean \pm SE. Bars that share the same superscript letter are not significantly different from each other ($P<0.05$).

Figure 4. An *in vitro* model of increased autophagy in undifferentiated (0d) and differentiated (7d) MC3T3-E1 cells was developed by subjecting them to treatment with 0 μ M (Con and DMSO) or 10 μ M rapamycin for 24 hr. Bafilomycin (BafA1) of was added to cultures 2 hr prior (e.g., 22 hr) to protein and RNA extraction. Representative images of western blot analyses of LC3B-II abundance from undifferentiated (A) and differentiated (B) MC3T3-E1 cells are shown. LC3B-II protein abundance was determined by quantifying density light units (DLU) normalized to γ -tubulin DLU (C). qPCR analysis of *Maplc3a* (D) and *Maplc3b* (E), normalized to peptidylprolyl isomerase B (*Ppib*) and expressed as relative mRNA abundance. Data is presented as the mean \pm SE ($n=3$). Points that share the same superscript letter are not significantly different from each other ($P<0.05$).

Figure 5. To determine how autophagy would impact undifferentiated (0d) and differentiated (7d) MC3T3-E1 cells were treated with 0 μ M (Con and DMSO) or 10 μ M rapamycin for 24 hr. RNA was extracted and qPCR was performed to characterize genes involved in osteoblast differentiation, activity, and maturation including; *Ccnd1* (A), *Bmp2* (B), *Bmp4* (C), *Atf4* (D), *Cbfa1* (E), *Alpl* (F), *Colla1* (G), *Spp1* (H), and *Bglap* (I). All qPCR results were evaluated by the comparative cycle number at threshold (C_Q) method, and genes of interest were normalized to the invariant control, peptidylprolyl isomerase B (*Ppib*) and expressed as relative mRNA abundance. Data is presented as the mean \pm SE ($n=6$). Bars that share the same superscript letter are not significantly different from each other ($P<0.05$).

References

- 1 Centers for Disease Prevention and Control. National Diabetes Fact Sheet. 2011.
- 2 de Liefde II, van der Klift M, de Laet CE, van Daele PL, Hofman A, Pols HA. Bone mineral density and fracture risk in type-2 diabetes mellitus: the Rotterdam Study. *Osteoporos Int* 2005 Dec;16(12):1713-20.
- 3 Janghorbani M, Feskanich D, Willett WC, Hu F. Prospective study of diabetes and risk of hip fracture: the Nurses' Health Study. *Diabetes Care* 2006 Jul;29(7):1573-8.
- 4 Nicodemus KK, Folsom AR. Type 1 and type 2 diabetes and incident hip fractures in postmenopausal women. *Diabetes Care* 2001 Jul;24(7):1192-7.
- 5 Schwartz AV, Sellmeyer DE, Ensrud KE, Cauley JA, Tabor HK, Schreiner PJ, et al. Older women with diabetes have an increased risk of fracture: a prospective study. *J Clin Endocrinol Metab* 2001 Jan;86(1):32-8.
- 6 Farr JN, Drake MT, Amin S, Melton LJ, III, McCready LK, Khosla S. In Vivo assessment of bone quality in postmenopausal women with type 2 diabetes. *J Bone Miner Res* 2013 Oct 1.
- 7 Schwartz AV, Vittinghoff E, Bauer DC, Hillier TA, Strotmeyer ES, Ensrud KE, et al. Association of BMD and FRAX score with risk of fracture in older adults with type 2 diabetes. *JAMA* 2011 Jun 1;305(21):2184-92.
- 8 Lu XM, Zhao H, Wang EH. A high-fat diet induces obesity and impairs bone acquisition in young male mice. *Mol Med Rep* 2013 Apr;7(4):1203-8.
- 9 Bursch W, Karwan A, Mayer M, Dornetshuber J, Frohwein U, Schulte-Hermann R, et al. Cell death and autophagy: cytokines, drugs, and nutritional factors. *Toxicology* 2008 Dec 30;254(3):147-57.
- 10 Masini M, Bugliani M, Lupi R, del GS, Boggi U, Filippini F, et al. Autophagy in human type 2 diabetes pancreatic beta cells. *Diabetologia* 2009 Jun;52(6):1083-6.
- 11 Jansen HJ, van EP, Koenen T, Joosten LA, Netea MG, Tack CJ, et al. Autophagy activity is up-regulated in adipose tissue of obese individuals and modulates proinflammatory cytokine expression. *Endocrinology* 2012 Dec;153(12):5866-74.
- 12 Nunez CE, Rodrigues VS, Gomes FS, de Moura RF, Victorio SC, Bombassaro B, et al. Defective regulation of adipose tissue autophagy in obesity. *Int J Obes (Lond)* 2013 Mar 12.
- 13 Ost A, Svensson K, Ruishalme I, Branmark C, Franck N, Krook H, et al. Attenuated mTOR signaling and enhanced autophagy in adipocytes from obese patients with type 2 diabetes. *Mol Med* 2010 Jul;16(7-8):235-46.

- 14 Liu HY, Han J, Cao SY, Hong T, Zhuo D, Shi J, et al. Hepatic autophagy is suppressed in the presence of insulin resistance and hyperinsulinemia: inhibition of FoxO1-dependent expression of key autophagy genes by insulin. *J Biol Chem* 2009 Nov 6;284(45):31484-92.
- 15 Yang YH, Chen K, Li B, Chen JW, Zheng XF, Wang YR, et al. Estradiol inhibits osteoblast apoptosis via promotion of autophagy through the ER-ERK-mTOR pathway. *Apoptosis* 2013 Nov;18(11):1363-75.
- 16 Gunaratnam K, Vidal C, Gimble JM, Duque G. Mechanisms of Palmitate-Induced Lipotoxicity in Human Osteoblasts. *Endocrinology* 2013 Oct 29.
- 17 Xia X, Kar R, Gluhak-Heinrich J, Yao W, Lane NE, Bonewald LF, et al. Glucocorticoid-induced autophagy in osteocytes. *J Bone Miner Res* 2010 Nov;25(11):2479-88.
- 18 Onal M, Piemontese M, Xiong J, Wang Y, Han L, Ye S, et al. Suppression of autophagy in osteocytes mimics skeletal aging. *J Biol Chem* 2013 Jun 14;288(24):17432-40.
- 19 Liu F, Fang F, Yuan H, Yang D, Chen Y, Williams L, et al. Suppression of autophagy by FIP200 deletion leads to osteopenia in mice through the inhibition of osteoblast terminal differentiation. *J Bone Miner Res* 2013 Nov;28(11):2414-30.
- 20 Noda T, Matsuura A, Wada Y, Ohsumi Y. Novel system for monitoring autophagy in the yeast *Saccharomyces cerevisiae*. *Biochem Biophys Res Commun* 1995 May 5;210(1):126-32.
- 21 Eisenberg-Lerner A, Bialik S, Simon HU, Kimchi A. Life and death partners: apoptosis, autophagy and the cross-talk between them. *Cell Death Differ* 2009 Jul;16(7):966-75.
- 22 Lanyon LE. Osteocytes, strain detection, bone modeling and remodeling. *Calcif Tissue Int* 1993;53 Suppl 1:S102-S106.
- 23 Bonewald LF. The amazing osteocyte. *J Bone Miner Res* 2011 Feb;26(2):229-38.
- 24 Chen ZF, Li YB, Han JY, Wang J, Yin JJ, Li JB, et al. The double-edged effect of autophagy in pancreatic beta cells and diabetes. *Autophagy* 2011 Jan;7(1):12-6.
- 25 Mizushima N, Yoshimori T. How to interpret LC3 immunoblotting. *Autophagy* 2007 Nov;3(6):542-5.
- 26 Wirth M, Joachim J, Tooze SA. Autophagosome formation--the role of ULK1 and Beclin1-PI3KC3 complexes in setting the stage. *Semin Cancer Biol* 2013 Oct;23(5):301-9.
- 27 Kang R, Zeh HJ, Lotze MT, Tang D. The Beclin 1 network regulates autophagy and apoptosis. *Cell Death Differ* 2011 Apr;18(4):571-80.
- 28 Gurkar AU, Chu K, Raj L, Bouley R, Lee SH, Kim YB, et al. Identification of ROCK1 kinase as a critical regulator of Beclin1-mediated autophagy during metabolic stress. *Nat Commun* 2013;4:2189.

- 29 Kim J, Kim YC, Fang C, Russell RC, Kim JH, Fan W, et al. Differential regulation of distinct Vps34 complexes by AMPK in nutrient stress and autophagy. *Cell* 2013 Jan 17;152(1-2):290-303.

Table 1. Alterations in Trabecular Microarchitecture of the Femoral Neck after 2, 8, and 16 Wk

	2 Wk		8 Wk		16 Wk	
	Con	HF	Con	HF	Con	HF
BV/TV (%)	39.1 ± 1.8 ^B	41.2 ± 3.4 ^B	58.6 ± 3.7 ^A	45.4 ± 3.0 ^B	54.8 ± 2.7 ^A	46.7 ± 1.7 ^B
Tb.N. (1/mm)	8.7 ± 0.2 ^A	8.8 ± 0.2 ^A	8.8 ± 0.3 ^A	8.4 ± 0.3 ^A	8.1 ± 0.2 ^{AB}	7.6 ± 0.2 ^B
Tb.Th. (µm)	56.3 ± 1.9 ^E	60.2 ± 2.9 ^{DE}	80.8 ± 4.9 ^{AB}	66.5 ± 2.4 ^{CD}	85.7 ± 4.6 ^A	74.6 ± 1.8 ^{BC}
Tb.Sp. (µm)	101.5 ± 2.7	99.3 ± 4.9	89.7 ± 4.5	100.8 ± 7.0	102.1 ± 4.9	112.3 ± 3.1
Conn.Dens. (1/mm³)	453.3 ± 33.5 ^A	404.3 ± 21.2 ^A	253.6 ± 13.2 ^{BC}	284.3 ± 24.4 ^C	179.2 ± 14.3 ^D	215.7 ± 8.7 ^{BD}
SMI	0.56 ± 0.13 ^A	0.41 ± 0.33 ^{AB}	-1.73 ± 0.36 ^C	-0.28 ± 0.23 ^{BD}	-1.10 ± 0.23 ^C	-0.44 ± 0.11 ^D

MicroCT analyses of trabecular bone in the femoral neck at 2, 8, and 16 weeks on a control (Con=10 % kcal from fat) or HF (60% kcal from fat) diet. Trabecular parameters includes bone volume/ total volume (BV/TV), trabecular number (Tb.N.), thickness (Tb.Th.), and separation (Tb.Sp), as well as connectivity density (Conn.Dens.) and structural model index (SMI). Values are expressed as mean ± SE. Rows that share the same superscript letter are not significantly different from each other ($P < 0.05$).

Table 2. Target genes used for qPCR Analyses

NCBI Accession Number	Protein/ Gene Name	Gene Symbol	Primer Sequence
NM_007431	Alkaline phosphatase, liver/ bone/ kidney	<i>Alpl</i>	QF 5'- GGT ATG GGC GTC TCC ACA GT -3' QR 5'- GCC CGT GTT GTG GTG TAG CT -3'
NM_009716	Activating transcript factor 4	<i>Atf4</i>	QF 5'- GCA GTG TTG CTG TAA CGG ACA -3' QR 5'- TCG CTG TTC AGG AAG CTC ATC -3'
NM_019584	Beclin1	<i>Becn1</i>	QF 5'- TTC AAT GCC ACC TTC CAC AT -3' QR 5'- AAG CGA CCC AGT CTG AAA TTA TT -3'
NM_0074541	Osteocalcin/ Bone gamma carboxyglutamate protein	<i>Bglap</i>	QF 5'- TGA GCT TAA CCC TGC TTG TGA CGA -3' QR 5'- AGG GCA GCA CAG GTC CTA AAT AGT -3'
NM_007553	Bone morphogenetic protein 2	<i>Bmp2</i>	QF 5'- GGA CAT CCG CTC CAC AAA -3' QR 5'- GGC GCT TCC GCT GTT T -3'
NM_007554	Bone morphogenetic protein 4	<i>Bmp4</i>	QF 5'- GCC GAG CCA ACA CTG TGA -3' QR 5'- TGG TCC CTG GGA TGT TCT C -3'
NM_009810	Caspase 3	<i>Casp3</i>	QF 5'- CAT AAG AGC ACT GGA ATG TCA TCT C -3' QR 5'- CCC ATG AAT GTC TCT CTG AGG TT -3'
NM_001146038	Core-binding factor subunit alpha-1/ Runt-related transcription factor 2	<i>Cbfa1/ Runx2</i>	QF 5'- CGA CAG TCC CAA CTT CCT GT -3' QR 5'- CGG TAA CCA CAG TCC CAT CT -3'
NM_07631	Cyclin D1	<i>Ccnd1</i>	QF 5'- GCC CTC CGT ATC TTA CTT CAA G -3' QR 5'- GCG GTC CAG GTA GTT CAT G -3'
NM_007742	Collagen, type 1, alpha 1	<i>Colla1</i>	QF 5'- CGT CTG GTT TGG AGA GAG CAT -3' QR 5'- GGT CAG CTG GAT AGC GAC ATC -3'
NM_025735	Microtubule-associated protein light chain 3 alpha	<i>Maplc3a</i>	QF 5'- CTG TAA GGA GGT GCA GCA GAT -3' QR 5'- CCC TTG TAG CGC TCG ATG AT -3'
NM_026160	Microtubule-associated protein light chain 3 beta	<i>Maplc3b</i>	QF 5'- TTT CTC TCC TGG TTT GAA TTC TGT -3' QR 5'- TAA GGC CAG CGC TTG CT -3'
NM_011149	Peptidylproyl isomerase B	<i>Ppib</i>	QF 5'- TGG AGA GCA CCA AGA CAG ACA -3' QR 5'- TGC CGG AGT CGA CAA TGA -3'
NM_001204201	Osteopontin/ Secreted phosphoprotein	<i>Spp1</i>	QF 5'- ACT CCA ATC GTC CCT ACA GTC G -3' QR 5'- TGA GGT CCT CAT CTG TGG CAT -3'

Figure 1.

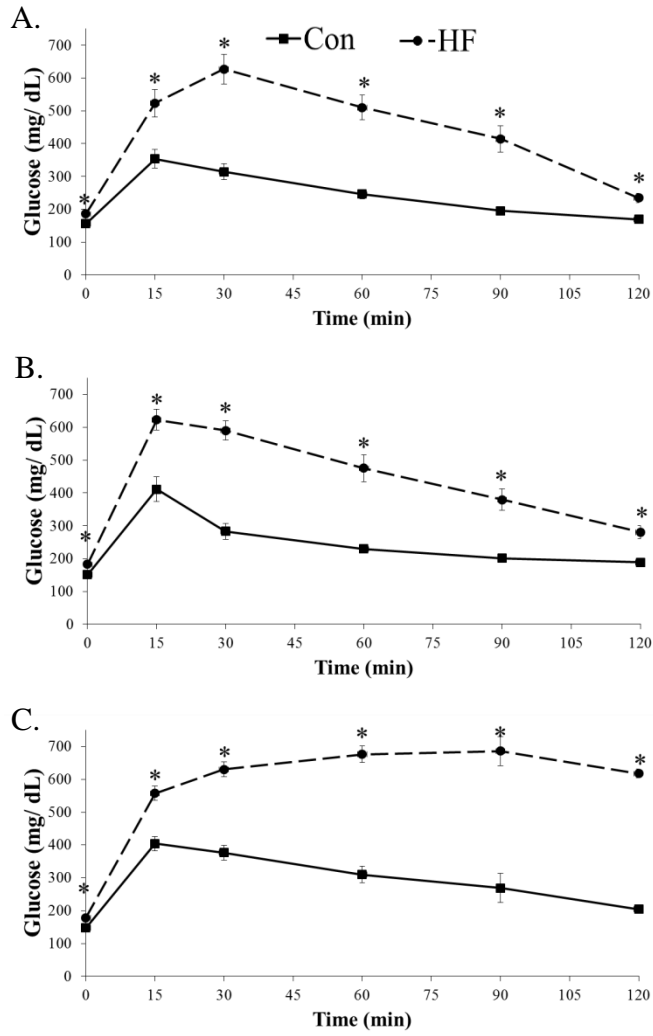


Figure 2.

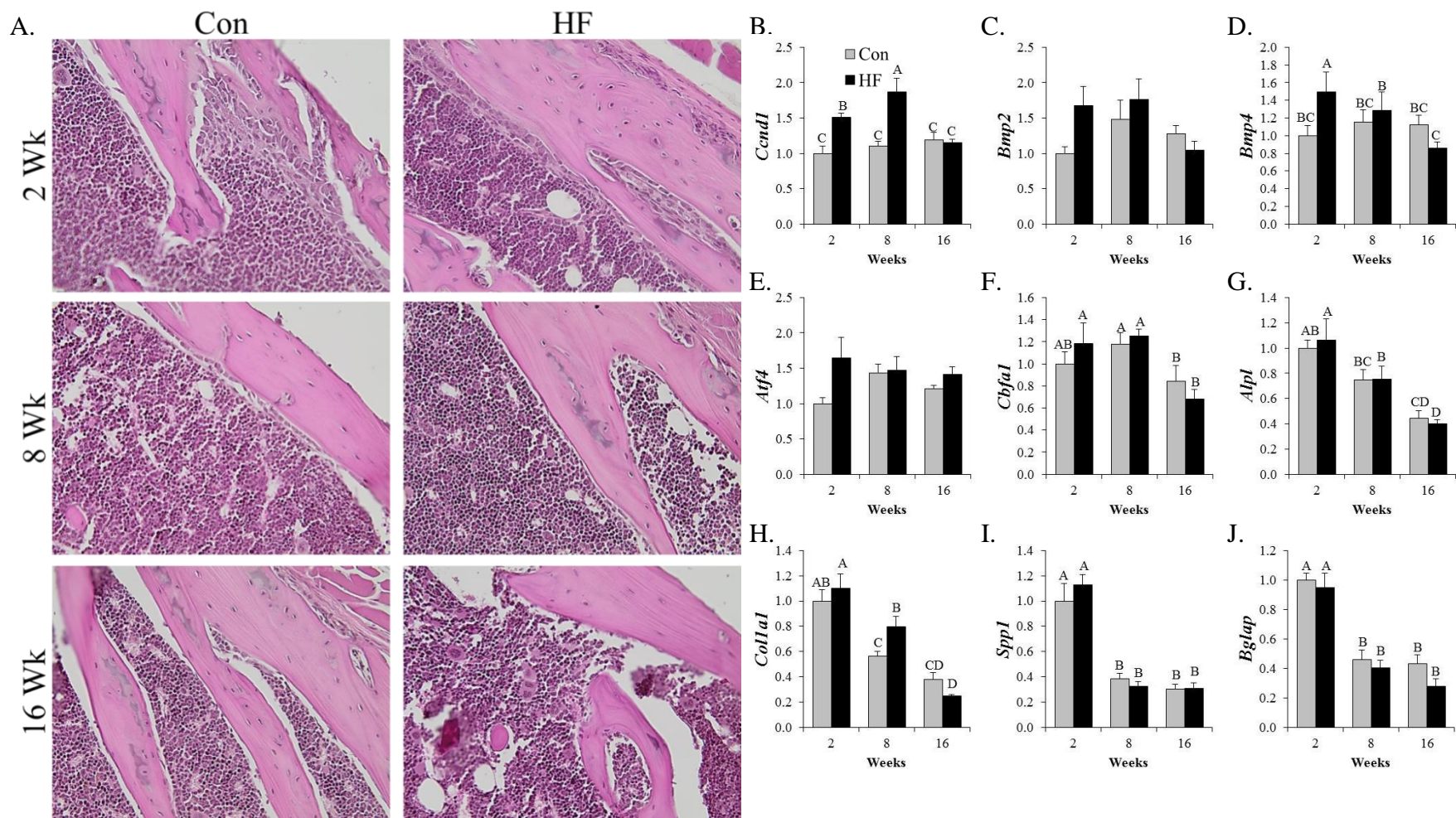


Figure 3.

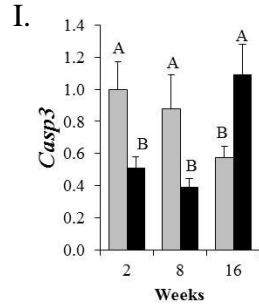
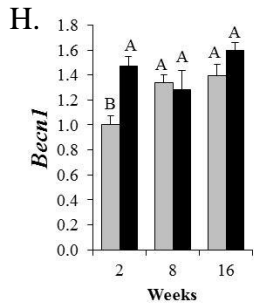
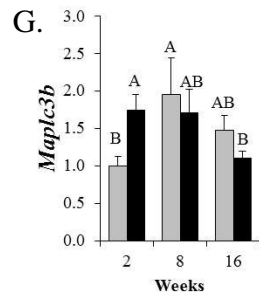
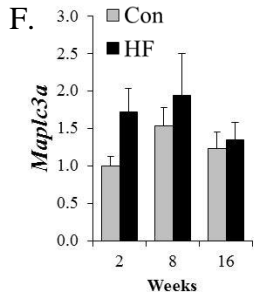
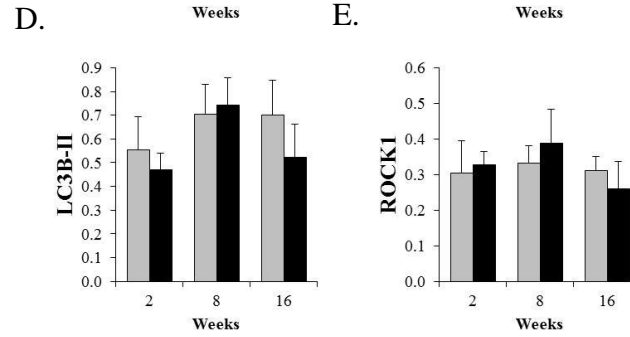
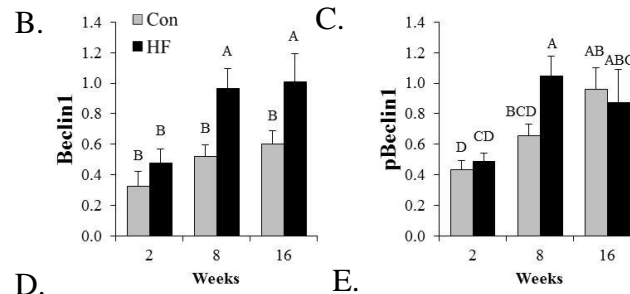
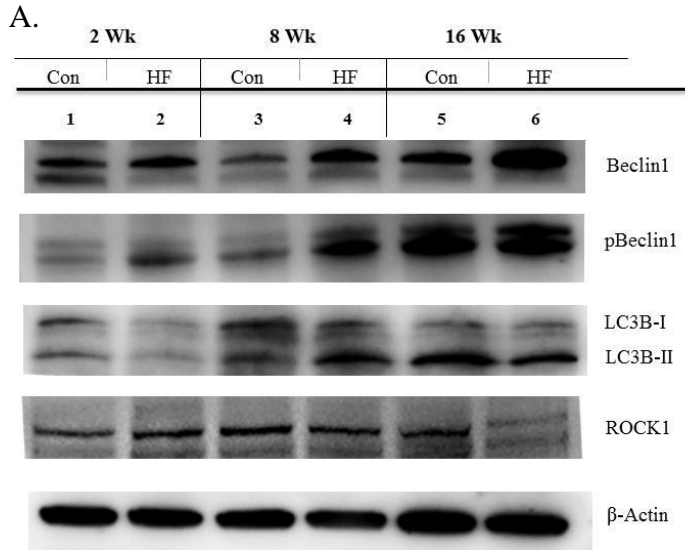


Figure 4.

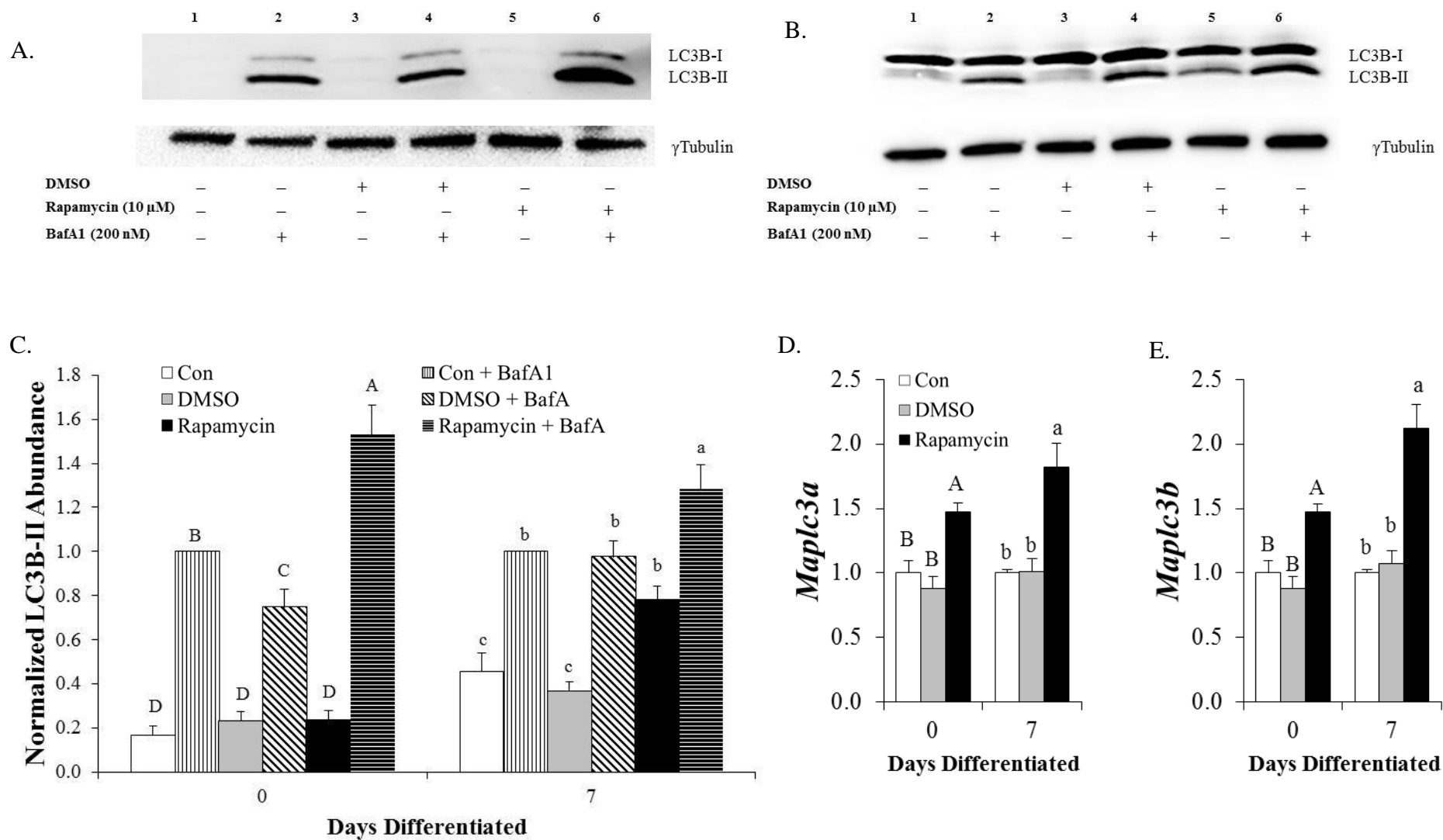
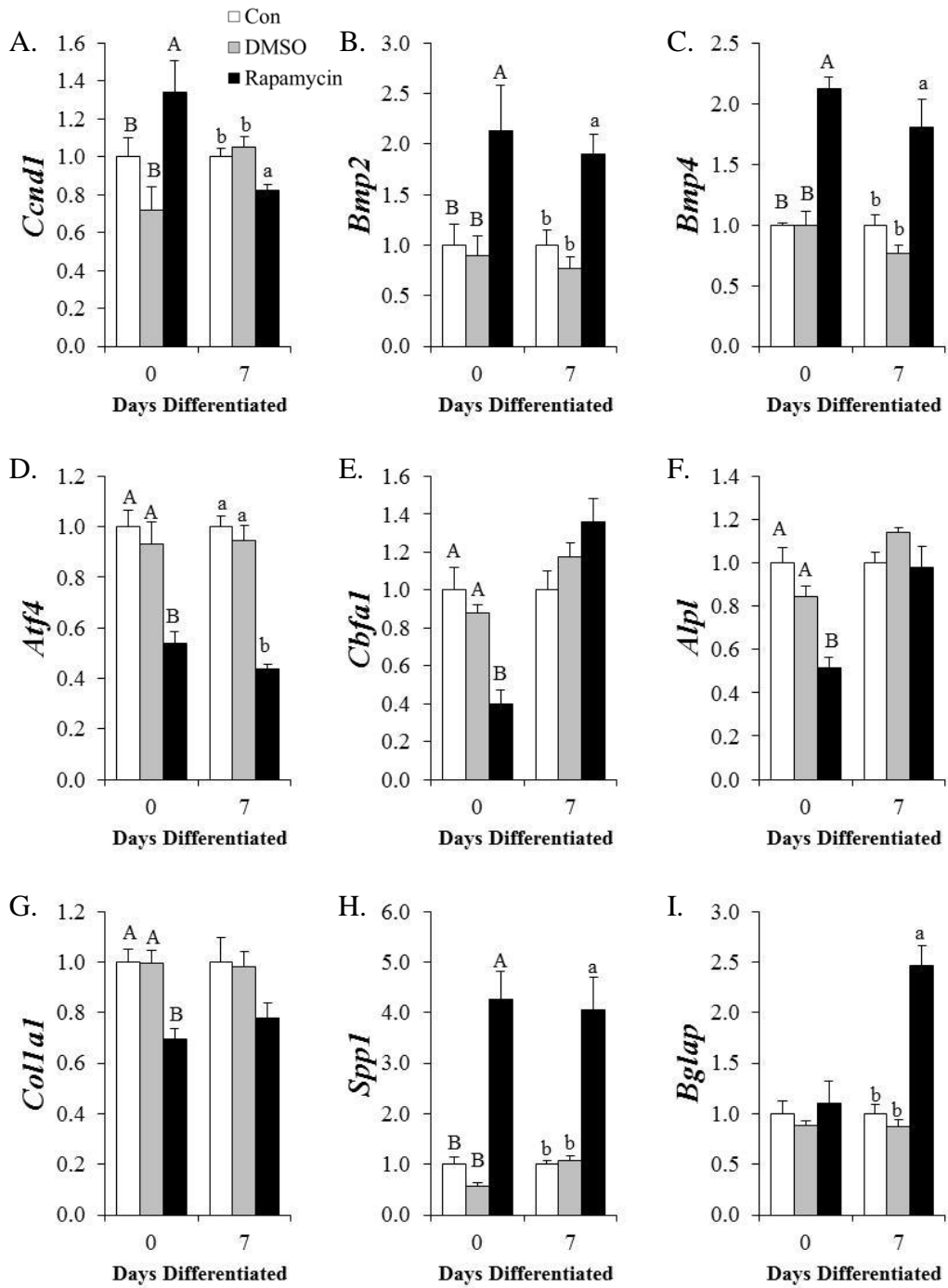


Figure 5.



CHAPTER VI

SUMMARY, CONCLUSIONS, AND RECOMMENDATIONS

Summary

The purpose of this project was to advance our understanding of the molecular mechanism contributing to dysregulation of bone metabolism during the development and progression of T2DM. To accomplish the overarching purpose, three studies were carried out. Study 1 was designed to investigate the long-term metabolic and skeletal response of two commonly used C57BL/6 substrains (i.e., C57BL/6 and C57BL/6N) to a high fat diet. The findings of this study show that the C57BL/6J and the C57BL/6N mouse differ in their metabolic and skeletal response to a high fat diet (i.e., 45 % kcal from fat) over a 24 wk study period. The aim of Study 2 was to investigate

the role TLR-4 contributes to the dysregulation of bone metabolism during the initiation and progression of T2DM. The C3H/HeJ mice with a non-functional TLR-4, were somewhat protected from the metabolic changes induced by a HF diet as evidenced by their IGTT response and ability to normalize blood glucose with a hyperinsulinemic response at week 16. These animals also demonstrated a delay in the development of a skeletal phenotype characterized as a decrease in BMD after 16 wk and no changes in trabecular bone. By comparison, the C57BL/6 mice on a HF diet exhibited early impaired glucose tolerance (i.e., 2 wks) and glucose intolerance at 8 and 16 wks. The mice on the HF diet demonstrated a lower whole body BMD and trabecular BV/TV of the distal femur metaphysis, attributed to decreased osteoblastogenesis and osteoclastogenesis at 8 wks and suppression of bone turnover by 16 wks. Together, these findings show that impaired glucose homeostasis results in lower trabecular bone in young, growing mice compared to controls and suggests a role for TLR-4 in the dysregulation of bone metabolism in this T2DM model. Study 3 was designed to determine the role of autophagy focused on the osteoblasts during hyperglycemia and altered insulin signaling. Autophagy appeared to be initiated in the bone as early as 2 wk on a high fat diet, and as impaired glucose tolerance progresses, autophagic flux was enhanced as evidenced by the increased protein abundance of pBeclin1 (Thr119) and no change in LC3B-II. Histological evaluation and characterization of genes involved in osteoblast maturation revealed that the development and progression of impaired glucose tolerance was associated with osteoblast maturation and an apparent increase in osteocytes. The ability of autophagy to drive osteoblast maturation was further confirmed by the ability of rapamycin-mediated autophagy to shift the phenotype of

MC3T3-E1 towards that of a more mature osteoblast. These findings provide evidence that suggest that Beclin1 mediated autophagy contributes to the attenuation of bone accrual during hyperglycemia by shifting the osteoblast towards a non-mineralizing, mature phenotype.

Conclusions

The *purpose* of this project is to: 1) determine the alterations in bone metabolism and their effects on bone microarchitectural and biomechanical properties during the development and progression of T2DM in a young, growing animal; 2) determine the role of TLR-4 in this skeletal response; and (3) explore the extent to which the autophagic pathway in bone cells is altered in response to impaired insulin signaling and glucose availability.

Hypothesis 1: The young growing C57BL/6 mice will exhibit compromised bone mass, structure and quality with increasing time on the high fat diet compared to their C3H/HeJ counterparts.

The C57BL/6 exhibited lower whole body BMD during the progression of impaired glucose tolerance to glucose intolerance (i.e., after 8 and 16 wk on a high fat diet), and longitudinal bone growth was attenuated at the 16 wk time point, the time at which a metabolic profile similar to that of T2DM was observed. However, the C3H/HeJ mice on a high fat diet demonstrated a delayed skeletal response, only exhibiting a lower

whole body BMD at the 16 wk time point. Moreover, the C57BL/6 mice had less trabecular bone at the distal femur metaphysis compared to their respective control groups that was explained by the attenuation of bone accrual (i.e., between 2 and 8 wk), whereas this was not observed in C3H/HeJ animals. Furthermore, biomechanical properties determined by reference point ID suggested that the C57BL/6 mice have a weaker bone after 8 and 16 wk on a high fat diet in the distal femur metaphysis. By 16 wk, both the C57BL/6 and C3H/HeJ mice on the high fat diet had compromised bone strength in the femur mid-diaphysis as evidenced by an increase in ID. These structural and biomechanical changes were accompanied with a decrease in osteoblastogenesis after 8 and 16 wk on the HF diet only in the C57BL/6 mice. Both the C57BL/6 and C3H/HeJ mice on a HF diet demonstrated an increase in osteoclastogenesis after 8 wk on HF diet, however, bone turnover was apparently decreased in the C57BL/6 during prolonged hyperglycemia. Based on the difference in skeletal response (i.e., bone structure, microarchitecture, and biomechanical properties) between the C57BL/6 and C3H/HeJ mice in a diet-induced obesity model, we fail to reject Hypothesis 1.

Hypothesis 2: Autophagy associated with the metabolic changes occurring in T2DM will contribute to the dysregulation of skeletal metabolism, resulting in deterioration of bone quality

Based on the increase in *Maplc3b* and *Becn1* mRNA at 2 wk, along with pBeclin1 protein abundance in the femur at 8 wk, autophagy appears to be up-regulated in the bone

during impaired glucose tolerance. Although autophagy provides an acute protective role, prolonged autophagy at the 16 wk time point begins to induce apoptosis as evidenced by *Casp3* mRNA abundance. Histological evaluation revealed that there was an apparent decrease in active, osteoblasts and an increase in osteocyte number during impaired glucose tolerance at the 2 and 8 wk time point. Furthermore, *in vitro* studies of undifferentiated and differentiated osteoblast-like MC3T3-E1 cell line confirmed that rapamycin-induced autophagy drives osteoblast maturation. Given these results demonstrating that glucose intolerance promotes osteoblast maturation and impairing bone accrual due to Beclin1-mediated autophagy, we fail to reject Hypothesis 2.

Recommendations

The current project provides new insight into how the development and progression of impaired glucose tolerance attenuates bone accrual and in certain phases of the metabolic changes may promote bone loss in young growing animals. Impaired bone accrual in young, growing children not only has the potential to lead to an increase in fracture risk during childhood and adolescence, but also predisposes these children to fragility-related fracture later in life (Valerio et al., 2012). This data suggest that bone accrual is attenuated in obese children experiencing mild hyperglycemia, and implies that longitudinal bone growth is impaired. Given that the alterations on bone growth and accrual appear to partly be reflective of impaired osteoblastogenesis, fracture repair may also be impaired in this population. Therefore, the results of these studies raise the issue of whether or not dietary and/or mechanical interventions, specifically geared to alleviate

the deleterious skeletal impact of impaired glucose tolerance, should be developed for this young population. Furthermore, questions arise about how altered glucose homeostasis during pregnancy (i.e., gestational diabetes mellitus) impacts fetal skeletal development. Due to the increased prevalence of childhood obesity and T2DM, the results from the current study emphasize the importance of maintaining glucose homeostasis during these critical years of bone accrual.

The fact that the C3H/HeJ mice were protected from the attenuated trabecular bone accrual suggests a role of TLR-4. Further studies of the activation of TLR-4 signaling should be carried out in osteoblasts and osteoclasts during impaired glucose tolerance and glucose intolerance. This could be accomplished by extracting protein from flushed femur or calvaria specimens (i.e., samples enriched for osteoblasts) and bone marrow (i.e., population enriched for osteoclasts and progenitor cells) at the 2, 8, and 16 wk time point and assessing key proteins involved in TLR-4 signaling (i.e., MyD88, TRIF, IRAK1, TRAF6, etc.).

We have shown that impaired bone accrual coincides with enhanced autophagy, presumably, shifting the osteoblast towards a more mature, non-mineralizing phenotype. However, the precise mechanism by which the metabolic alterations occurring within the diet-induced obesity model are regulating autophagy in bone remains elusive. First and foremost, experiments should be conducted using dynamic and static histomorphometry to determine whether actual alterations occurred in bone mineralization and to quantify osteocytes. While it is hypothesized that autophagy is altered by impaired intracellular glucose availability or insulin signaling, further studies are warranted to determine the pathway by which autophagy is regulated in this model. One approach would be to

administer an intraperitoneal injection of insulin prior to the end of the study, as opposed to fasting animals. This would allow for the quantification of proteins involved in the insulin signaling pathway (e.g., pIRS1, pAkt, etc.), which could offer insight in to the alterations occurring in the flushed femur during impaired glucose tolerance. Although ROCK1 protein abundance was not altered in the current study, given this kinase's ability to phosphorylate Beclin1 at Thr119, the enzymatic activity of ROCK1 should be determined (Gurkar et al., 2013). Lastly, future studies should include the osteoblast-specific knockout of *Becn1* to determine whether pBeclin1 is sufficient and necessary to mediate autophagy, leading to the maturation of the osteoblast. Driving the osteoblast towards a more mature, non-mineralizing phenotype resulting in the attenuation of bone formation is also a novel concept in the field of bone and mineral research. It puts into question the current opinion of anabolic agents, and whether they act by up-regulating osteoblast mineralization or maturation, which could have profound and opposing consequences. The terminal differentiation of an osteoblast into an osteocyte provokes more questions about the osteocyte. For example, does an increase in osteocyte number render the skeleton more sensitive to mechanical loading, and if so, why would it be associated with osteopenia? Studies aimed to further investigate the role of autophagy associated glucose intolerance and alterations in bone metabolism, may lead to the potential development of therapeutic treatments.

To test the hypothesis that autophagy is up-regulated in the osteoblast due to impaired intracellular glucose, the primary GLUT would need to be to be regulated in an insulin sensitive manner. Previously, GLUT1 and GLUT3 were identified as the primary GLUTs reported on osteoblasts and osteoblast-like cells (i.e., mice, rats, and humans)

(Thomas et al., 1996). While our preliminary experiment revealed that MC3T3-E1 cells differentiated over a time course expressed GLUT1 and GLUT3, both GLUT3 and GLUT4 are present (mRNA and protein) in the flushed femur. This unexpected observation created a scenario in which we questioned the use of MC3T3-E1 cells as an appropriate model to study GLUTs relative to the osteoblast *in vivo*. Given that MC3T3-E1 cells were derived from a newborn calvaria sample, we evaluated mouse calvaria samples for GLUT3 and GLUT4, to which it was confirmed that both of these GLUTs are expressed at a transcriptional level. A possible confounding factor that was not considered was the age of the mice of the samples tested in the current study compared to the neonatal origin of the MC3T3-E1 cell line, which could account for the differences in GLUT expression. It has been hypothesized, however, that GLUT3 functions as the primary GLUT on osteoblasts given its low K_m (Simpson et al., 2008). While osteoblast-specific knockout of GLUT4 does not result in a bone phenotype (Zhu Li et al., 2013), further investigation of GLUT3 is needed. For example, it remains to be determined if GLUT3's subcellular localization is dependent on insulin stimulation on the osteoblast. Experiments would need to be designed to include primary osteoblasts cultured with and without insulin, and the subcellular location of GLUT3 would need to be determined by indirect immunofluorescence, subcellular fractionation and western blot analyses. Moreover, flushed femur samples are believed to provide a mixed cell population enriched for osteoblasts and osteocytes, therefore, the characterization of GLUTs on the osteocyte is warranted. If, as the MC3T3-E1 cell lines suggest, pre-/immature osteoblasts only express GLUT1 and GLUT3, and the osteocyte expresses GLUT3 and GLUT4, these discrepancies may be explained. An initial approach would be to culture the

immortalized MLO-Y4 cell line and/or primary osteocytes for transcriptional and protein abundance of GLUT1-4.

The results from the current project advance that field of bone and mineral research by providing mechanistic insight in to how the development and progression of impaired glucose tolerance exerts a detrimental impact to bone, and suggests the involvement of TLR-4 and autophagy. Based on the findings from these studies it appears that TLR-4 activation during glucose intolerance down-regulates bone turnover, resulting in the attenuation of longitudinal bone growth and bone accrual in young male mice. Furthermore, we provide mechanistic data suggesting that increased autophagy in the bone coincides with advanced osteoblast maturation, resulting in a non-mineralizing phenotype. *In vitro* studies confirm that autophagy induced by rapamycin treatment in osteoblastic-like cells decreases mineralization and promotes cellular maturation.

LITERATURE CITED

- e, H., Yamada, N., Kamata, K., Kuwaki, T., Shimada, M., Osuga, J. et al. (1998). Hypertension, hypertriglyceridemia, and impaired endothelium-dependent vascular relaxation in mice lacking insulin receptor substrate-1. *J.Clin.Invest*, *101*, 1784-1788.
- Abrahamsen, B., Bonnevie-Nielsen, V., Ebbesen, E. N., Gram, J., & Beck-Nielsen, H. (2000). Cytokines and bone loss in a 5-year longitudinal study--hormone replacement therapy suppresses serum soluble interleukin-6 receptor and increases interleukin-1-receptor antagonist: the Danish Osteoporosis Prevention Study. *J Bone Miner.Res.*, *15*, 1545-1554.
- Adams, A. L., Kessler, J. I., Deramerian, K., Smith, N., Black, M. H., Porter, A. H. et al. (2013). Associations between childhood obesity and upper and lower extremity injuries. *Inj.Prev.*, *19*, 191-197.
- Agusti, A. & Soriano, J. B. (2008). COPD as a systemic disease. *COPD.*, *5*, 133-138.
- Almehed, K., Forsblad, d. H., Kvist, G., Ohlsson, C., & Carlsten, H. (2007). Prevalence and risk factors of osteoporosis in female SLE patients-extended report. *Rheumatology.(Oxford)*, *46*, 1185-1190.
- Anastos, K., Lu, D., Shi, O., Mulligan, K., Tien, P. C., Freeman, R. et al. (2007). The association of bone mineral density with HIV infection and antiretroviral treatment in women. *Antivir.Ther.*, *12*, 1049-1058.
- Araki, E., Lipes, M. A., Patti, M. E., Bruning, J. C., Haag, B., III, Johnson, R. S. et al. (1994). Alternative pathway of insulin signalling in mice with targeted disruption of the IRS-1 gene. *Nature*, *372*, 186-190.
- .

- Ashcroft, S. J. (1976). The control of insulin release by sugars. *Ciba Found.Symp.*, 41, 117-139.
- Avruch, J. (1998). Insulin signal transduction through protein kinase cascades. *Mol.Cell Biochem.*, 182, 31-48.
- Bandow, K., Maeda, A., Kakimoto, K., Kusuyama, J., Shamoto, M., Ohnishi, T. et al. (2010). Molecular mechanisms of the inhibitory effect of lipopolysaccharide (LPS) on osteoblast differentiation. *Biochem.Biophys.Res.Comm.*, 402, 755-761.
- Beamer, W. G., Donahue, L. R., Rosen, C. J., & Baylink, D. J. (1996). Genetic variability in adult bone density among inbred strains of mice. *Bone*, 18, 397-403.
- Berenson, G. S. (2012). Health consequences of obesity. *Pediatr.Blood Cancer*, 58, 117-121.
- Bilan, P. J., Mitsumoto, Y., Maher, F., Simpson, I. A., & Klip, A. (1992). Detection of the GLUT3 facilitative glucose transporter in rat L6 muscle cells: regulation by cellular differentiation, insulin and insulin-like growth factor-I. *Biochem.Biophys.Res.Comm.*, 186, 1129-1137.
- Bu, S. Y., Hunt, T. S., & Smith, B. J. (2008). Dried plum polyphenols attenuate the detrimental effects of TNF-alpha on osteoblast function coincident with up-regulation of Runx2, Osterix and IGF-I. *J.Nutr.Biochem.*
- Burks, D. J., Font de, M. J., Schubert, M., Withers, D. J., Myers, M. G., Towery, H. H. et al. (2000). IRS-2 pathways integrate female reproduction and energy homeostasis. *Nature*, 407, 377-382.
- Bursch, W., Karwan, A., Mayer, M., Dornetshuber, J., Frohwein, U., Schulte-Hermann, R. et al. (2008). Cell death and autophagy: cytokines, drugs, and nutritional factors. *Toxicology*, 254, 147-157.
- Cani, P. D., Bibiloni, R., Knauf, C., Waget, A., Neyrinck, A. M., Delzenne, N. M. et al. (2008). Changes in gut microbiota control metabolic endotoxemia-induced inflammation in high-fat diet-induced obesity and diabetes in mice. *Diabetes*, 57, 1470-1481.
- Center for Disease Control and Prevention. (1-1-2008). National Health and Nutrition Examination Survey, 2007-2008.
Ref Type: Generic
- Center for Disease Control and Prevention. (2011). Obesity Data and Trends.
Ref Type: Generic
- Centers for Disease Control and Prevention (2013). *Children and Diabetes*.

Centers for Disease Prevention and Control. (2011). National Diabetes Fact Sheet. Ref Type: Generic

Chalhoub, N. & Baker, S. J. (2009). PTEN and the PI3-kinase pathway in cancer. *Annu.Rev.Pathol.*, 4, 127-150.

Chan, E. Y. (2012). Regulation and function of uncoordinated-51 like kinase proteins. *Antioxid.Redox.Signal.*, 17, 775-785.

Chatakun, P., Nunez-Toldra, R., Diaz Lopez, E. J., Gil-Recio, C., Martinez-Sarra, E., Hernandez-Alfaro, F. et al. (2014). The effect of five proteins on stem cells used for osteoblast differentiation and proliferation: a current review of the literature. *Cell Mol.Life Sci.*, 71, 113-142.

Chen, Z. F., Li, Y. B., Han, J. Y., Wang, J., Yin, J. J., Li, J. B. et al. (2011). The double-edged effect of autophagy in pancreatic beta cells and diabetes. *Autophagy*, 7, 12-16.

Chun, K. H., Araki, K., Jee, Y., Lee, D. H., Oh, B. C., Huang, H. et al. (2012). Regulation of glucose transport by ROCK1 differs from that of ROCK2 and is controlled by actin polymerization. *Endocrinology*, 153, 1649-1662.

Cole, Z. A., Harvey, N. C., Kim, M., Ntani, G., Robinson, S. M., Inskip, H. M. et al. (2012). Increased fat mass is associated with increased bone size but reduced volumetric density in pre pubertal children. *Bone*, 50, 562-567.

Collins, S., Martin, T. L., Surwit, R. S., & Robidoux, J. (2004). Genetic vulnerability to diet-induced obesity in the C57BL/6J mouse: physiological and molecular characteristics. *Physiol Behav.*, 81, 243-248.

Copps, K. D. & White, M. F. (2012). Regulation of insulin sensitivity by serine/threonine phosphorylation of insulin receptor substrate proteins IRS1 and IRS2. *Diabetologia*, 55, 2565-2582.

Cortizo, A. M., Lettieri, M. G., Barrio, D. A., Mercer, N., Etcheverry, S. B., & McCarthy, A. D. (2003). Advanced glycation end-products (AGEs) induce concerted changes in the osteoblastic expression of their receptor RAGE and in the activation of extracellular signal-regulated kinases (ERK). *Mol.Cell Biochem.*, 250, 1-10.

Curry, D. L., Bennett, L. L., & Grodsky, G. M. (1968). Dynamics of insulin secretion by the perfused rat pancreas. *Endocrinology*, 83, 572-584.

Dasu, M. R., Devaraj, S., Zhao, L., Hwang, D. H., & Jialal, I. (2008). High glucose induces toll-like receptor expression in human monocytes: mechanism of activation. *Diabetes*, 57, 3090-3098.

Dasu, M. R., Ramirez, S., & Isseroff, R. R. (2012). Toll-like receptors and diabetes: a therapeutic perspective. *Clin.Sci.(Lond)*, 122, 203-214.

- Davis, J. E., Gabler, N. K., Walker-Daniels, J., & Spurlock, M. E. (2008). Tlr-4 deficiency selectively protects against obesity induced by diets high in saturated fat. *Obesity.(Silver.Spring)*, 16, 1248-1255.
- de Liefde, I. I., van der Klift, M., de Laet, C. E., van Daele, P. L., Hofman, A., & Pols, H. A. (2005). Bone mineral density and fracture risk in type-2 diabetes mellitus: the Rotterdam Study. *Osteoporos.Int.*, 16, 1713-1720.
- DeSelm, C. J., Miller, B. C., Zou, W., Beatty, W. L., van, M. E., Takahata, Y. et al. (2011). Autophagy proteins regulate the secretory component of osteoclastic bone resorption. *Dev.Cell*, 21, 966-974.
- Ebstein, W. (1876). Zur therapie des Diabetes mellitus, insbesondere uber die Anwendung des salicylsauren Matron bei demselben. *Berliner Klinische Wochenschrift*, 13, 337-340.
- Eisenberg-Lerner, A., Bialik, S., Simon, H. U., & Kimchi, A. (2009). Life and death partners: apoptosis, autophagy and the cross-talk between them. *Cell Death.Differ.*, 16, 966-975.
- Emerton, K. B., Hu, B., Woo, A. A., Sinofsky, A., Hernandez, C., Majeska, R. J. et al. (2010). Osteocyte apoptosis and control of bone resorption following ovariectomy in mice. *Bone*, 46, 577-583.
- Exton, J. H., Harper, S. C., Tucker, A. L., & Ho, R. J. (1973). Effects of insulin on gluconeogenesis and cyclic AMP levels in perfused livers from diabetic rats. *Biochim.Biophys.Acta*, 329, 23-40.
- Fang, Y., Wang, Z. Y., Mao, Y., Xin, H. T., Ren, G. L., & Bai, X. F. (2006). Effects of insulin-like growth factor I on the development of osteoblasts in hyperglycemia. *Diabetes Res.Clin.Pract.*, 73, 95-97.
- Farr, J. N., Drake, M. T., Amin, S., Melton, L. J., III, McCready, L. K., & Khosla, S. (2013). In Vivo assessment of bone quality in postmenopausal women with type 2 diabetes. *J.Bone Miner.Res.*
- Finkelstein, E. A., Trogdon, J. G., Cohen, J. W., & Dietz, W. (2009). Annual medical spending attributable to obesity: payer-and service-specific estimates. *Health Aff.(Millwood.)*, 28, w822-w831.
- Flegal, K. M., Carroll, M. D., Ogden, C. L., & Curtin, L. R. (2010). Prevalence and trends in obesity among US adults, 1999-2008. *JAMA*, 303, 235-241.
- Fu, Y., Maianu, L., Melbert, B. R., & Garvey, W. T. (2004). Facilitative glucose transporter gene expression in human lymphocytes, monocytes, and macrophages: a role for GLUT isoforms 1, 3, and 5 in the immune response and foam cell formation. *Blood Cells Mol.Dis.*, 32, 182-190.

- Ganguly, A. & Devaskar, S. U. (2008). Glucose transporter isoform-3-null heterozygous mutation causes sexually dimorphic adiposity with insulin resistance. *Am.J.Physiol Endocrinol.Metab*, 294, E1144-E1151.
- Gerstenfeld, L. C., McLean, J., Healey, D. S., Stapleton, S. N., Silkman, L. J., Price, C. et al. (2010). Genetic variation in the structural pattern of osteoclast activity during post-natal growth of mouse femora. *Bone*, 46, 1546-1554.
- Geurs, N. C. (2007). Osteoporosis and periodontal disease. *Periodontol.2000.*, 44, 29-43.
- Gilbert, L., He, X., Farmer, P., Boden, S., Kozlowski, M., Rubin, J. et al. (2000). Inhibition of osteoblast differentiation by tumor necrosis factor-alpha. *Endocrinology*, 141, 3956-3964.
- Gonzalez, I., Romero, J., Rodriguez, B. L., Perez-Castro, R., & Rojas, A. (2013). The immunobiology of the receptor of advanced glycation end-products: trends and challenges. *Immunobiology*, 218, 790-797.
- Goulding, A., Jones, I. E., Taylor, R. W., Williams, S. M., & Manning, P. J. (2001). Bone mineral density and body composition in boys with distal forearm fractures: a dual-energy x-ray absorptiometry study. *J.Pediatr.*, 139, 509-515.
- Goulding, A., Jones, I. E., Williams, S. M., Grant, A. M., Taylor, R. W., Manning, P. J. et al. (2005). First fracture is associated with increased risk of new fractures during growth. *J.Pediatr.*, 146, 286-288.
- Goulding, A., Taylor, R. W., Jones, I. E., McAuley, K. A., Manning, P. J., & Williams, S. M. (2000). Overweight and obese children have low bone mass and area for their weight. *Int.J.Obes.Relat Metab Disord.*, 24, 627-632.
- Grassi, W., De, A. R., Lamanna, G., & Cervini, C. (1998). The clinical features of rheumatoid arthritis. *Eur.J.Radiol.*, 27 Suppl 1, S18-S24.
- Grodsky, G. M., Curry, D., Landahl, H., & Bennett, L. (1969). [Further studies on the dynamic aspects of insulin release in vitro with evidence for a two-compartmental storage system]. *Acta Diabetol.Lat.*, 6 Suppl 1, 554-578.
- Grodsky, G. M., Curry, D. L., Bennett, L. L., & Rodrigo, J. J. (1968). [Factors influencing different rates of insulin release in vitro]. *Acta Diabetol.Lat.*, 5 Suppl 1, 140-161.
- Gunaratnam, K., Vidal, C., Gimble, J. M., & Duque, G. (2013). Mechanisms of Palmitate-Induced Lipotoxicity in Human Osteoblasts. *Endocrinology*.
- Guo, C., Yuan, L., Wang, J. G., Wang, F., Yang, X. K., Zhang, F. H. et al. (2013). Lipopolysaccharide (LPS) Induces the Apoptosis and Inhibits Osteoblast Differentiation Through JNK Pathway in MC3T3-E1 Cells. *Inflammation*.

- Gurkar, A. U., Chu, K., Raj, L., Bouley, R., Lee, S. H., Kim, Y. B. et al. (2013). Identification of ROCK1 kinase as a critical regulator of Beclin1-mediated autophagy during metabolic stress. *Nat. Commun.*, *4*, 2189.
- Hahn, T. J., Westbrook, S. L., Sullivan, T. L., Goodman, W. G., & Halstead, L. R. (1988). Glucose transport in osteoblast-enriched bone explants: characterization and insulin regulation. *J. Bone Miner. Res.*, *3*, 359-365.
- Hajer, G. R., van Haefen, T. W., & Visseren, F. L. (2008). Adipose tissue dysfunction in obesity, diabetes, and vascular diseases. *Eur. Heart J*, *29*, 2959-2971.
- Heath, H., III, Melton, L. J., III, & Chu, C. P. (1980). Diabetes mellitus and risk of skeletal fracture. *N. Engl. J. Med.*, *303*, 567-570.
- Hedekov, C. J. (1980). Mechanism of glucose-induced insulin secretion. *Physiol Rev.*, *60*, 442-509.
- Hofmann, M. A., Drury, S., Fu, C., Qu, W., Taguchi, A., Lu, Y. et al. (1999). RAGE mediates a novel proinflammatory axis: a central cell surface receptor for S100/calgranulin polypeptides. *Cell*, *97*, 889-901.
- INGLE, D. J. (1949). A simple means of producing obesity in the rat. *Proc. Soc. Exp. Biol. Med.*, *72*, 604.
- Ionova-Martin, S. S., Wade, J. M., Tang, S., Shahnazari, M., Ager, J. W., III, Lane, N. E. et al. (2011). Changes in cortical bone response to high-fat diet from adolescence to adulthood in mice. *Osteoporos. Int.*, *22*, 2283-2293.
- Ituarte, E. A., Halstead, L. R., Iida-Klein, A., Ituarte, H. G., & Hahn, T. J. (1989). Glucose transport system in UMR-106-01 osteoblastic osteosarcoma cells: regulation by insulin. *Calcif. Tissue Int.*, *45*, 27-33.
- Iwai-Kanai, E., Yuan, H., Huang, C., Sayen, M. R., Perry-Garza, C. N., Kim, L. et al. (2008). A method to measure cardiac autophagic flux in vivo. *Autophagy.*, *4*, 322-329.
- Janghorbani, M., Feskanich, D., Willett, W. C., & Hu, F. (2006). Prospective study of diabetes and risk of hip fracture: the Nurses' Health Study. *Diabetes Care*, *29*, 1573-1578.
- Jilka, R. L. (1998). Cytokines, bone remodeling, and estrogen deficiency: a 1998 update. *Bone*, *23*, 75-81.
- Johnson, G. B., Riggs, B. L., & Platt, J. L. (2004). A genetic basis for the "Adonis" phenotype of low adiposity and strong bones. *FASEB J.*, *18*, 1282-1284.
- Kang, R., Zeh, H. J., Lotze, M. T., & Tang, D. (2011). The Beclin 1 network regulates autophagy and apoptosis. *Cell Death. Differ.*, *18*, 571-580.

- Kearns, A. E., Khosla, S., & Kostenuik, P. J. (2008). Receptor activator of nuclear factor kappaB ligand and osteoprotegerin regulation of bone remodeling in health and disease. *Endocr.Rev.*, *29*, 155-192.
- Kenney, W. E. (1946). A NOTE ON THE INCIDENCE OF DIABETES MELLITUS IN FRACTURE OF THE HIP. *Yale Journal of Biology and Medicine*, 578-581.
- Kessler, J., Koebnick, C., Smith, N., & Adams, A. (2013). Childhood obesity is associated with increased risk of most lower extremity fractures. *Clin.Orthop.Relat Res.*, *471*, 1199-1207.
- Kim, J., Kim, Y. C., Fang, C., Russell, R. C., Kim, J. H., Fan, W. et al. (2013a). Differential regulation of distinct Vps34 complexes by AMPK in nutrient stress and autophagy. *Cell*, *152*, 290-303.
- Kim, J. E., Hsieh, M. H., Soni, B. K., Zayzafoon, M., & Allison, D. B. (2013b). Childhood obesity as a risk factor for bone fracture: a mechanistic study. *Obesity.(Silver.Spring)*, *21*, 1459-1466.
- Kim, J. J. & Sears, D. D. (2010). TLR4 and Insulin Resistance. *Gastroenterol.Res.Pract.*, *2010*.
- Kim, J. Y., Zhao, H., Martinez, J., Doggett, T. A., Kolesnikov, A. V., Tang, P. H. et al. (2013c). Noncanonical autophagy promotes the visual cycle. *Cell*, *154*, 365-376.
- Klein, K. O., Larmore, K. A., de, L. E., Brown, J. M., Considine, R. V., & Hassink, S. G. (1998). Effect of obesity on estradiol level, and its relationship to leptin, bone maturation, and bone mineral density in children. *J.Clin.Endocrinol.Metab*, *83*, 3469-3475.
- Klionsky, D. J., Abeliovich, H., Agostinis, P., Agrawal, D. K., Aliev, G., Askew, D. S. et al. (2008). Guidelines for the use and interpretation of assays for monitoring autophagy in higher eukaryotes. *Autophagy.*, *4*, 151-175.
- Knowles, H. J. & Athanasou, N. A. (2008). Hypoxia-inducible factor is expressed in giant cell tumour of bone and mediates paracrine effects of hypoxia on monocyte-osteoclast differentiation via induction of VEGF. *J Pathol.*, *215*, 56-66.
- Lamothe, B., Lai, Y., Xie, M., Schneider, M. D., & Darnay, B. G. (2013). TAK1 is essential for osteoclast differentiation and is an important modulator of cell death by apoptosis and necroptosis. *Mol.Cell Biol.*, *33*, 582-595.
- Lamothe, B., Webster, W. K., Gopinathan, A., Besse, A., Campos, A. D., & Darnay, B. G. (2007). TRAF6 ubiquitin ligase is essential for RANKL signaling and osteoclast differentiation. *Biochem.Biophys.Res.Commun.*, *359*, 1044-1049.
- Lanyon, L. E. (1992). Control of bone architecture by functional load bearing. *J.Bone Miner.Res.*, *7 Suppl 2*, S369-S375.

- Lanyon, L. E. (1993). Osteocytes, strain detection, bone modeling and remodeling. *Calcif.Tissue Int.*, 53 Suppl 1, S102-S106.
- Lee, D. H., Shi, J., Jeung, N. H., Kim, M. S., Zabolotny, J. M., Lee, S. W. et al. (2009a). Targeted disruption of ROCK1 causes insulin resistance in vivo. *J.Biol.Chem.*, 284, 11776-11780.
- Lee, J. Y., Sohn, K. H., Rhee, S. H., & Hwang, D. (2001). Saturated fatty acids, but not unsaturated fatty acids, induce the expression of cyclooxygenase-2 mediated through Toll-like receptor 4. *J Biol.Chem.*, 276, 16683-16689.
- Lee, K. W., Yook, J. Y., Son, M. Y., Kim, M. J., Koo, D. B., Han, Y. M. et al. (2009b). Rapamycin promotes the osteoblastic differentiation of human embryonic stem cells by blocking the mTOR pathway and stimulating the BMP/Smad pathway. *Stem Cells Dev.*
- Lee, S. H., Huang, H., Choi, K., Lee, D. H., Shi, J., Liu, T. et al. (2014). ROCK1 isoform-specific deletion reveals a role for diet-induced insulin resistance. *Am.J.Physiol Endocrinol.Metab*, 306, E332-E343.
- Lemaitre, B., Nicolas, E., Michaut, L., Reichhart, J. M., & Hoffmann, J. A. (1996). The dorsoventral regulatory gene cassette spatzle/Toll/cactus controls the potent antifungal response in *Drosophila* adults. *Cell*, 86, 973-983.
- Leonard, M. B., Shults, J., Wilson, B. A., Tershakovec, A. M., & Zemel, B. S. (2004). Obesity during childhood and adolescence augments bone mass and bone dimensions. *Am.J.Clin.Nutr.*, 80, 514-523.
- Li, X., Zhang, Y., Kang, H., Liu, W., Liu, P., Zhang, J. et al. (2005). Sclerostin binds to LRP5/6 and antagonizes canonical Wnt signaling. *J.Biol.Chem.*, 280, 19883-19887.
- Lin, N. Y., Stefanica, A., & Distler, J. H. (2013). Autophagy: A key pathway of TNF-induced inflammatory bone loss. *Autophagy*, 9, 1253-1255.
- Linkhart, T. A., Linkhart, S. G., Kodama, Y., Farley, J. R., Dimai, H. P., Wright, K. R. et al. (1999). Osteoclast formation in bone marrow cultures from two inbred strains of mice with different bone densities. *J.Bone Miner.Res.*, 14, 39-46.
- Liu, F., Fang, F., Yuan, H., Yang, D., Chen, Y., Williams, L. et al. (2013). Suppression of autophagy by FIP200 deletion leads to osteopenia in mice through the inhibition of osteoblast terminal differentiation. *J.Bone Miner.Res.*, 28, 2414-2430.
- Lu, X. M., Zhao, H., & Wang, E. H. (2013). A high-fat diet induces obesity and impairs bone acquisition in young male mice. *Mol.Med.Rep.*, 7, 1203-1208.
- Ma, P., Xiong, W., Liu, H., Ma, J., Gu, B., & Wu, X. (2011). Extraparacrine roles of glimepiride on osteoblasts from rat mandibular bone in vitro: Regulation of cytodifferentiation through PI3-kinases/Akt signalling pathway. *Arch.Oral Biol.*, 56, 307-316.

- Mabilleau, G., Chappard, D., & Sabokbar, A. (2011). Role of the A20-TRAF6 axis in lipopolysaccharide-mediated osteoclastogenesis. *J.Biol.Chem.*, 286, 3242-3249.
- Manolagas, S. C. & Parfitt, A. M. (2010). What old means to bone. *Trends Endocrinol.Metab*, 21, 369-374.
- Maratou, E., Dimitriadis, G., Kollias, A., Boutati, E., Lambadiari, V., Mitrou, P. et al. (2007). Glucose transporter expression on the plasma membrane of resting and activated white blood cells. *Eur.J.Clin.Invest*, 37, 282-290.
- Masini, M., Bugliani, M., Lupi, R., del, G. S., Boggi, U., Filipponi, F. et al. (2009). Autophagy in human type 2 diabetes pancreatic beta cells. *Diabetologia*, 52, 1083-1086.
- Mathieu, P., Lemieux, I., & Despres, J. P. (2010). Obesity, inflammation, and cardiovascular risk. *Clin.Pharmacol.Ther.*, 87, 407-416.
- May, A. L., Freedman, D., Sherry, B., & Blanck, H. M. (2013). Obesity - United States, 1999-2010. *MMWR Surveill Summ.*, 62 Suppl 3, 120-128.
- McClung, M. R., Grauer, A., Boonen, S., Bolognese, M. A., Brown, J. P., Diez-Perez, A. et al. (2014). Romosozumab in postmenopausal women with low bone mineral density. *N.Engl.J.Med.*, 370, 412-420.
- Medvedev, A. E., Piao, W., Shoenfelt, J., Rhee, S. H., Chen, H., Basu, S. et al. (2007). Role of TLR4 tyrosine phosphorylation in signal transduction and endotoxin tolerance. *J.Biol.Chem.*, 282, 16042-16053.
- Medzhitov, R., Preston-Hurlburt, P., & Janeway, C. A., Jr. (1997). A human homologue of the Drosophila Toll protein signals activation of adaptive immunity. *Nature*, 388, 394-397.
- Melton, L. J., III, Leibson, C. L., Achenbach, S. J., Therneau, T. M., & Khosla, S. (2008). Fracture risk in type 2 diabetes: update of a population-based study. *J Bone Miner.Res.*, 23, 1334-1342.
- Mizushima, N. & Yoshimori, T. (2007). How to interpret LC3 immunoblotting. *Autophagy.*, 3, 542-545.
- Nakamura, H., Fukusaki, Y., Yoshimura, A., Shiraishi, C., Kishimoto, M., Kaneko, T. et al. (2008). Lack of Toll-like receptor 4 decreases lipopolysaccharide-induced bone resorption in C3H/HeJ mice in vivo. *Oral Microbiol.Immunol.*, 23, 190-195.
- Nakashima, K. & de, C. B. (2003). Transcriptional mechanisms in osteoblast differentiation and bone formation. *Trends Genet.*, 19, 458-466.
- National Institutes of Health (1998). *Clinical guidelines on the identification, evaluation, and treatment of overweight and obesity in adults- The evidence report*. *Obes Res* 6 (Suppl 2).

- National Institutes of Health (2000). *Osteoporosis prevention, diagnosis, and therapy*.
- Nicodemus, K. K. & Folsom, A. R. (2001). Type 1 and type 2 diabetes and incident hip fractures in postmenopausal women. *Diabetes Care*, *24*, 1192-1197.
- Noda, T., Matsuura, A., Wada, Y., & Ohsumi, Y. (1995). Novel system for monitoring autophagy in the yeast *Saccharomyces cerevisiae*. *Biochem.Biophys.Res.Commun.*, *210*, 126-132.
- Nunez, C. E., Rodrigues, V. S., Gomes, F. S., de Moura, R. F., Victorio, S. C., Bombassaro, B. et al. (2013). Defective regulation of adipose tissue autophagy in obesity. *Int.J.Obes.(Lond)*.
- Ogasawara, T., Katagiri, M., Yamamoto, A., Hoshi, K., Takato, T., Nakamura, K. et al. (2004). Osteoclast differentiation by RANKL requires NF-kappaB-mediated downregulation of cyclin-dependent kinase 6 (Cdk6). *J.Bone Miner.Res.*, *19*, 1128-1136.
- Ogawa, N., Yamaguchi, T., Yano, S., Yamauchi, M., Yamamoto, M., & Sugimoto, T. (2007). The combination of high glucose and advanced glycation end-products (AGEs) inhibits the mineralization of osteoblastic MC3T3-E1 cells through glucose-induced increase in the receptor for AGEs. *Horm.Metab Res.*, *39*, 871-875.
- Ogden, C. L., Carroll, M. D., Kit, B. K., & Flegal, K. M. (2012). Prevalence of obesity and trends in body mass index among US children and adolescents, 1999-2010. *JAMA*, *307*, 483-490.
- Ogden, C. L., Carroll, M. D., Kit, B. K., & Flegal, K. M. (2013). Prevalence of obesity among adults: United States, 2011-2012. *NCHS.Data Brief.*, 1-8.
- Onal, M., Piemontese, M., Xiong, J., Wang, Y., Han, L., Ye, S. et al. (2013). Suppression of autophagy in osteocytes mimics skeletal aging. *J.Biol.Chem.*, *288*, 17432-17440.
- Ost, A., Svensson, K., Ruishalme, I., Brannmark, C., Franck, N., Krook, H. et al. (2010). Attenuated mTOR signaling and enhanced autophagy in adipocytes from obese patients with type 2 diabetes. *Mol.Med.*, *16*, 235-246.
- Pacifici, R., Rifas, L., McCracken, R., Vered, I., McMurtry, C., Avioli, L. V. et al. (1989). Ovarian steroid treatment blocks a postmenopausal increase in blood monocyte interleukin 1 release. *Proc.Natl.Acad.Sci.U.S.A*, *86*, 2398-2402.
- Pal, D., Dasgupta, S., Kundu, R., Maitra, S., Das, G., Mukhopadhyay, S. et al. (2012). Fetuin-A acts as an endogenous ligand of TLR4 to promote lipid-induced insulin resistance. *Nat.Med.*, *18*.
- Parhami, F., Tintut, Y., Beamer, W. G., Gharavi, N., Goodman, W., & Demer, L. L. (2001). Atherogenic high-fat diet reduces bone mineralization in mice. *J.Bone Miner.Res.*, *16*, 182-188.

- Parikh, N. I., Pencina, M. J., Wang, T. J., Lanier, K. J., Fox, C. S., D'Agostino, R. B. et al. (2007). Increasing trends in incidence of overweight and obesity over 5 decades. *Am.J.Med.*, 120, 242-250.
- Patsch, J. M., Kiefer, F. W., Varga, P., Pail, P., Rauner, M., Stupphann, D. et al. (2011). Increased bone resorption and impaired bone microarchitecture in short-term and extended high-fat diet-induced obesity. *Metabolism*, 60, 243-249.
- Pfeilschifter, J. (2003). Role of cytokines in postmenopausal bone loss. *Curr.Osteoporos.Rep.*, 1, 53-58.
- Piao, W., Song, C., Chen, H., Wahl, L. M., Fitzgerald, K. A., O'Neill, L. A. et al. (2008). Tyrosine phosphorylation of MyD88 adapter-like (Mal) is critical for signal transduction and blocked in endotoxin tolerance. *J.Biol.Chem.*, 283, 3109-3119.
- Poggi, M., Bastelica, D., Gual, P., Iglesias, M. A., Gremeaux, T., Knauf, C. et al. (2007). C3H/HeJ mice carrying a toll-like receptor 4 mutation are protected against the development of insulin resistance in white adipose tissue in response to a high-fat diet. *Diabetologia*, 50, 1267-1276.
- Porte, D., Jr. (1991). Banting lecture 1990. Beta-cells in type II diabetes mellitus. *Diabetes*, 40, 166-180.
- Previs, S. F., Withers, D. J., Ren, J. M., White, M. F., & Shulman, G. I. (2000). Contrasting effects of IRS-1 versus IRS-2 gene disruption on carbohydrate and lipid metabolism in vivo. *J.Biol.Chem.*, 275, 38990-38994.
- Ramasamy, R., Yan, S. F., & Schmidt, A. M. (2011). Receptor for AGE (RAGE): signaling mechanisms in the pathogenesis of diabetes and its complications. *Ann.N.Y.Acad.Sci.*, 1243, 88-102.
- Ravikumar, B., Sarkar, S., Davies, J. E., Futter, M., Garcia-Arencibia, M., Green-Thompson, Z. W. et al. (2010). Regulation of mammalian autophagy in physiology and pathophysiology. *Physiol Rev.*, 90, 1383-1435.
- REID, J., MACDOUGALL, A. I., & ANDREWS, M. M. (1957). Aspirin and diabetes mellitus. *Br.Med.J.*, 2, 1071-1074.
- Reinehr, T. (2013). Type 2 diabetes mellitus in children and adolescents. *World J.Diabetes*, 4, 270-281.
- Reyna, S. M., Ghosh, S., Tantiwong, P., Meka, C. S., Eagan, P., Jenkinson, C. P. et al. (2008). Elevated toll-like receptor 4 expression and signaling in muscle from insulin-resistant subjects. *Diabetes*, 57, 2595-2602.
- Rishaug, U., Birkeland, K. I., Falch, J. A., & Vaaler, S. (1995). Bone mass in non-insulin-dependent diabetes mellitus. *Scand.J.Clin.Lab Invest*, 55, 257-262.

- Robins, S. P. & Bailey, A. J. (1972). Age-related changes in collagen: the identification of reducible lysine-carbohydrate condensation products. *Biochem.Biophys.Res.Comm.*, 48, 76-84.
- Roggia, C., Gao, Y., Cenci, S., Weitzmann, M. N., Toraldo, G., Isaia, G. et al. (2001). Up-regulation of TNF-producing T cells in the bone marrow: a key mechanism by which estrogen deficiency induces bone loss in vivo. *Proc.Natl.Acad.Sci U.S.A.*, 98, 13960-13965.
- Saito, M., Fujii, K., Mori, Y., & Marumo, K. (2006). Role of collagen enzymatic and glycation induced cross-links as a determinant of bone quality in spontaneously diabetic WBN/Kob rats. *Osteoporos.Int.*, 17, 1514-1523.
- Sarfstein, R. & Werner, H. (2013). Minireview: nuclear insulin and insulin-like growth factor-1 receptors: a novel paradigm in signal transduction. *Endocrinology*, 154, 1672-1679.
- Schaeffler, A., Gross, P., Buettner, R., Bollheimer, C., Buechler, C., Neumeier, M. et al. (2009). Fatty acid-induced induction of Toll-like receptor-4/nuclear factor-kappaB pathway in adipocytes links nutritional signalling with innate immunity. *Immunology*, 126, 233-245.
- Scheidt-Nave, C., Bismar, H., Leidig-Bruckner, G., Woitge, H., Seibel, M. J., Ziegler, R. et al. (2001). Serum interleukin 6 is a major predictor of bone loss in women specific to the first decade past menopause. *J.Clin.Endocrinol.Metab*, 86, 2032-2042.
- Schiller, M., Metze, D., Luger, T. A., Grabbe, S., & Gunzer, M. (2006). Immune response modifiers--mode of action. *Exp.Dermatol.*, 15, 331-341.
- Schmidt, A. M., Yan, S. D., Wautier, J. L., & Stern, D. (1999). Activation of receptor for advanced glycation end products: a mechanism for chronic vascular dysfunction in diabetic vasculopathy and atherosclerosis. *Circ.Res.*, 84, 489-497.
- Schriefer, J. L., Robling, A. G., Warden, S. J., Fournier, A. J., Mason, J. J., & Turner, C. H. (2005). A comparison of mechanical properties derived from multiple skeletal sites in mice. *J.Biomech.*, 38, 467-475.
- Schwartz, A. V., Sellmeyer, D. E., Ensrud, K. E., Cauley, J. A., Tabor, H. K., Schreiner, P. J. et al. (2001). Older women with diabetes have an increased risk of fracture: a prospective study. *J.Clin.Endocrinol.Metab*, 86, 32-38.
- Schwartz, A. V., Vittinghoff, E., Bauer, D. C., Hillier, T. A., Strotmeyer, E. S., Ensrud, K. E. et al. (2011). Association of BMD and FRAX score with risk of fracture in older adults with type 2 diabetes. *JAMA*, 305, 2184-2192.
- Sheng, M. H., Baylink, D. J., Beamer, W. G., Donahue, L. R., Lau, K. H., & Wergedal, J. E. (2002). Regulation of bone volume is different in the metaphyses of the femur and vertebra of C3H/HeJ and C57BL/6J mice. *Bone*, 30, 486-491.

Sheng, M. H., Lau, K. H., Beamer, W. G., Baylink, D. J., & Wergedal, J. E. (2004). In vivo and in vitro evidence that the high osteoblastic activity in C3H/HeJ mice compared to C57BL/6J mice is intrinsic to bone cells. *Bone*, 35, 711-719.

Sheng, M. H., Lau, K. H., Mohan, S., Baylink, D. J., & Wergedal, J. E. (2006). High osteoblastic activity in C3H/HeJ mice compared to C57BL/6J mice is associated with low apoptosis in C3H/HeJ osteoblasts. *Calcif.Tissue Int.*, 78, 293-301.

Shi, H., Kokoeva, M. V., Inouye, K., Tzameli, I., Yin, H., & Flier, J. S. (2006). TLR4 links innate immunity and fatty acid-induced insulin resistance. *J.Clin.Invest*, 116, 3015-3025.

Simpson, I. A., Dwyer, D., Malide, D., Moley, K. H., Travis, A., & Vannucci, S. J. (2008). The facilitative glucose transporter GLUT3: 20 years of distinction. *Am.J.Physiol Endocrinol.Metab*, 295, E242-E253.

Singha, U. K., Jiang, Y., Yu, S., Luo, M., Lu, Y., Zhang, J. et al. (2008). Rapamycin inhibits osteoblast proliferation and differentiation in MC3T3-E1 cells and primary mouse bone marrow stromal cells. *J.Cell Biochem.*, 103, 434-446.

Smith, B. J., Lerner, M. R., Bu, S. Y., Lucas, E. A., Hanas, J. S., Lightfoot, S. A. et al. (2006). Systemic bone loss and induction of coronary vessel disease in a rat model of chronic inflammation. *Bone*, 38, 378-386.

Son, M. J., Lee, S. B., Byun, Y. J., Lee, H. O., Kim, H. S., Kwon, O. J. et al. (2010). Sodium nitroprusside induces autophagic cell death in glutathione-depleted osteoblasts. *J.Biochem.Mol.Toxicol.*, 24, 313-322.

Stolk, R. P., van Daele, P. L., Pols, H. A., Burger, H., Hofman, A., Birkenhager, J. C. et al. (1996). Hyperinsulinemia and bone mineral density in an elderly population: The Rotterdam Study. *Bone*, 18, 545-549.

Sultzter, B. M. (1968). Genetic control of leucocyte responses to endotoxin. *Nature*, 219, 1253-1254.

Takeda, K. & Akira, S. (2007). Toll-like receptors. *Curr.Protoc.Immunol.*, Chapter 14, Unit.

Tanida, I., Ueno, T., & Kominami, E. (2004). LC3 conjugation system in mammalian autophagy. *Int.J.Biochem.Cell Biol.*, 36, 2503-2518.

Thomas, D. M., Maher, F., Rogers, S. D., & Best, J. D. (1996). Expression and regulation by insulin of GLUT 3 in UMR 106-01, a clonal rat osteosarcoma cell line. *Biochem.Biophys.Res.Commun.*, 218, 789-793.

Tilich, M. & Arora, R. R. (2011). Modulation of toll-like receptors by insulin. *Am.J.Ther.*, 18, e130-e137.

- Tresse, E., Salomons, F. A., Vesa, J., Bott, L. C., Kimonis, V., Yao, T. P. et al. (2010). VCP/p97 is essential for maturation of ubiquitin-containing autophagosomes and this function is impaired by mutations that cause IBMPFD. *Autophagy*, 6, 217-227.
- Tsukumo, D. M., Carvalho-Filho, M. A., Carvalheira, J. B., Prada, P. O., Hirabara, S. M., Schenka, A. A. et al. (2007). Loss-of-function mutation in Toll-like receptor 4 prevents diet-induced obesity and insulin resistance. *Diabetes*, 56, 1986-1998.
- Valerio, G., Galle, F., Mancusi, C., Di, O., V, Guida, P., Tramontano, A. et al. (2012). Prevalence of overweight in children with bone fractures: a case control study. *BMC.Pediatr.*, 12, 166.
- van Daele, P. L., Stolk, R. P., Burger, H., Algra, D., Grobbee, D. E., Hofman, A. et al. (1995). Bone density in non-insulin-dependent diabetes mellitus. The Rotterdam Study. *Ann.Intern.Med.*, 122, 409-414.
- Vashishth, D. (2007). The role of the collagen matrix in skeletal fragility. *Curr.Osteoporos.Rep.*, 5, 62-66.
- Wei, S., Kitaura, H., Zhou, P., Ross, F. P., & Teitelbaum, S. L. (2005). IL-1 mediates TNF-induced osteoclastogenesis. *J.Clin.Invest*, 115, 282-290.
- WINEGRAD, A. I. & RENOLD, A. E. (1958). Studies on rat adipose tissue in vitro. I. Effects of insulin on the metabolism of glucose, pyruvate, and acetate. *J.Biol.Chem.*, 233, 267-272.
- Wirth, M., Joachim, J., & Tooze, S. A. (2013). Autophagosome formation--the role of ULK1 and Beclin1-PI3KC3 complexes in setting the stage. *Semin.Cancer Biol.*, 23, 301-309.
- World Health Organization (2004). *WHO Scientific Group on the Assessment of Osteoporosis at Primary Health Care Level*.
- Xia, X., Kar, R., Gluhak-Heinrich, J., Yao, W., Lane, N. E., Bonewald, L. F. et al. (2010). Glucocorticoid-induced autophagy in osteocytes. *J.Bone Miner.Res.*, 25, 2479-2488.
- Yang, Y. H., Chen, K., Li, B., Chen, J. W., Zheng, X. F., Wang, Y. R. et al. (2013). Estradiol inhibits osteoblast apoptosis via promotion of autophagy through the ER-ERK-mTOR pathway. *Apoptosis*, 18, 1363-1375.
- Yang, Z. & Klionsky, D. J. (2010). Mammalian autophagy: core molecular machinery and signaling regulation. *Curr.Opin.Cell Biol.*, 22, 124-131.
- Zhao, Y., Chen, G., Zhang, W., Xu, N., Zhu, J. Y., Jia, J. et al. (2011). Autophagy regulates hypoxia-induced osteoclastogenesis through the HIF-1alpha/BNIP3 signaling pathway. *J Cell Physiol*.

Zhou, Z., Han, J. Y., Xi, C. X., Xie, J. X., Feng, X., Wang, C. Y. et al. (2008). HMGB1 regulates RANKL-induced osteoclastogenesis in a manner dependent on RAGE. *J.Bone Miner.Res.*, 23, 1084-1096.

Zhou, Z., Immel, D., Xi, C. X., Bierhaus, A., Feng, X., Mei, L. et al. (2006). Regulation of osteoclast function and bone mass by RAGE. *J.Exp.Med.*, 203, 1067-1080.

Zhu Li, Julie Leslie, Guang William Wong, Barbara Kahn, Ryan Riddle, and Thomas Clemans. (10-5-2013). Expression of Glucose Transporter-4 by the osteoblast is required for global glucose metabolism. American Society for Bone and Mineral Research .
Ref Type: Abstract

Zoidis, E., Ghirlanda-Keller, C., & Schmid, C. (2011). Stimulation of glucose transport in osteoblastic cells by parathyroid hormone and insulin-like growth factor I. *Mol.Cell Biochem.*, 348, 33-42.

Zou, W. & Bar-Shavit, Z. (2002). Dual modulation of osteoclast differentiation by lipopolysaccharide. *J.Bone Miner.Res.*, 17, 1211-1218.

APPENDICES

APPENDIX A

SUPPLEMENTAL MATERIALS FOR CHAPTER III

Table 1. Plasma Total (Gla-) and Undercarboxylated (Glu-) OCN

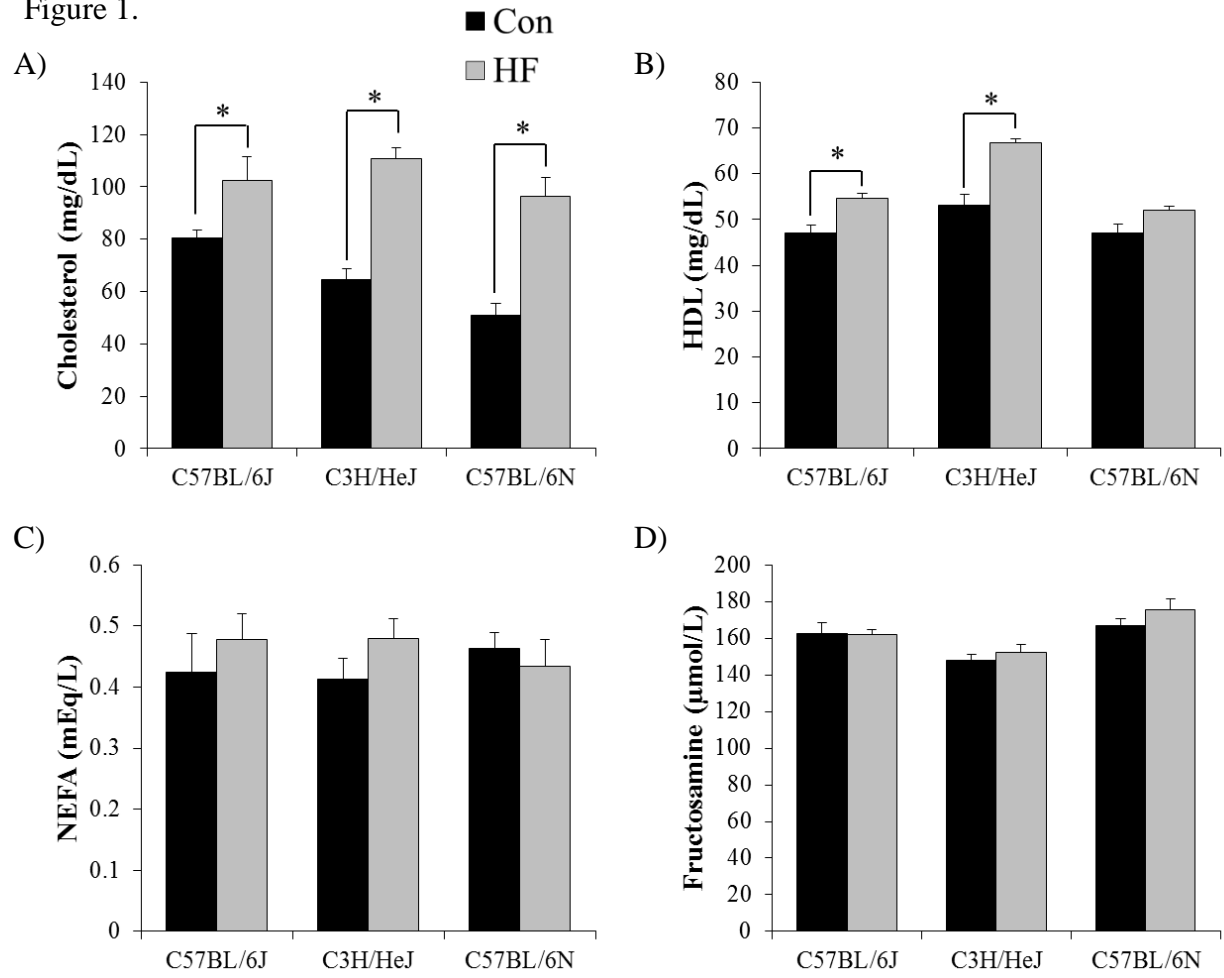
Figure 1. Blood profile of cholesterol (A), high-density lipoprotein (HDL) (B), non-esterified fatty acids (NEFA) (C), and fructosamine (D) were determined in C57BL/6J, C3H/HeJ, and C57BL/6N mice following 24 wk on a control (Con=AIN 93M) or high fat (HF=45% kcal from fat). Values are means \pm SE. Symbol, *, represents a significant difference ($P < 0.05$) between dietary treatments within a given strain.

Table 1. Plasma Total (Gla-) and Undercarboxylated (Glu-) OCN

	C57BL/6J			C57BL/6N			C3H/HeJ		
	Con	HF	<i>p-value</i>	Con	HF	<i>p-value</i>	Con	HF	<i>p-value</i>
Gla-OCN (ng/mL)	46.77 ± 6.73	43.84 ± 3.65	0.7072	35.83 ± 2.31	40.51 ± 4.35	0.3583	35.02 ± 1.56	31.96 ± 2.09	0.2594
Glu-OCN (ng/mL)	1.28 ± 0.16	1.21 ± 0.10	0.7015	1.11 ± 0.7	1.01 ± 0.13	0.5152	0.89 ± 0.14	0.95 ± 0.18	0.8038
Glu-OCN/Gla-OCN (%)	2.86 ± 0.31	2.79 ± 0.15	0.8304	3.18 ± 0.25	2.48 ± 0.13*	0.0254	2.56 ± 0.37	3.02 ± 0.61	0.5252

Total (Gla-) and undercarboxylated (Glu-) osteocalcin (OCN) was determined in the plasma from C57BL/6J, C57BL/6N, and C3H/HeJ mice following 24 wk on a control (Con=AIN 93M) or high fat (HF=45% kcal from fat) using a commercially available ELISA kit (Clontech Takara Bio, Mountain View, CA). Values are means ± SE. Symbol, *, represents a significant difference ($P < 0.05$) between dietary treatments within a given strain.

Figure 1.



APPENDIX B

SUPPLEMENTAL MATERIALS FOR CHAPTER IV

Table 1. Whole Body DXA Analysis and Tibia Length after 2, 8, and 16 wk on a Control or High Fat Diet.

Table 2. Cortical Bone Parameters of the Femur Mid-Diaphysis

Table 3. Alterations in Biomechanical Properties of the Distal Femur Metaphysis and Mid-Diaphysis

Table 4. Trabecular Bone Parameters of the Distal Femur Metaphysis

Table 5. Plasma Leptin and Adiponectin in C57BL/6 and C3H/HeJ Mice

Figure 1. Intraperitoneal glucose tolerance test (IGTT) was performed on C57BL/6 and C3H/HeJ mice receiving a control (Con; AIN93M) or high fat (HF; 60% kcal from fat) diet for 2, 8, and 16 wk by administering an intraperitoneal injection of glucose solution (2 g glucose/ kg bodyweight) and blood glucose was monitored at 15, 30, 60, 90, and 120 minutes. Symbol (*, C57BL/6; +, C3H/HeJ) represents a significant difference ($P < 0.05$) at a given time point between dietary treatments within a given strain.

Figure 2. The advanced glycation end product (AGE), pentosidine, was determined in the humerus from C57BL/6 and C3H/HeJ mice on control (Con; AIN93M) or high fat (HF; 60% kcal from fat) diet for at 2, 8, and 16 wk, and expressed as total pentosidine (A), collagen (B), pentosidine or AGEs/ collagen (C), and AGEs/ wet weight of the humerus (D). Values are means \pm SE. Comparisons were made at a given time point between dietary treatments within a given strain.

Table 1. Whole Body DXA Analysis and Tibia Length after 2, 8, and 16 wk on a Control or High Fat Diet.

	C57BL/6		C3H/HeJ	
	Control	HF	Control	HF
2 Week				
<i>BMA (cm²)</i>	9.17 ± 0.14	8.89 ± 0.19	10.01 ± 0.11	9.84 ± 0.27
<i>BMC (mg)</i>	385.3 ± 8.3	381.8 ± 8.9	486.9 ± 9.2	482.3 ± 18.5
<i>BMD (mg/cm²)</i>	42.0 ± 0.4	42.9 ± 0.4	48.6 ± 0.6	48.9 ± 0.6
<i>Tibia Length (mm)</i>	16.3 ± 0.1	16.2 ± 0.1	16.2 ± 0.1	16.34 ± 0.2
8 Week				
<i>BMA (cm²)</i>	10.29 ± 0.44	8.40 ± 0.18*	12.05 ± 0.14	10.8 ± 0.16*
<i>BMC (mg)</i>	513.7 ± 31.4	393.9 ± 12.1*	700.7 ± 14.1	598.7 ± 10.0*
<i>BMD (mg/cm²)</i>	49.6 ± 0.9	46.9 ± 0.5*	58.1 ± 0.5	57.1 ± 0.4
<i>Tibia Length (mm)</i>	17.4 ± 0.2	17.0 ± 0.2	17.3 ± 0.2	17.4 ± 0.2
16 Week				
<i>BMA (cm²)</i>	10.61 ± 0.17	8.28 ± 0.13*	12.46 ± 0.11	10.92 ± 0.11*
<i>BMC (mg)</i>	529.0 ± 11.7	401.4 ± 8.4*	782.3 ± 10.1	657.8 ± 10.0*
<i>BMD (mg/cm²)</i>	49.8 ± 0.4	48.5 ± 0.4*	62.7 ± 0.5	60.2 ± 0.4*
<i>Tibia Length (mm)</i>	18.2 ± 0.2	17.6 ± 0.2*	17.9 ± 0.2	17.7 ± 0.1

Whole body bone mineral area (BMA), content (BMC), and density (BMD) determined by dual-energy x-ray absorptiometry (DXA) and tibia length from C57BL/6 and C3H/HeJ on control (Con; AIN93M) or high fat (HF; 60% kcal from fat) diet. Values are expressed as mean ± SE. Symbol * indicates significant differences ($P = 0.05$) between dietary treatments within mouse strain at a given time point.

Table 2. Cortical Bone Parameters of the Femur Mid-Diaphysis

	C57BL/6		C3H/HeJ	
	Con	HF	Con	HF
2 Week				
<i>Porosity (%)</i>	5.68 ± 0.27	5.30 ± 0.16	3.73 ± 0.23	3.91 ± 0.08
<i>Cortical Thickness (mm)</i>	0.155 ± 0.004	0.163 ± 0.0035	0.240 ± 0.007	0.235 ± 0.003
<i>Cortical Area (mm²)</i>	0.042 ± 0.001	0.043 ± 0.001	0.057 ± 0.0019	0.057 ± 0.002
<i>Medullary Area (mm²)</i>	0.040 ± 0.001	0.038 ± 0.001	0.035 ± 0.002	0.036 ± 0.001
8 Week				
<i>Porosity (%)</i>	4.27 ± 0.17	4.59 ± 0.14	2.61 ± 0.08	2.71 ± 0.08
<i>Cortical Thickness (mm)</i>	0.202 ± 0.004	0.187 ± .002*	0.325 ± 0.003	0.326 ± 0.005
<i>Cortical Area (mm²)</i>	0.059 ± 0.003	0.051 ± 0.001*	0.088 ± 0.001	0.081 ± 0.002
<i>Medullary Area (mm²)</i>	0.042 ± 0.003	0.038 ± 0.001	0.033 ± 0.001	0.035 ± 0.001
16 Week				
<i>Porosity (%)</i>	4.22 ± 0.15	4.45 ± 0.18	3.15 ± 0.29	2.65 ± 0.08
<i>Cortical Thickness (mm)</i>	0.195 ± 0.003	0.192 ± 0.003	0.329 ± 0.007	0.348 ± 0.005*
<i>Cortical Area (mm²)</i>	0.055 ± 0.001	0.052 ± 0.001	0.088 ± 0.003	0.088 ± 0.002
<i>Medullary Area (mm²)</i>	0.038 ± 0.001	0.039 ± 0.002	0.045 ± 0.004	0.038 ± 0.002

Table 2. Alterations in cortical bone were assessed by microCT analyses of the femur mid-diaphysis at 2, 8, and 16 wk on control (Con; AIN93M) or high fat (HF; 60% kcal from fat) diet in C57BL/6 and C3H/HeJ mice. Values are expressed as mean ± SE. Symbol * indicates significant differences ($P = 0.05$) between dietary treatments within a mouse strain at a given time point.

Table 3. Alterations in Biomechanical Properties of the Distal Femur Metaphysis and Mid-Diaphysis

	C57BL/6		C3H/HeJ	
	Con	HF	Con	HF
2 Week				
<i>ID Distal Metaphysis(μm)</i>	75.6 \pm 13.3	89.5 \pm 9.9	129.3 \pm 13.5	125.8 \pm 9.7
<i>ID Mid-Diaphysis(μm)</i>	53.1 \pm 1.7	54.5 \pm 2.6	42.6 \pm 2.8	37.9 \pm 0.6*
8 Week				
<i>ID Distal Metaphysis(μm)</i>	68.3 \pm 5.6	91.5 \pm 8.1*	58.2 \pm 5.6	62.6 \pm 6.8
<i>ID Mid-Diaphysis(μm)</i>	36.2 \pm 0.7	38.3 \pm 0.8	33.1 \pm 0.5	34.7 \pm 1.6
16 Week				
<i>ID Distal Metaphysis(μm)</i>	73.7 \pm 3.0	95.2 \pm 9.1*	58.6 \pm 2.1	59.0 \pm 2.8
<i>ID Mid-Diaphysis(μm)</i>	32.5 \pm 1.2	35.7 \pm 1.2*	28.9 \pm 0.6	33.3 \pm 1.7*

Table 3. First cycle indentation distance (ID) was determined by reference point indentation (RPI) performed on the lateral surface of the distal femur metaphysis and anterior surface of the femur mid-diaphysis in C57BL/6 and C3H/HeJ mice on control (Con; AIN93M) or high fat (HF; 60% kcal from fat) diet for at 2, 8, and 16 wk. Values are expressed as mean \pm SE. Symbol * indicates significant differences ($P = 0.05$) between dietary treatments within a mouse strain at a given time point.

Table 4. Trabecular Bone Parameters of the Distal Femur Metaphysis

	C57BL/6		C3H/HeJ	
	Con	HF	Con	HF
2 Week				
<i>BV/TV (%)</i>	13.29 ± 0.43	15.51 ± 1.74	22.85 ± 2.74	23.83 ± 2.9
<i>Tb.N. (mm)</i>	5.43 ± 0.19	5.52 ± 0.16	5.64 ± 0.21	5.56 ± 0.27
<i>Tb.Th. (mm)</i>	0.0382 ± 0.0006	0.0421 ± 0.0019	0.0564 ± 0.0021	0.0546 ± 0.0023
<i>Tb.Sp. (mm)</i>	0.177 ± 0.004	0.175 ± 0.006	0.166 ± 0.007	0.172 ± 0.010
8 Week				
<i>BV/TV (%)</i>	16.33 ± 1.78	11.70 ± 0.55*	19.98 ± 2.67	18.41 ± 1.36
<i>Tb.N. (mm)</i>	5.01 ± 0.19	4.38 ± 0.97	4.30 ± 0.31	4.16 ± 0.16
<i>Tb.Th. (mm)</i>	0.0500 ± 0.0031	0.0467 ± 0.0017*	0.0610 ± 0.0021	0.0622 ± 0.0024
<i>Tb.Sp. (mm)</i>	0.191 ± 0.007	0.220 ± 0.005	0.223 ± 0.019	0.228 ± 0.010
16 Week				
<i>BV/TV (%)</i>	10.92 ± 1.31	6.82 ± 0.54*	17.47 ± 1.70	15.36 ± 0.84
<i>Tb.N. (mm)</i>	3.02 ± 0.32	2.06 ± 0.18	3.95 ± 0.27	3.30 ± 0.14
<i>Tb.Th. (mm)</i>	0.0360 ± 0.0097	0.0334 ± 0.0014*	0.0437 ± 0.0018	0.0465 ± 0.0014
<i>Tb.Sp. (mm)</i>	0.318 ± 0.043	0.468 ± 0.044	0.215 ± 0.018	0.259 ± 0.013

Table 4. MicroCT analyses of the trabecular bone in the distal femur metaphysis C57BL/6 and C3H/HeJ mice on control (Con; AIN93M) or high fat (HF; 60% kcal from fat) diet for at 2, 8, and 16 wk. Parameters include bone volume/ total volume (BV/TV), trabecular number (Tb.N.), thickness (Tb.Th.), and separation (Tb.Sp.). Symbol, *, represents a significant difference ($P < 0.05$) between dietary treatments for a given strain.

Table 5. Plasma Leptin and Adiponectin in C57BL/6 and C3H/HeJ Mice

	C57BL/6		C3H/HeJ	
	Con	HF	Con	HF
2 Week				
<i>Plasma Leptin (ng/mL)</i>	1.80 ± 0.36	4.08 ± 0.57*	0.62 ± 0.10	4.09 ± 0.71*
<i>Plasma Adiponectin (µg/mL)</i>	5.98 ± 0.39	5.02 ± 0.31	2.78 ± 0.25	3.18 ± 0.24
8 Week				
<i>Plasma Leptin (ng/mL)</i>	4.21 ± 0.83	29.92 ± 3.20*	0.93 ± 0.35	24.93 ± 2.44*
<i>Plasma Adiponectin (µg/mL)</i>	5.89 ± 0.37	8.50 ± 0.80*	3.85 ± 0.21	4.57 ± 0.19*
16 Week				
<i>Plasma Leptin (ng/mL)</i>	6.44 ± 1.25	96.94 ± 10.58*	1.60 ± 0.20	25.03 ± 1.98*
<i>Plasma Adiponectin (µg/mL)</i>	8.71 ± 0.37	9.87 ± 0.53	5.27 ± 0.39	4.81 ± 0.21

Table 5. Plasma leptin and adiponectin after 24 wk on a control (Con=AIN-93M) or a high fat diet (HF=45% kcal from fat) in C57BL/6 and C3H/HeJ mice, assessed by commercially ELISA kits (EMD Millipore, Billerica, MA) following the manufacturer's protocol. Values are means ± SE, $n = 15$ mice in each group. Symbol, *, represents a significant difference ($P < 0.05$) between dietary treatments within a given strain.

Figure 1.

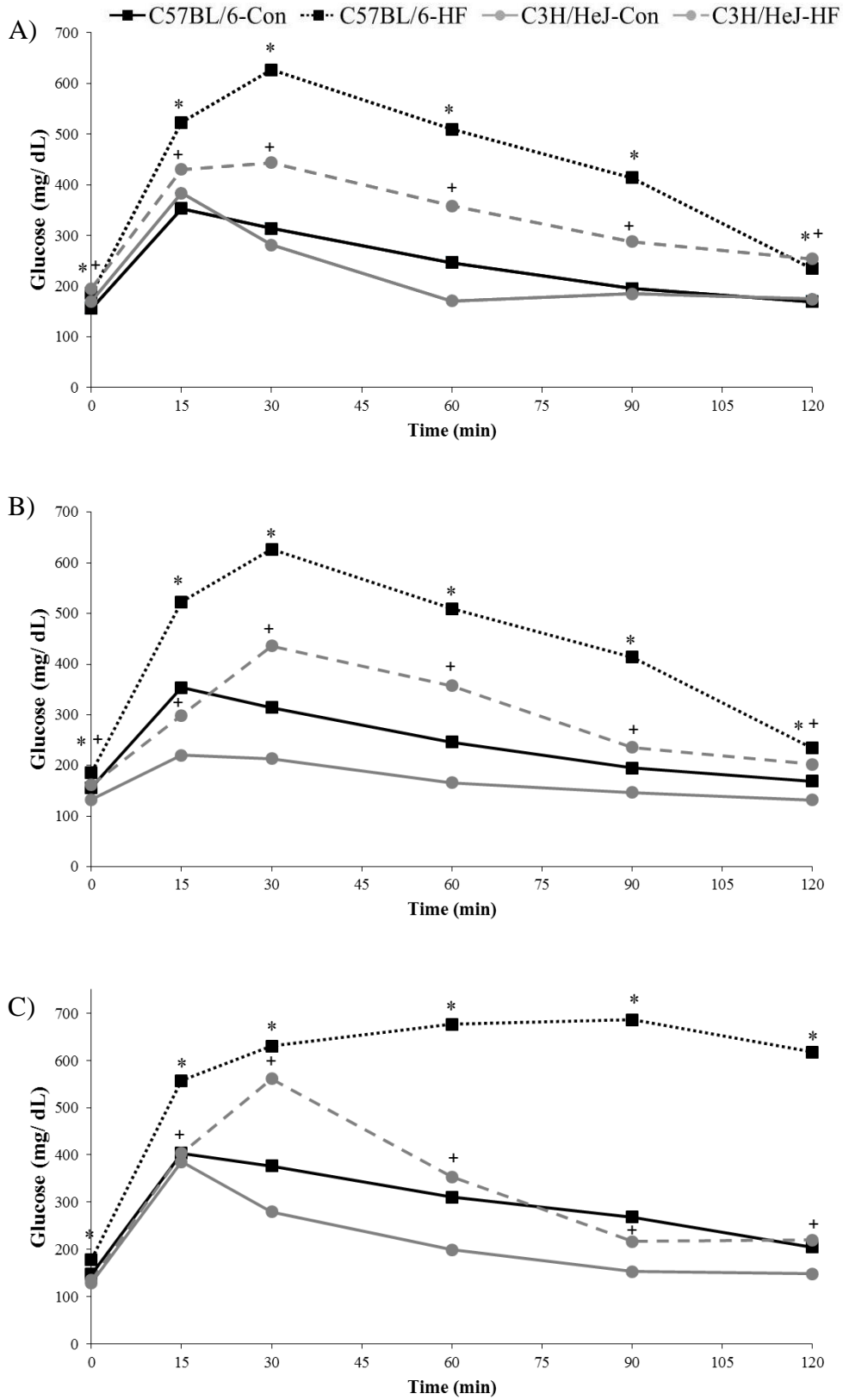
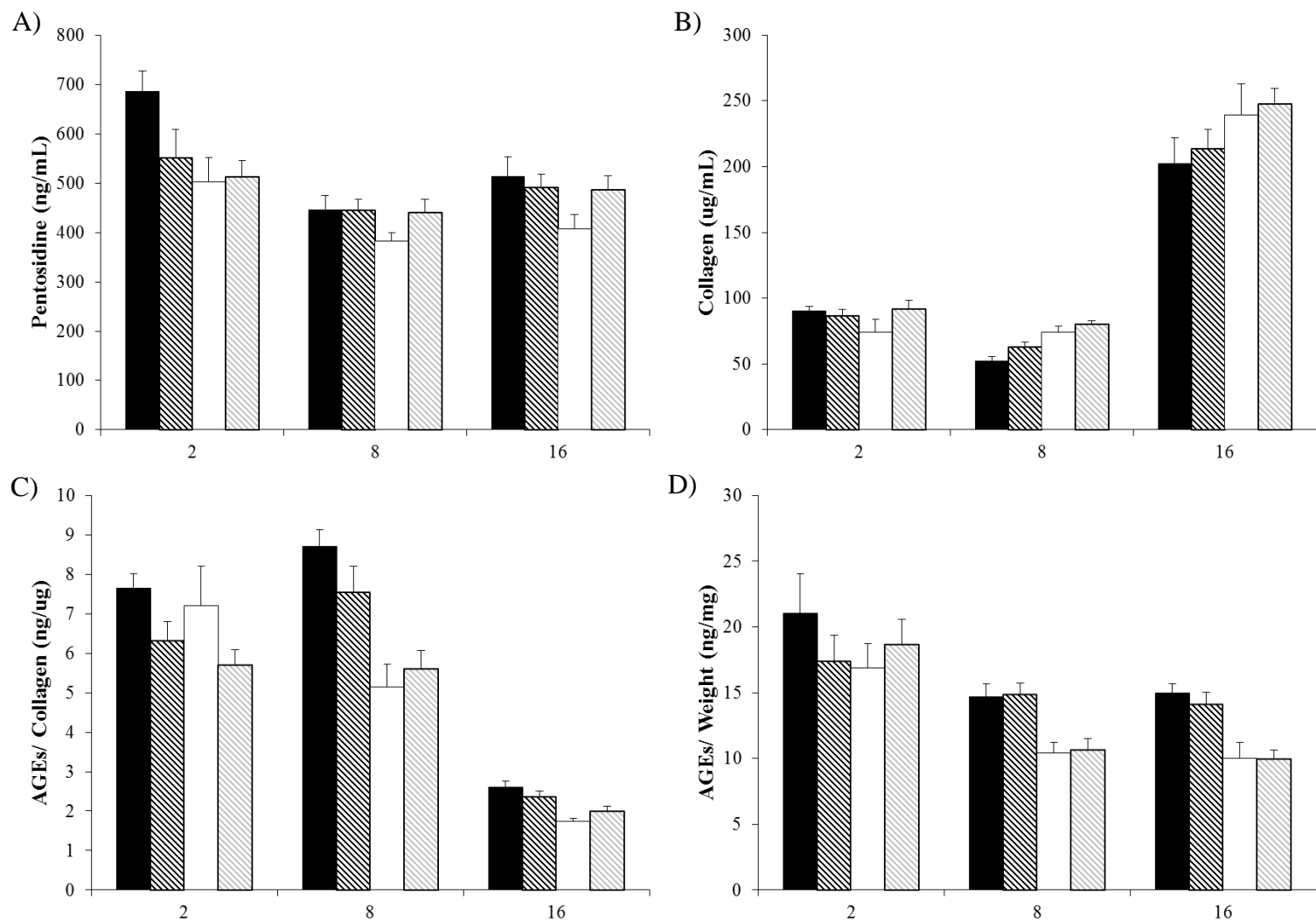


Figure 2.

■ C57BL/6-Con ▨ C57BL/6-HF □ C3H/HeJ-Con ▩ C3H/HeJ-HF



APPENDIX C

SUPPLEMENTAL MATERIALS FOR CHAPTER V

Figure 1. Alterations occurring in autophagy of the flushed femur samples from mice (C57BL/6N) on a control (\emptyset =Con; AIN93M) or high fat (HF; 60% kcal from fat) diet for at 2, 8, and 16 wk was assessed by determining protein abundance by western blot technique. Quantification was performed using OptiQuant software and density light units (DLU, 1×10^3) are reported under each blot and correspond to a given sample.

Figure 2. Initial experiments for an *in vitro* model for autophagy induction in MC3T3-E1 cells began with treatments including 55 μ M rapamycin (Rap), 200nM bafilomycin A1 (BafA1), and 500 μ M H₂O₂ for 4, 8, 16, and 24 hr, followed by LC3b-II protein abundance. Quantification was determined by OptiQuant Software and LC3B-II protein abundance is expressed relative to γ -tubulin abundance, and normalized to control.

Figure 3. MC3T3-E1 cells treated with nothing (Con), vehicle (DMSO), and 10, 30, or 55 μ M rapamycin for 4 (A) or 8 (B) hr. Bafilomycin A1 (200 nM) was added to each treatment 2 hr prior to the termination of each time point to stabilize LC3B-II protein expression. PARP and cleaved PARP (cPARP) was also determined to monitor apoptosis. γ Tubulin was used as the loading control. Representative images are shown from an $n=3$.

Figure 4. Rapamycin (Rap) (0 μ M, Con and DMSO or 10 μ M) was added to MC3T3-E1 cultures for 4 (A), 8 (B), or 24 (C) hrs. Bafilomycin A1 (BafA1) was also added 2 hours prior to protein harvest. LC3B-II protein abundance was determined to as an indicator of autophagy while PARP cleavage was monitored for apoptosis. γ Tubulin was used as the loading control

Figure 5. Established *in vitro* model of increased autophagy in undifferentiated (0d) and differentiated (7d) MC3T3-E1 cells was developed by subjecting them to treatment with 0 μ M (Con and DMSO) or 10 μ M rapamycin for 24 hr. Bafilomycin (BafA1) of was added to cultures 2 hr prior (e.g., 22 hr) to protein extraction. Representative images ($n=3$) of western blot analyses of LC3B-II abundance from undifferentiated (A) and differentiated (B) MC3T3-E1 cells are shown. No changes in cPARP, Beclin1 or pBeclin1 (Thr119) were noted.

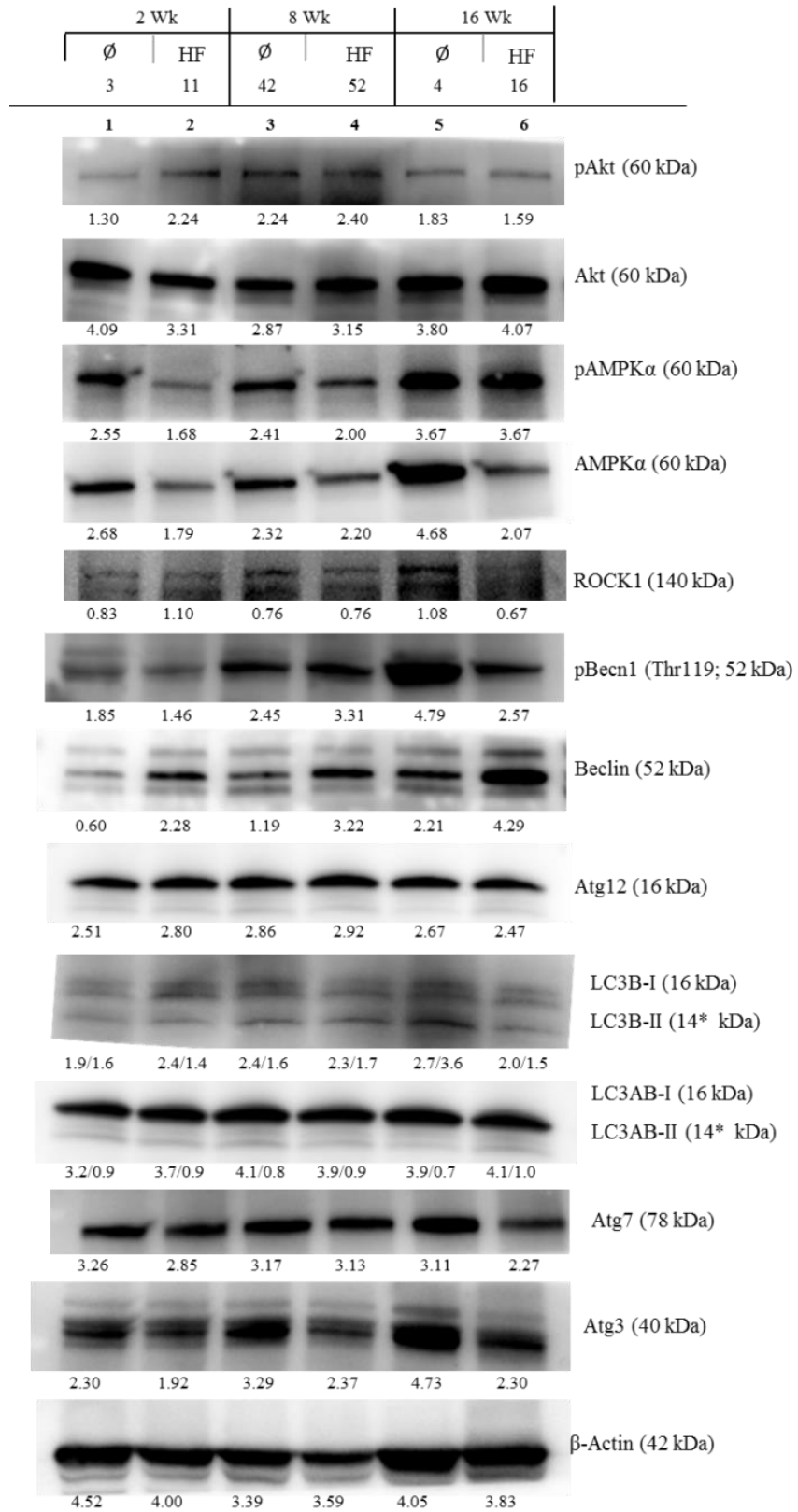
Figure 6. Following de-calcification and fixation in 2% glutaraldehyde, 0.15 M EDTA, 1M sodium cacodylate, tibias to be processed for TEM were washed 3 times for 20 min each in wash buffer, followed by post-fixation in 1% osmium tetroxide (60 min). After fixation, the samples were washed 3 times for 20 min each wash with buffer and then dehydrated by passing through multiple ethanol dehydration steps (e.g., 50%, 70%, 80%, 90%, 95%, and 100% for 3 changes). Tissues were then washed three times for 20 minutes each in propylene oxide. Tissues were infiltrated by 1:1 propylene oxide and Poly/Bed resin for five days. Propylene oxide was allowed to evaporate off, and then tissues were embedded in 100% poly/bed resin and placed in a 60°C oven for 48 hr. Thin sections (75 nm) were cut using a Reichert-Jung UltraCut E microtome and a Diatome diamond knife. Thin sections were positioned on grids and stained with uranyl acetate and Reynold's lead citrate. These sections were then imaged on a JEOL JEM-2100 TEM (JEOL USA, Inc, Peabody, MA). Representative images are shown at 4000x direct magnification.

Figure 7. Characterization of glucose transporter (GLUT)1 or *Slc2a1* (A), GLUT2 or *Slc2a2* (B), GLUT3 or *Slc2a3* (C), and GLUT4 or *Slc2a4* (D) in MC3T3 cells cultured in complete (control) α MEM or osteogenic (complete α MEM supplemented with 10 mM β -glycerophosphate and 25 μ g/ mL ascorbic acid) over time. All qPCR results were evaluated by the comparative cycle number at threshold (C_Q) method, and genes of interest were normalized to the invariant control, peptidylprolyl isomerase B (*Ppib*) and expressed as relative mRNA abundance. Data is presented as the mean \pm SEM. Bars that share the same superscript letter are not significantly different from each other ($P < 0.05$).

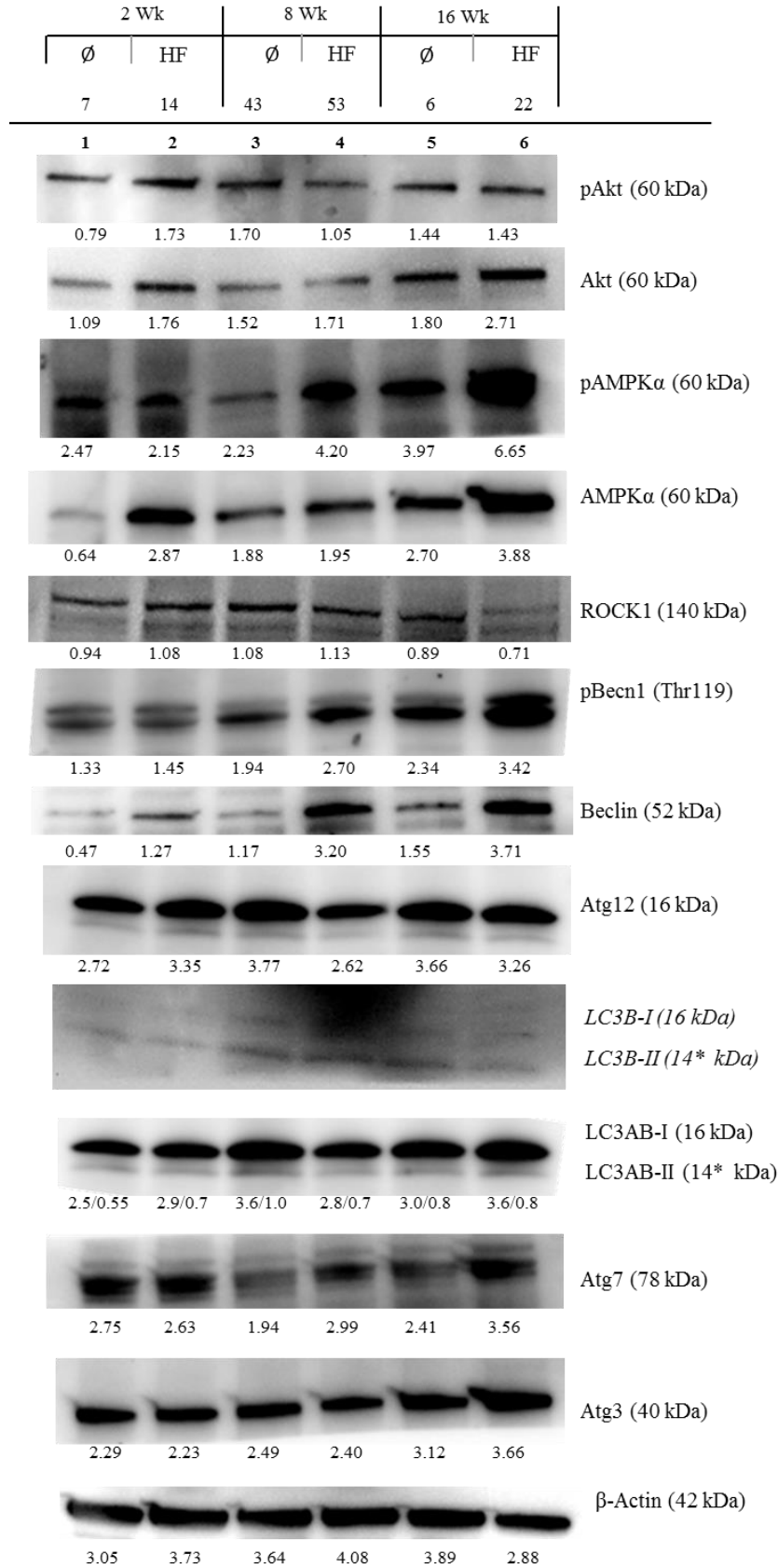
Figure 8. Characterization of glucose transporters (GLUTs) in the flushed femur at the mRNA and protein level from C57BL/6N mice on a control (Con; AIN93M) or high fat (HF; 60% kcal from fat) diet for at 2, 8, and 16 wk. qPCR was performed to determine GLUT3 or *Slc2a3* (A) or GLUT4 or *Slc2a4* (B) mRNA abundance, normalized to the invariant control, peptidylprolyl isomerase B (*Ppib*). Protein abundance of GLUT3 and GLUT4 from flushed femur samples (C-E).

Figure 1.

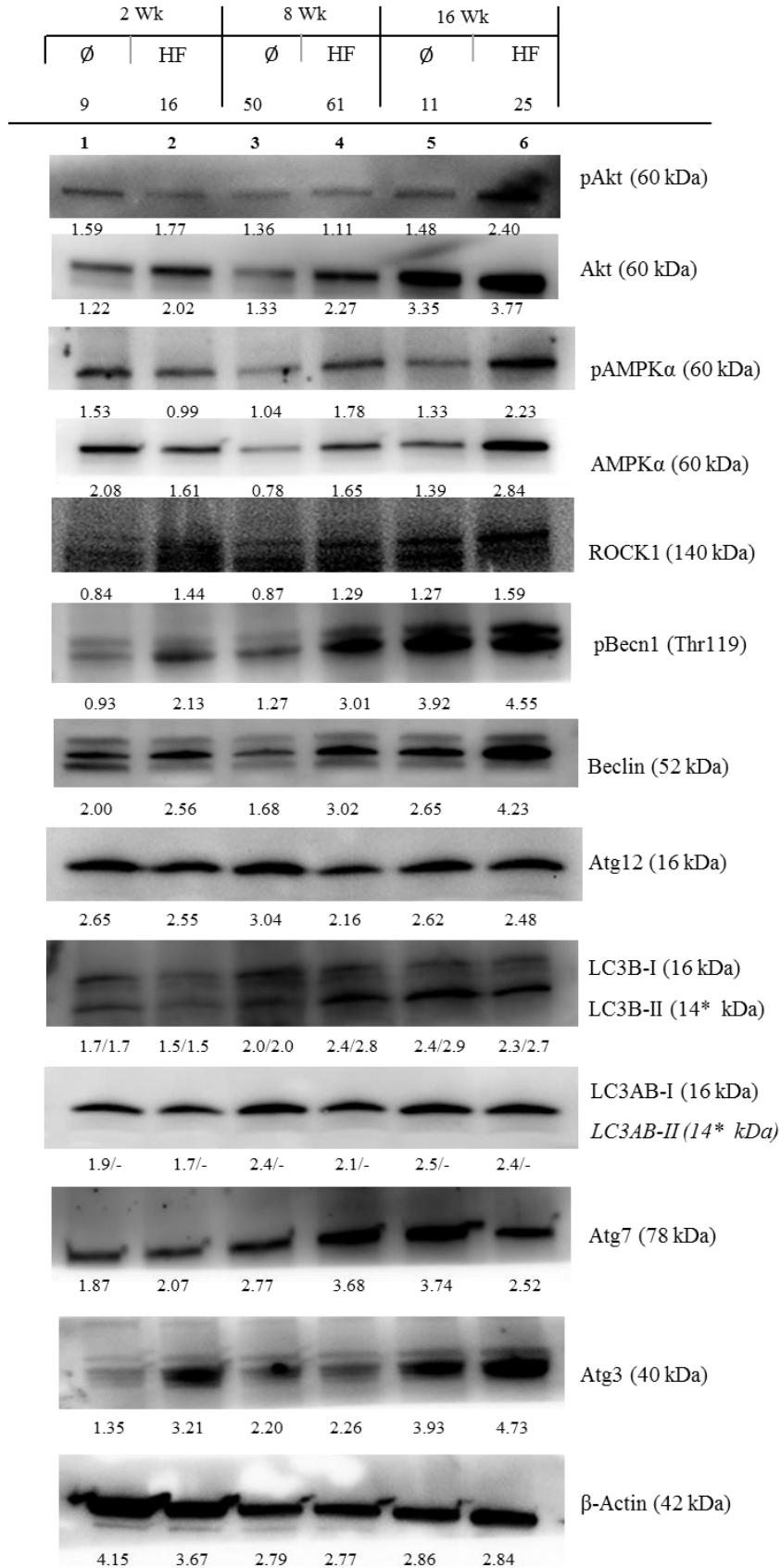
A)



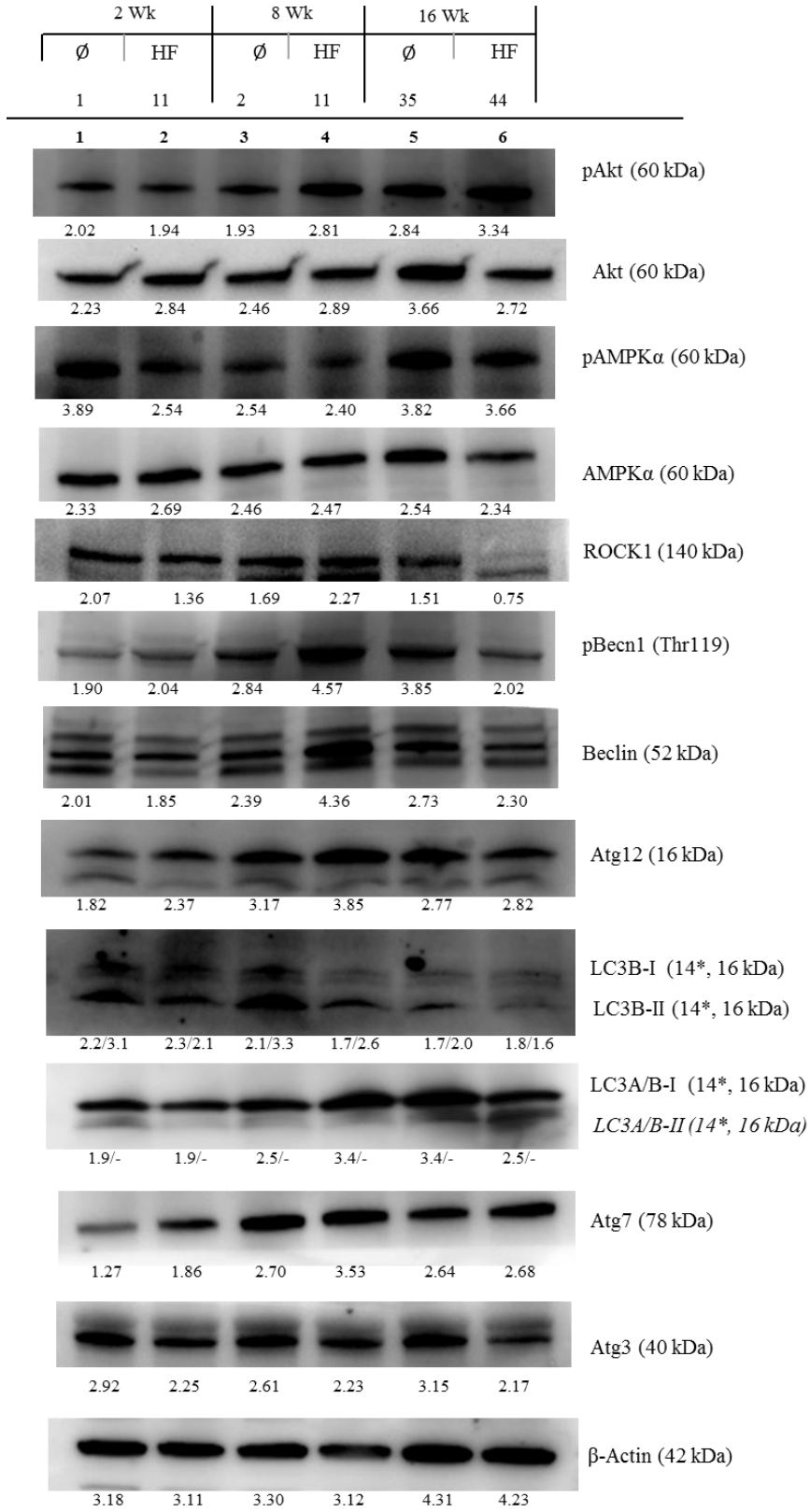
B)



C)



D)



E)

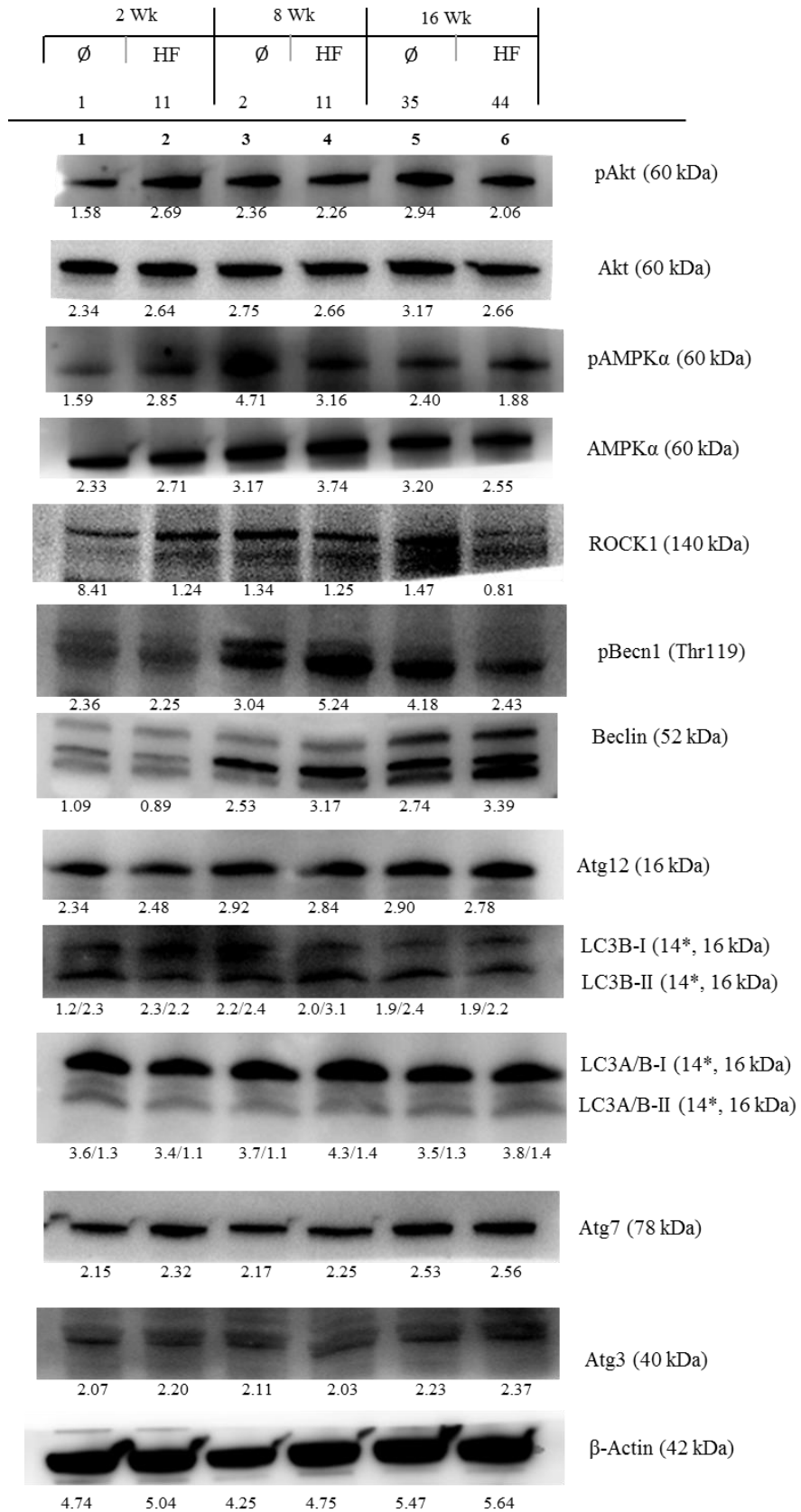


Figure 2.

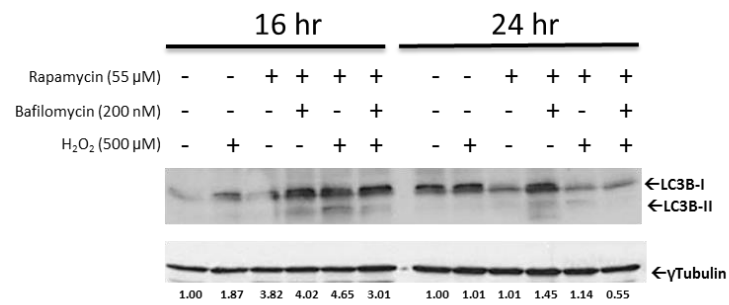
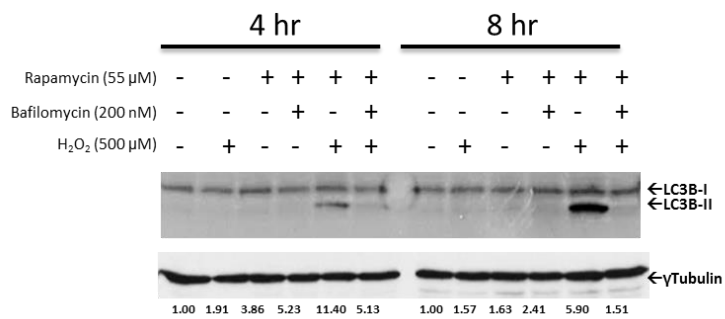
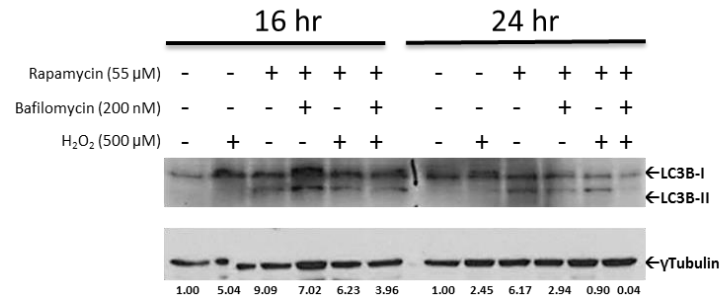
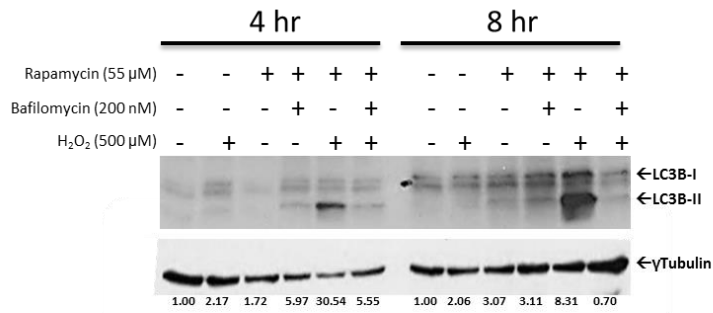
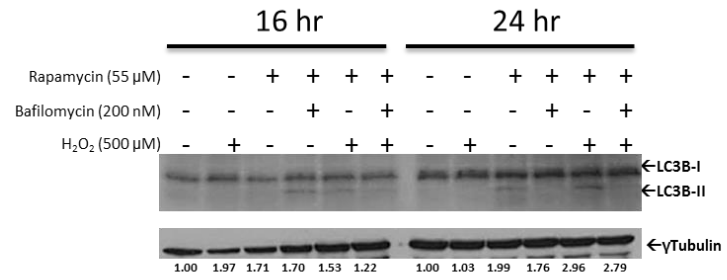
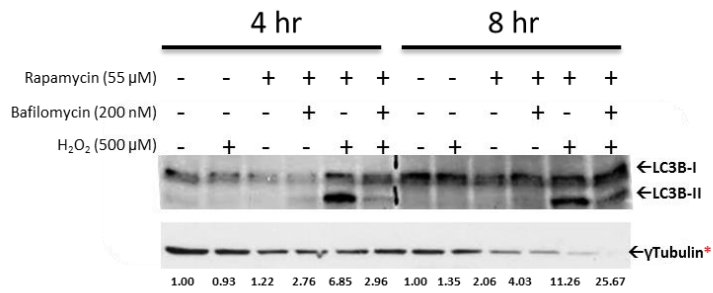
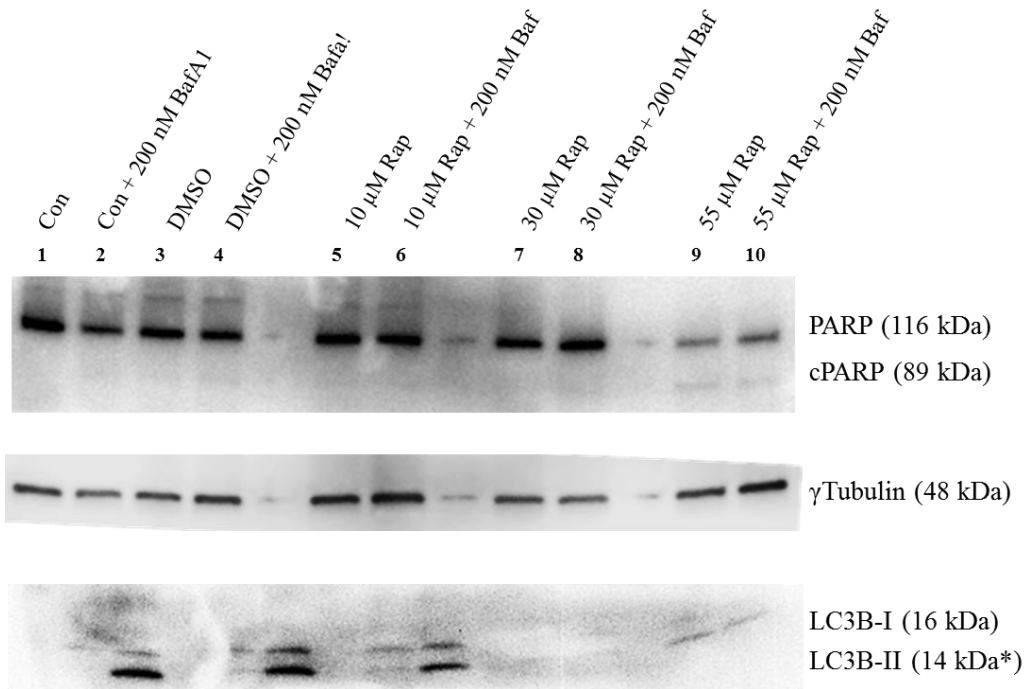


Figure 3.

A)



B)

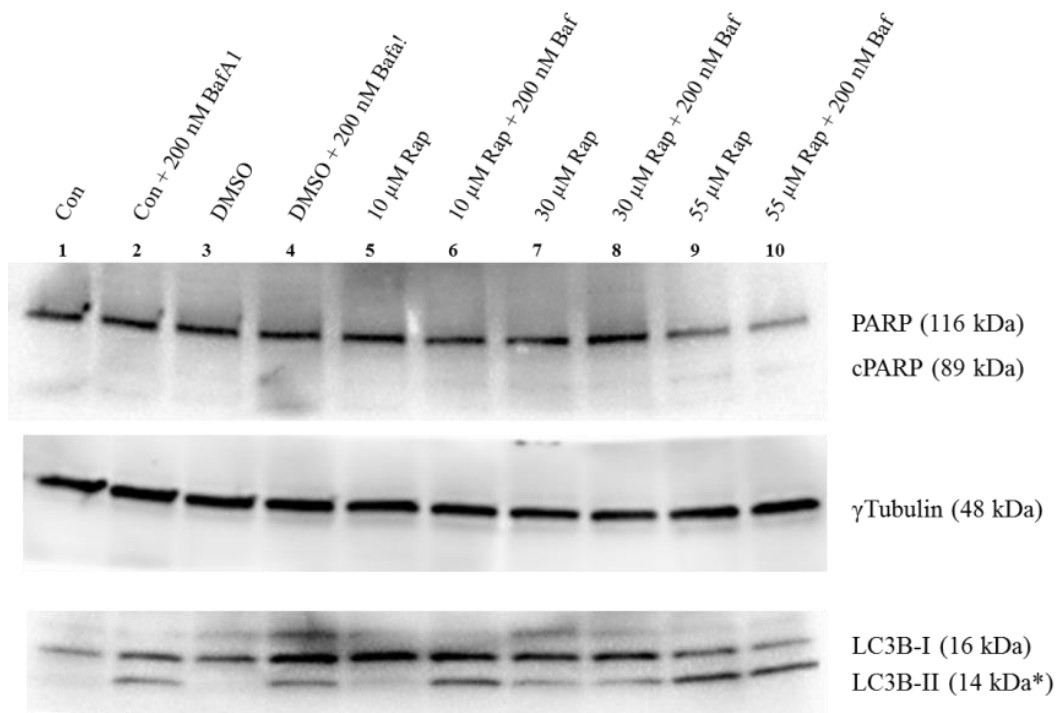
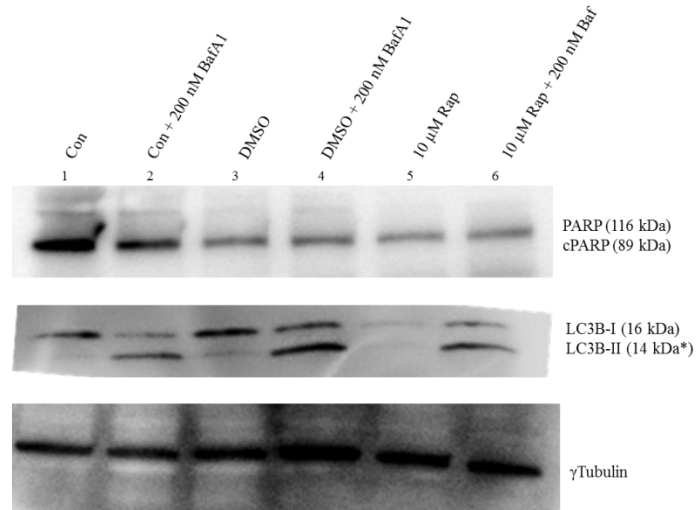
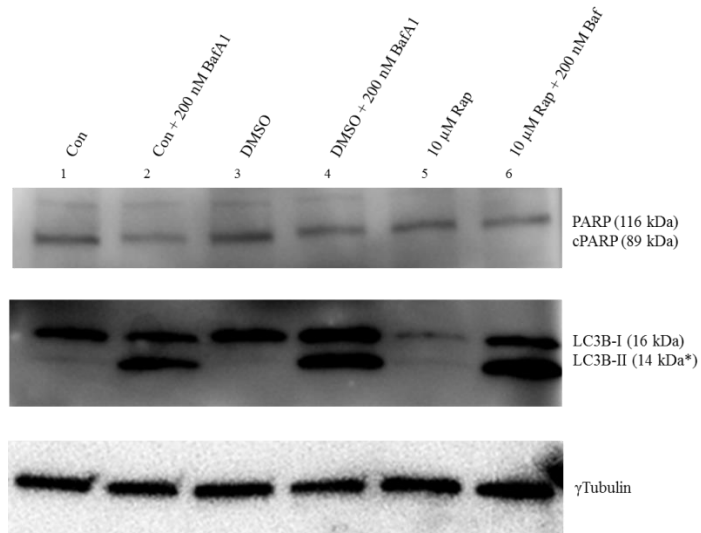


Figure 4.

A)



B)



C)

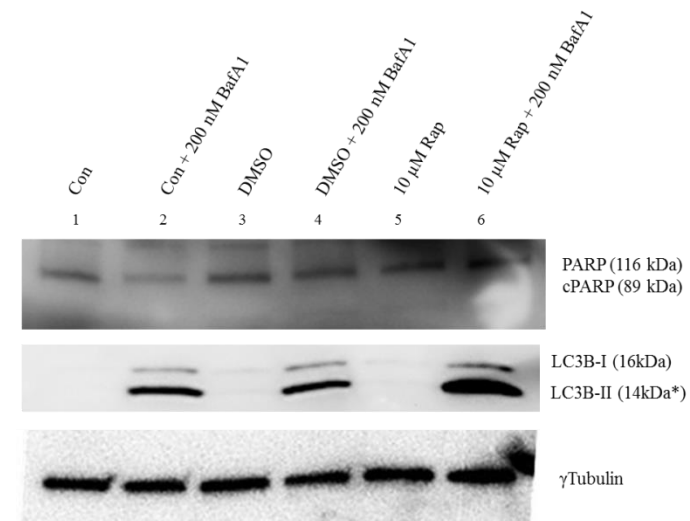
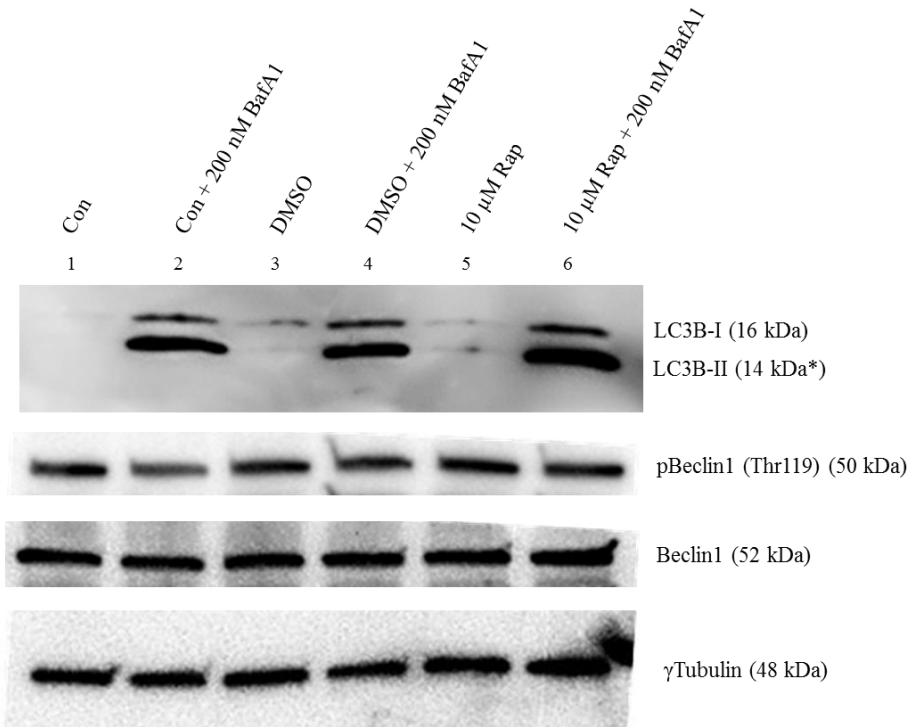


Figure 5.

A)



B)

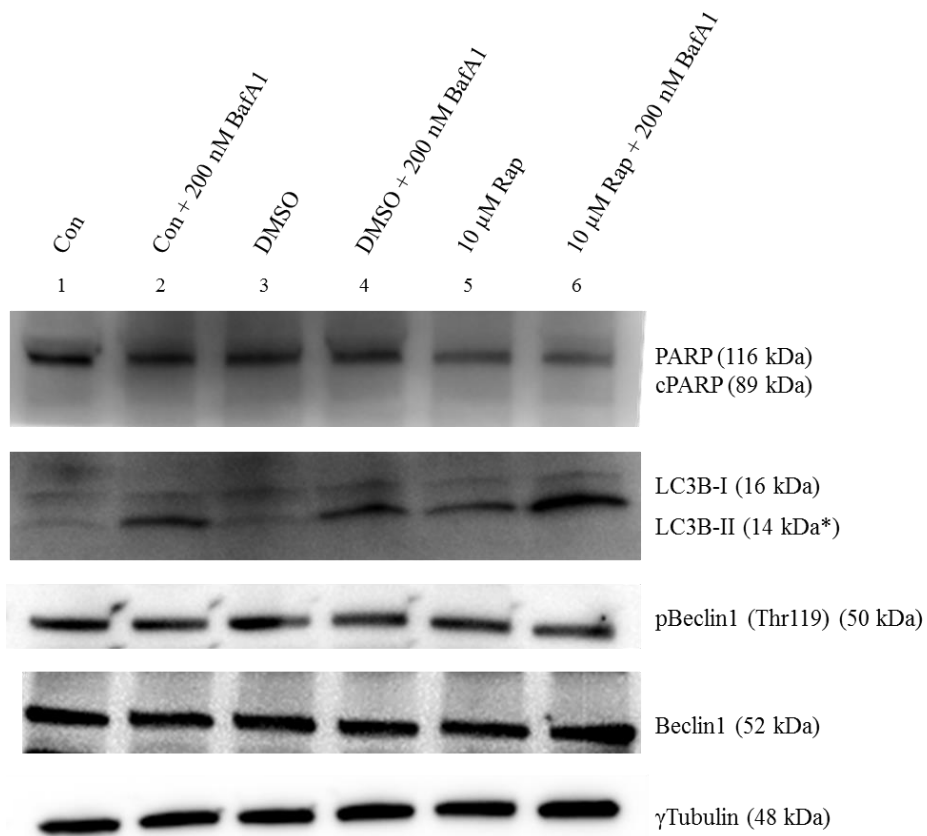


Figure 6.

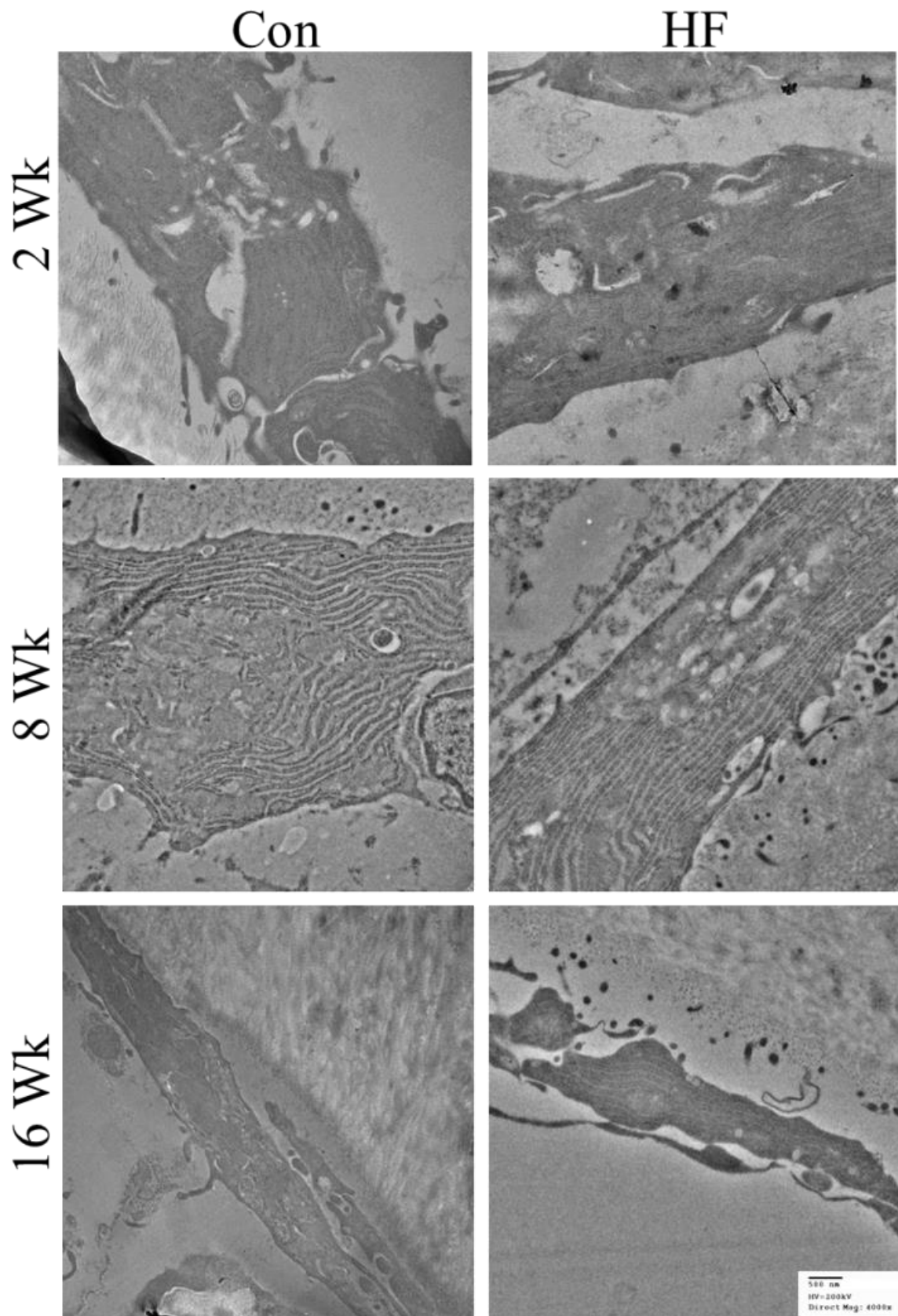


Figure 7.

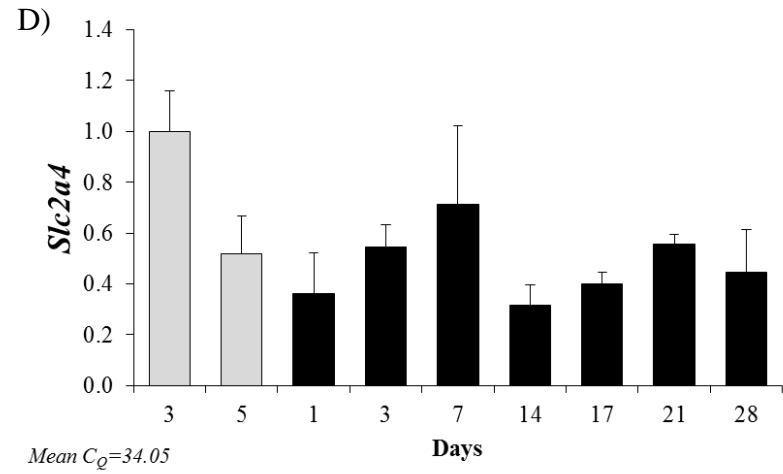
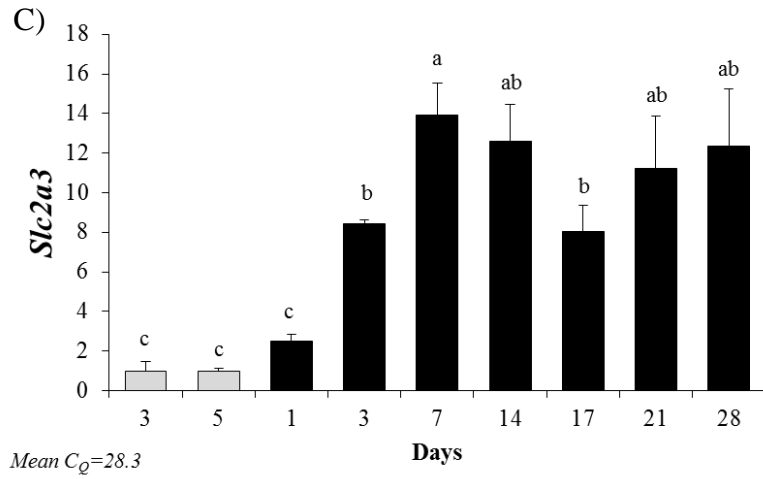
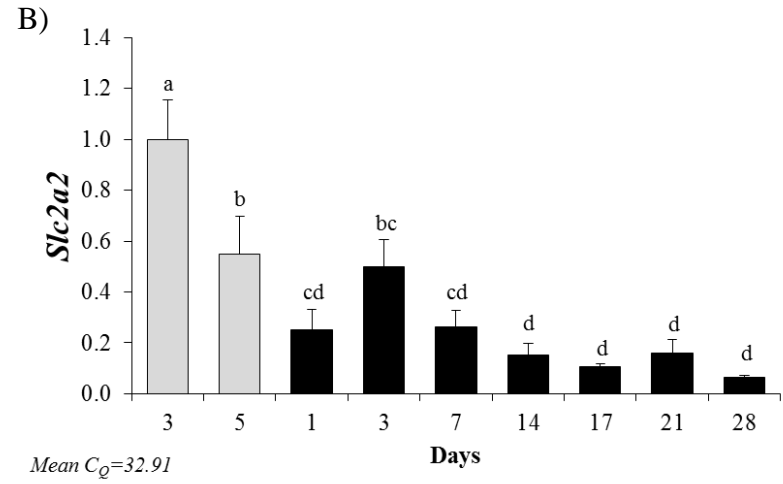
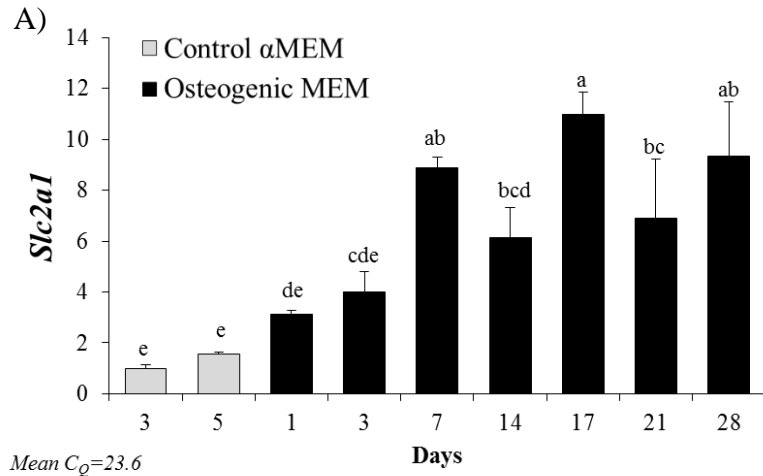
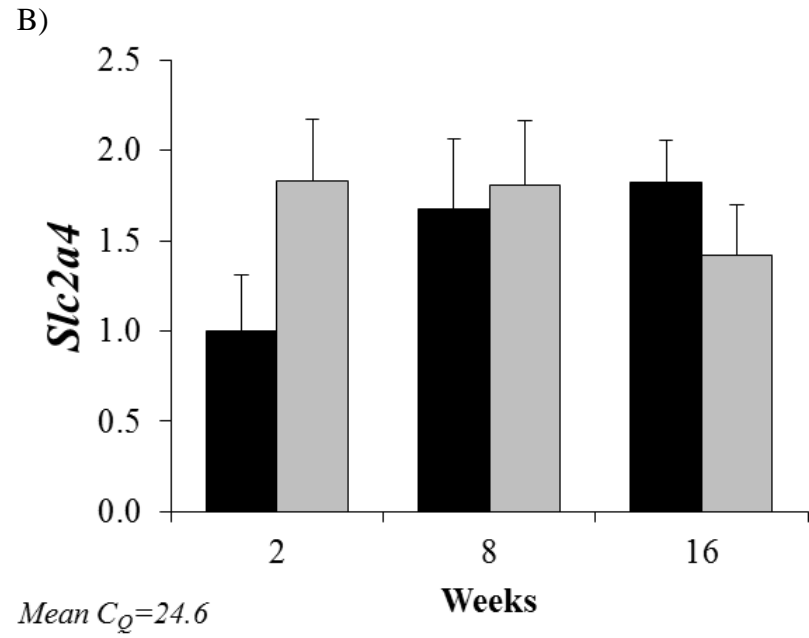
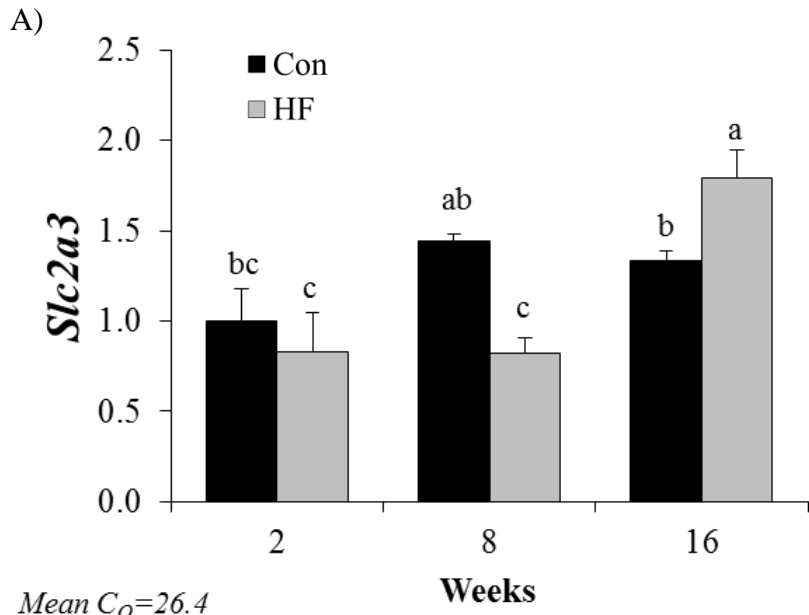
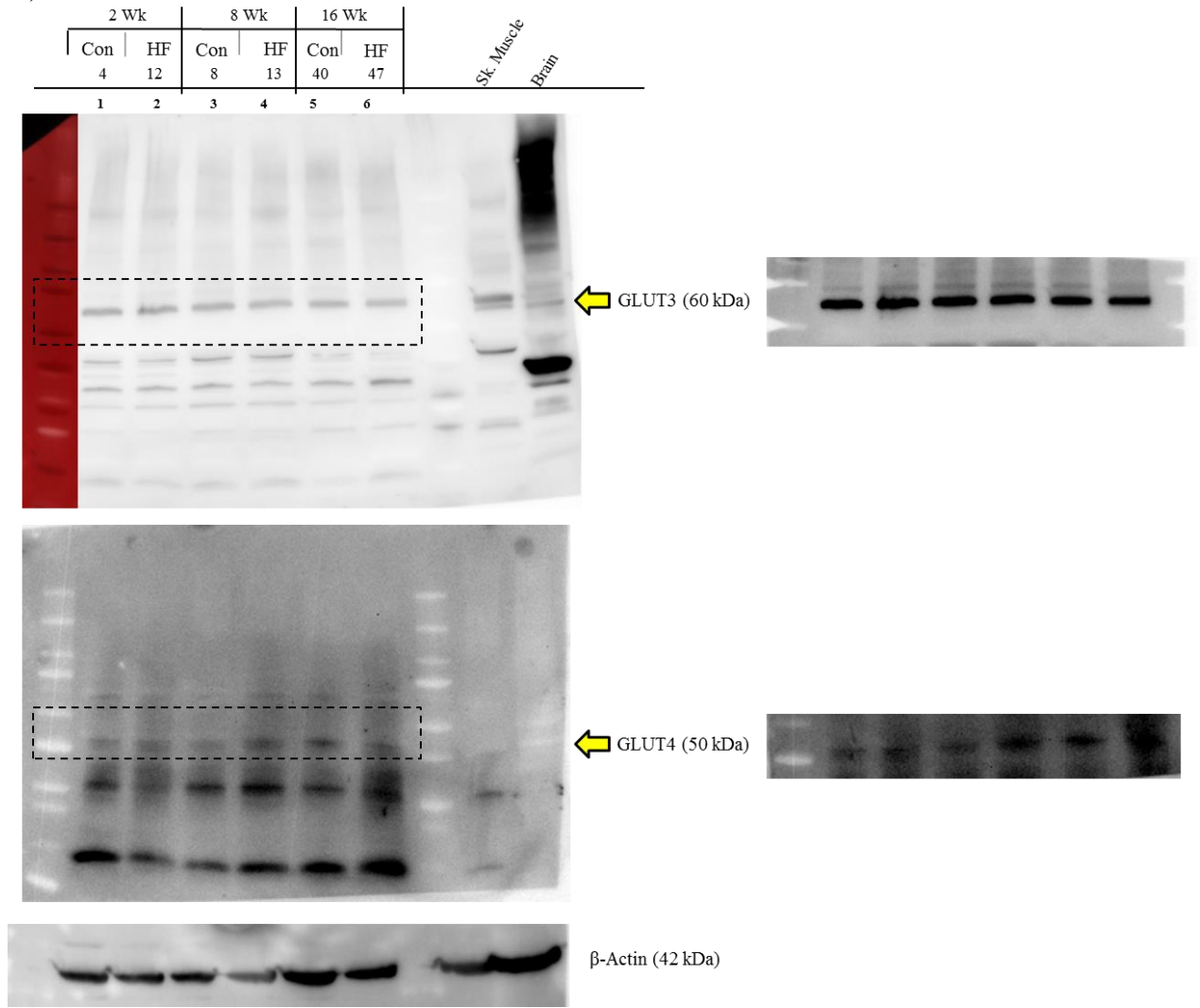


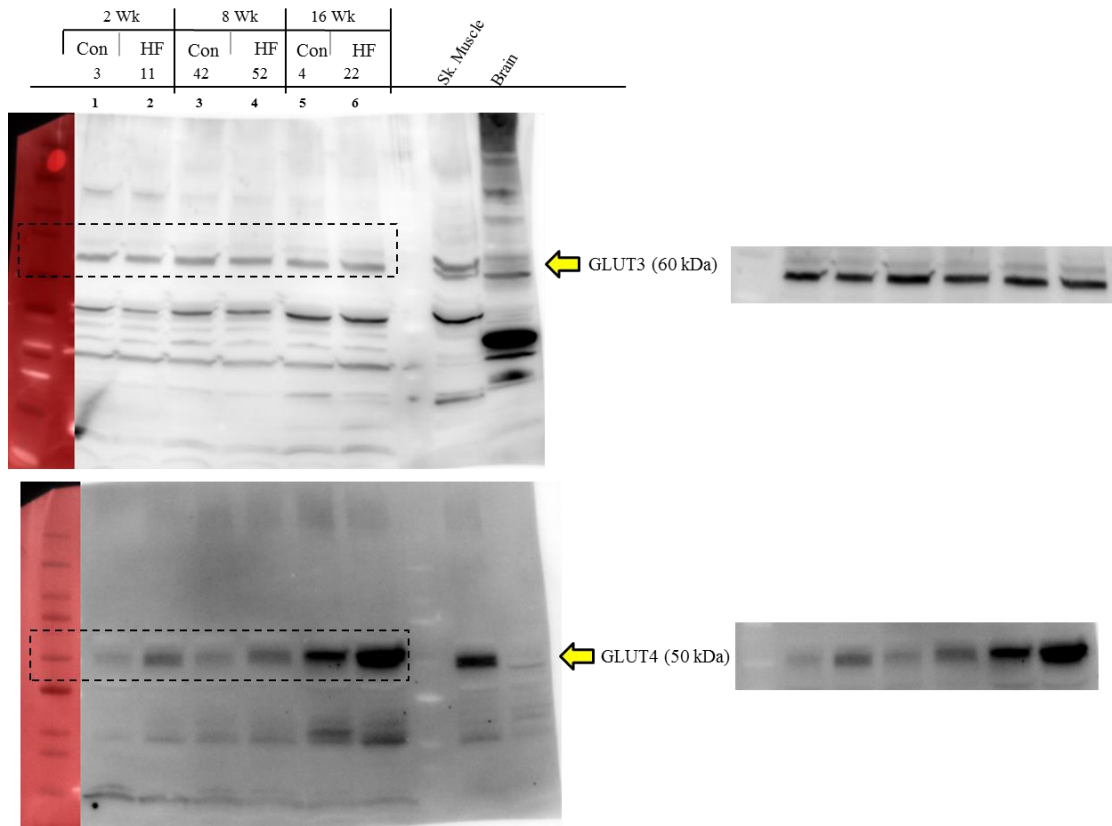
Figure 8.



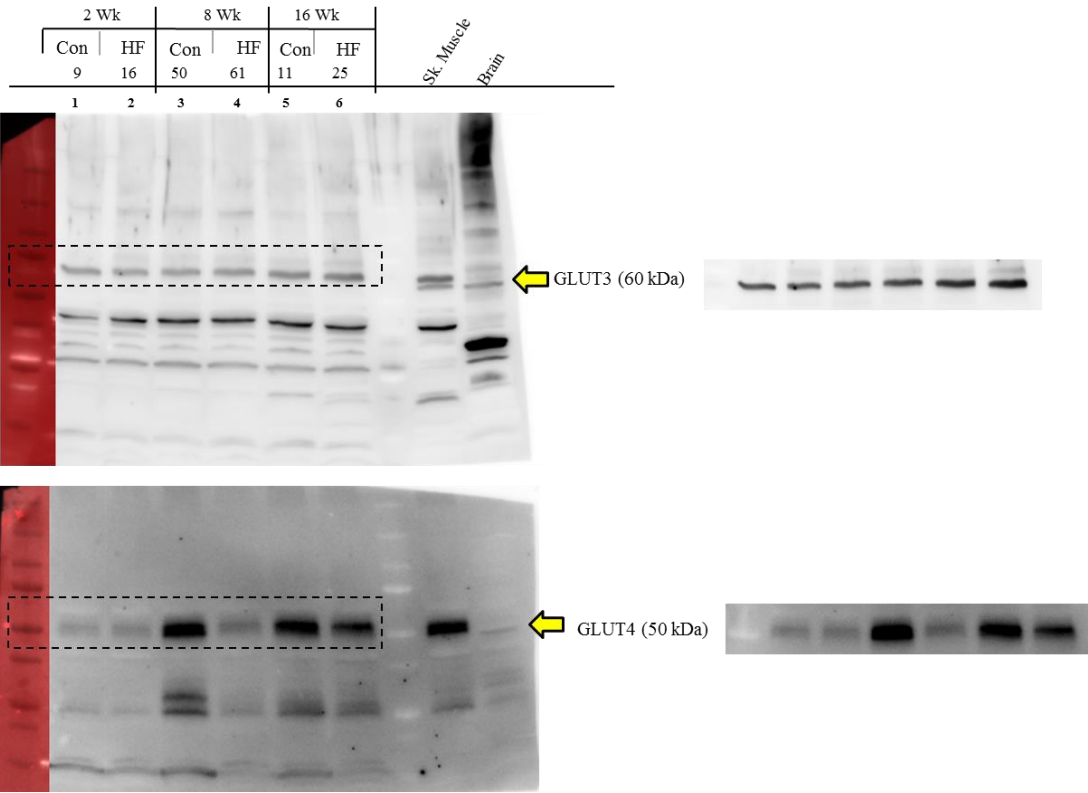
C)



D)



E)



Oklahoma State University
Institutional Animal Care and Use Committee (IACUC)

Protocol Expires: 7/5/2012

Date: Monday, July 06, 2009

Animal Care and Use Protocol (ACUP) No: HE092

Proposal Title: Dysregulation of Bone Metabolism in Type 2 Diabetes

Principal
Investigator:

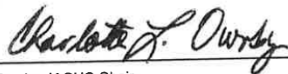
Brenda J. Smith
Nutritional Sciences
301 HES
Campus

Reviewed and Processed as: Full Committee

Approval Status Recommended by Reviewer(s): Approved

The revised protocol is approved as written. You are approved for a maximum of 90 C57BL/6 mice and 90 C3H/HeJ mice for the next three years.

Signatures



Charlotte Ownby, IACUC Chair

Monday, July 06, 2009

Date

cc: Department Head, Human Environmental Sciences
Director, Animal Resources

Approvals are valid for three calendar years, after which time a request for renewal must be submitted. Any modifications to the research project, course, or testing procedure must be submitted for review and approval by the IACUC, prior to initiating any changes. Modifications do not affect the original approval period. Approved projects are subject to monitoring by the IACUC. OSU is a USDA registered research facility and maintains an Animal Welfare Assurance document with the Public Health Service Office of Laboratory Animal Welfare, Assurance number AA3722-01.

Oklahoma State University
Institutional Animal Care and Use Committee (IACUC)

Protocol Expires: 7/5/2012

Date : Thursday, August 04, 2011

Animal Care and Use Protocol (ACUP) No: HE092

Proposal Title: Dysregulation of Bone Metabolism in Type 2 Diabetes

Principal
Investigator:

Brenda J. Smith
Nutritional Sciences
301 HES
Campus

Reviewed and
Processed as: Special Review **Modification**

Approval Status Recommended by Reviewer(s) : Approved

The modification request for additional mice and change in type of mice is approved. You are approved for an additional 62 C57BL/6 male mice and 62 C3H/HeJ male mice. You are also approved to use 40 C3H mice as a C3H control. This makes a total of 164 additional mice approved for this protocol.

164
180
344

Signatures


Dr. Charlotte Ownby, IACUC Chair

Thursday, August 04, 2011
Date

cc: Department Head, Human Sciences
LAR

Approvals are valid for three calendar years, after which time a request for renewal must be submitted. Any modifications to the research project, course, or testing procedures must be submitted for review and approval by the IACUC, prior to initiating any changes. Modifications do not affect the original approval period. Modification approvals are valid for the duration of the protocol approval (see protocol expiration date). Approved projects are subject to monitoring by the IACUC. OSU is a USDA registered research facility and maintains an Animal Welfare Assurance document with the Public Health Service Office of Laboratory Animal Welfare, Assurance number AA3722-01.

Abbreviation	Description
ADP	adenosine diphosphate
AGE	advanced glycation end-products
<i>Alp/ Alpl</i>	alkaline phosphatase
AMBRA	activating molecule in beclin-1 regulator autophagy
AMP	adenosine monophosphate
AMPK	AMP-activated protein kinase
Ap-1/ cFos	activator protein-1
<i>Atf4</i>	activating transcription factor 4
ATG/ Atg	autophagy related protein
ATP	adenosine triphosphate
AUC	area under the curve
BafA1	bafilomycin A1
Barkor/ Atg14L	beclin 1-associated autophagy-related key regulator
Bcl-2	B-cell lymphoma-2
Beclin1/ <i>Becn1</i>	Bcl-2-interacting myosin-like coiled-coil protein
BMA	bone mineral area
BMC	bone mineral content
BMD	bone mineral density
BMI	body mass index
BMP/ <i>Bmp</i>	bone morphogenic proteins
BSP/ <i>Ibsp</i>	bone sialoprotein/ integrin binding sialoprotein
BV/TV	bone volume/ total volume
<i>Casp3</i>	caspase 3
CD14	cluster of differentiation 14
CDC	Center for Disease Control and Prevention
cDNA	complementary DNA
CFU	colony forming units
<i>Colla1/ Colla1</i>	collagen type 1 alpha 1
Con	control
ConnDens	connectivity density
COPD	chronic obstructive pulmonary disorder
Cre	causes recombination
CTSK/ <i>Ctsk</i>	cathepsin K
CTX	cross-linked telopeptides of type I collagen
<i>Cxcl10</i>	chemokine (C-X-C motif) ligand 10
DAMP	damage-associated molecular pattern
DAPK	death-associated protein kinase
Deptor	DEP domain-containing mTOR-interacting protein
DMP	dentin matrix protein
DNA	deoxyribonucleic acid

DXA	dual energy x-ray absorptiometry
ECF	extracellular fluid
EF1	translational elongation factor 1
ELISA	enzyme-linked immunosorbent assay
<i>Fasn</i>	fatty acid synthase
FetA	fetuin A
FIP200	focal adhesion kinase family-interacting protein of 200 kDa
FoxO3	forkhead box O3
<i>Fra1/ Fos11</i>	Fos-related antigen 1
FRAX	Fracture Risk Algorithm
FRB	FKBP12–rapamycin-binding domain
GABARAP	GABA(A) receptor-associated protein
GABARAPL2/	
GATE16	GABA(A) receptor-associated protein-like 2
GFP	green fluorescence protein
Gla-OCN	total carboxylated OCN
Glu-OCN	undercarboxylated OCN
GLUT/ <i>Slc2a</i>	glucose transporter/ solute carrier family 2
<i>Gpx1</i>	glutathione peroxidase
hESC	human embryonic stem cells
HF	high fat
HIF	hypoxia inducible factor
HIV	human immunodeficiency virus
HMGB1	High-mobility group protein B1
HSC	hematopoietic stem cells
HSP	heat shock protein
ICAM1	Intercellular Adhesion Molecule 1
<i>Ifit1</i>	interferon-induced protein with tetratricopeptide repeats
IFN	interferon
IGF-1	insulin-like growth factor
IGTT	intraperitoneal glucose tolerance test
<i>Ihh</i>	Indian hedgehog
IKK	I κ B kinase
IL	interleukin
IR	insulin receptor
IRAK	IL-1 receptor-associated kinase
IRF	interferon regulatory factor
IRS	insulin receptor substrate
JNK	c-Jun NH(2)-terminal protein kinases
kcal	kilocalorie
K_m	Michaelis constant

LC3/ <i>Maplc3</i>	microtubule-associated protein 1 light chain 3
LDL	low density lipoprotein
<i>Lepr</i>	leptin receptor
LOX	lysyl oxidase
LPS	lipopolysaccharide
LRP	low density lipoprotein receptor-related protein
Mac-1	macrophage adhesion molecule-1
MAL	MyD88-adaptor-like
MEFs	mouse embryonic fibroblasts
microCT/ μ CT	micro-computerized tomography
mLST8/ G β L	mammalian lethal with SEC13 protein 8/ G protein β subunit-like protein
MSC	mesenchymal stem cells
mTORC	mechanistic target of rapamycin complex
MyD88	myeloid differentiation primary response 88
NAFLD	non-alcoholic fatty liver disease
NFATc1	nuclear factor of activated T-cells
NF- κ B	nuclear factor kappa-light-chain-enhancer of activated B cells
NNT	nicotinamide nucleotide transhydrogenase
NSAID	non-steroidal anti-inflammatory drug
\emptyset	control
OCN/ <i>Bglap</i>	osteocalcin/ bone gamma-carboxyglutamate (gla) protein
OPG	osteoprotegerin
OPN/ <i>Spp1</i>	osteopontin/ secreted phosphoprotein 1
<i>Osx/ Sp7</i>	osterix/ Sp7 transcription factor 7
PBMC	peripheral blood mononuclear cells
PDK	phosphoinositide dependent protein kinase
PE	phosphatidyl ethanolamine
PI3K	phosphatidylinositol 3 kinase
PIP	phosphatidylinositol 4, 5-bisphosphate 2
<i>Ppara</i>	peroxisome proliferative-activator α
<i>Ppib/ Cyclo</i>	peptidylprolyl isomerase B/ cyclophilin
Pras40	proline-rich AKT1 substrate 1
PRR	pattern recognition receptors
PTB	phosphotyrosine binding domain
PtdInsK	class III phosphatidylinositol 3-kinase
PTH	parathyroid hormone
PTHrP	PTH-related peptide
qPCR	quantitative real-time polymerase chain reaction
RA	rheumatoid arthritis
RAGE	receptor for advanced glycation end-products

RANK	receptor activator for NF- κ B
RANKL	RANK ligand
Rap	rapamycin
Raptor	regulatory-associated protein of mTOR
Rheb	ras homology enriched in brain
RNA	ribonucleic acid
ROCK1/ ROK β	Rho kinase 1
RR	relative risk
RTK	receptor tyrosine kinase
Rubicon	RUN domain protein as Beclin1 interacting and cysteine-rich containing
Runx2/ <i>Cbfa1</i>	runt-related transcription factor 2/ core binding factor alpha 1
SAS	statistical analysis software
SDS-PAGE	sodium dodecyl sulfate-polyacrylamide gel electrophoresis
SE	standard error
sFFA	saturated free fatty acids
SH2	Src homology 2
SLE	systemic lupus erythematosus
Smad	small body size, mothers against decapentaplegic
SMI	structural model index
SNP	sodium nitroprusside
SOF	Study of Osteoporotic Fracture
SOST/ <i>Sost1</i>	sclerostin
<i>Srebp1c</i>	sterol regulatory element-binding protein
T1DM	type 1 diabetes mellitus
T2DM	type 2 diabetes mellitus
TAK1	transforming growth factor (TGF)- β -activated kinase 1
Tb.N.	trabecular number
Tb.Sp	trabecular separation
Tb.Th.	trabecular thickness
TEM	transmission electron microscopy
TIP60	HIV-1 Tat interactive protein, 60 kD
TIR	toll/interleukin-1 receptor
TIRAP	toll/interleukin-1 receptor TIR adaptor protein
TLR-4	Toll-like receptor 4
TNF α	tumor necrosis factor alpha
TRAF	TNF receptor-associated factor
TRAP/ <i>Acp5</i>	tartrate resistant acid phosphatase/ acid phosphatase 5, tartrate resistant
TRIF	TIR domain-containing adaptor inducing IFN- β
TSC1/2	tuberous sclerosis complex

TZD	thiazolidinediones
ULK	unc-like kinase
UVRAG	UV radiation resistance-associated gene
VOI	volume of interest
Vps34	vacuole protein sorting
WBC	white blood cells
Wnt	wingless-related

VITA

Elizabeth Rendina-Ruedy

Candidate for the Degree of

Doctor of Philosophy

Thesis: DYSREGULATION OF BONE METABOLISM DURING TYPE 2
DIABETES MELLITUS: ROLE OF TOLL-LIKE RECEPTOR-4 AND
AUTOPHAGY

Major Field: Human Sciences; emphasis in Nutritional Sciences

Biographical:

Education:

Completed the requirements for the Master of Science in Nutritional Sciences at
Oklahoma State University, Stillwater, OK in 2009.

Completed the requirements for the Bachelor of Science in Biochemistry at
Oklahoma State University, Stillwater, OK in 2007.

Experience:

2012- Present

USDA-NIFA Pre-doctoral Fellowship;
Department of Nutritional Sciences, College of
Human Sciences, Oklahoma State University,
Stillwater, OK

2009- 2012

Research Assistant in Dr. Brenda J. Smith's
laboratory; Department of Nutritional Sciences,
College of Human Sciences, Oklahoma State
University, Stillwater, OK

Professional Memberships:

2009- Present

American Society of Bone and Mineral Research
(ASBMR)

2012- Present

Sigma Xi, The Scientific Research Society,
Associate Member